Sunrise on the Illinois Prairie – From My Study

OVERVIEW OF EFFECTS OF IRON REDOX IN CLAYS & SOILS

Joseph W. Stucki
University of Illinois

Brief Biographical Sketch

Brief Biographical Sketch

- Native of Rexburg, Idaho

Brief Biographical Sketch

- Native of Rexburg, Idaho
- Father was a professor of agriculture at Ricks College (now BYU-Idaho)

BYU-I

Brigham Young University -- Idaho

Brief Biographical Sketch

- Native of Rexburg, Idaho
- Father was a professor of agriculture at Ricks College (now BYU-Idaho)
- Grew up on a dairy


Work – Milking Cows

Brief Biographical Sketch

- Native of Rexburg, Idaho
- Father was a professor of agriculture at Ricks College (now BYU-Idaho)
- Grew up on a dairy
- Attended college in Idaho, Utah, and Indiana

My Colleges

Where I Grew Up.
Rexburg, Idaho

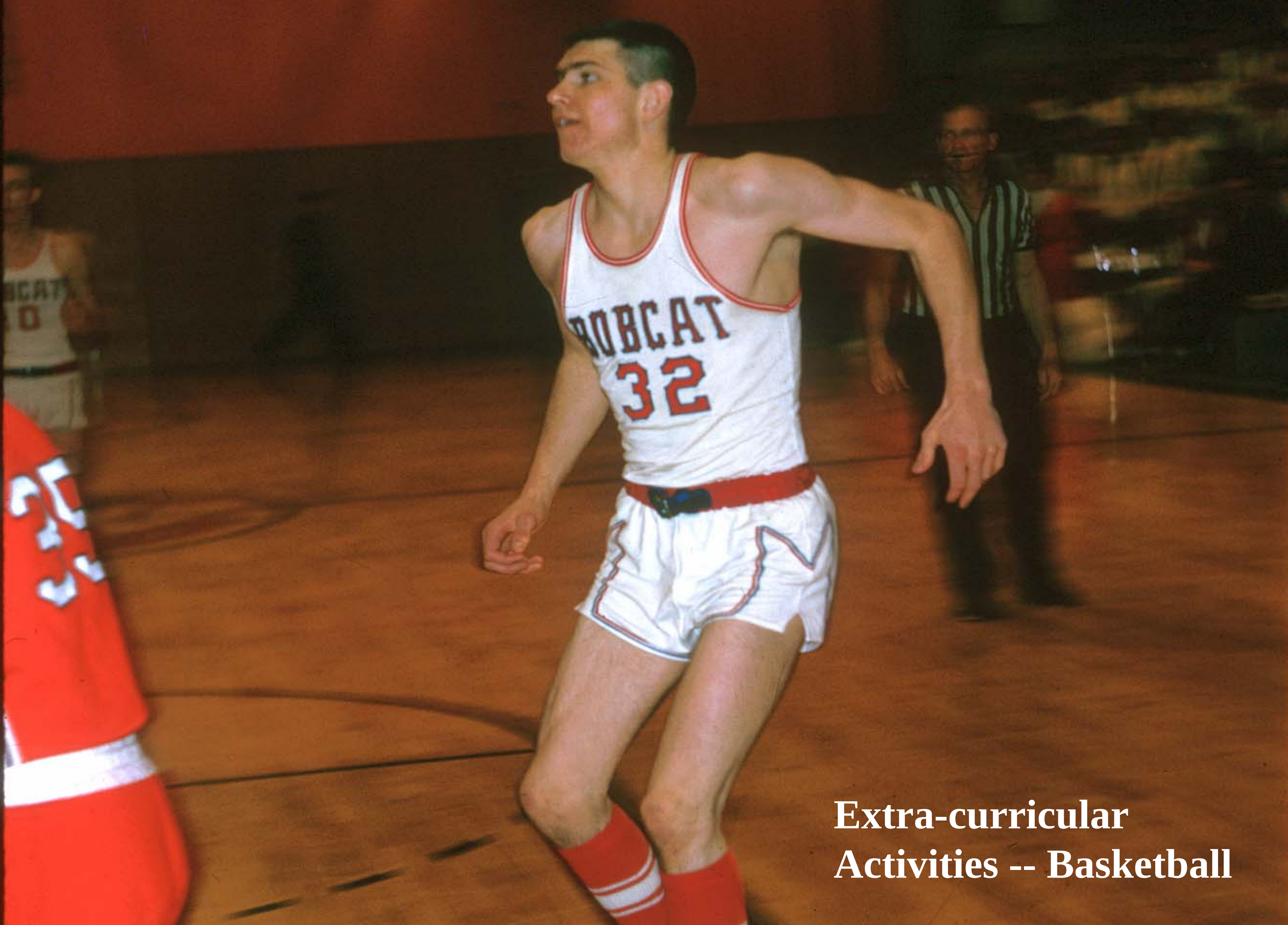

Extra-curricular Activities -- Basketball

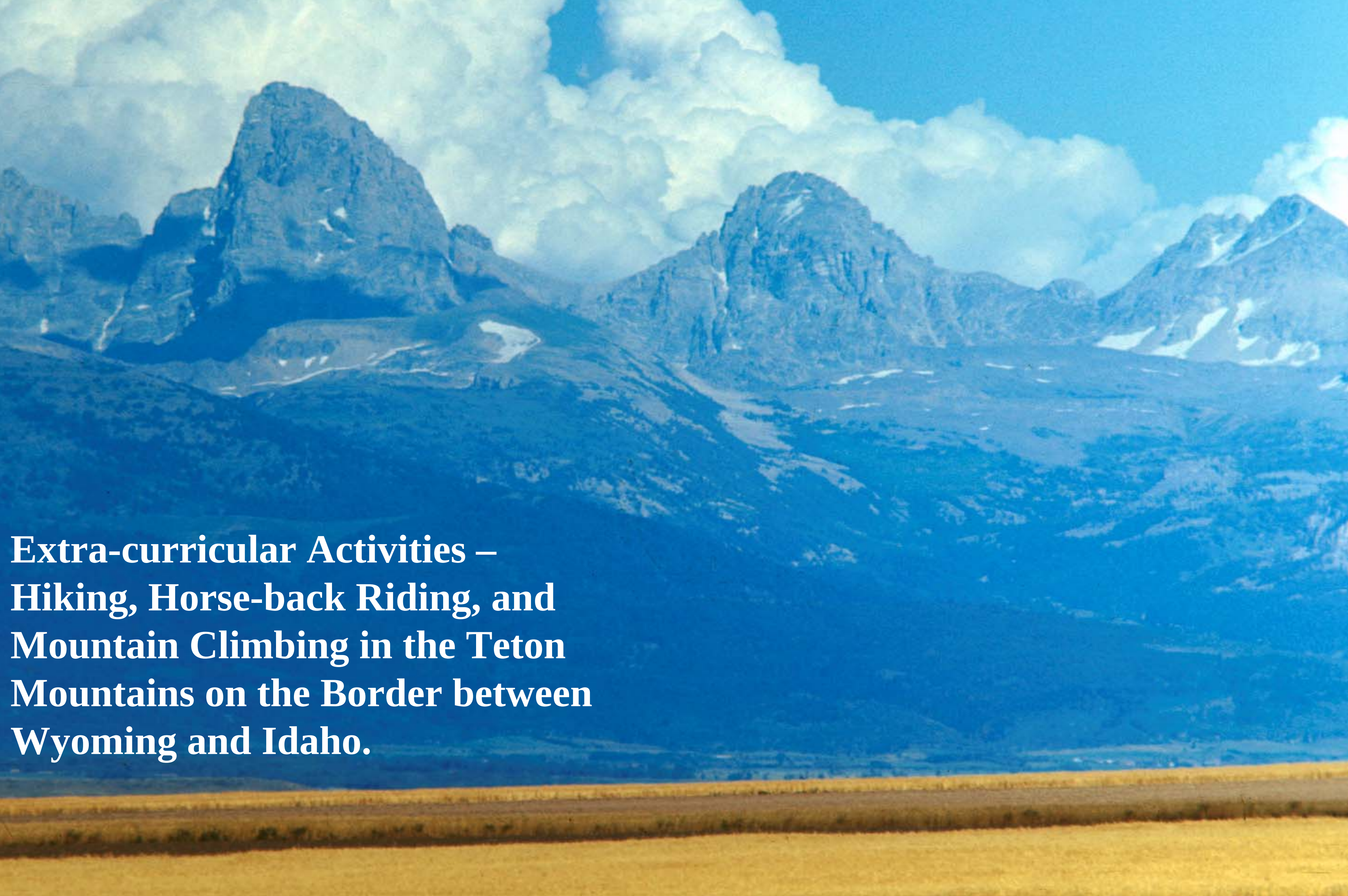
Extra-curricular Activities –
Hiking, Horse-back Riding, and
Mountain Climbing in the Teton
Mountains on the Border between
Wyoming and Idaho.

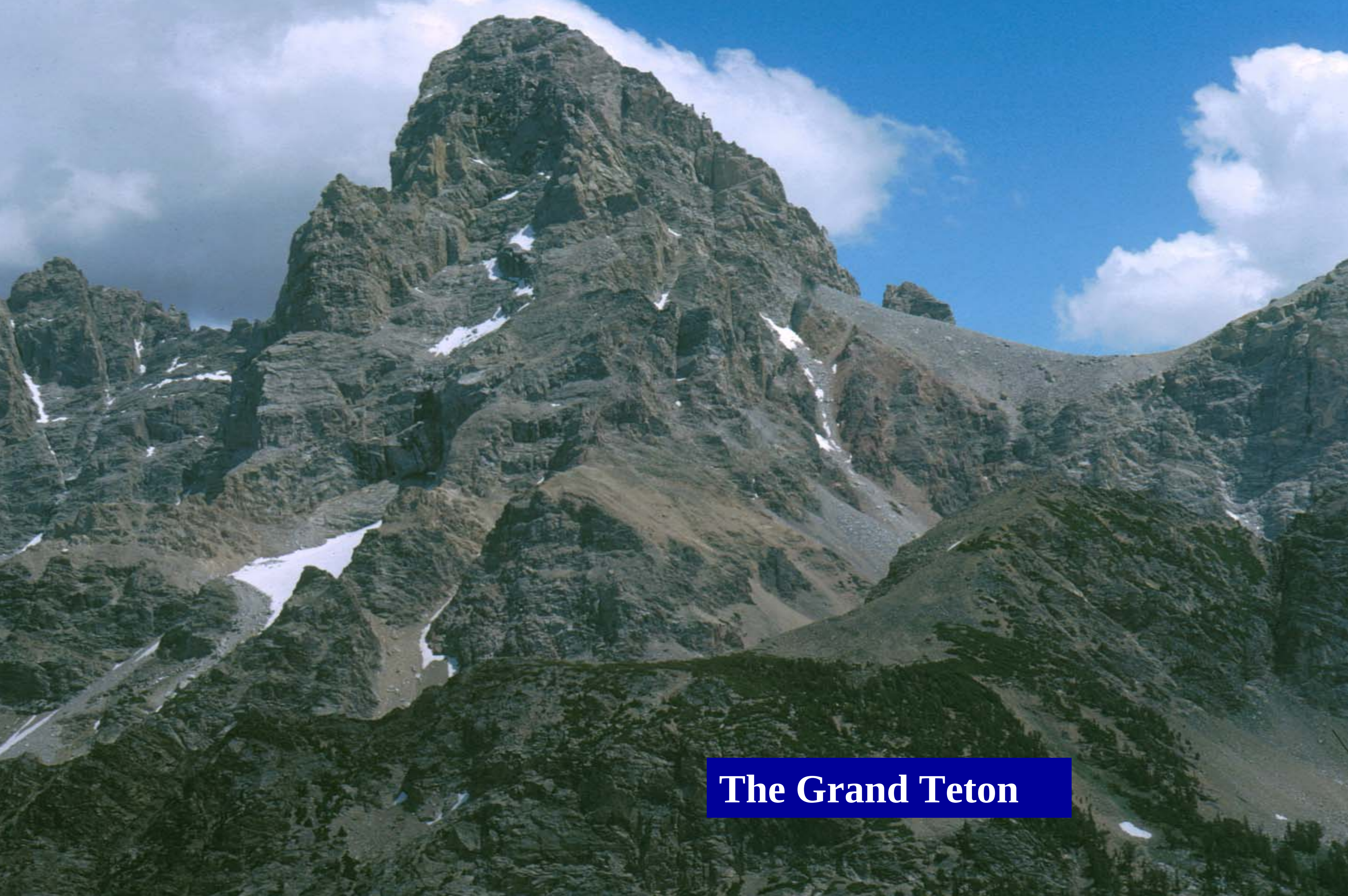
The Grand Teton


The Grand Teton Summit

My Youngest Daughter

Received B.S. in Chemistry

BYU
BRIGHAM YOUNG
UNIVERSITY
Provo, Utah

Mt. Timpo-nogas in Back-ground

Received M.S. in Soil Chemistry

PURDUE UNIVERSITY

Received Ph.D. in Physical Chemistry of Clays

Brief Biographical Sketch

- Native of Rexburg, Idaho
- Father was a professor of agriculture at Ricks College (now BYU-Idaho)
- Grew up on a dairy
- Attended college in Idaho, Utah, and Indiana
- Came to UIUC as assistant professor in 1976


UNIVERSITY of ILLINOIS
FOUNDED 1867

The University of Illinois

0161-15a.tif ACES-ITCS-Photo:


Raising a Family: 6 children; 9 grandchildren

Alma Mater

-- To thy happy children of the future, those of the past send greetings.

Hallene Gateway

Hallene Gateway

UIUC Classic Architecture

Altgeld Hall (Mathematics)

89003aa ACES-ITCS-Photo:

Morrow Plots – The U.S.'s Oldest Experimental Field

92061zza.tif ACES-ITCS-Photo:


UNIVERSITY OF ILLINOIS
OBSERVATORY

0340-33a.tif ACES-ITCS-Photo: Biotechnology

($Fe^{3+} \longrightarrow Fe^{2+}$)

Reduced Iron in Clay Minerals

Soil Fertility

($Fe^{3+} \longrightarrow Fe^{2+}$)

Reduced Iron in Clay Minerals

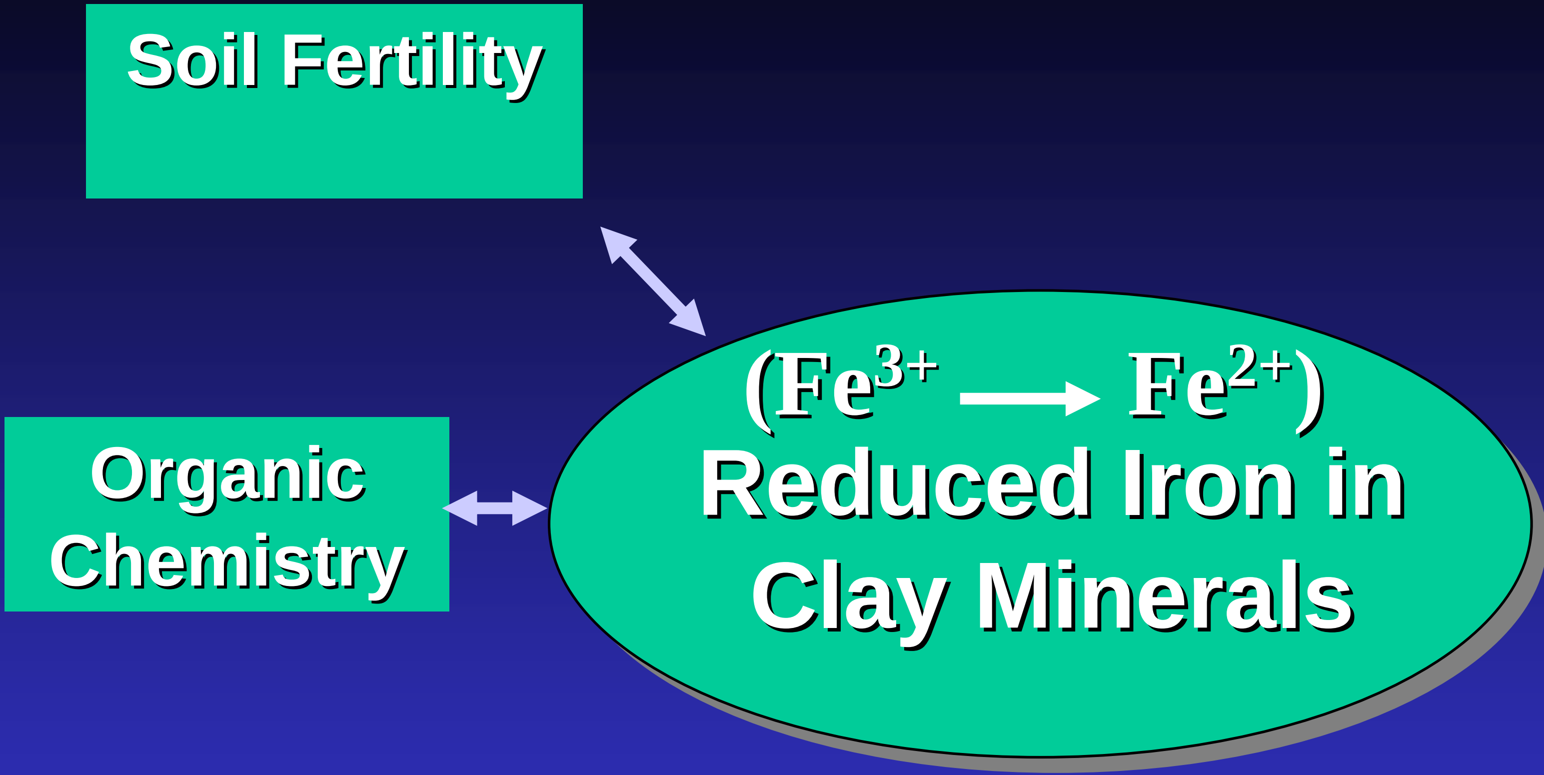
Soil Fertility
Organic Chemistry
($Fe^{3+} \longrightarrow Fe^{2+}$)
Reduced Iron in Clay Minerals

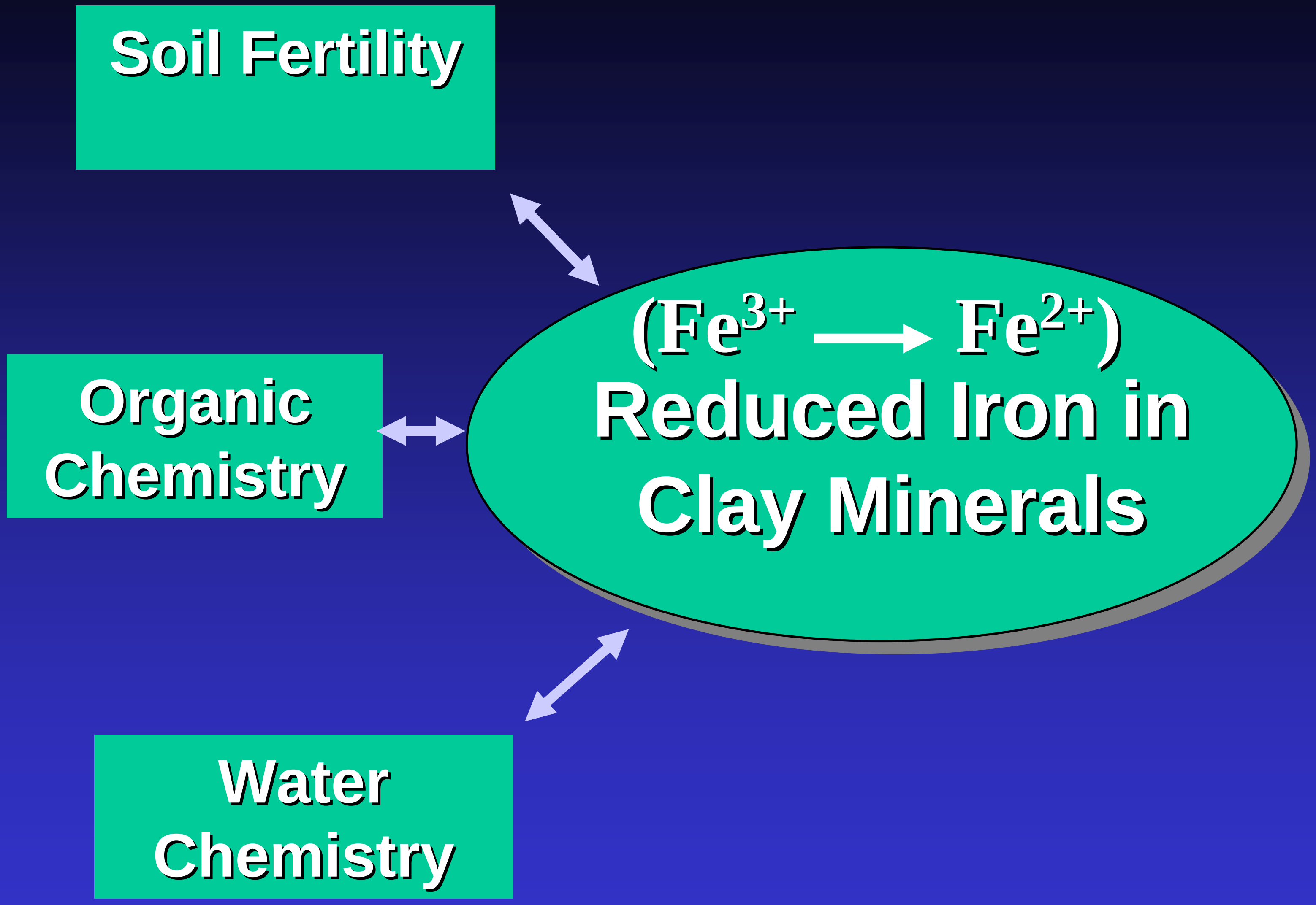
Soil Fertility
Organic Chemistry
Water Chemistry
($Fe^{3+} \longrightarrow Fe^{2+}$)
Reduced Iron in Clay Minerals

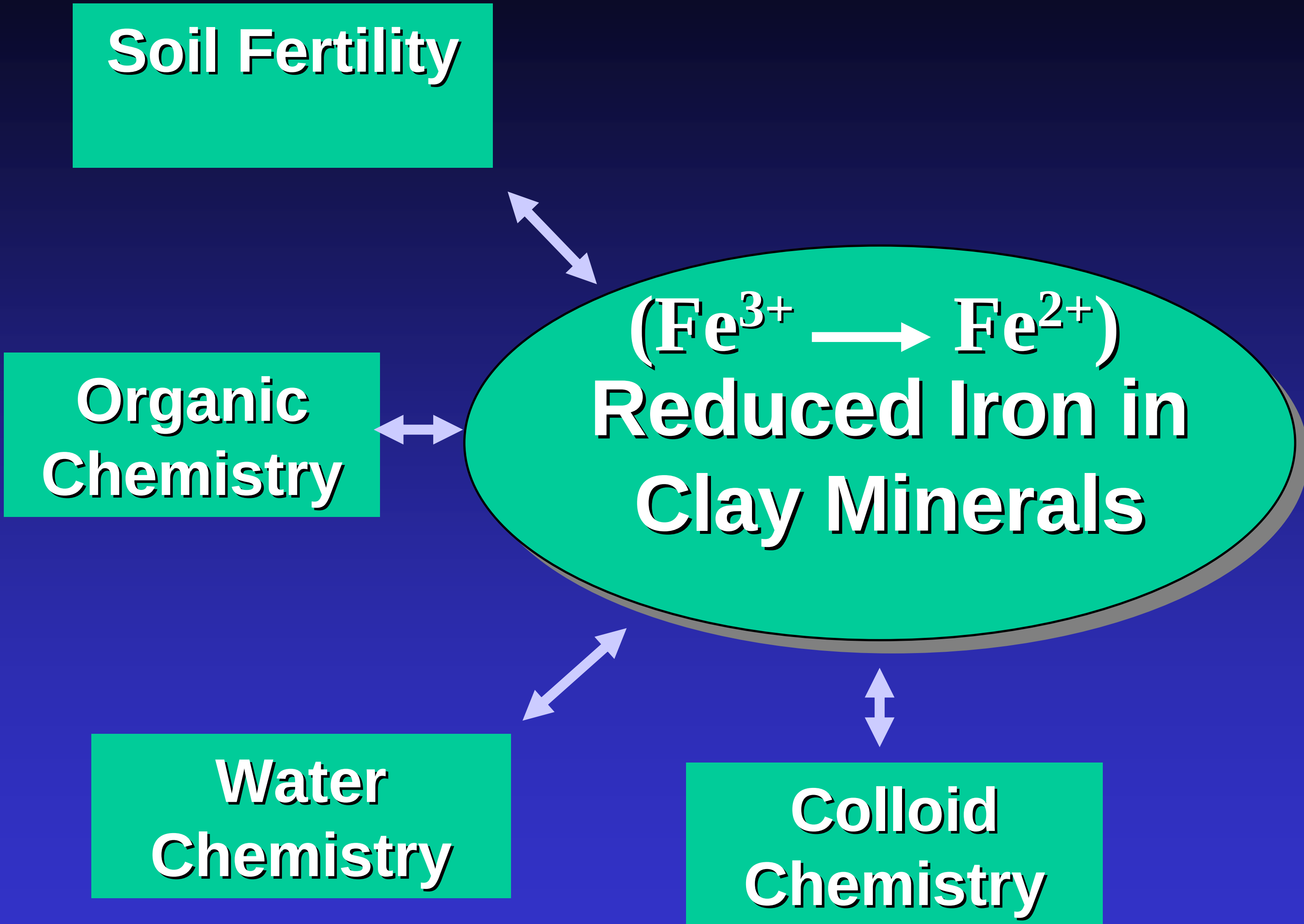
Soil Fertility
Organic Chemistry
($Fe^{3+} \longrightarrow Fe^{2+}$)
Reduced Iron in Clay Minerals
Water Chemistry
Colloid Chemistry

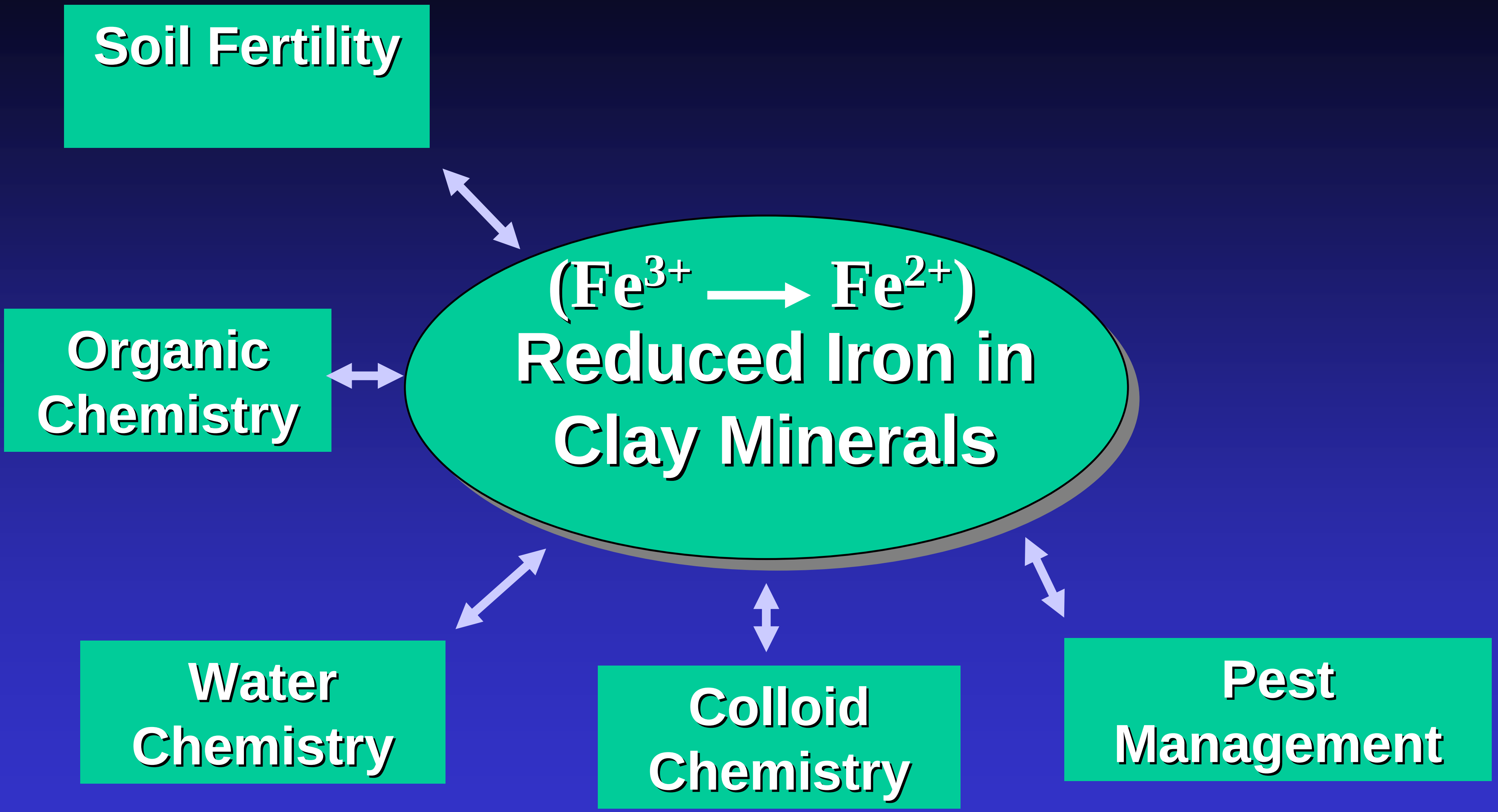
Soil Fertility
$(Fe^{3+} \longrightarrow Fe^{2+})$
Reduced Iron in Clay Minerals
Organic Chemistry
Water Chemistry
Colloid Chemistry
Pest Management

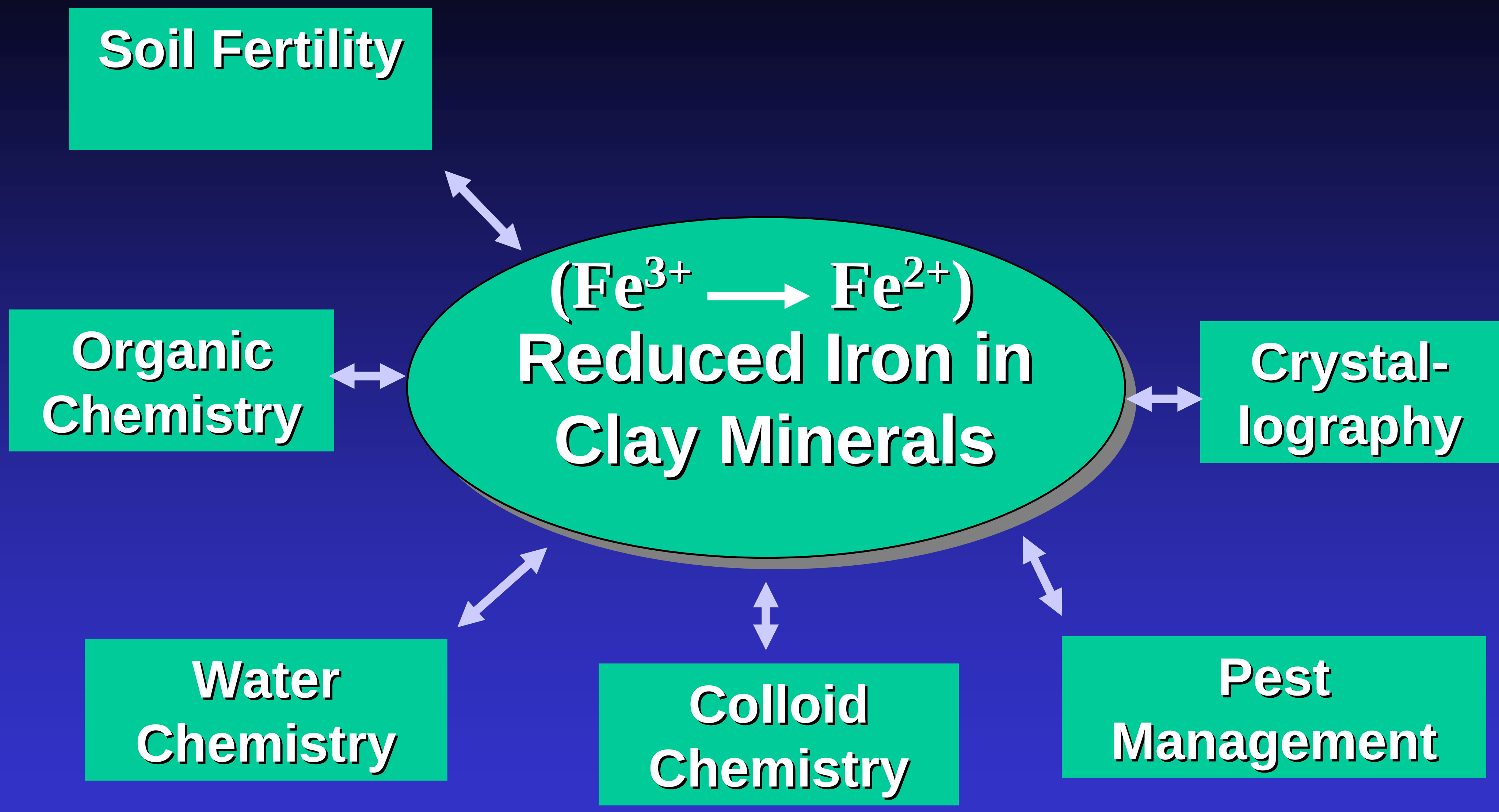
Soil Fertility
(Fe3+ → Fe2+)
Reduced Iron in Clay Minerals
Organic Chemistry
Crystal-lography
Water Chemistry
Colloid Chemistry
Pest Management

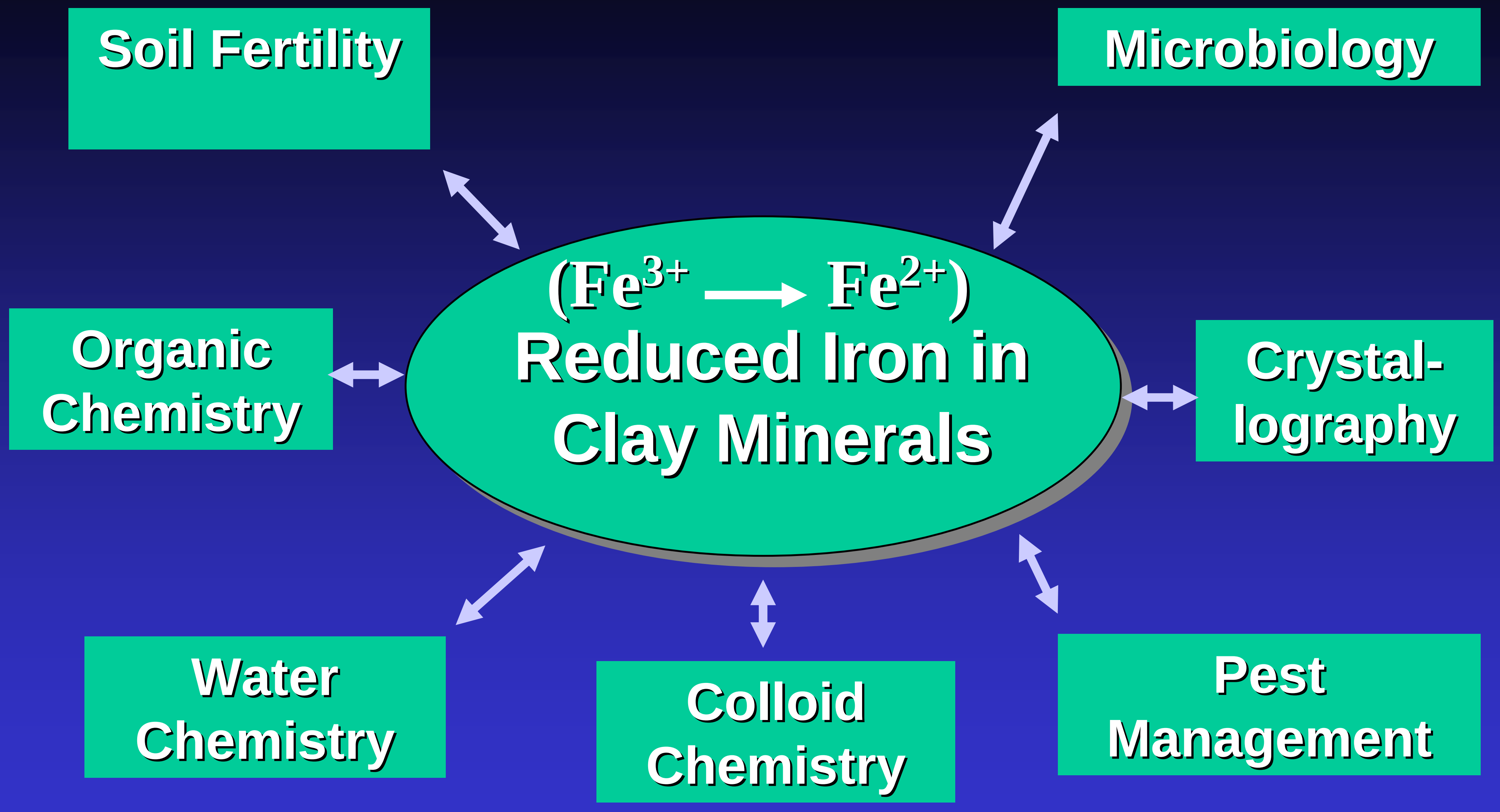

Soil Fertility
Microbiology
(Fe3+ → Fe2+)
Reduced Iron in Clay Minerals
Organic Chemistry
Crystal-lography
Water Chemistry
Colloid Chemistry
Pest Management

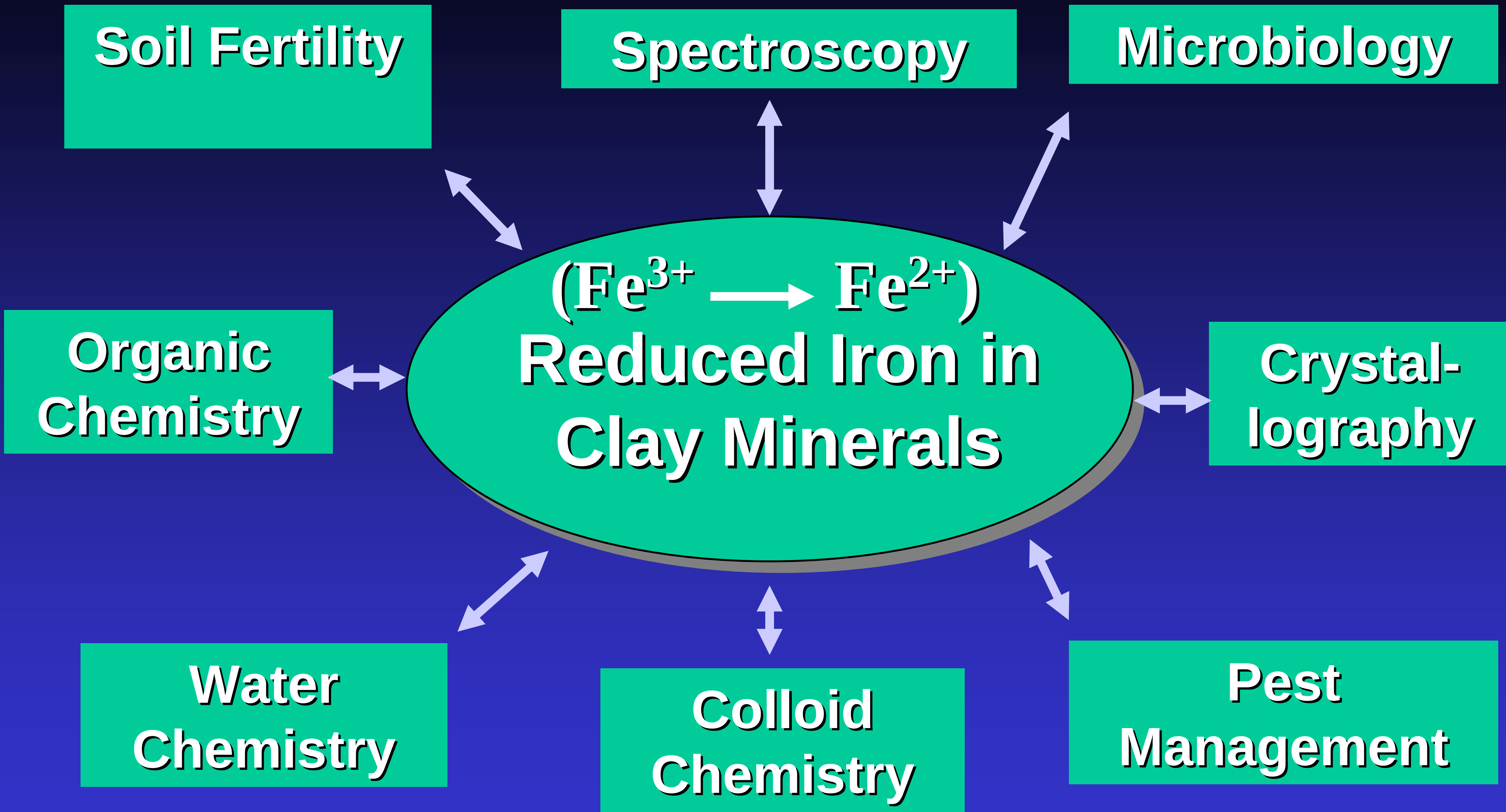

Soil Fertility
Spectroscopy
Microbiology
($Fe^{3+} \longrightarrow Fe^{2+}$)
Reduced Iron in Clay Minerals
Organic Chemistry
Crystal-lography
Water Chemistry
Colloid Chemistry
Pest Management

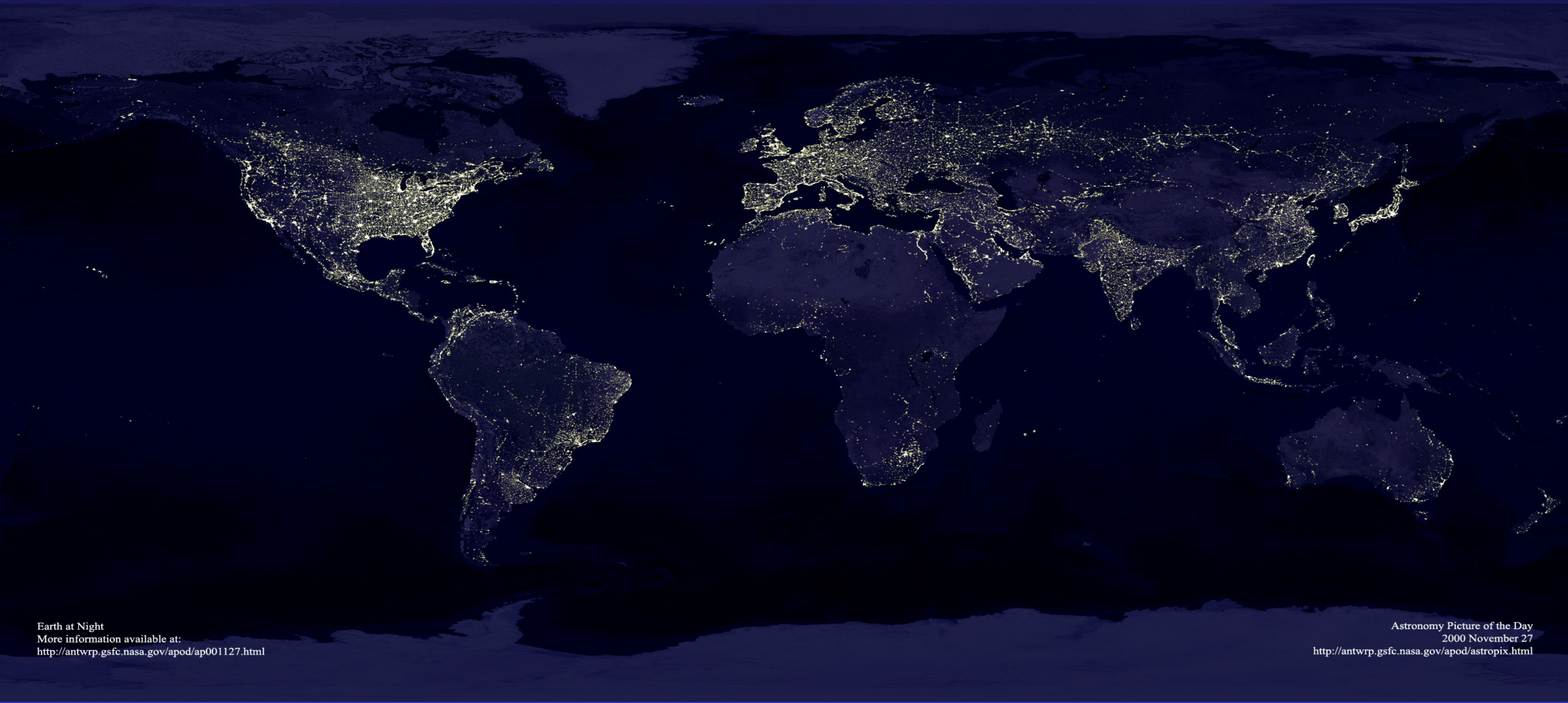

http://antwrp.gsfc.nasa.gov/apod/astropix.html

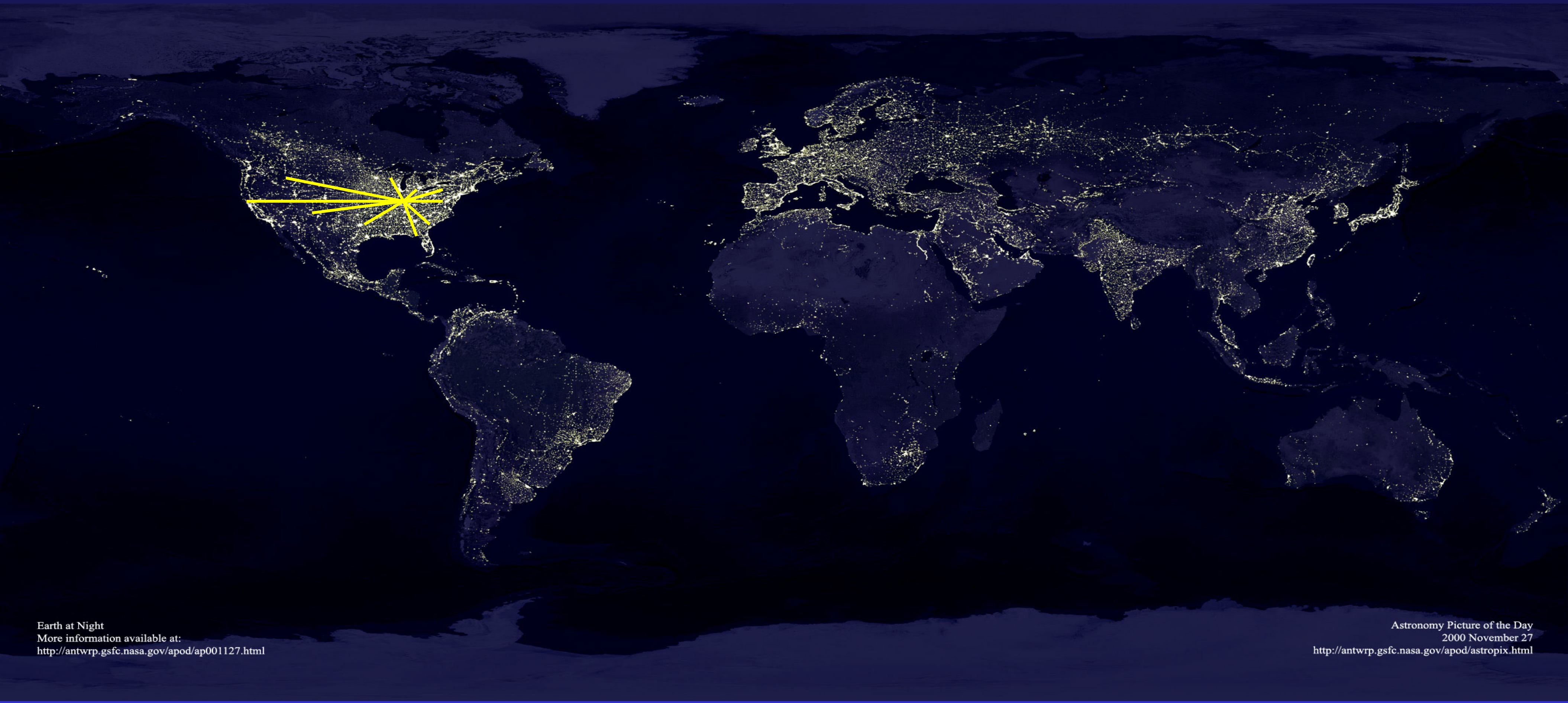

http://antwrp.gsfc.nasa.gov/apod/astropix.html

Illinois
Indiana
Wisconsin
Washington
California
Washington, D.C.

Florida
Georgia
Pennsylvania
Texas
New Mexico

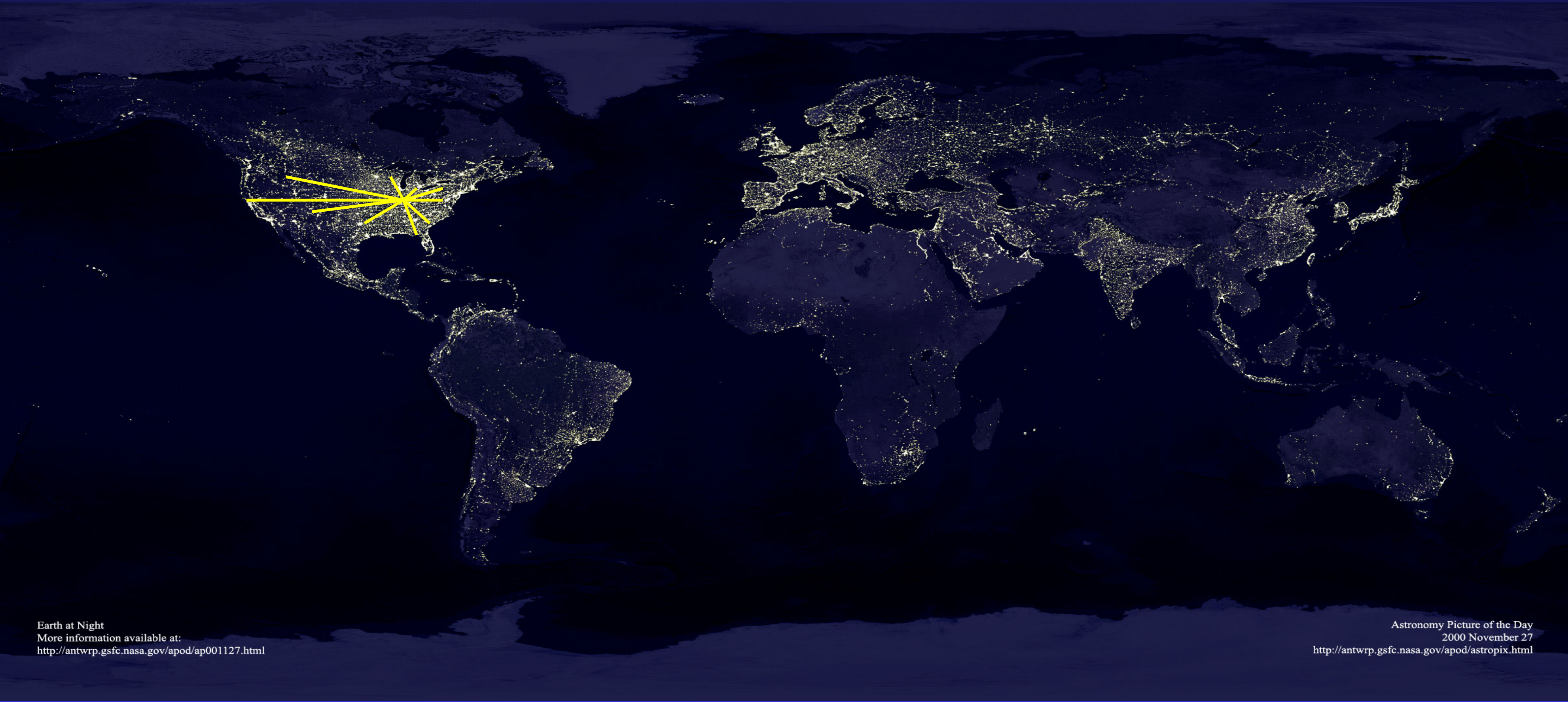

http://antwrp.gsfc.nasa.gov/apod/astropix.html

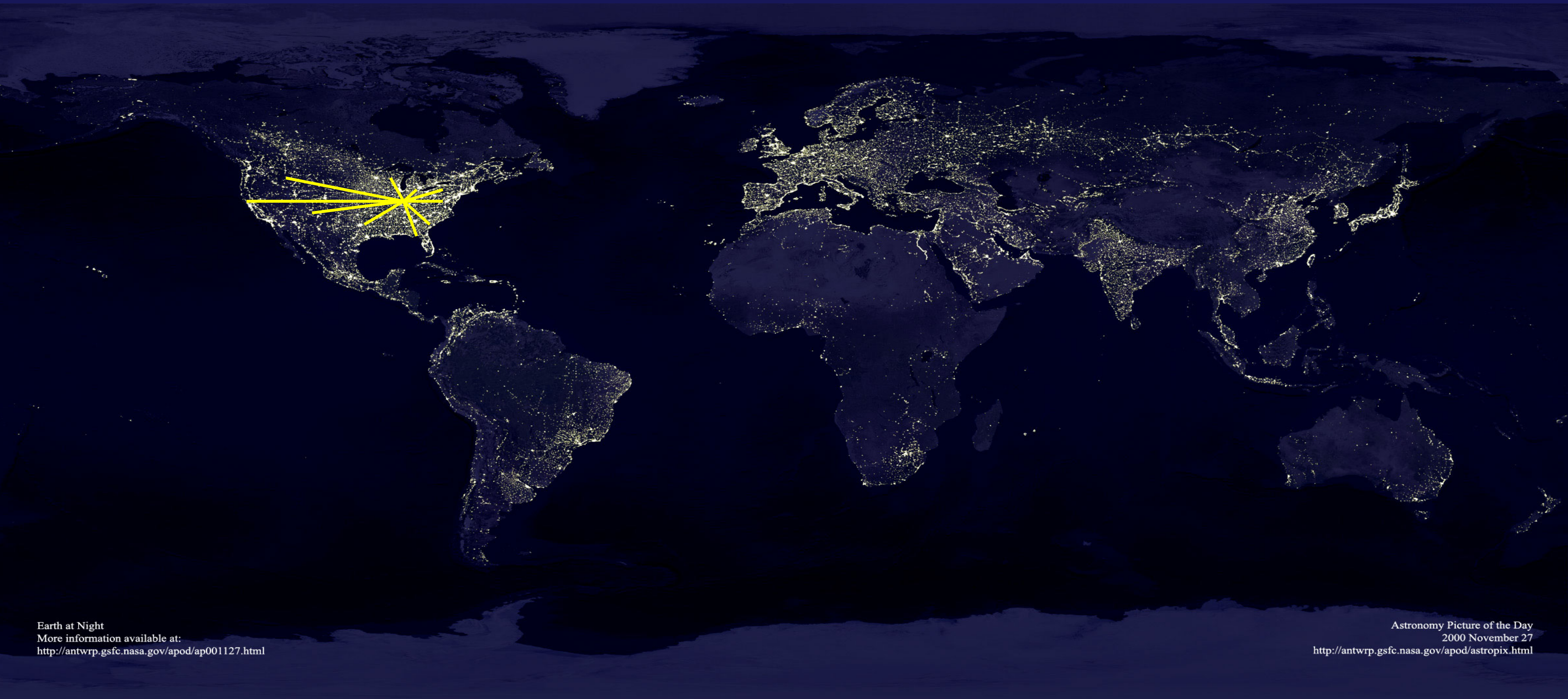

http://antwrp.gsfc.nasa.gov/apod/astropix.html

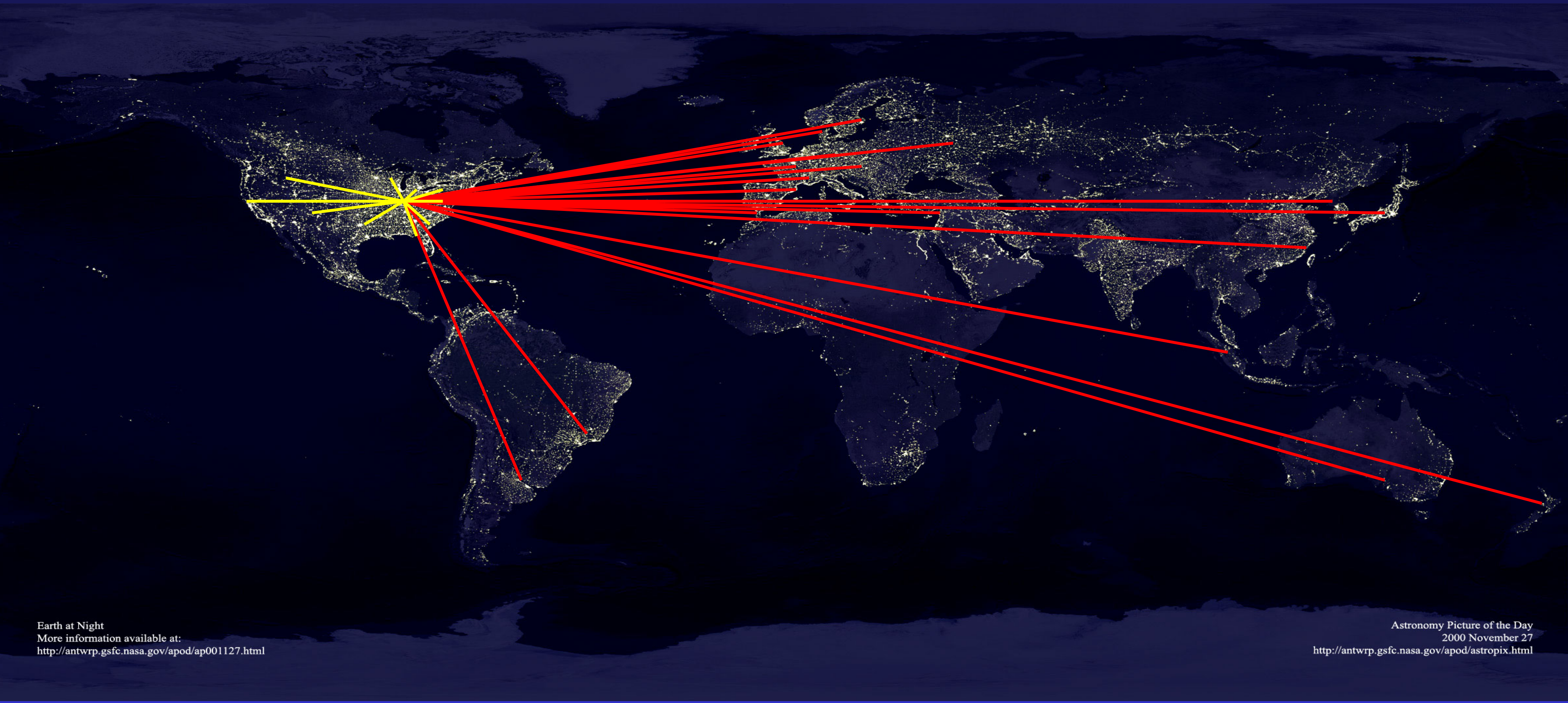

http://antwrp.gsfc.nasa.gov/apod/astropix.html

Argentina
Australia
Brazil
China
Denmark
England
France
Germany
Israel

Japan
Korea
New Zealand
Russia
Scotland
Singapore
Slovakia
Sweden
Switzerland
+ Visited 40 Others

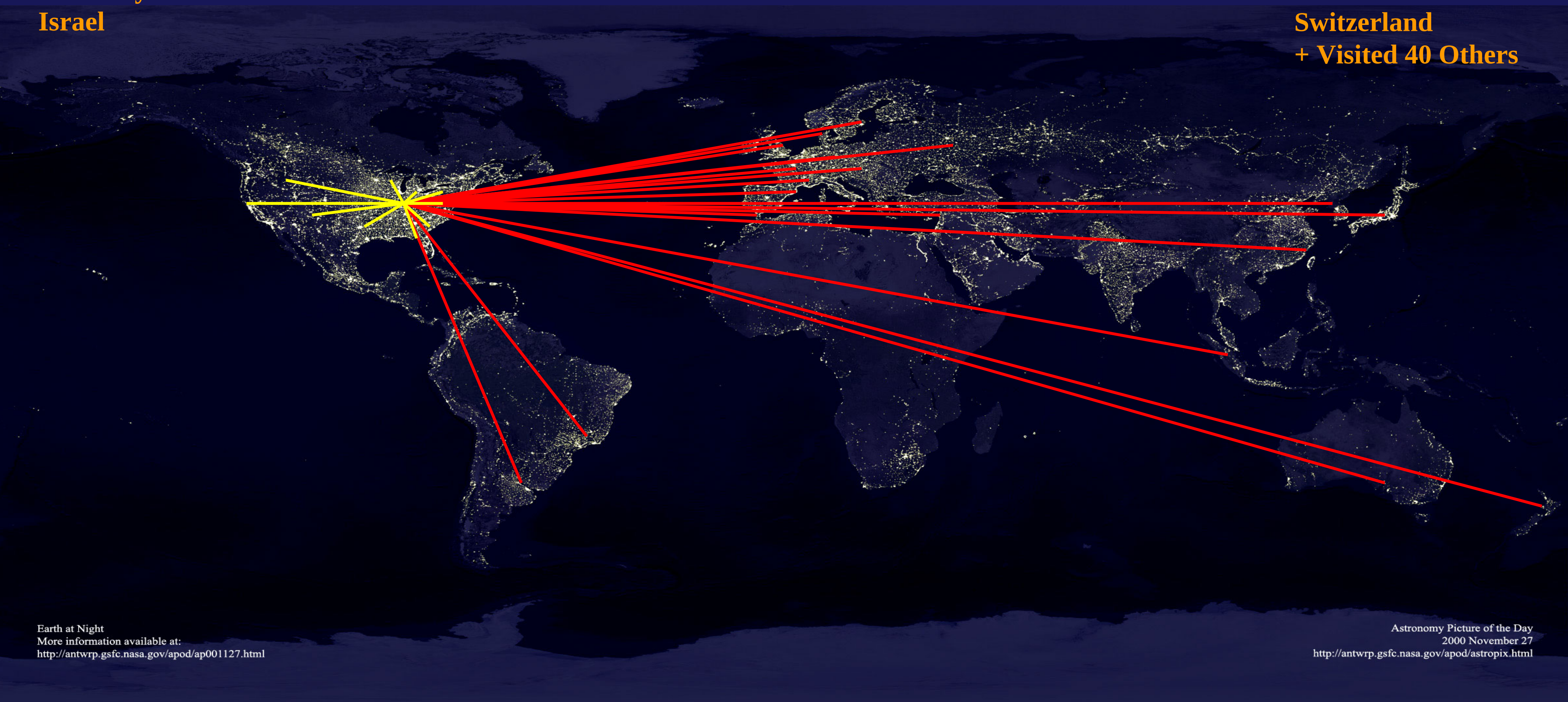

http://antwrp.gsfc.nasa.gov/apod/astropix.html

OUTLINE

- **Overview of Iron Reduction in Clays**

OUTLINE

- Overview of Iron Reduction in Clays
- Effects of Reduction on Smectite Structure and Iron Mineralogy

OUTLINE

- Overview of Iron Reduction in Clays
- Effects of Reduction on Clay-water & -organic Interactions

OUTLINE

- Overview of Iron Reduction in Clays
- Effects of Reduction on Clay-water & -organic Interactions
- **Application of Redox-treated Clays for the Remediation of Pesticide Toxicity**

Literature References

SEE HANDOUT

Most Common Soil Minerals

- Silicates and Aluminosilicates

Most Common Soil Minerals

- Silicates and Aluminosilicates
- Oxides and hydroxides of Fe, Al, and Mn

Most Common Soil Minerals

- Silicates and Aluminosilicates
- Oxides and hydroxides of Fe, Al, and Mn
- Carbonates

Most Common Soil Minerals

- Silicates and Aluminosilicates
- Oxides and hydroxides of Fe, Al, and Mn
- Carbonates
- Sulfates

Most Common Soil Minerals

- Silicates and Aluminosilicates

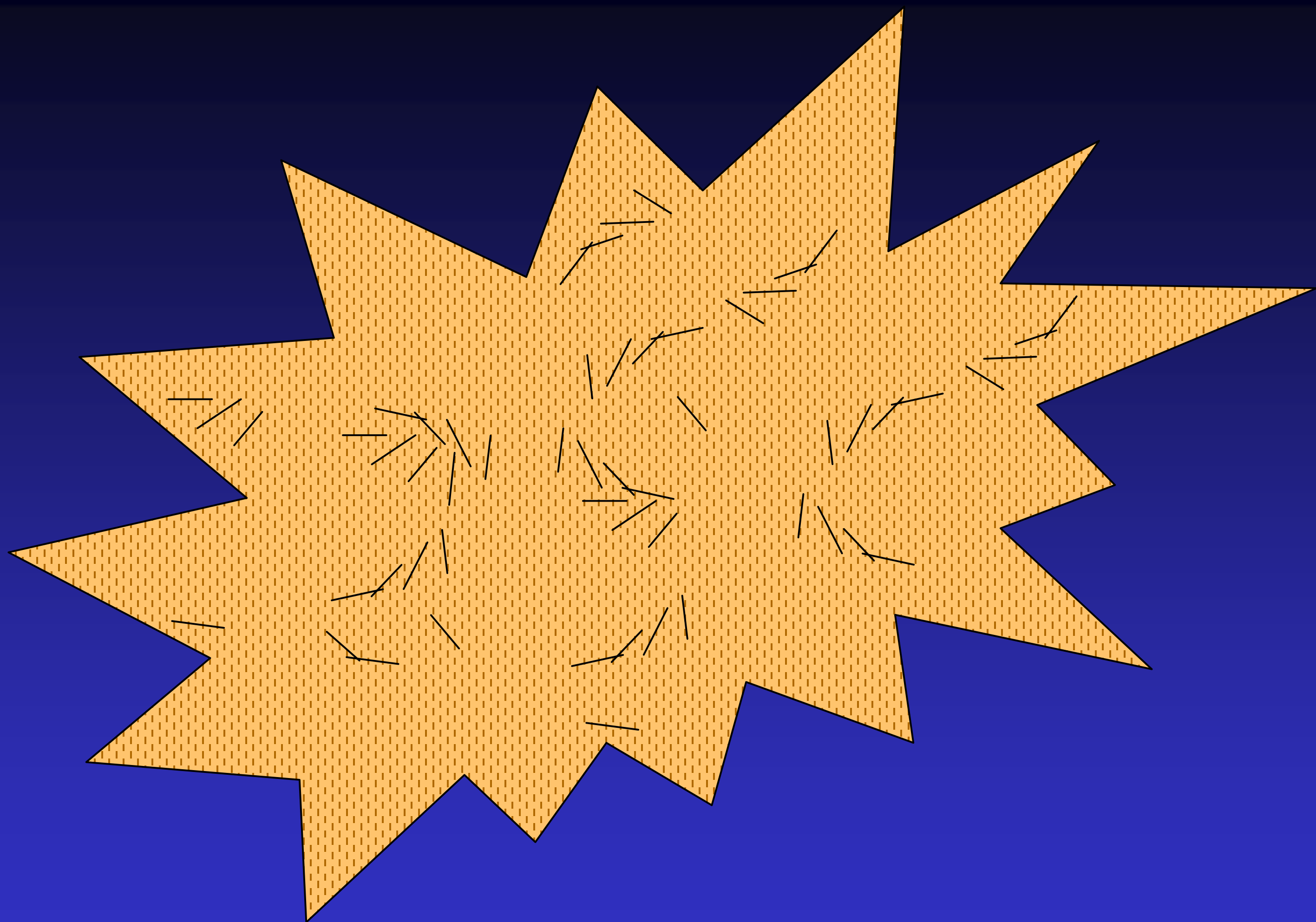

Soil Particle

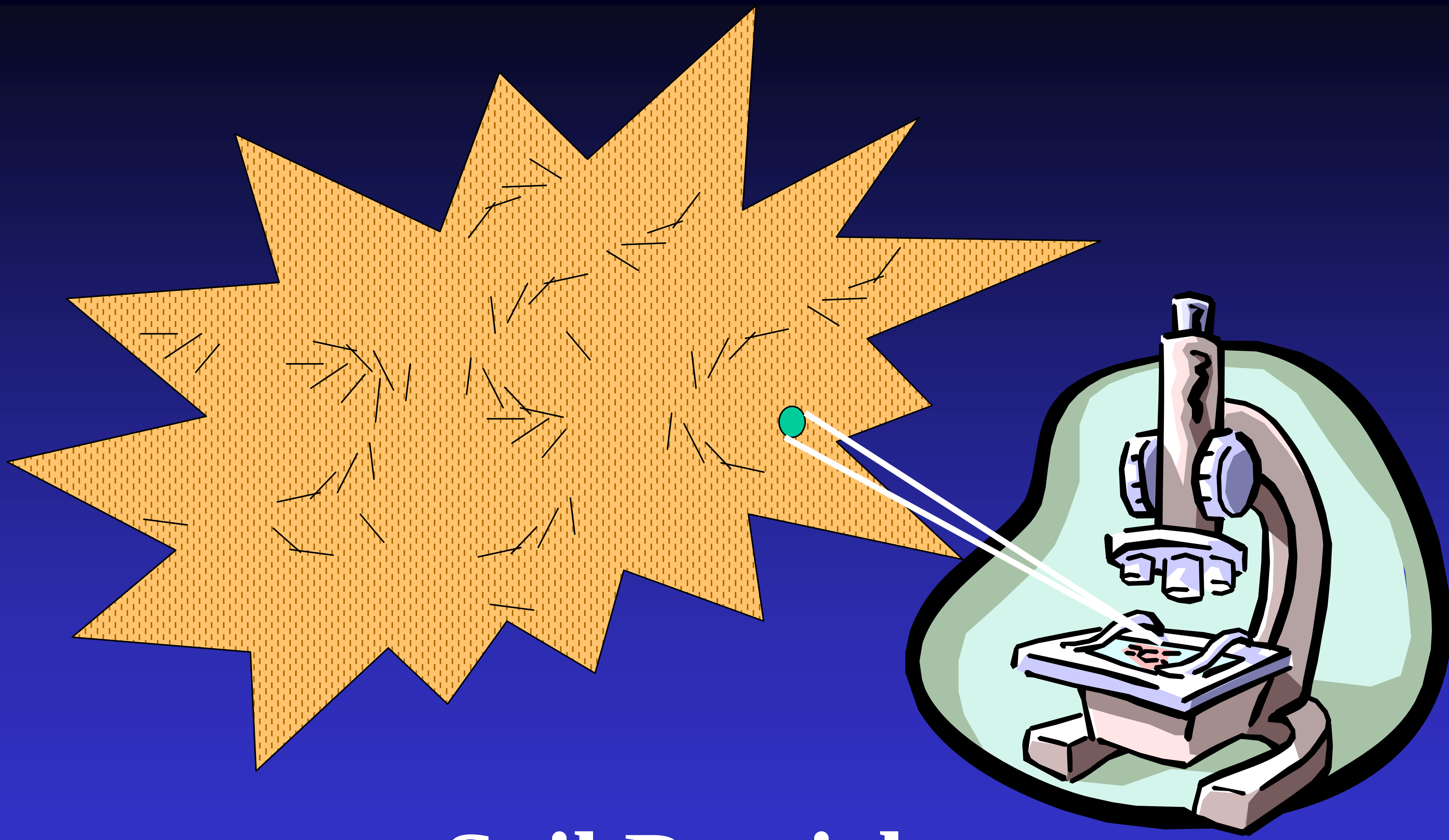

Soil Particle

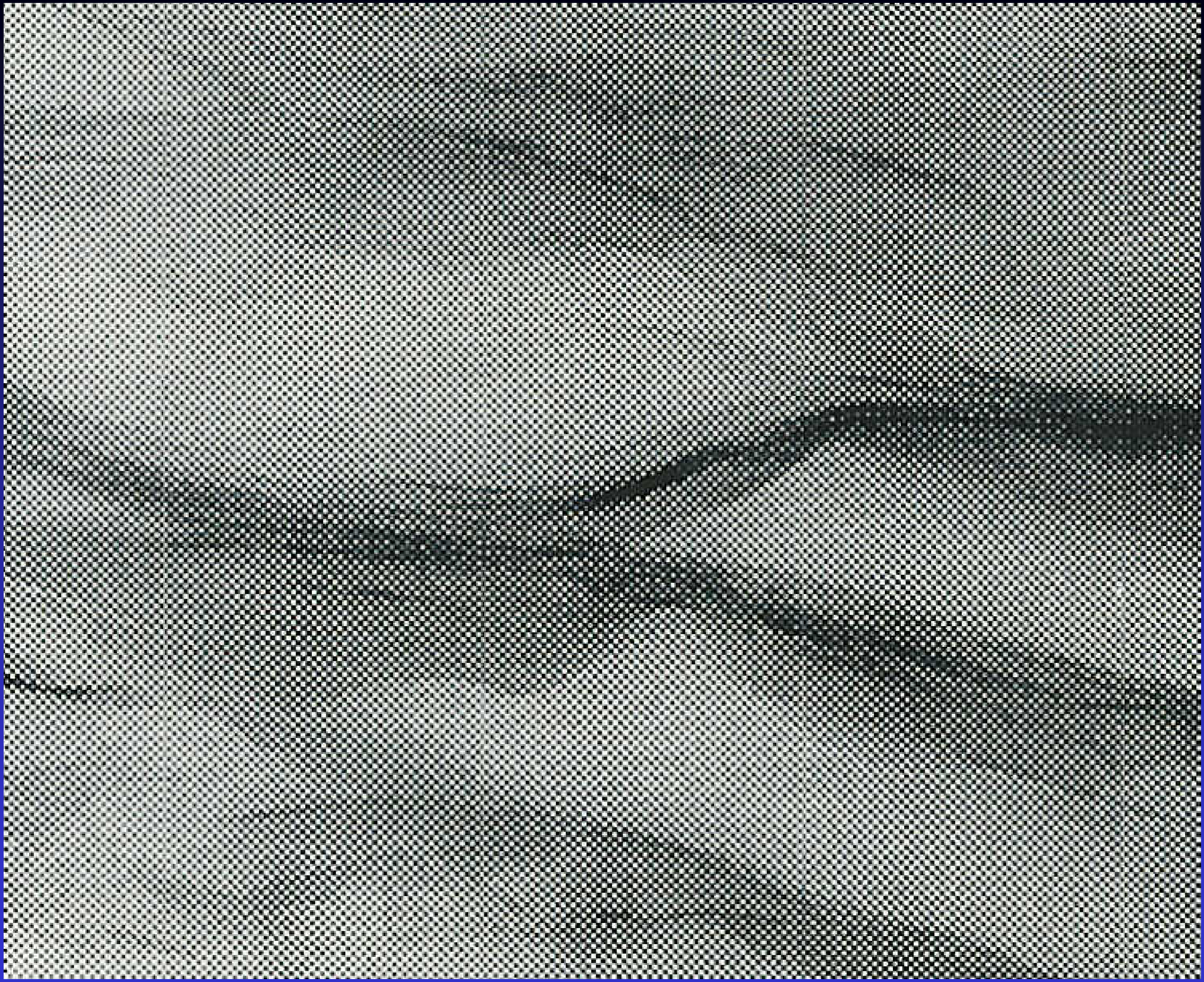

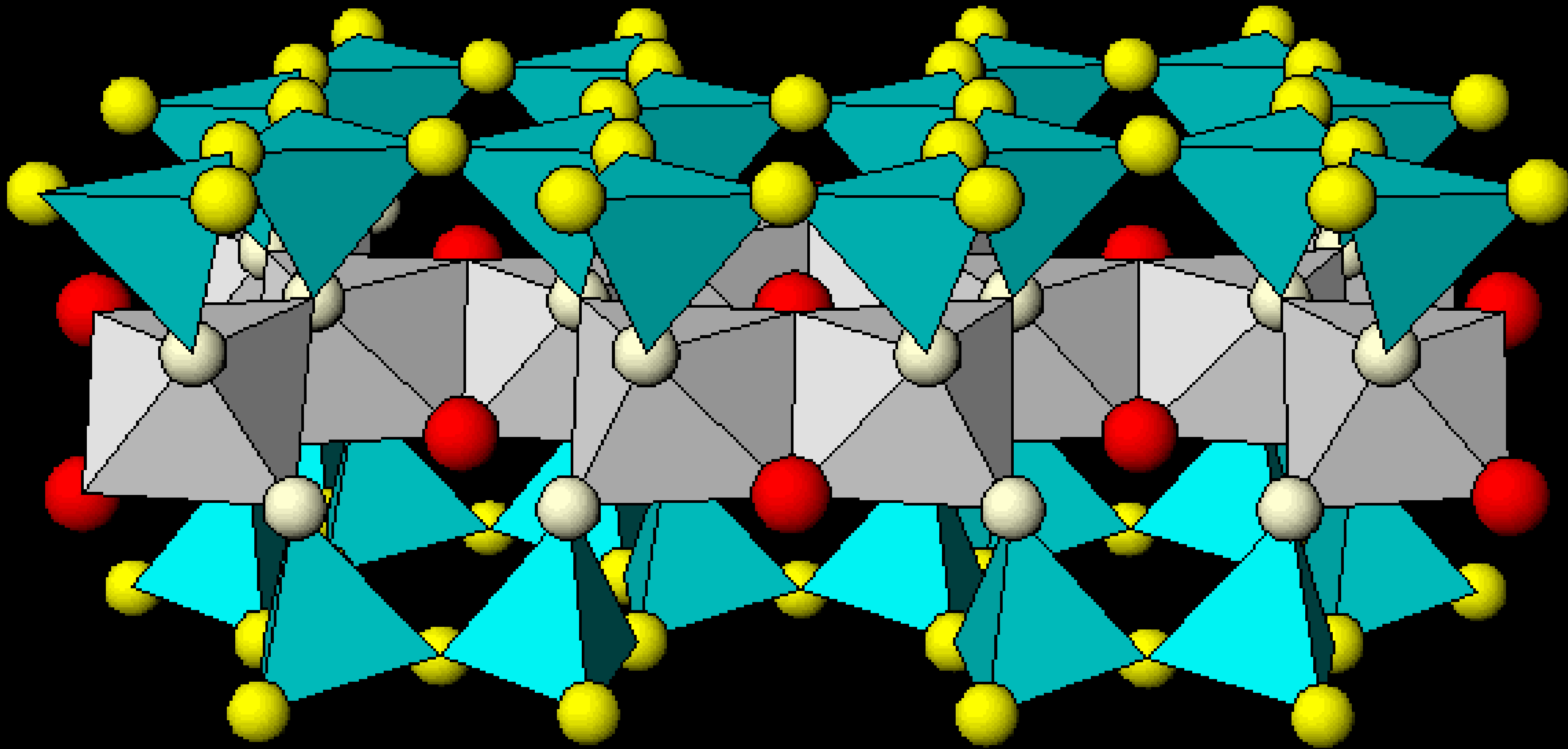

A Single Clay Layer
(2 μm wide x 0.00096 μm thick)

Drawing by Laibin Yan

The Silicon Tetrahedron

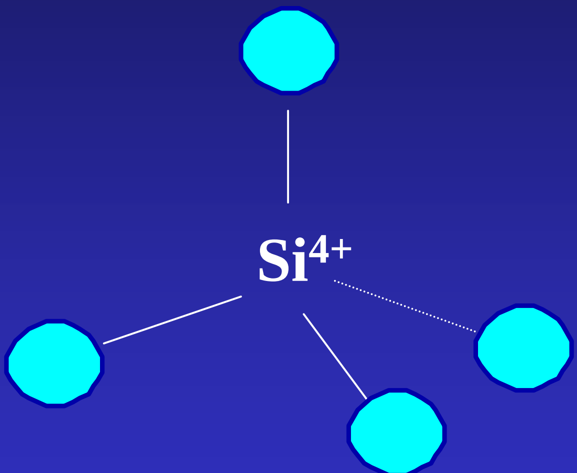

Ball and Stick Model

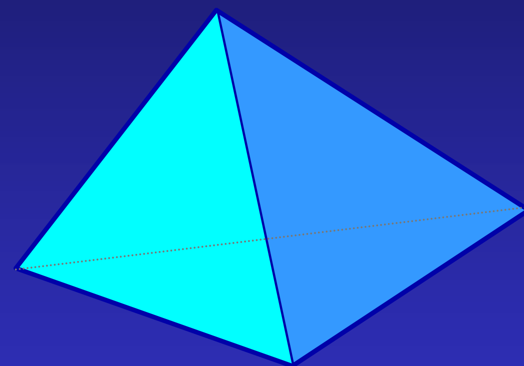

Polyhedral Model

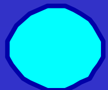 **Oxygen (2-)**

The Aluminum Octahedron

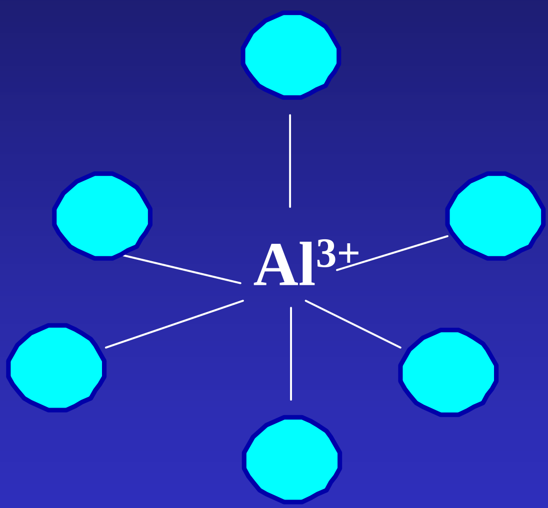

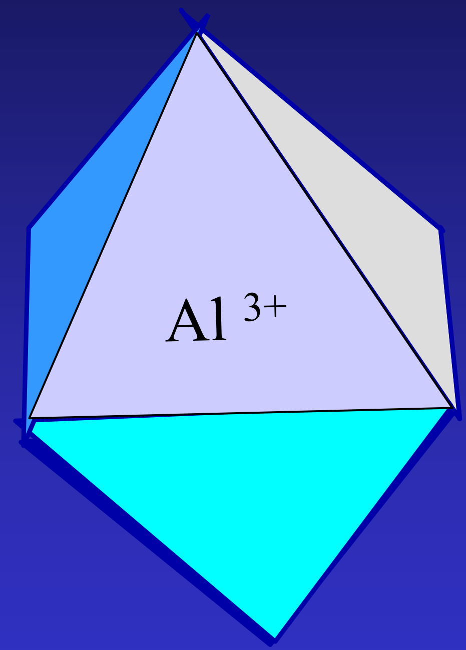

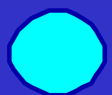

Oxygen (2-)

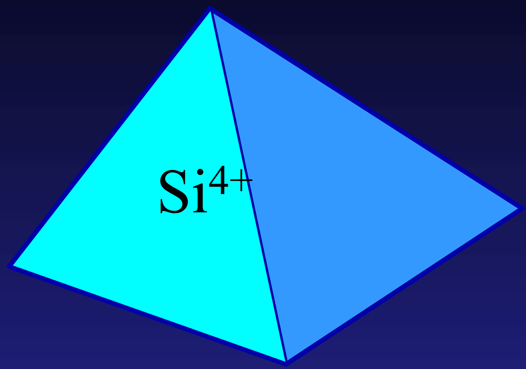

Polyhedral Model

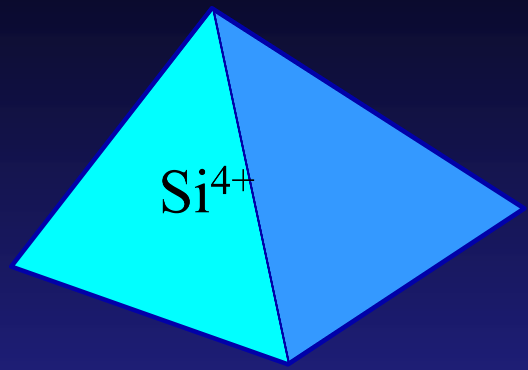

Polyhedral Model

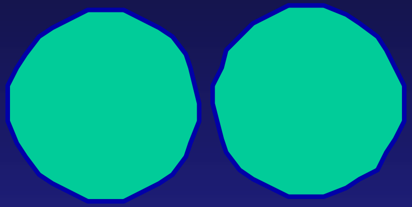

Close-packed Model

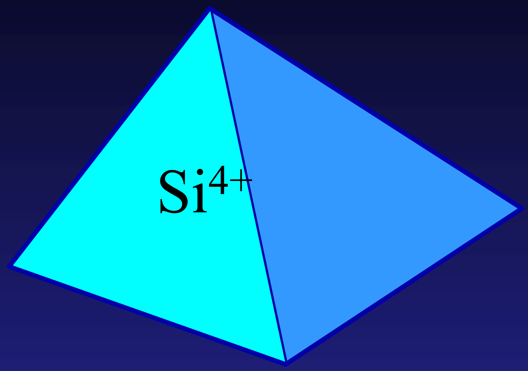

Polyhedral Model

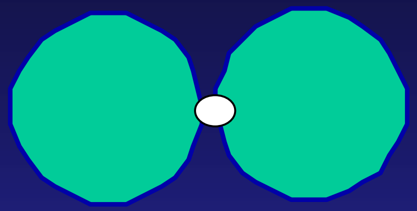

Close-packed Model

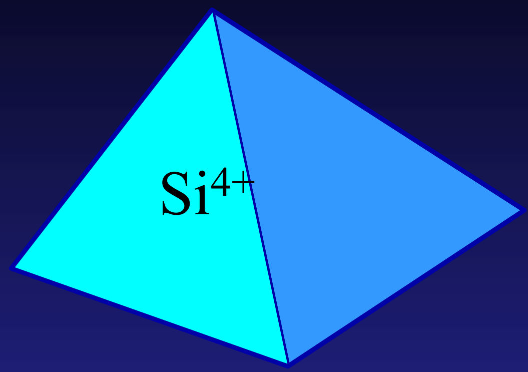

Polyhedral Model

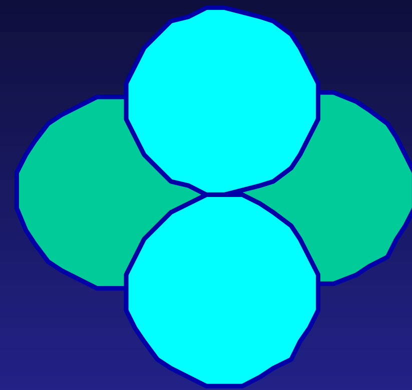

Close-packed Model

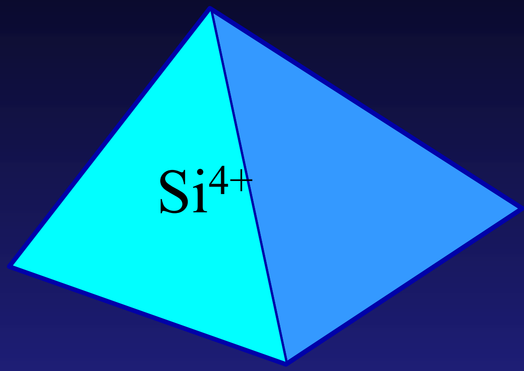

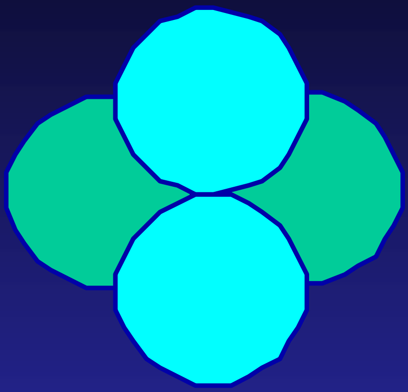

Polyhedral Model

Close-packed Model

Some of the Si^{4+} is sometimes replaced by Al^{3+} or Fe^{3+}

The Aluminum Octahedron

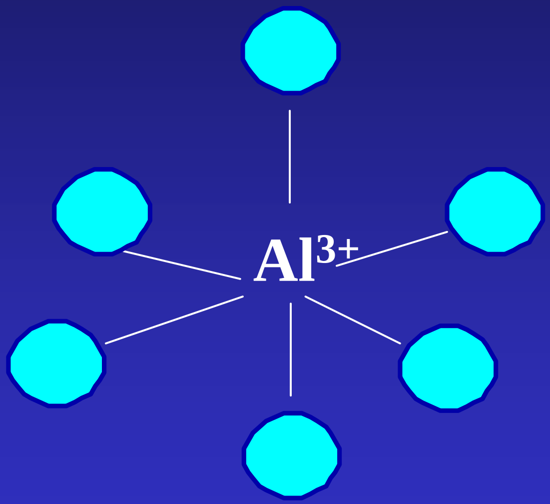

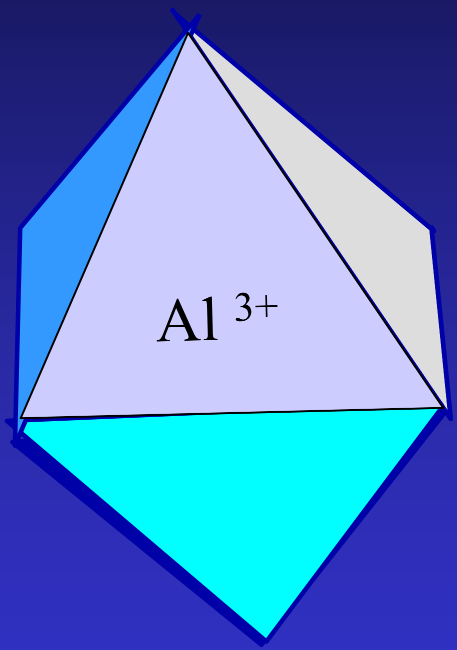

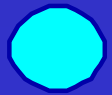 Oxygen (2-)

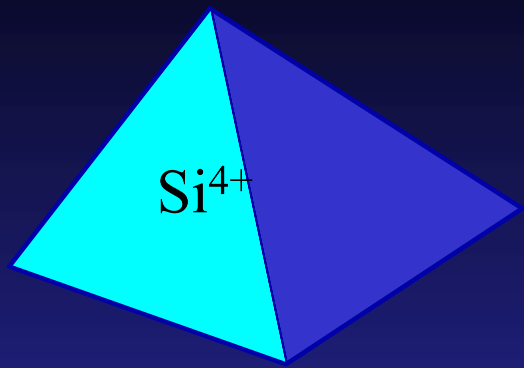

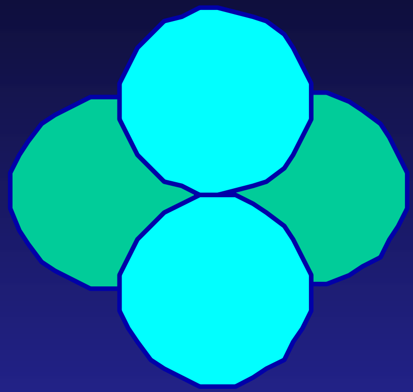

Polyhedral Model

Close-packed Model

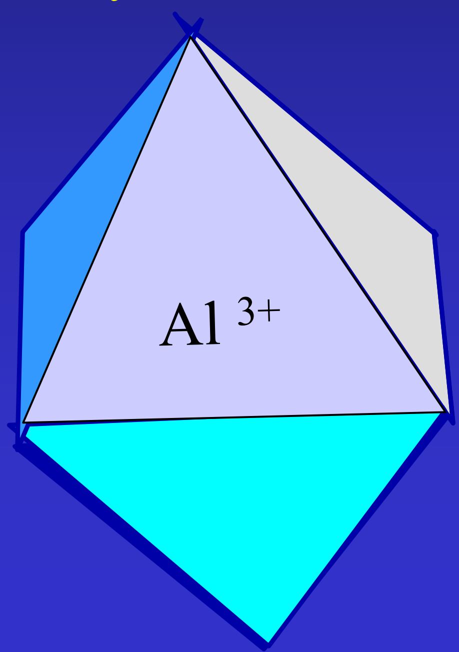

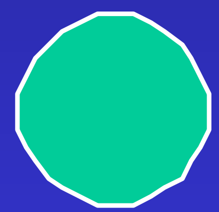

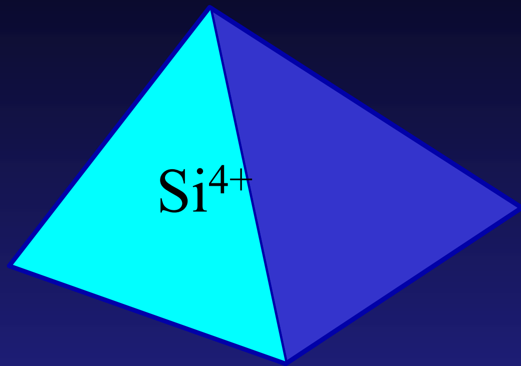

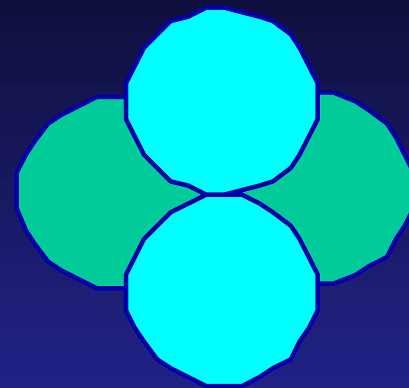

Polyhedral Model

Close-packed Model

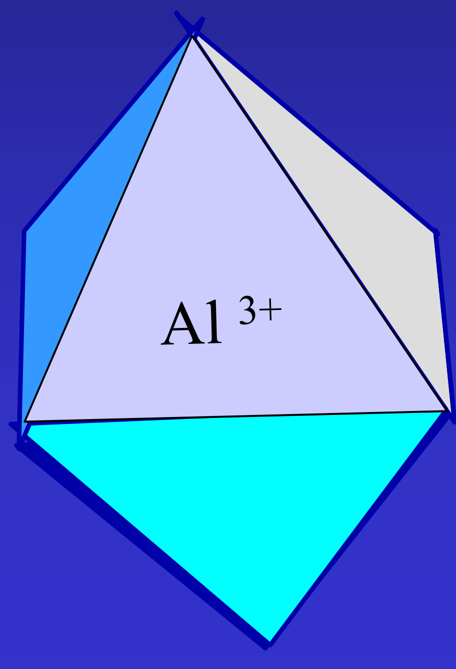

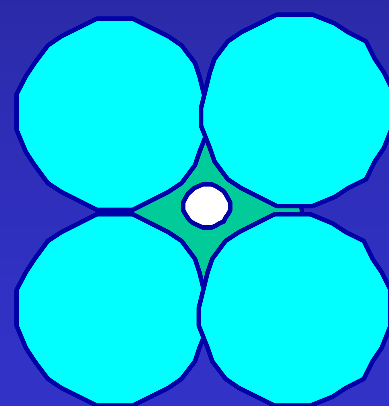

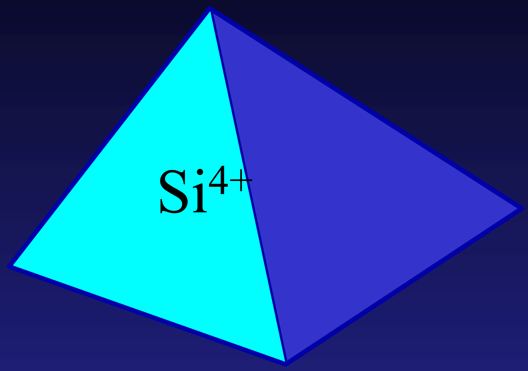

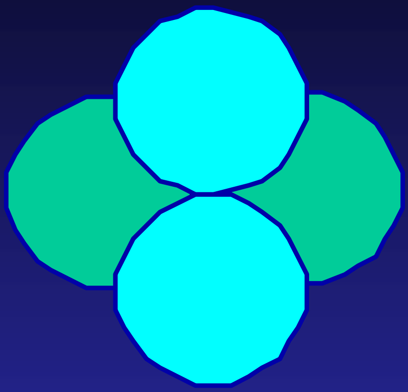

Polyhedral Model

Close-packed Model

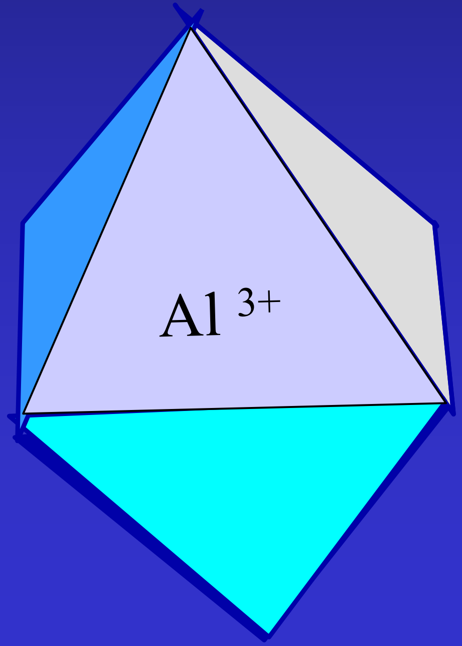

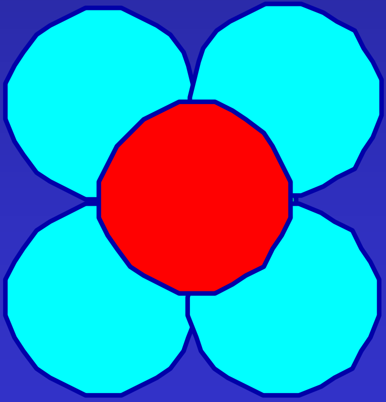

Tetrahedra Join At Corners

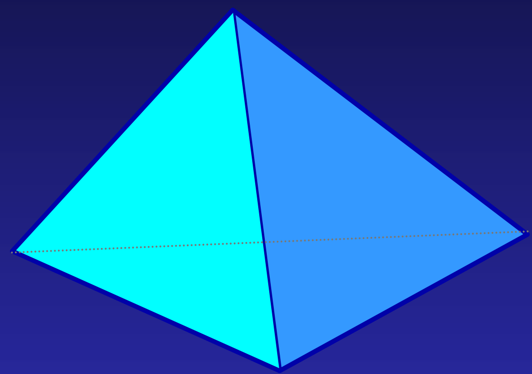

Tetrahedra Join At Corners

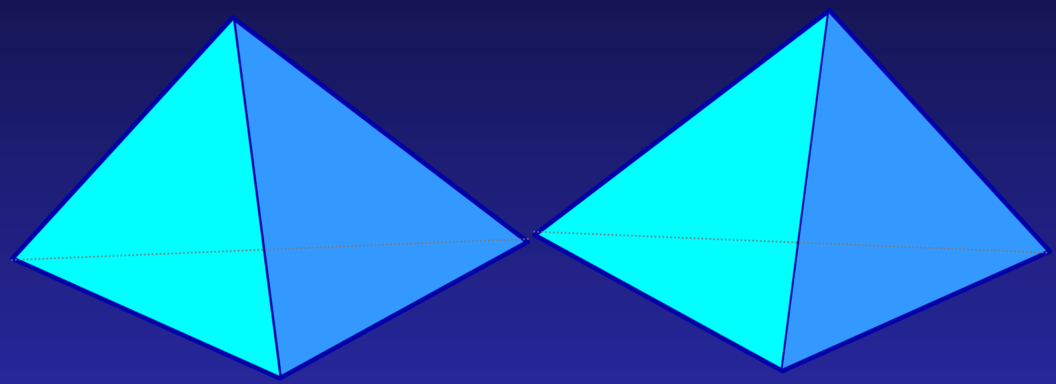

Tetrahedra Join At Corners

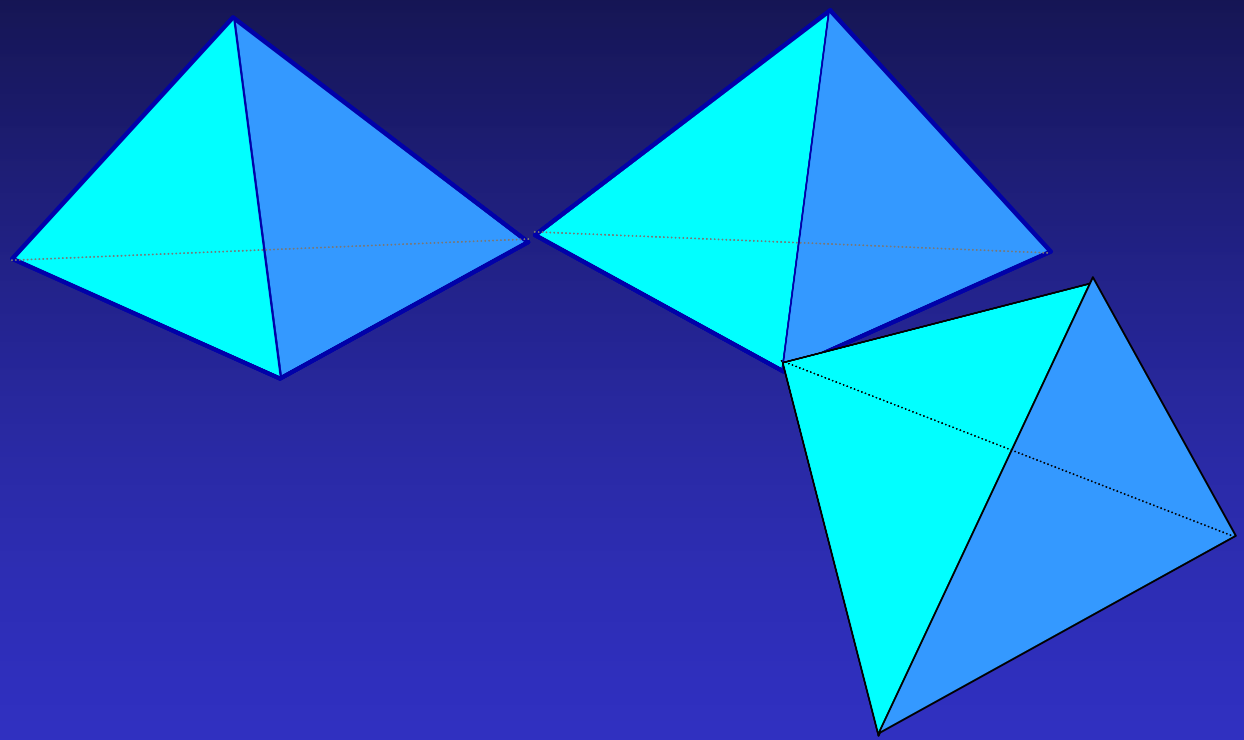

Tetrahedra Join At Corners

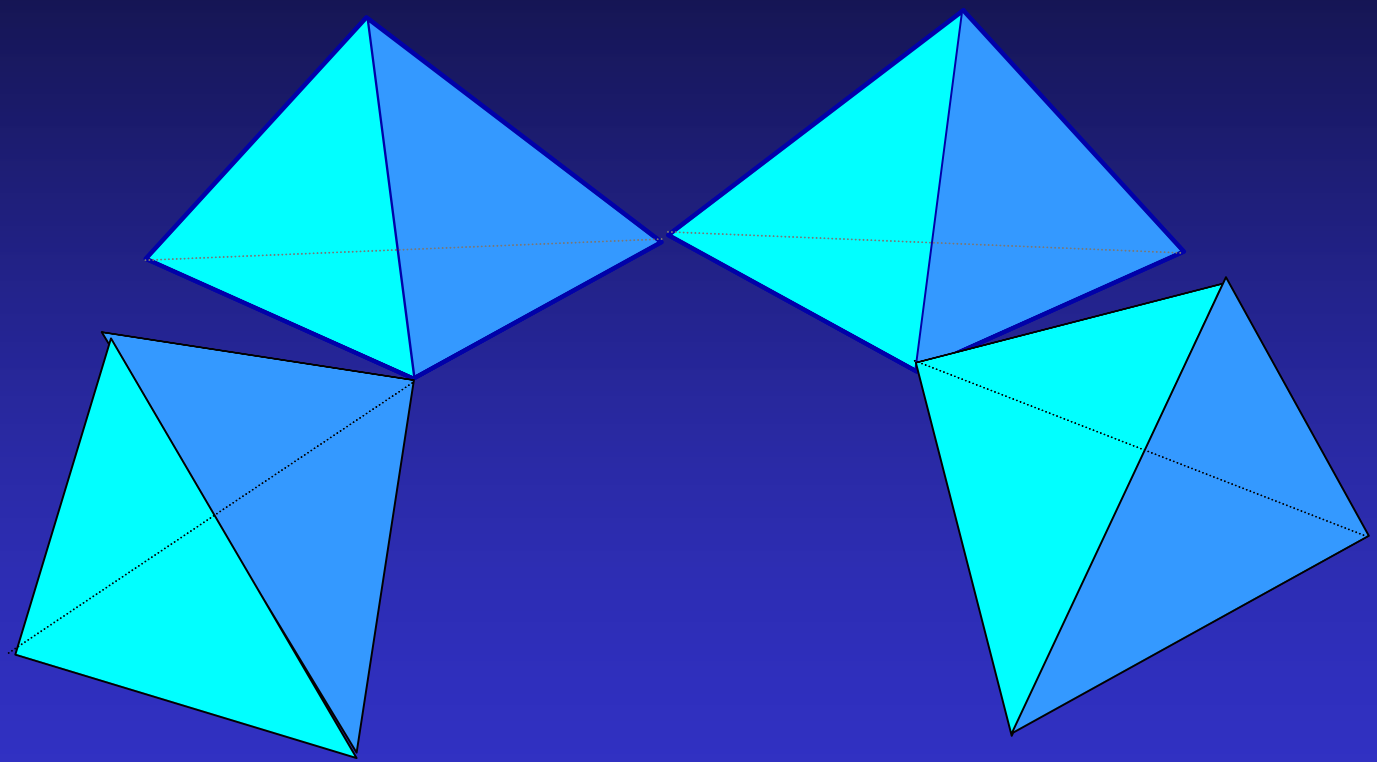

Tetrahedra Join At Corners

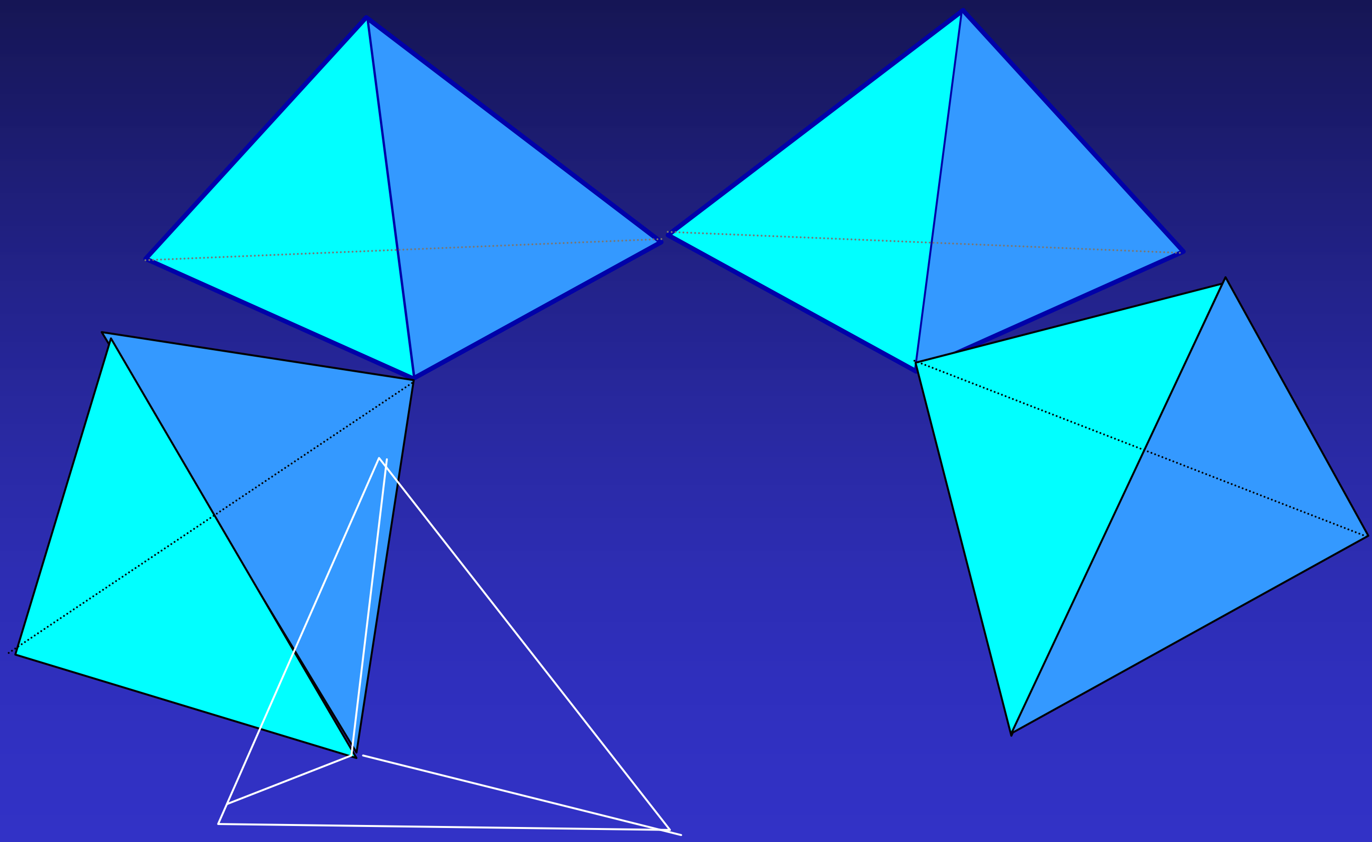

Tetrahedra Join At Corners

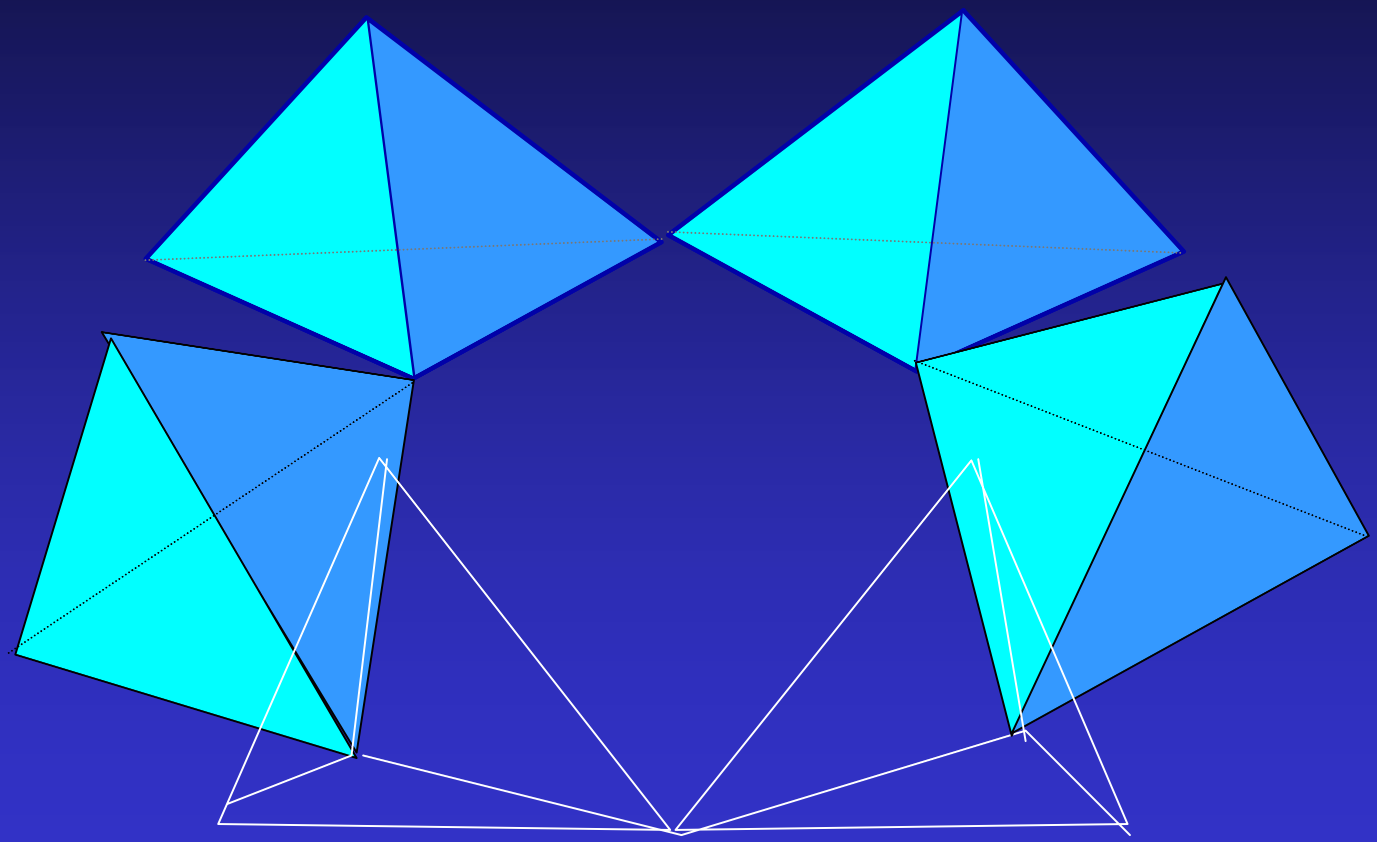

The Aluminum Octahedron

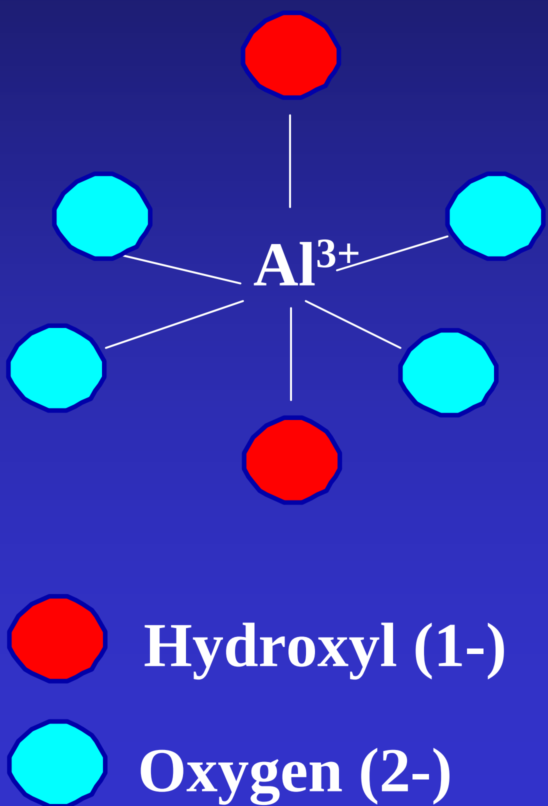

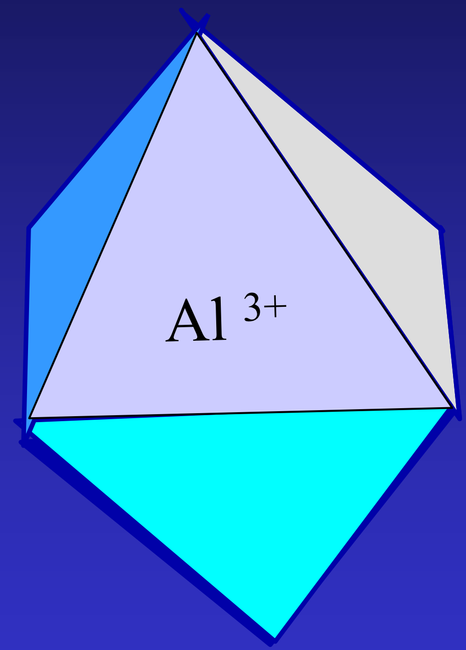

The Aluminum Octahedron

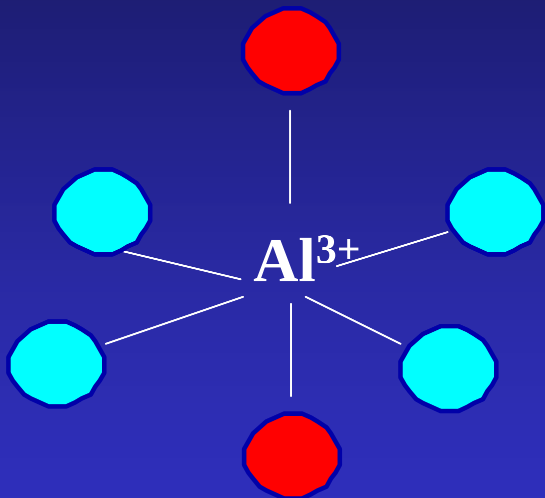

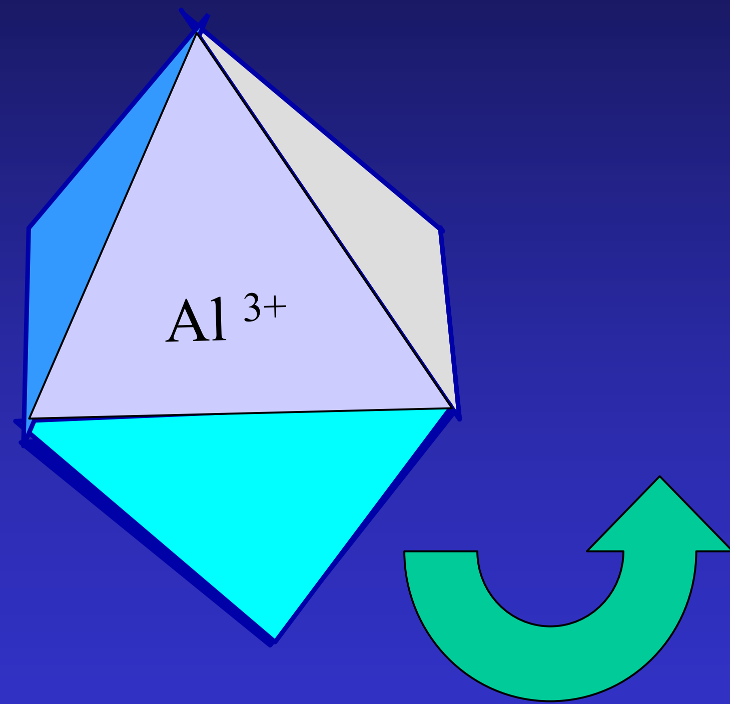

Hydroxyl (1-)

Oxygen (2-)

The Aluminum Octahedron

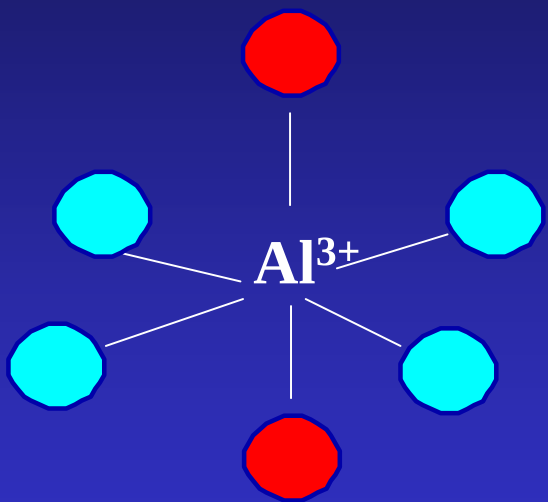

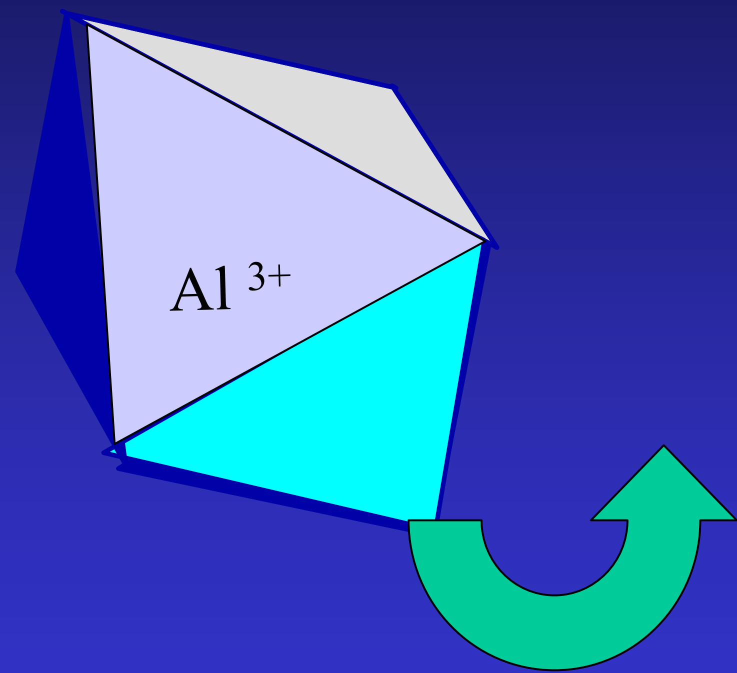

Hydroxyl (1-)

Oxygen (2-)

The Aluminum Octahedron

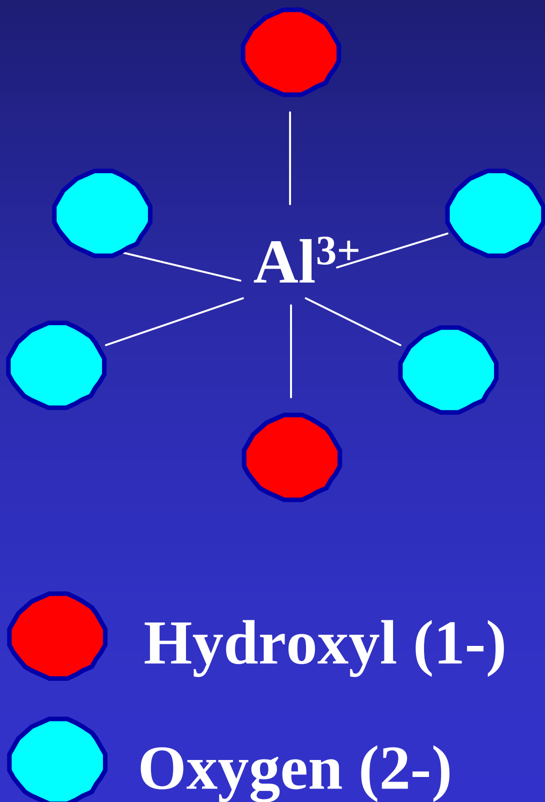

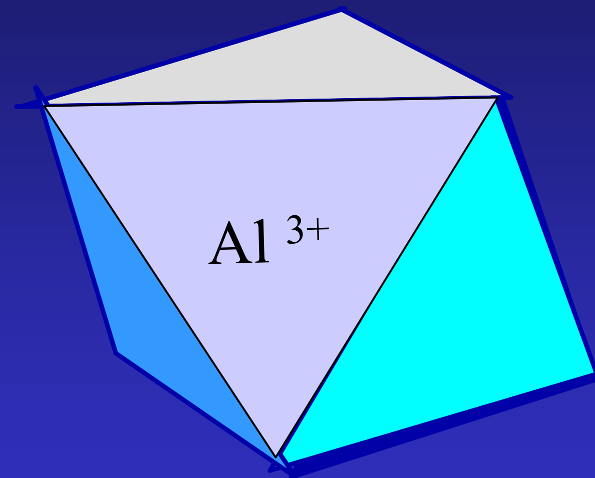

The Aluminum Octahedron

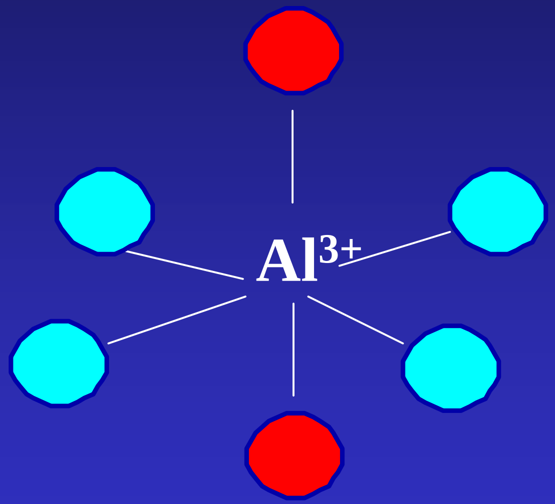

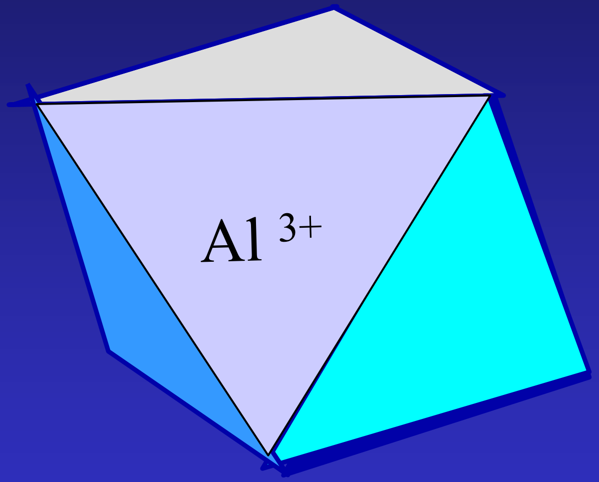

The Al^{3+} can be partially or completely replaced by Mg^{2+}, Fe^{3+}, or Fe^{2+}

Octahedra Join At Edges

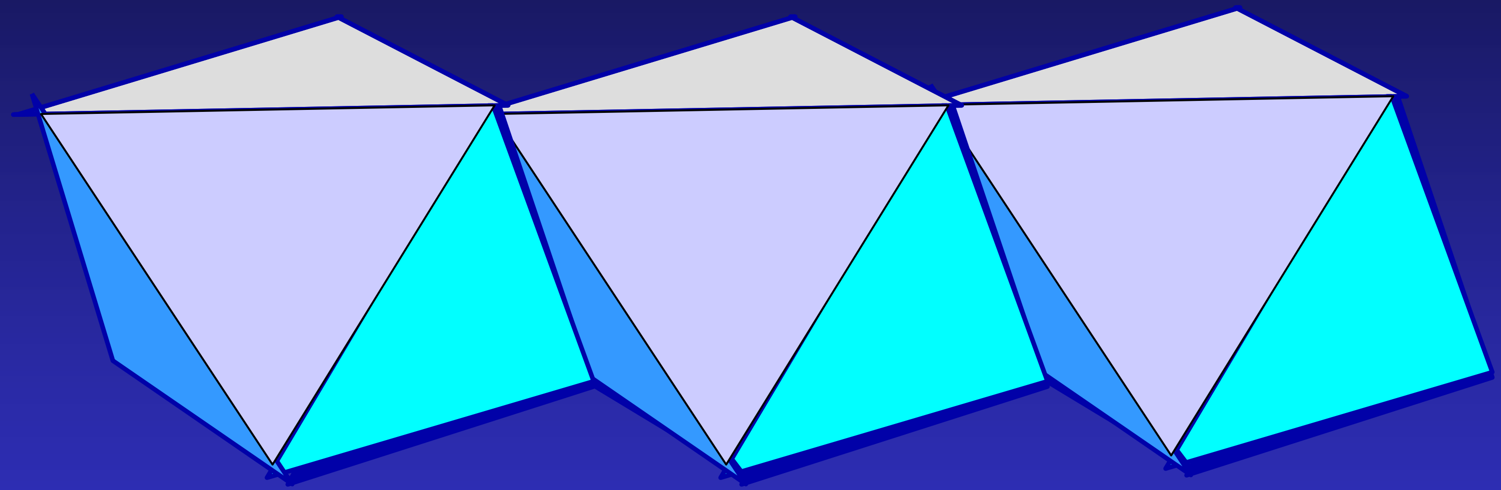

Octahedra Join At Edges

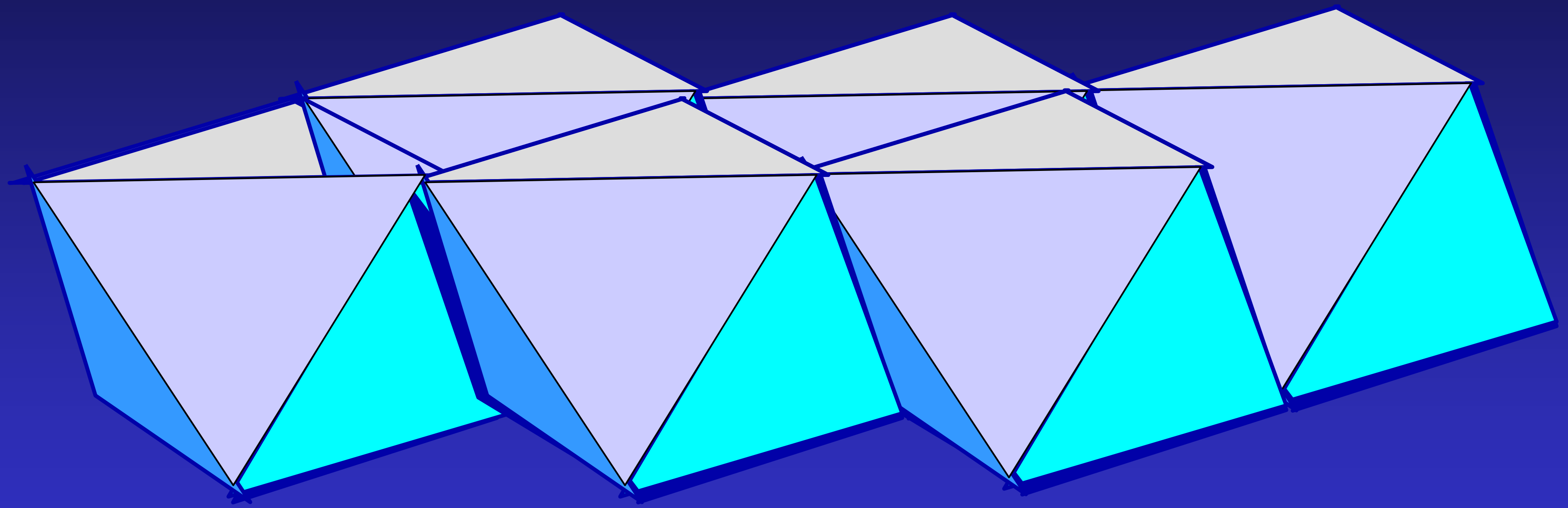

Octahedra Join At Edges

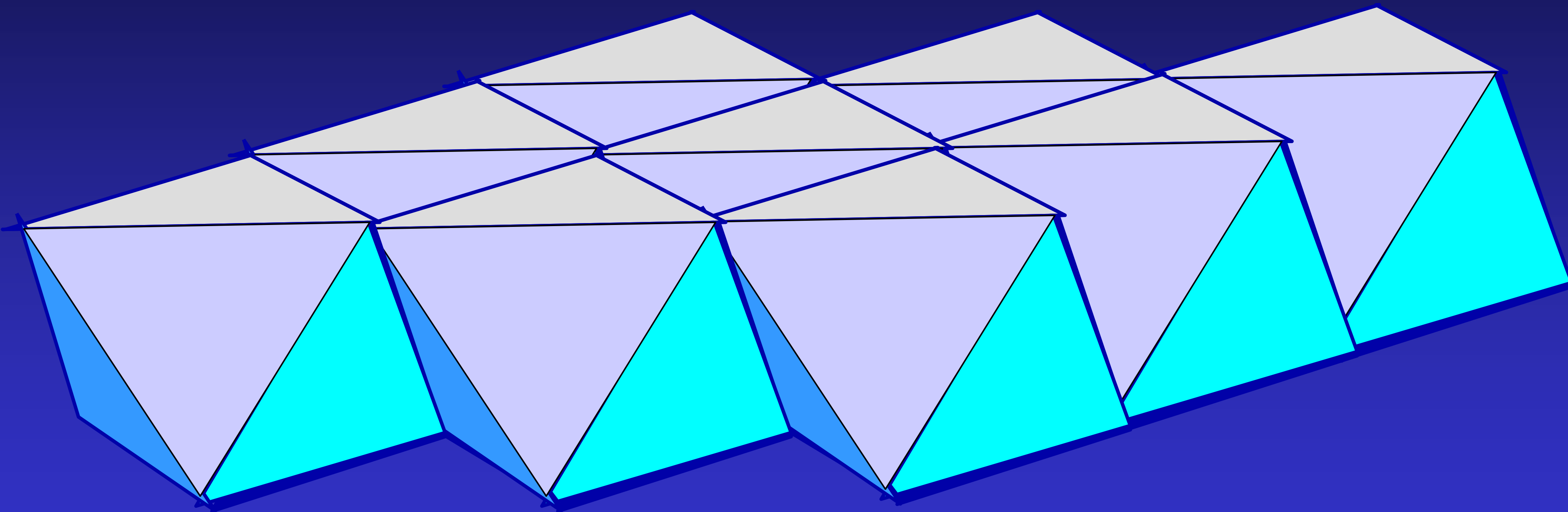

Octahedral Sheet

Combining O_h and T_d Sheets

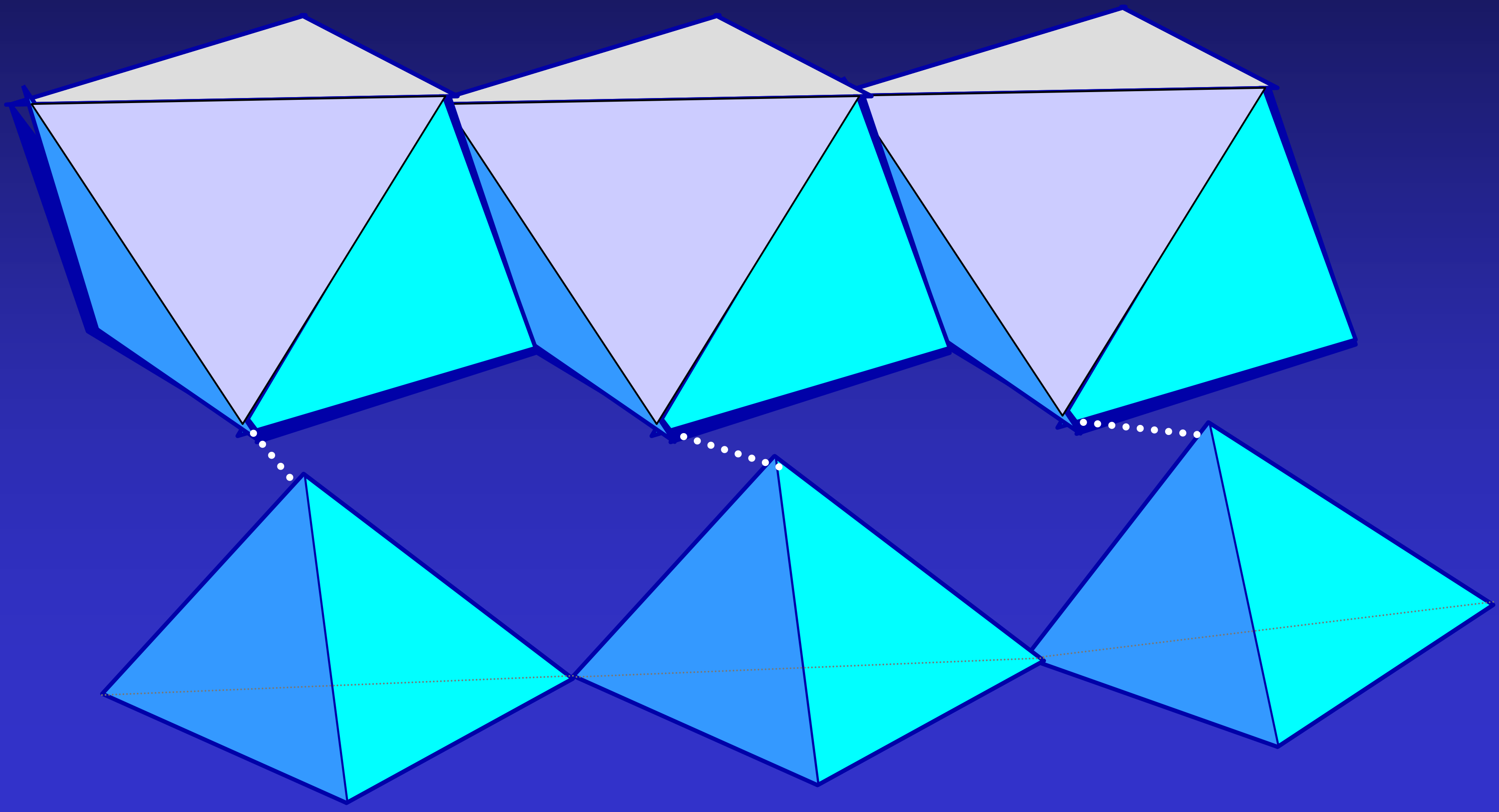

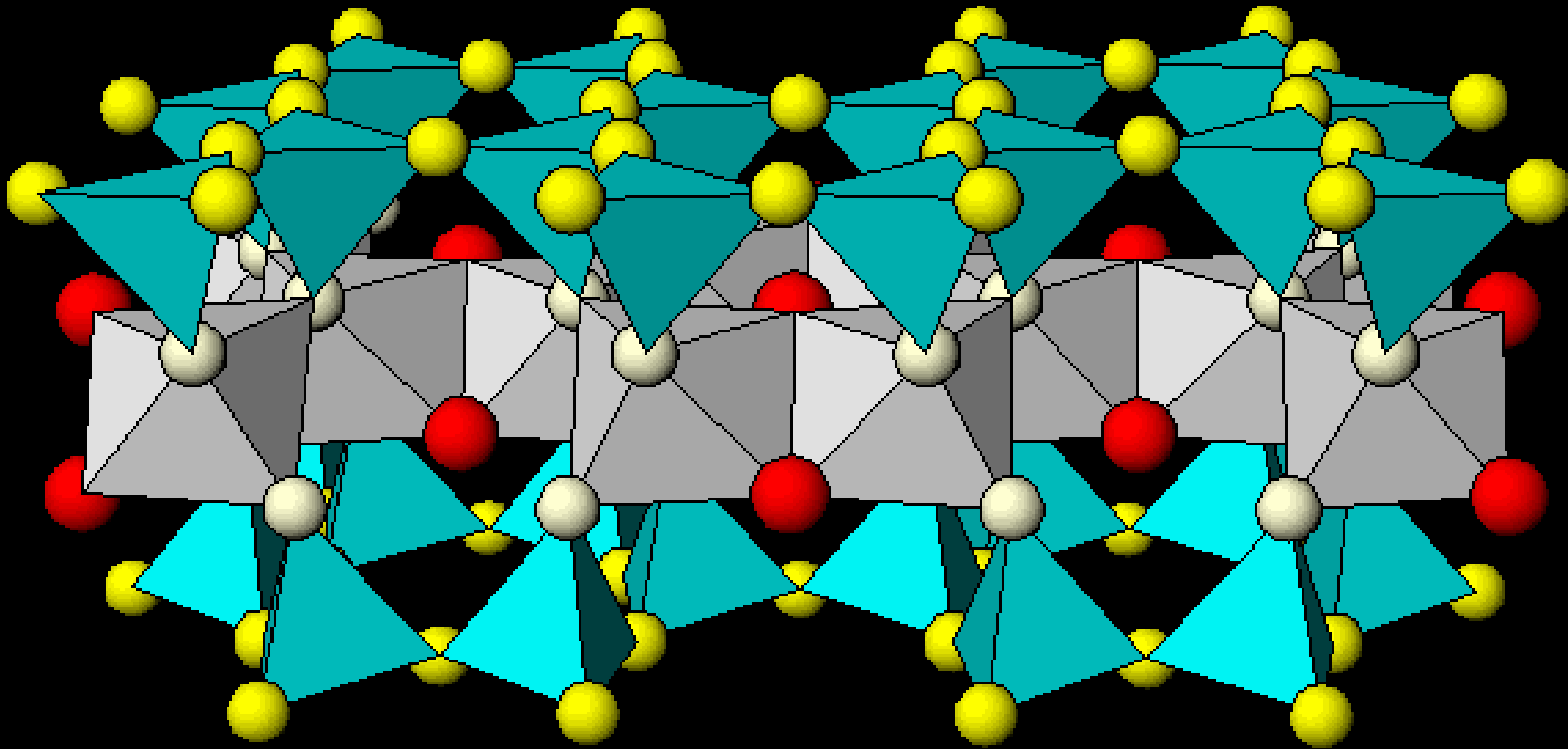

A Single Clay Layer
(2 µm wide x 0.00096 µm thick)

Drawing by Laibin Yan

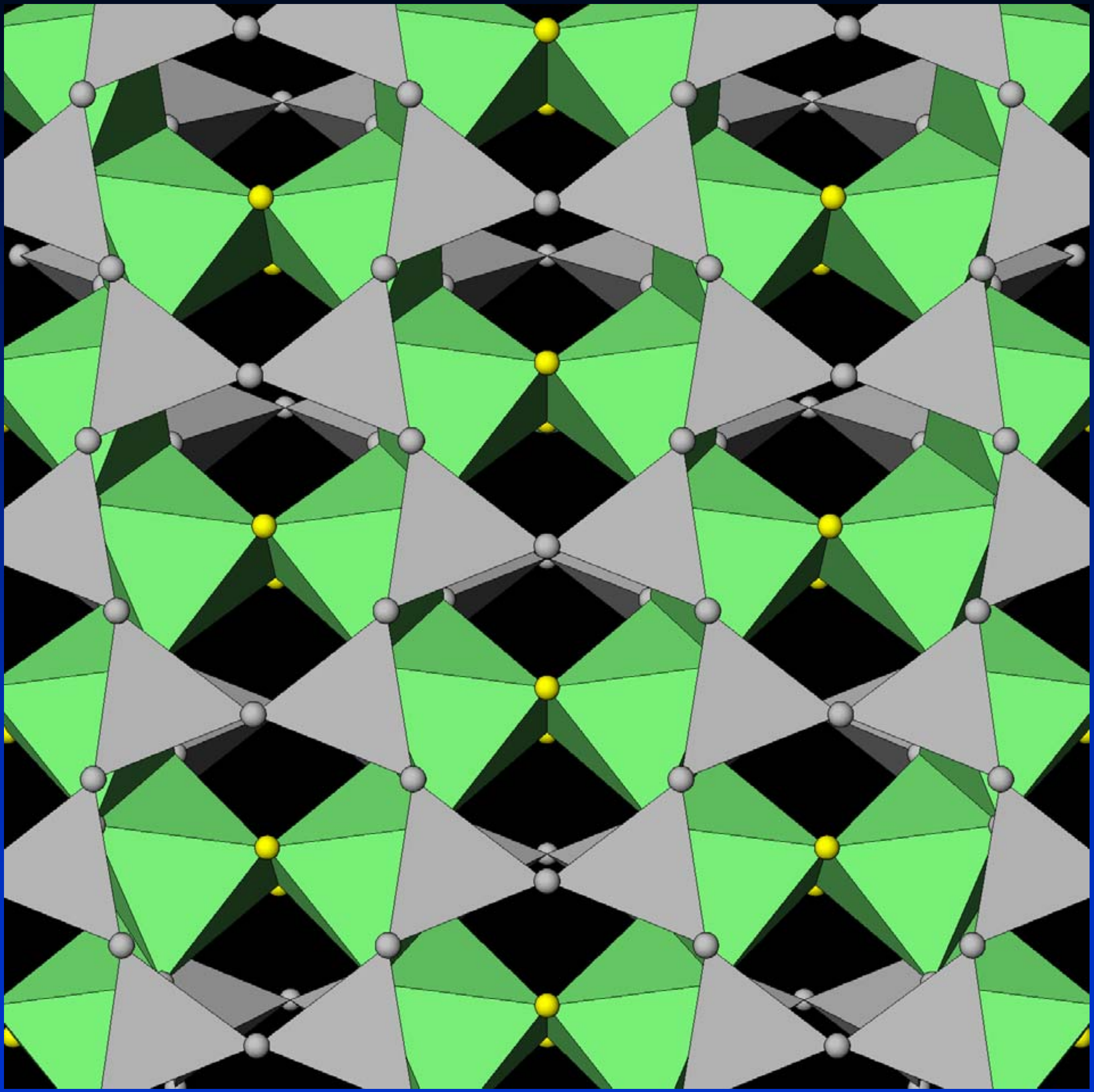

The Layers Stack One Upon Another

Tetrahedral

Octahedral

Tetrahedral

M^{n+}

O^{2-}

Si^{4+}, Fe^{3+}, Al^{3+}

OH^{-}, O^{2-}

Al^{3+}, Mg^{2+}, Fe^{3+}

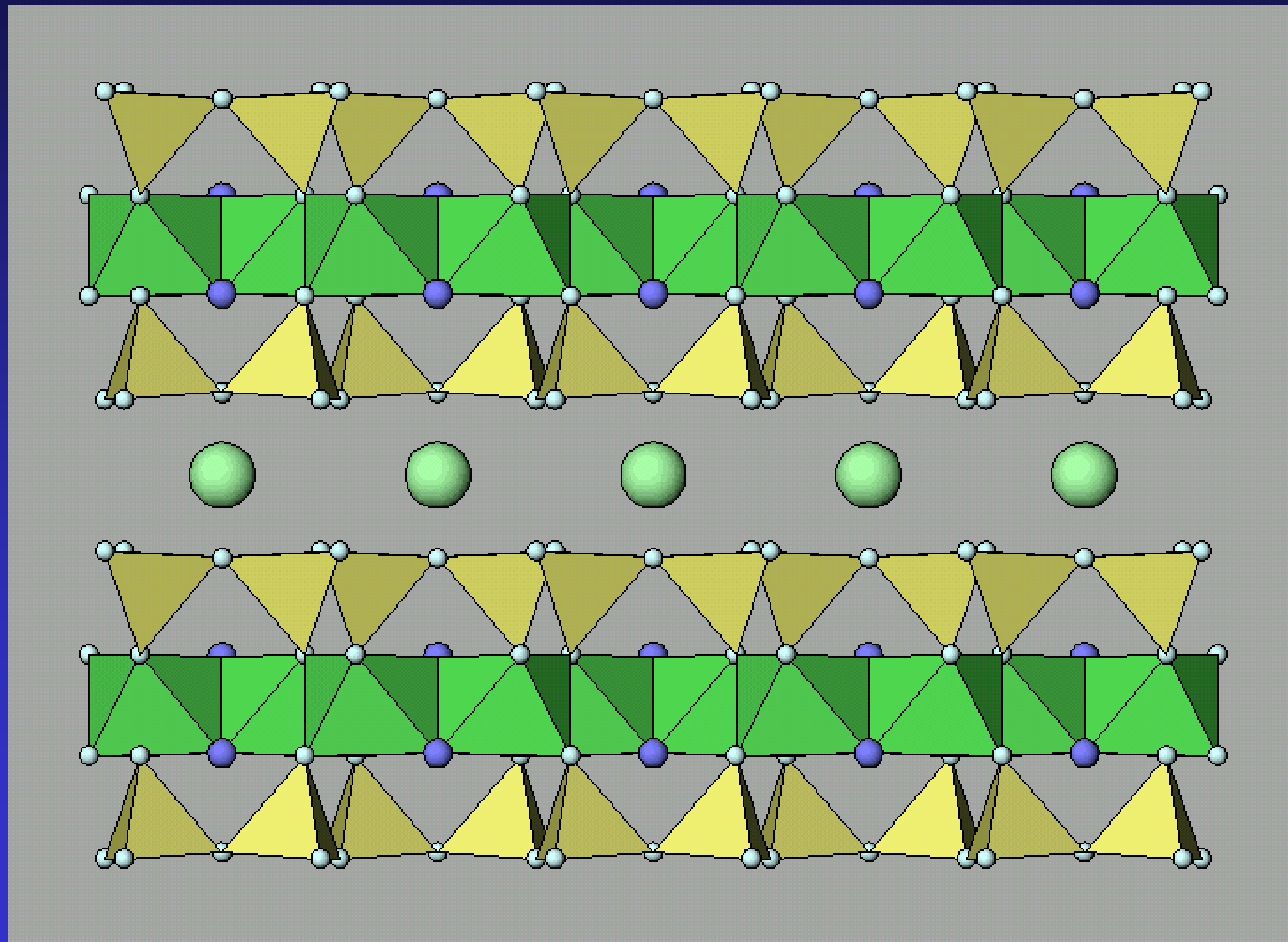

Drawing by Kangwon Lee

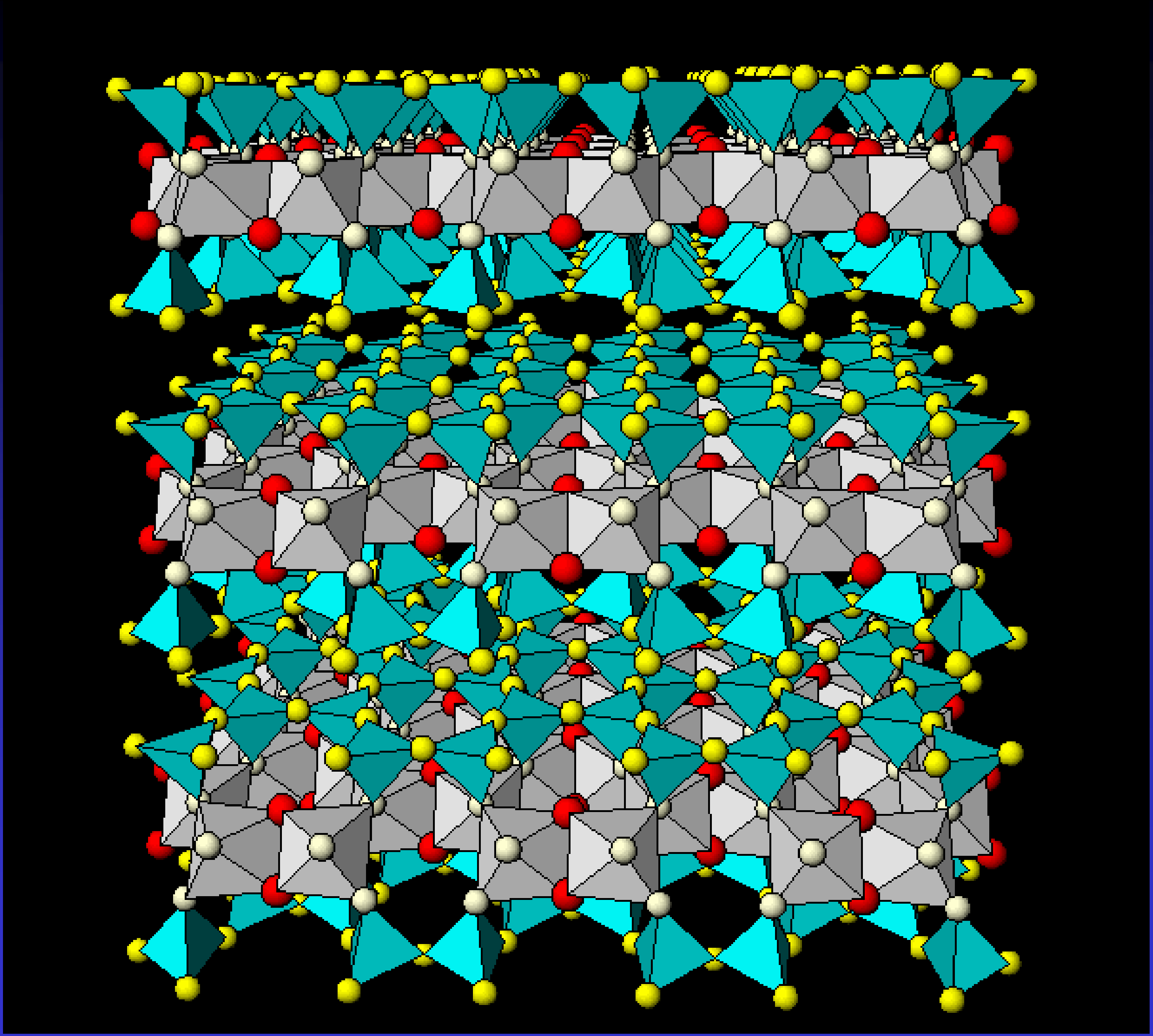

Iron in the Octahedral Sheet Can Be Reduced and Reoxidized

Tetrahedral

Octahedral

Tetrahedral

M^{n+}

O^{2-}

Si^{4+}, Fe^{3+}, Al^{3+}

OH^-, O^{2-}

Al^{3+}, Mg^{2+}, Fe^{3+}

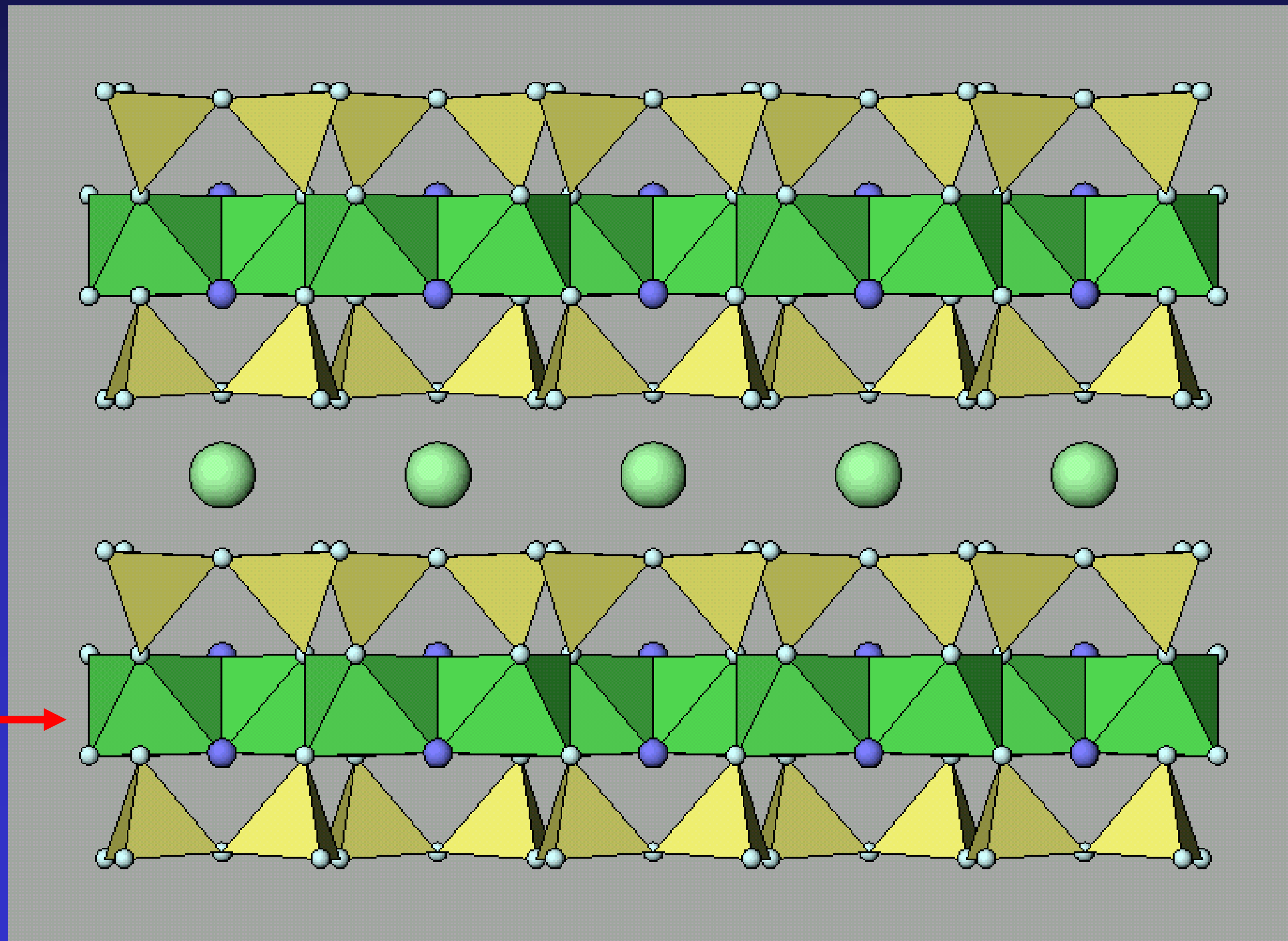

$$Fe^{3+} \rightarrow Fe^{2+}$$

Drawing by Kangwon Lee

Isomorphous Substitution in Clays

Cation	Replacement	**Change in Charge**
Al^{3+}	Fe^{3+}	**0**
Al^{3+}	Mg^{2+}	**-1**
Al^{3+}	Fe^{2+}	**-1**
Fe^{3+}	Fe^{2+}	**-1**
Si^{4+}	Al^{3+}	**-1**
Si^{4+}	Fe^{3+}	**-1**

Exchanged Cations Neutralize Isomorphous Substitution

Tetrahedral

Octahedral

Tetrahedral

M^{n+}

O^{2-}

Si^{4+}, Fe^{3+}, Al^{3+}

OH^-, O^{2-}

Al^{3+}, Mg^{2+}, Fe^{3+}

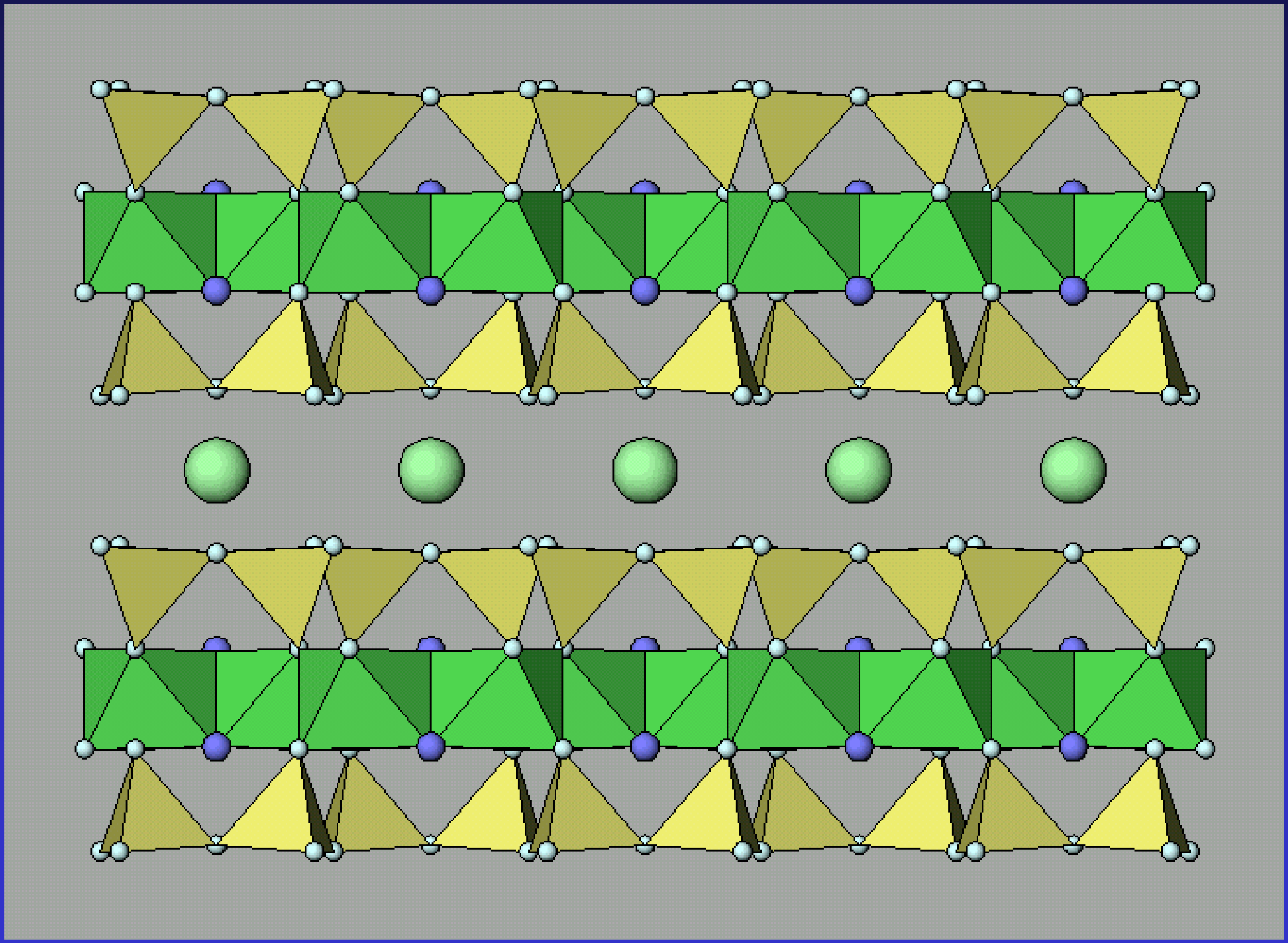

Drawing by Kangwon Lee

The Interlayer Region Is A Rich Chemical Environment

Tetrahedral

Octahedral

Tetrahedral

M^{n+}

O^{2-}

Si^{4+}, Fe^{3+}, Al^{3+}

OH^{-}, O^{2-}

Al^{3+}, Mg^{2+}, Fe^{3+}

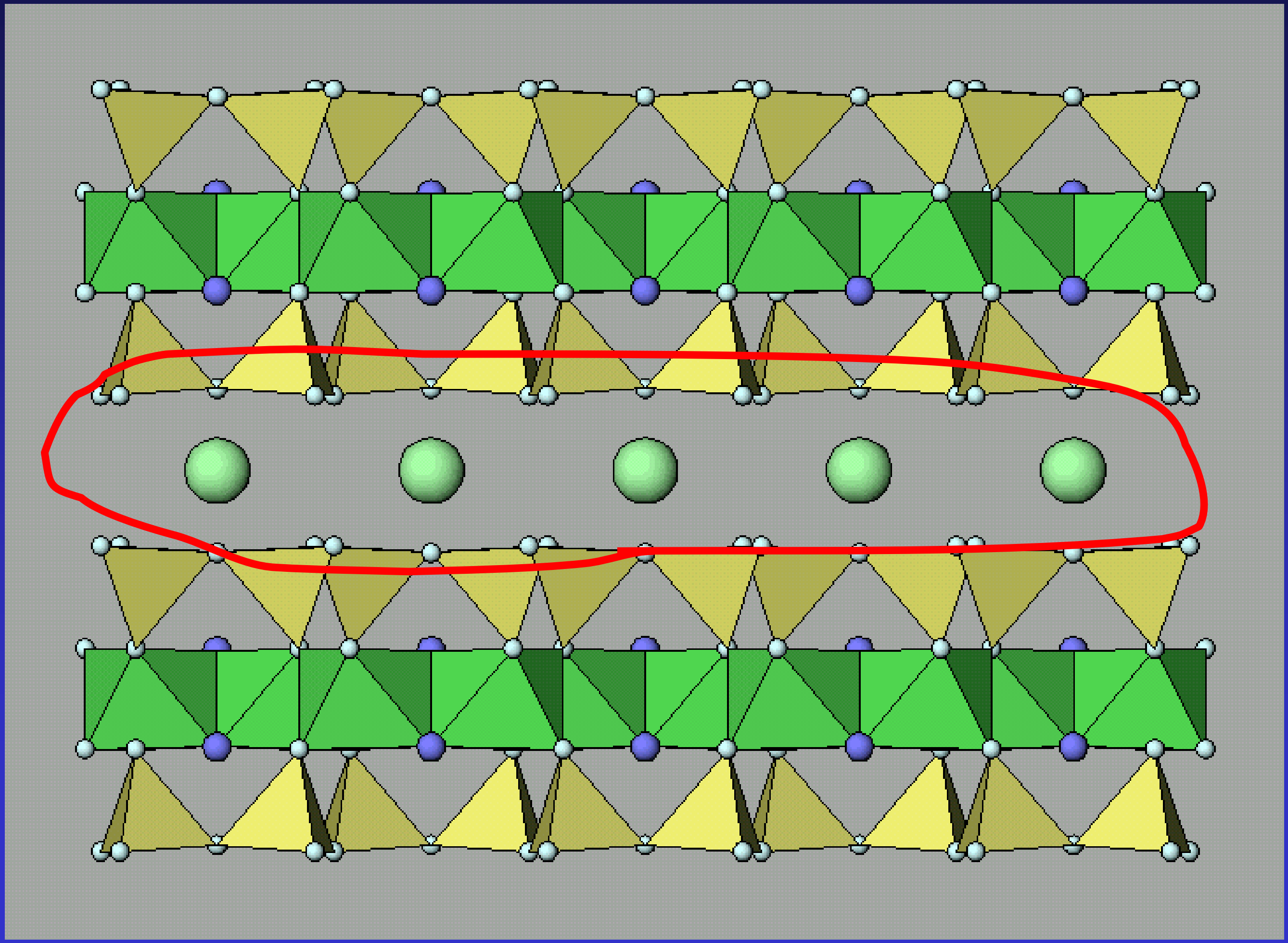

Drawing by Kangwon Lee

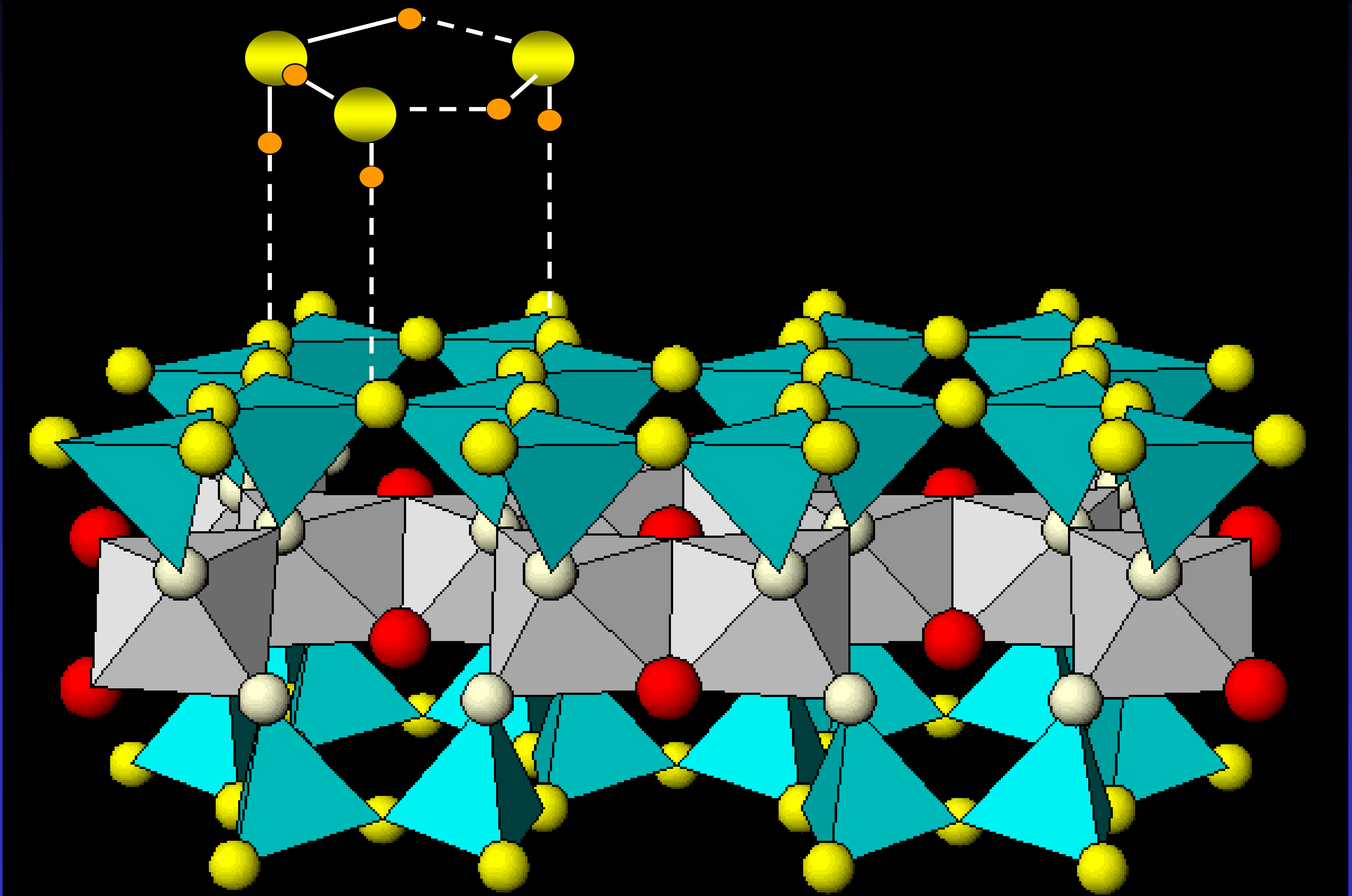

Iron Reduction Has Large Effect on Chemical Activity in the Interlayer

Tetrahedral

Octahedral

Tetrahedral

M^{n+}

O^{2-}

Si^{4+}, Fe^{3+}, Al^{3+}

OH^-, O^{2-}

Al^{3+}, Mg^{2+}, Fe^{3+}

$$Fe^{3+} \rightarrow Fe^{2+}$$

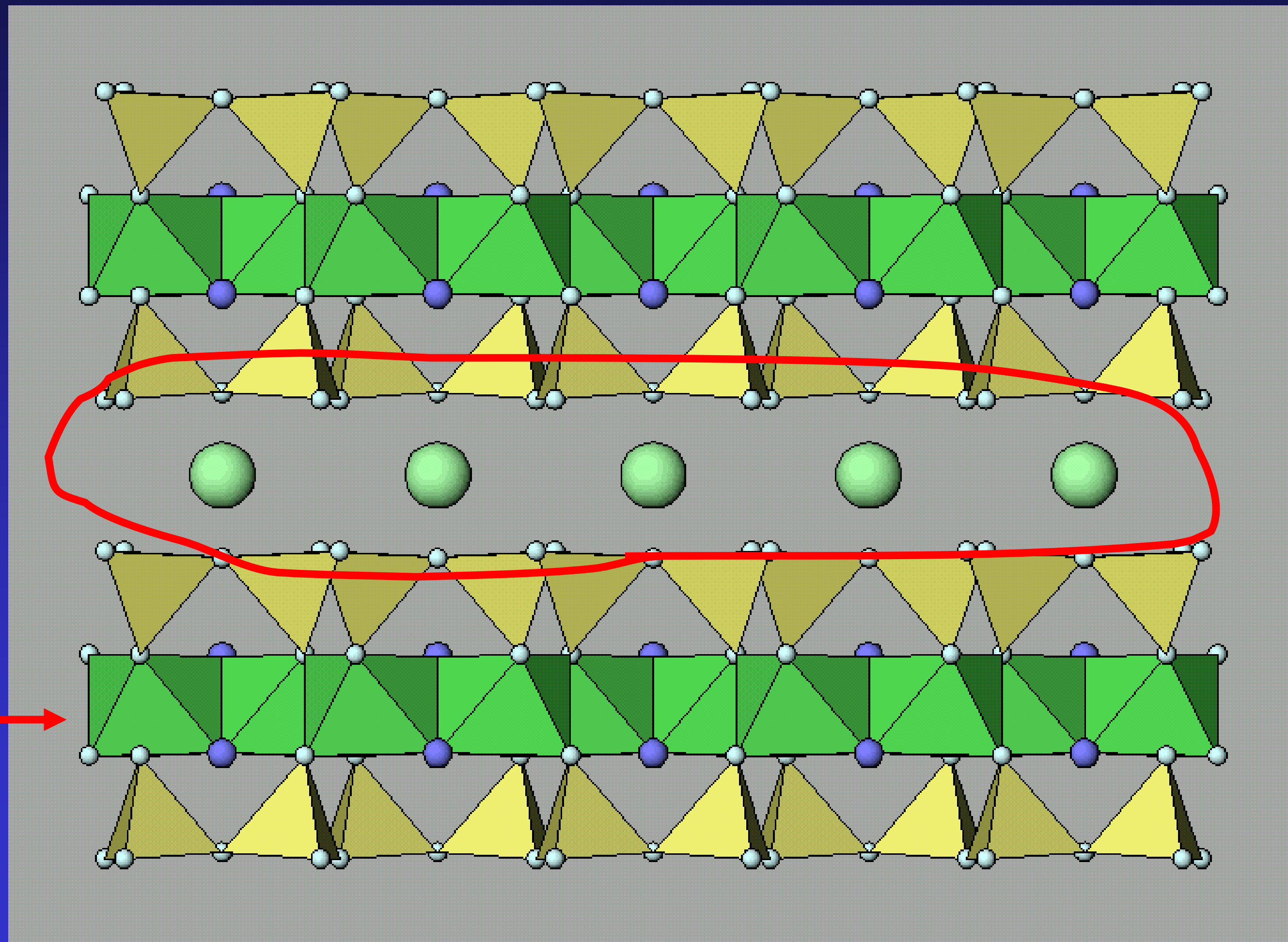

Drawing by Kangwon Lee

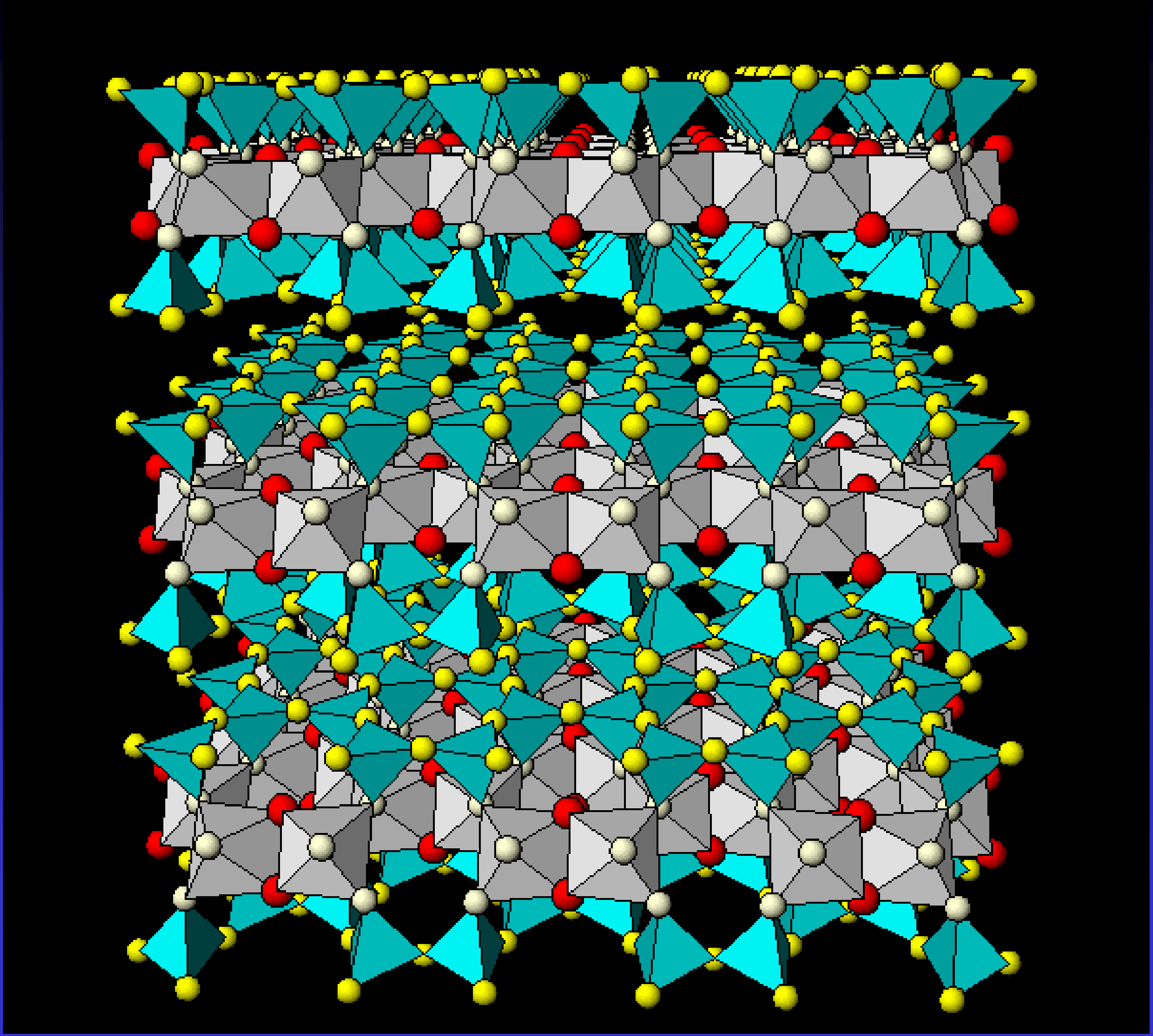

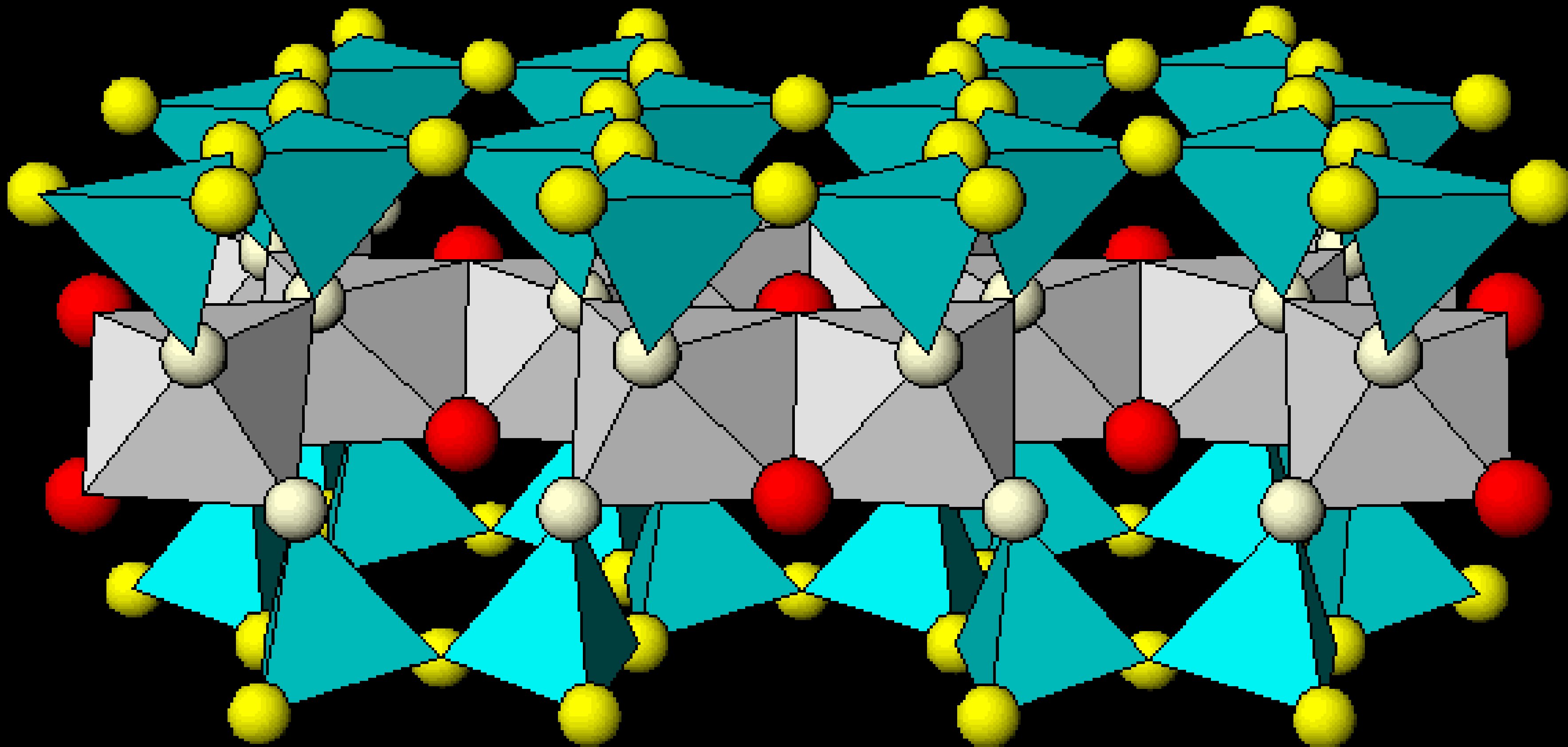

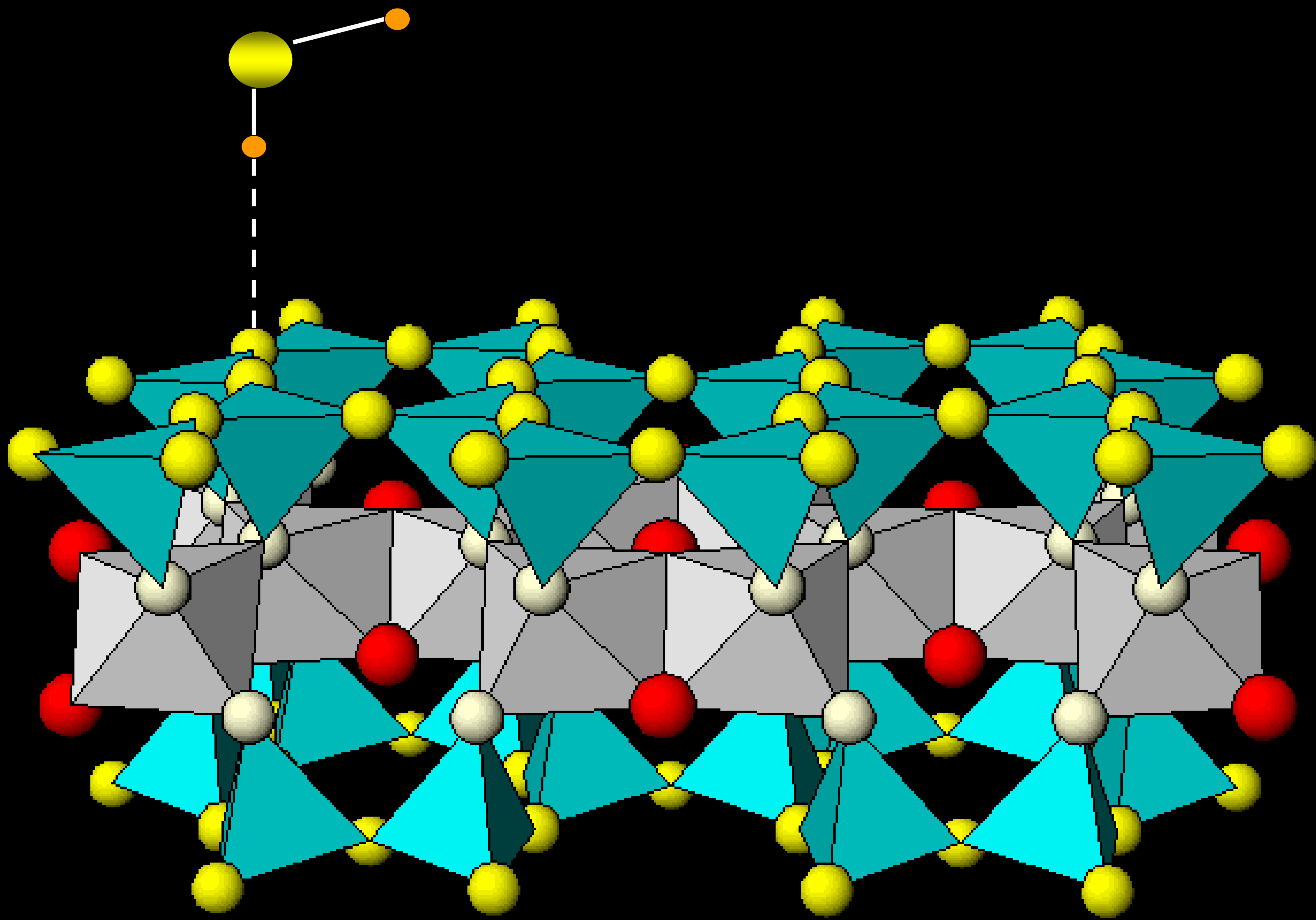

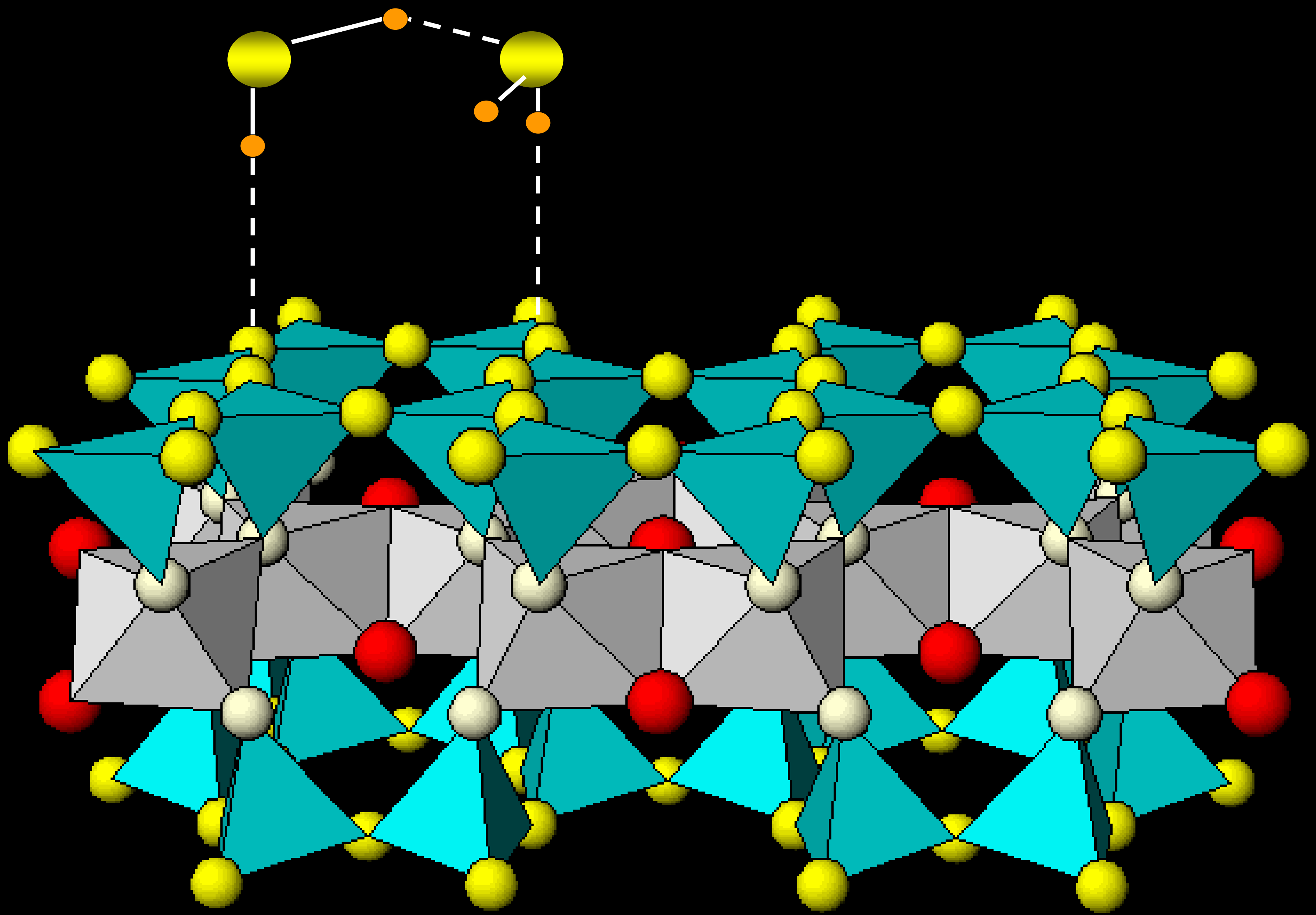

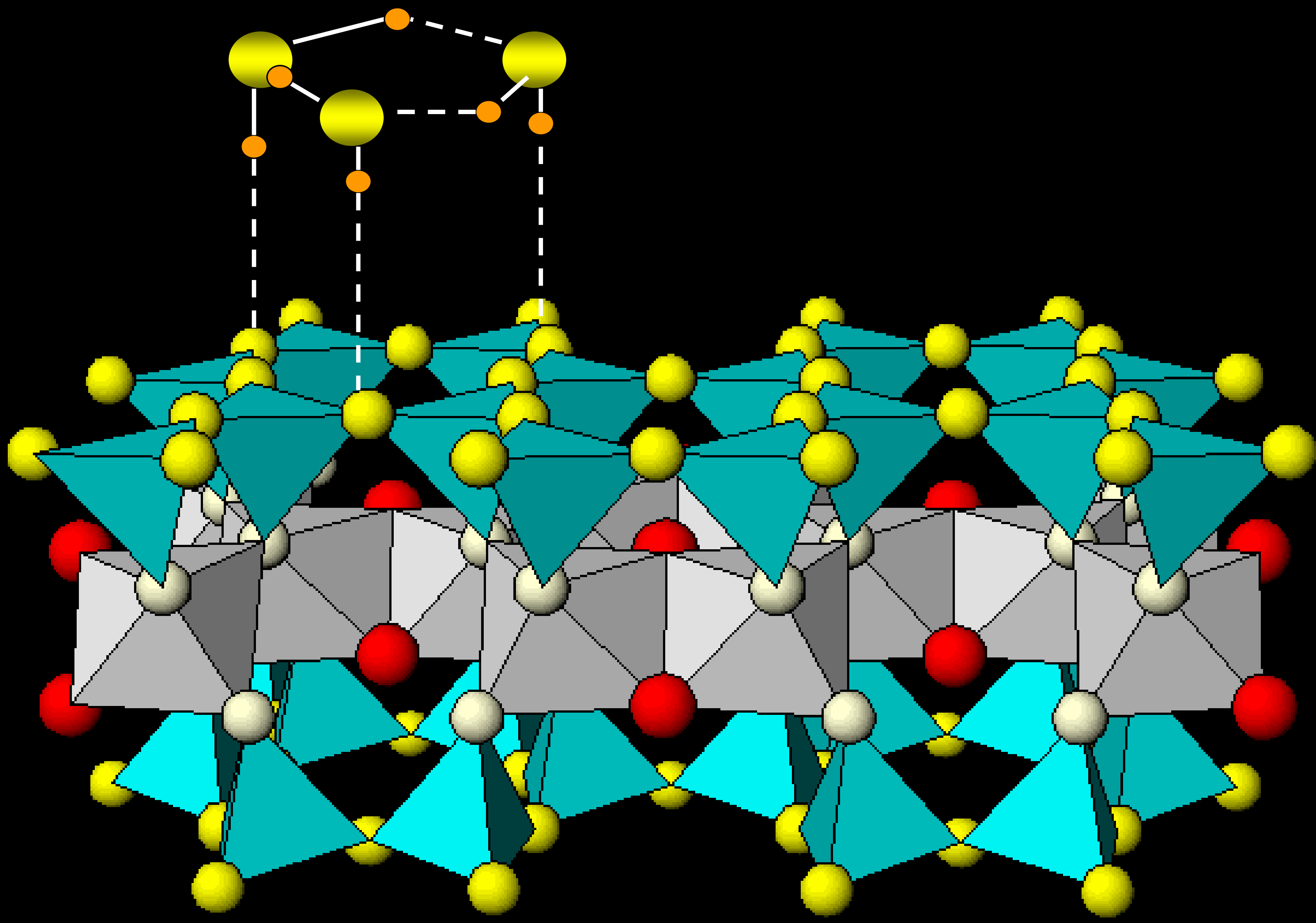

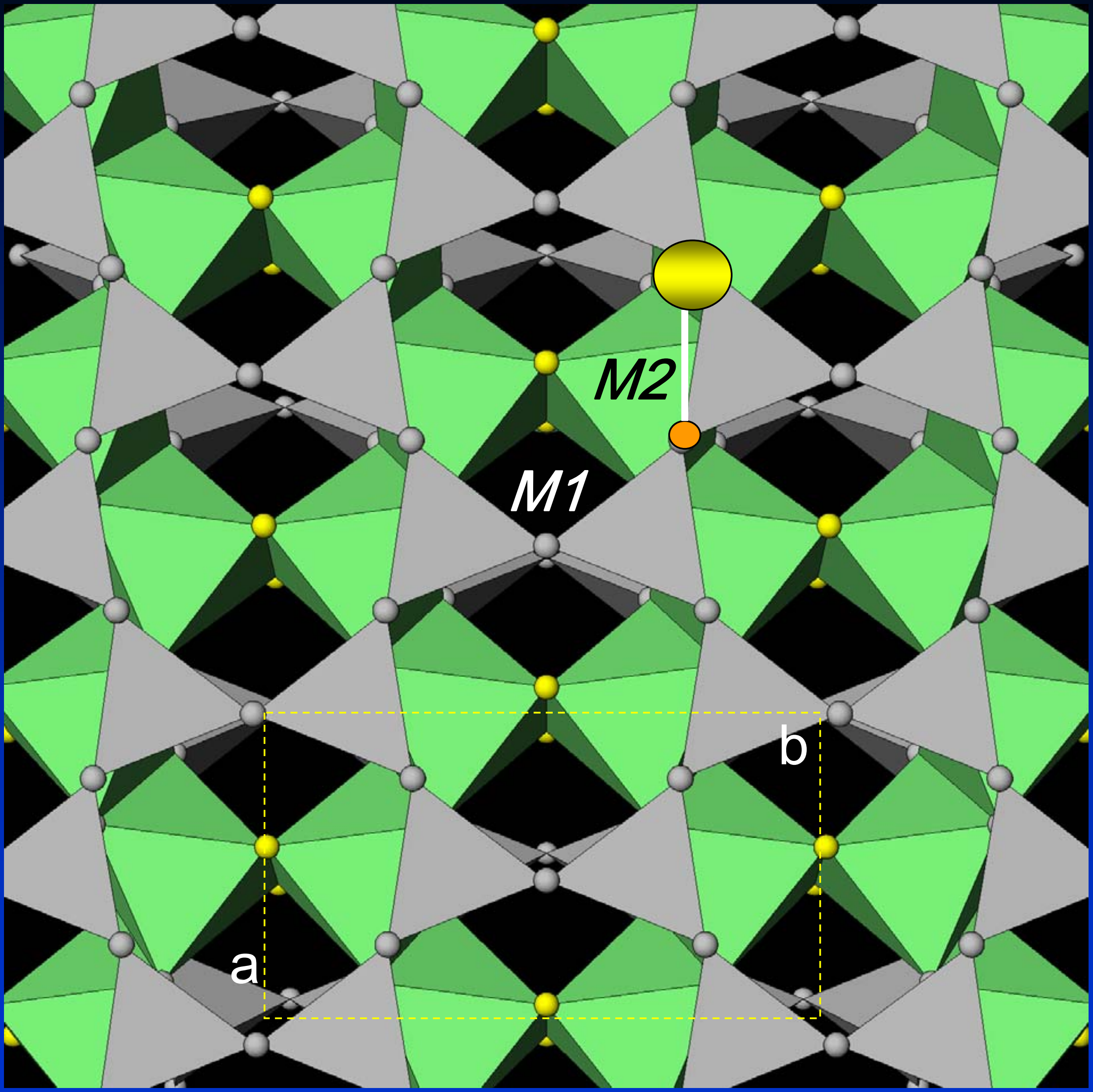
M2
M1
b
a

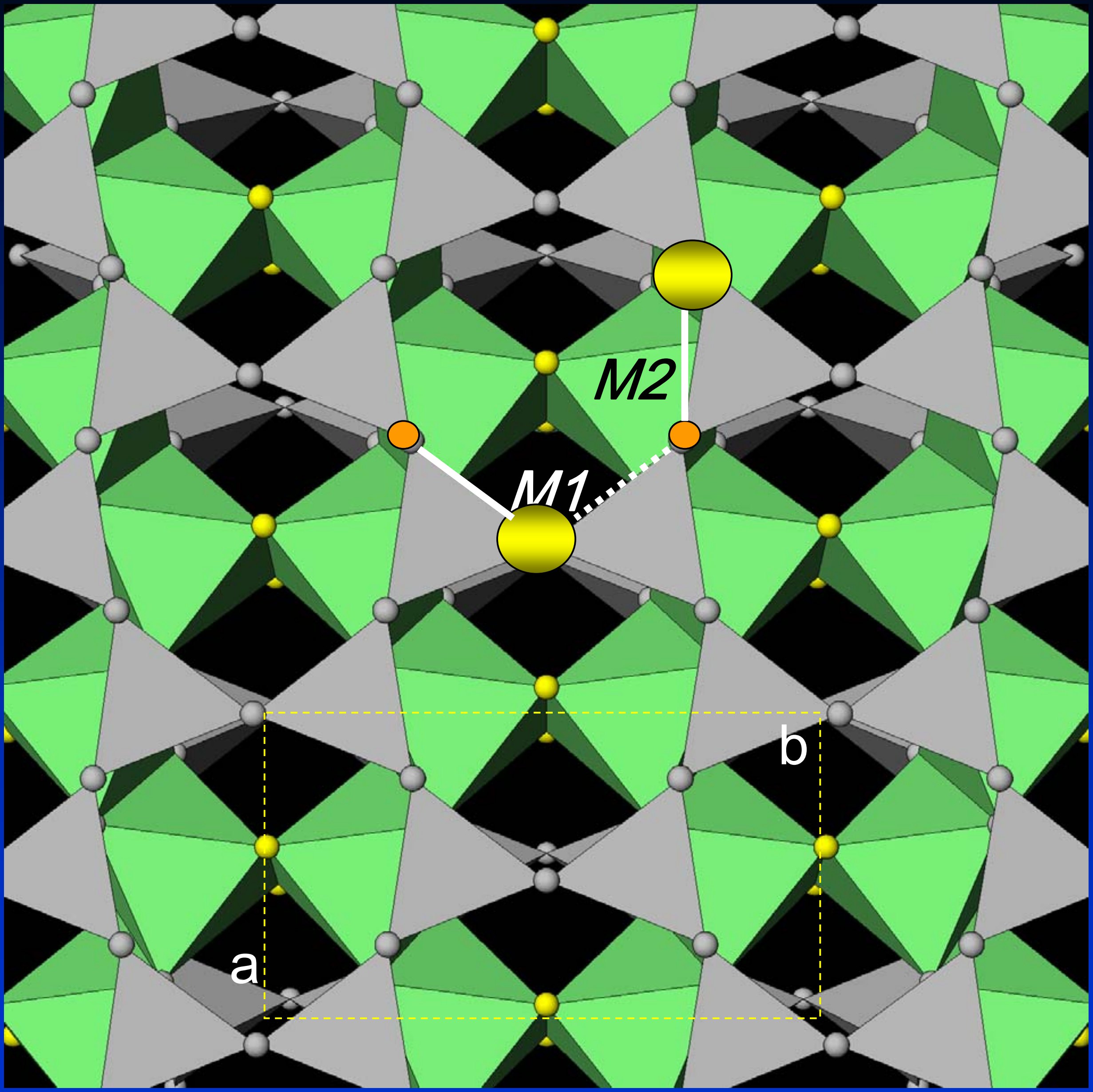
M2
M1
b
a

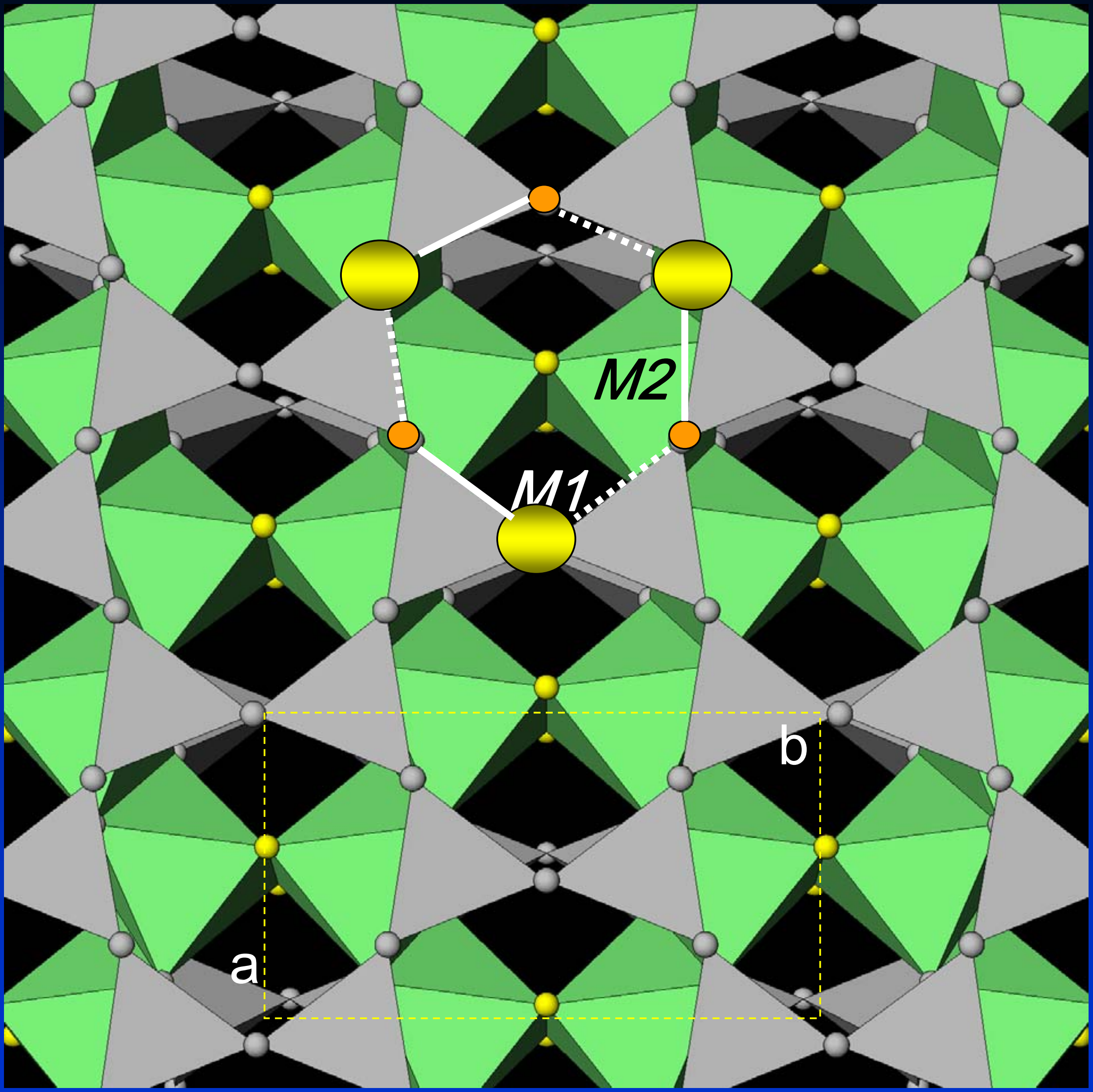

M2
M1
b
a

Iron in the Octahedral Sheet Can Be Reduced and Reoxidized

Tetrahedral

Octahedral

Tetrahedral

M^{n+}

O^{2-}

Si^{4+}, Fe^{3+}, Al^{3+}

OH^{-}, O^{2-}

Al^{3+}, Mg^{2+}, Fe^{3+}

$$Fe^{3+} \rightarrow Fe^{2+}$$

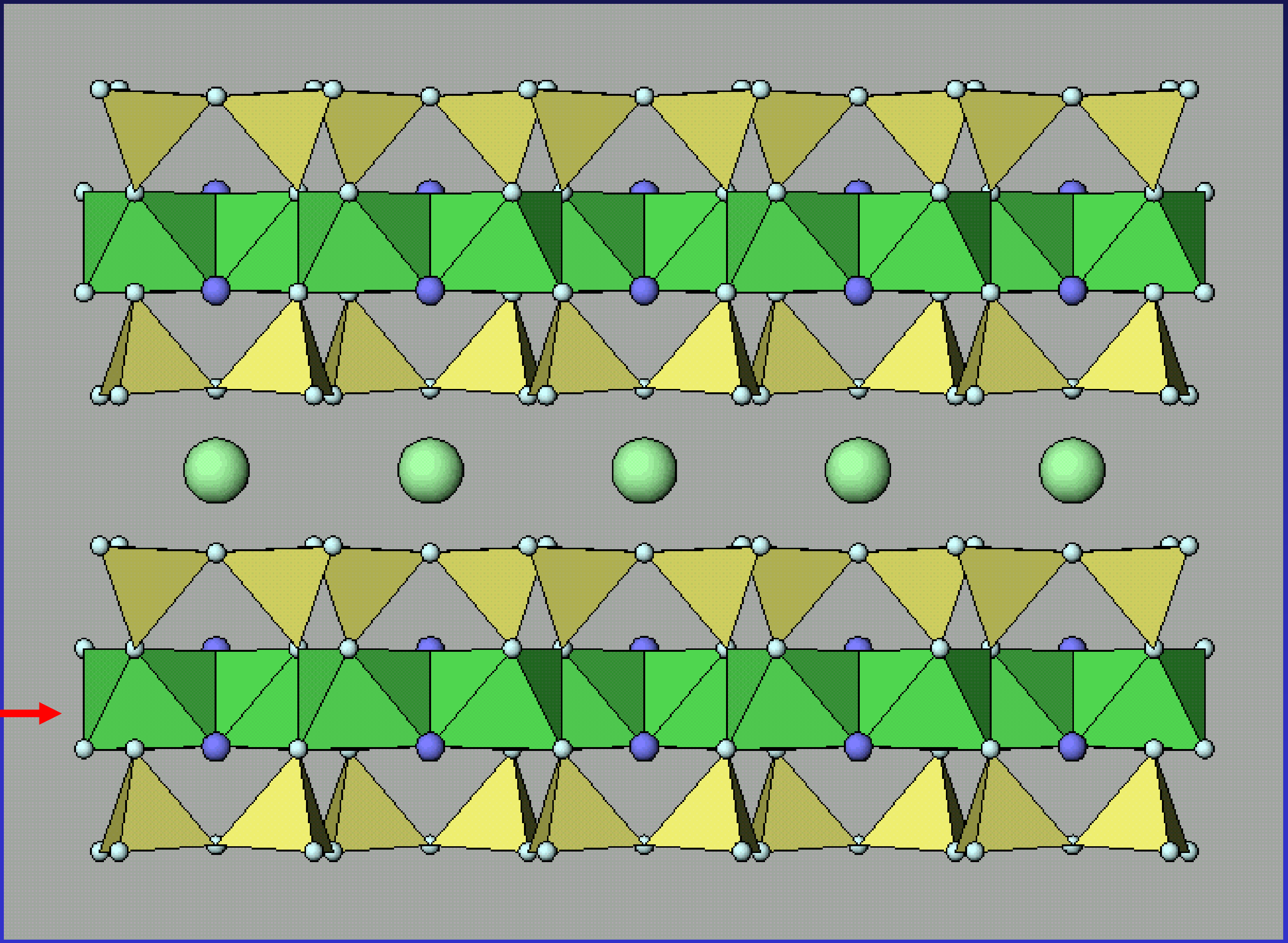

Drawing by Kangwon Lee

REDUCING AGENTS

- Dithionite
- Hydrazine
- Sulfide
- Hydrogen Gas
- Hydroquinone
- Nitrobenzene
- Tetraphenylboron
- Bacteria

REDUCING AGENTS

- Dithionite
- Hydrazine
- Sulfide
- Hydrogen Gas
- Hydroquinone
- Nitrobenzene
- Tetraphenylboron
- Bacteria

Normally not present in nature

REDUCING AGENTS

- Dithionite
- Hydrazine
- Sulfide
- Hydrogen Gas
- Hydroquinone
- Nitrobenzene
- Tetraphenylboron
- Bacteria

The most likely reducing agent in nature

REDUCING AGENTS

- **Dithionite**
- Hydrazine
- Sulfide
- Hydrogen Gas
- Hydroquinone
- Nitrobenzene
- Tetraphenylboron
- **Bacteria**

REDUCING AGENTS

- **Dithionite**

Garfield Nontronite Reduction with Dithionite

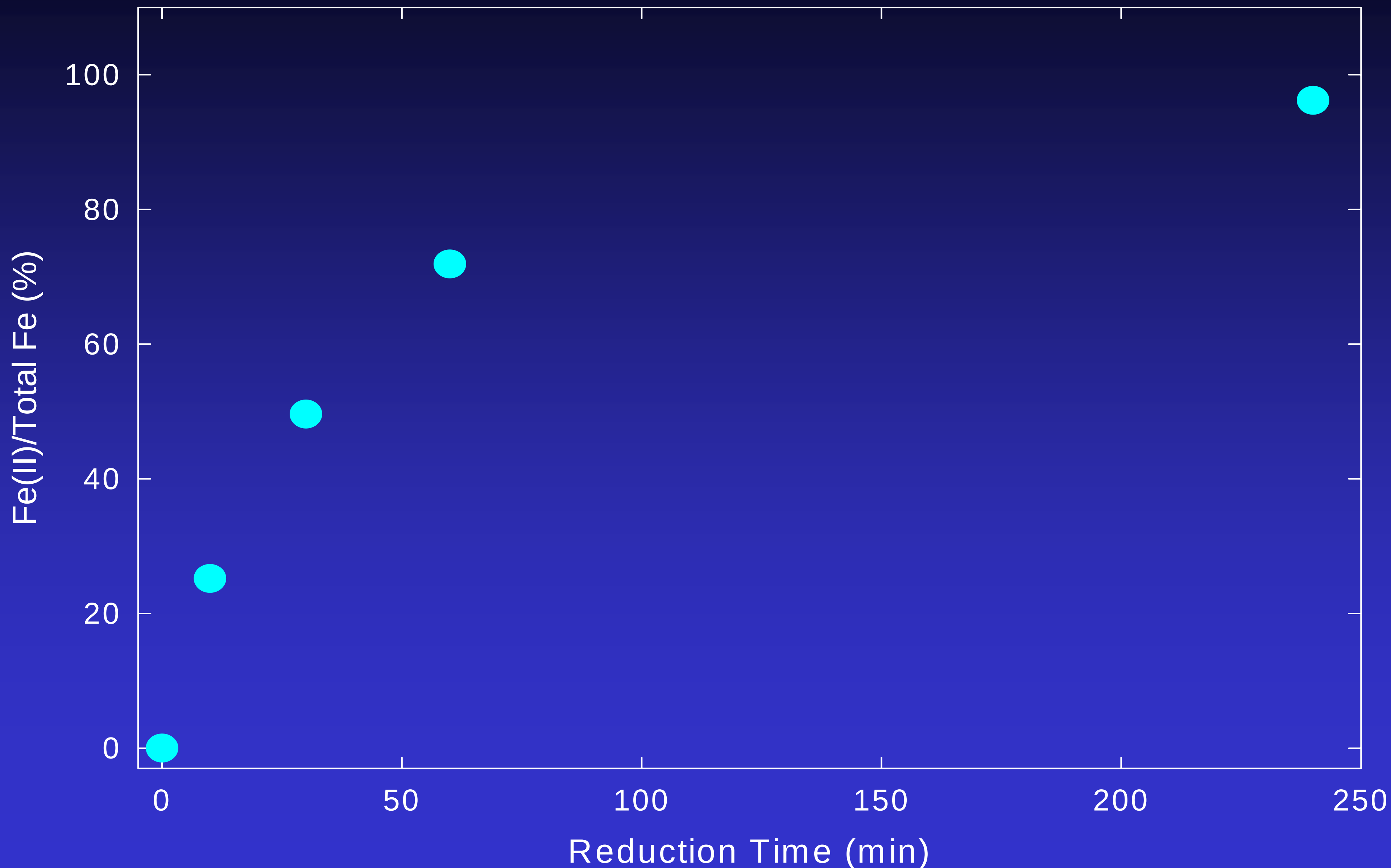


Oxidized
Smectite from Senegalese Soil
Dithionite
Reduced
Ferruginous Smectite SWa-1
Courtesy Pascal Boivin and Fabienne Favre

Visible Light Source
(Tungsten Lamp)

$$\Delta E_{vis} = h\nu$$

I_0

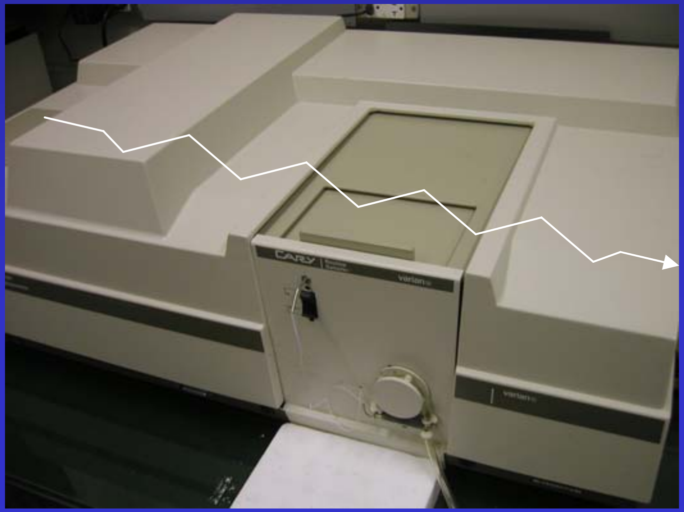

Visible Light Source
(Tungsten Lamp)

Sample

$$\Delta E_{vis} = h\nu$$

$$I_0$$

Visible Light Source
(Tungsten Lamp)

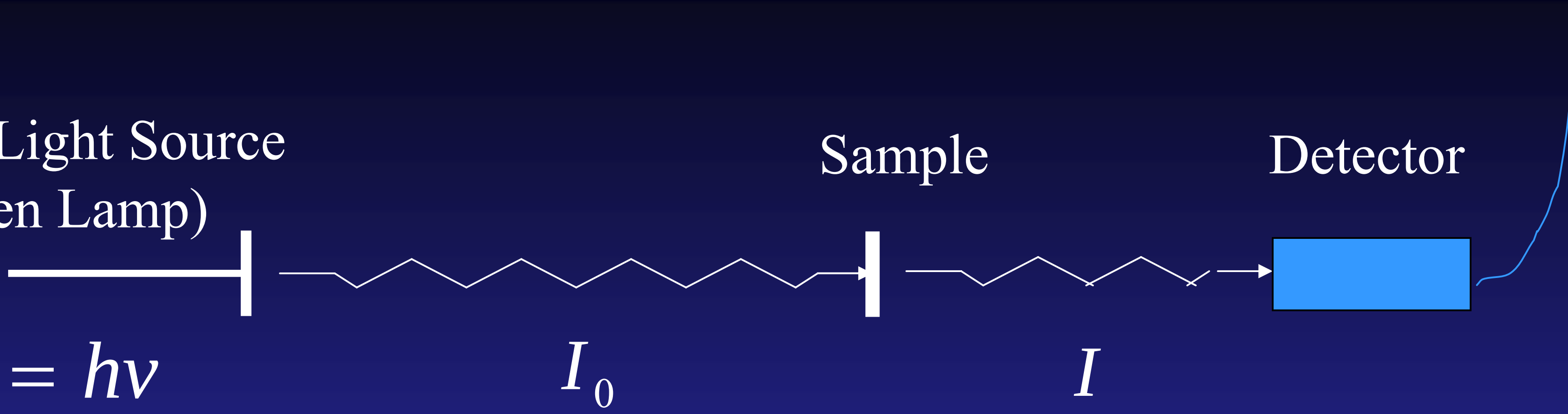

$$\Delta E_{vis} = h\nu$$

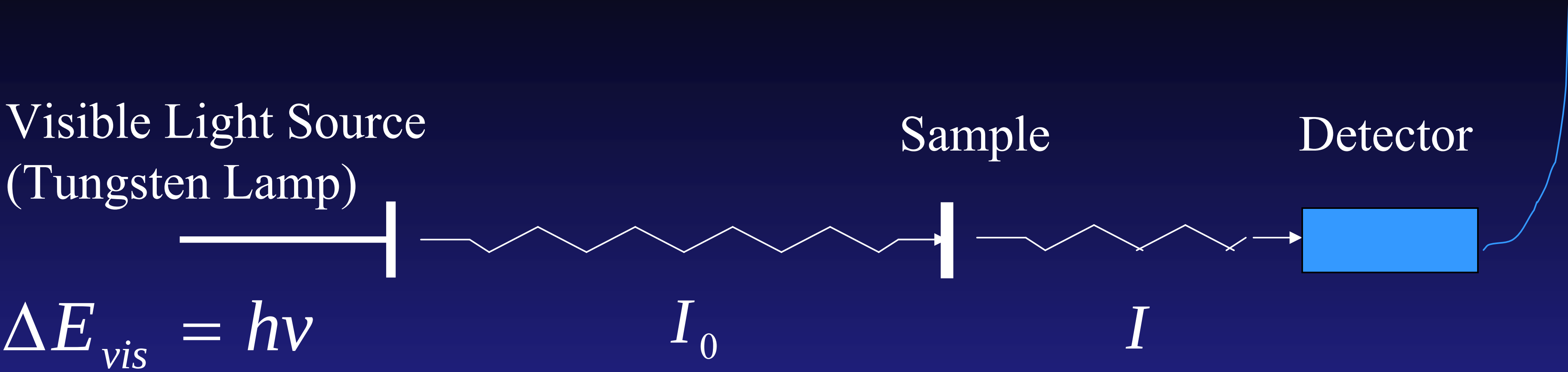

$$\Delta E_{vis} = h\nu$$

$$Absorbance = \log\left(I_0 / I\right)$$

Iron-Pair Combination

Iron-Pair Combination

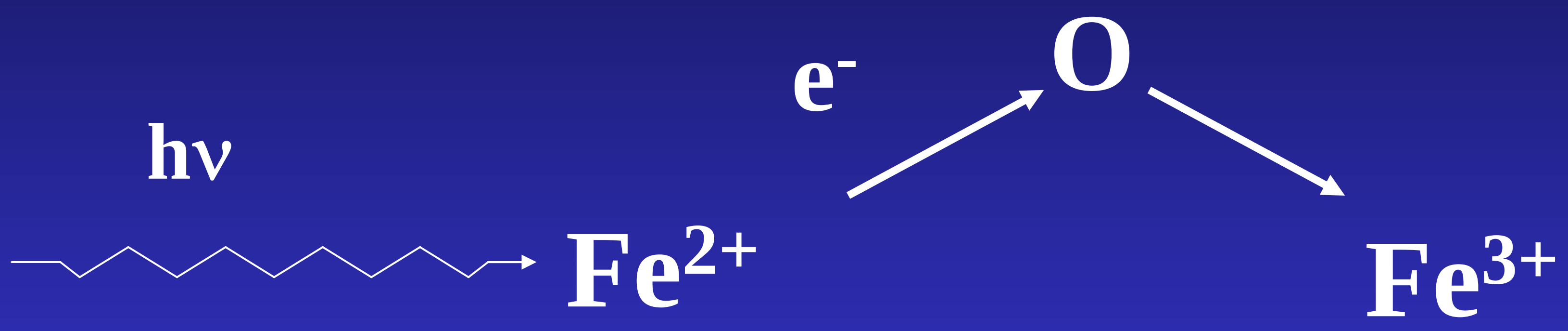

~730 nm

Iron-Pair Combination

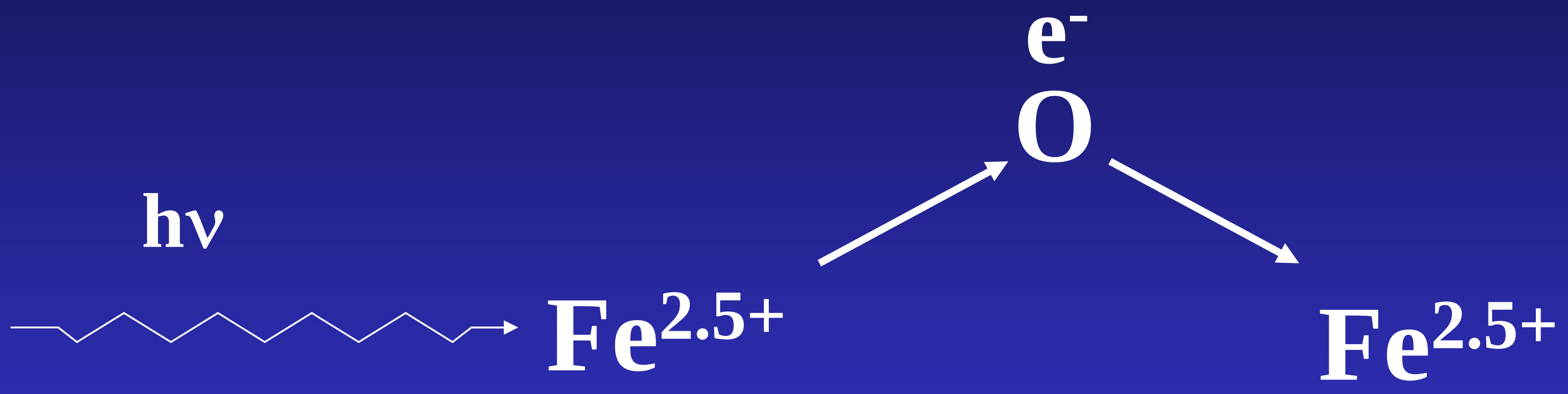

~730 nm

Iron-Pair Combination

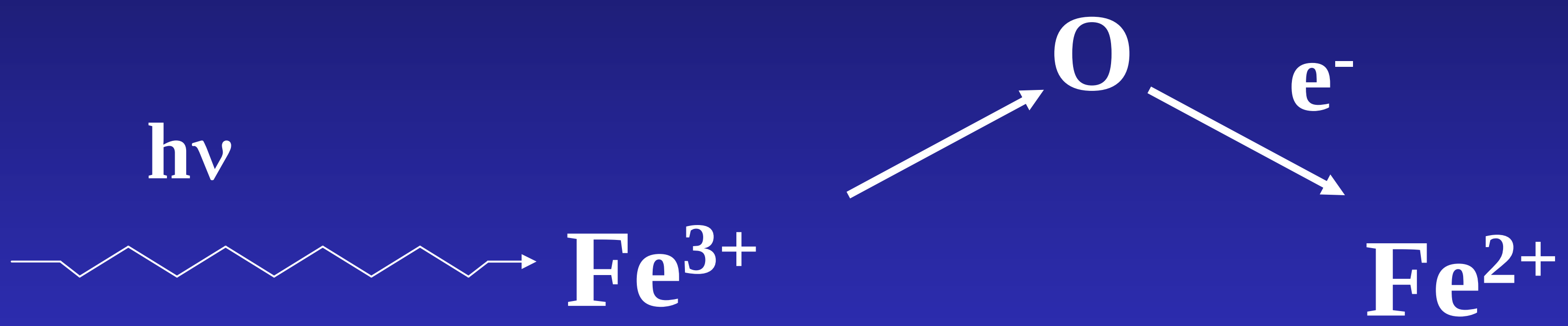

~730 nm

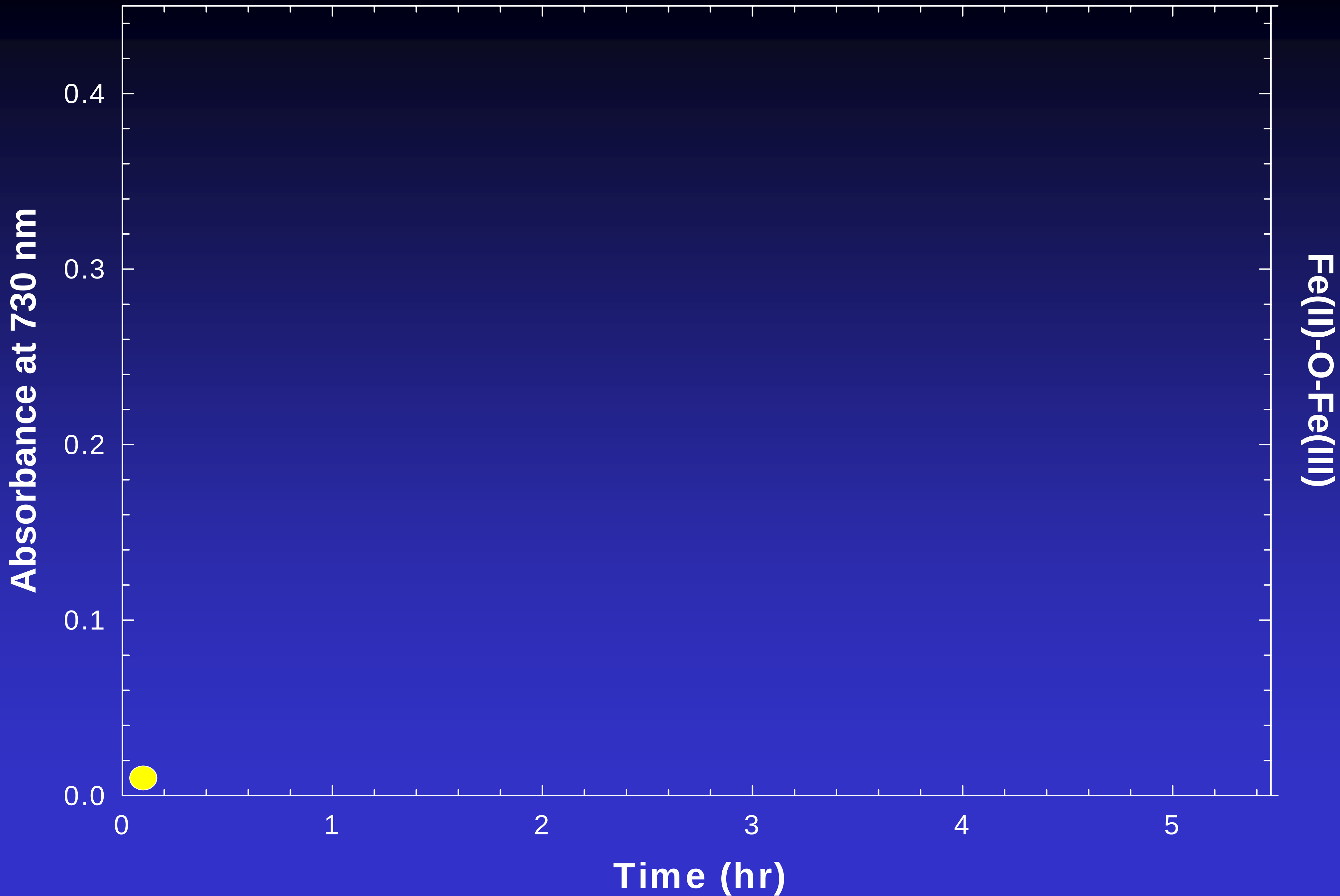

Absorbance at 730 nm
0.4
0.3
0.2
0.1
0.0
0
1
2
3
4
5
Time (hr)
Fe(II)-O-Fe(III)

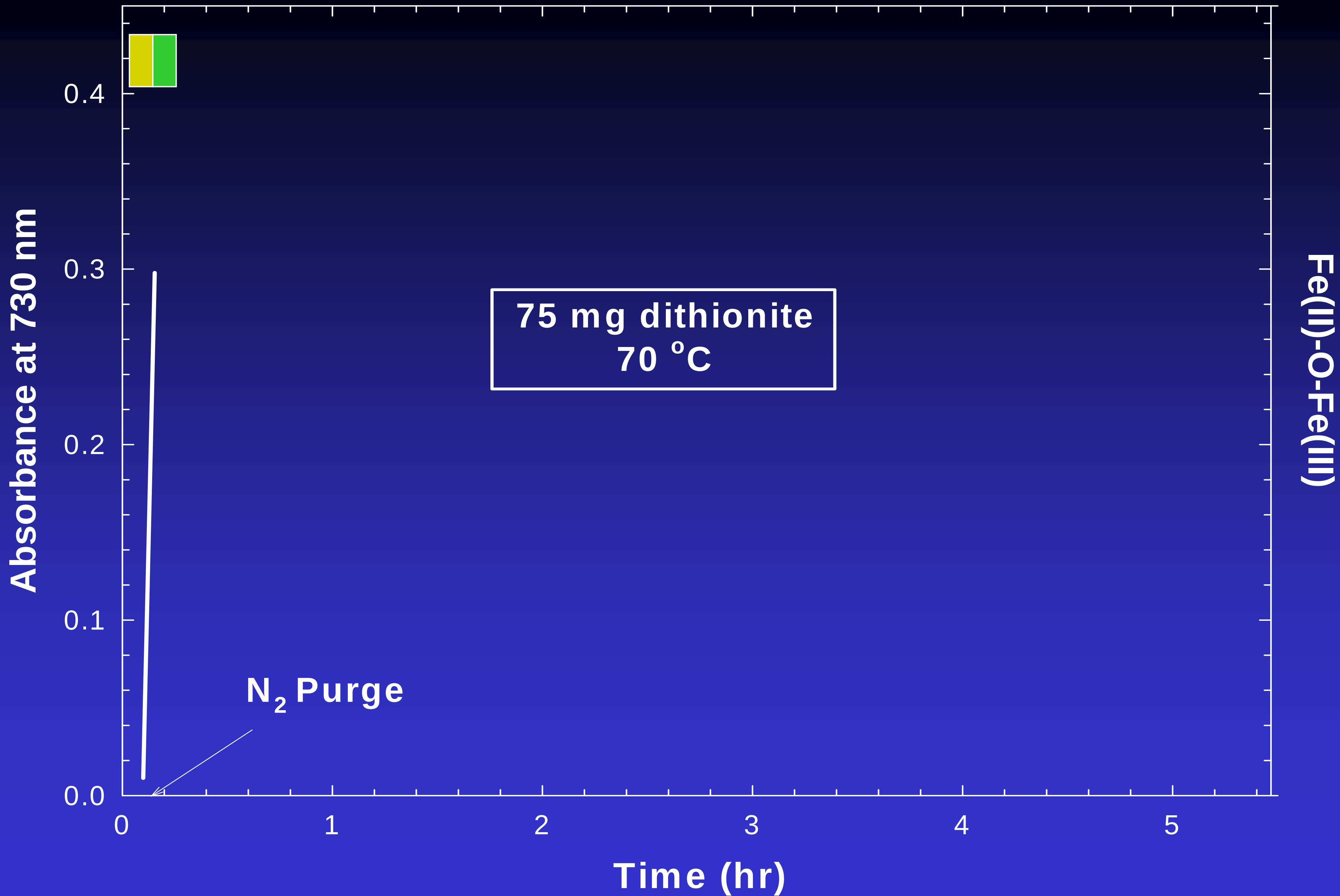

Absorbance at 730 nm
0.4
0.3
0.2
0.1
0.0
0
1
2
3
4
5
Time (hr)
Fe(II)-O-Fe(III)
75 mg dithionite
70 °C
N2 Purge

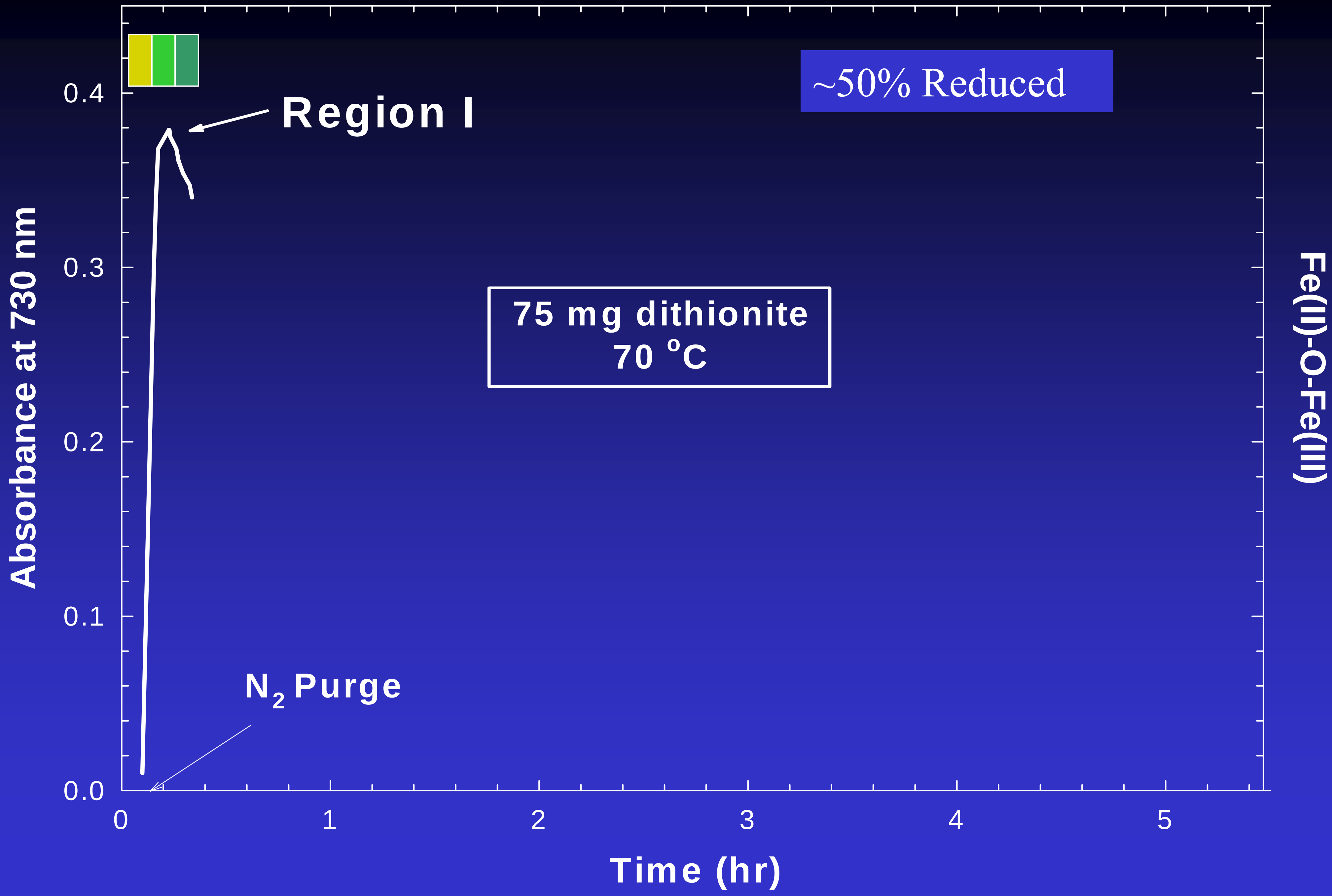

Region I
~50% Reduced
75 mg dithionite
70 °C
N_2 Purge
Absorbance at 730 nm
Fe(II)-O-Fe(III)
Time (hr)
0.0
0.1
0.2
0.3
0.4
0
1
2
3
4
5

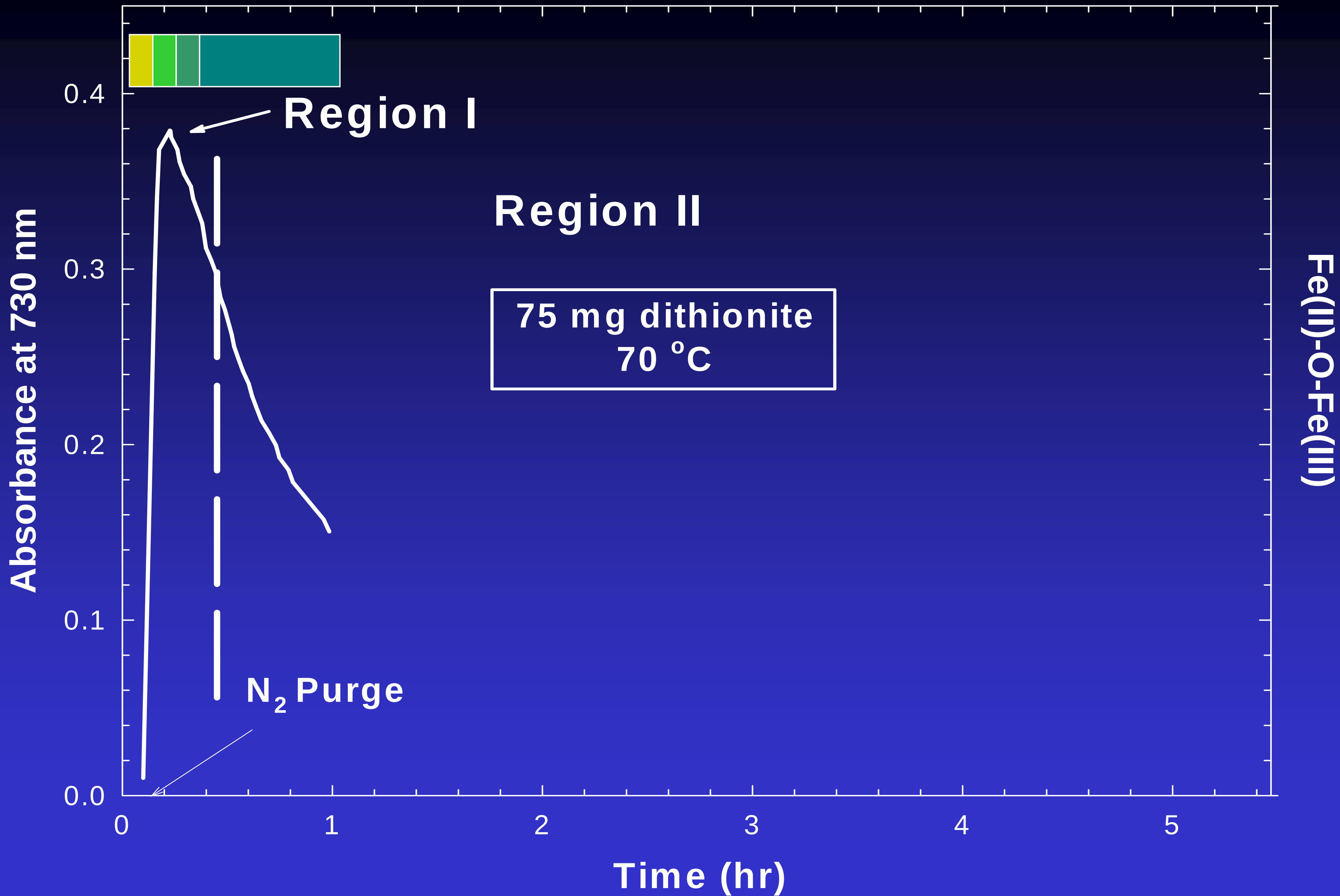
Region I
Region II
75 mg dithionite
70 °C
N2 Purge
Absorbance at 730 nm
Fe(II)-O-Fe(III)
Time (hr)
0.0
0.1
0.2
0.3
0.4
0
1
2
3
4
5

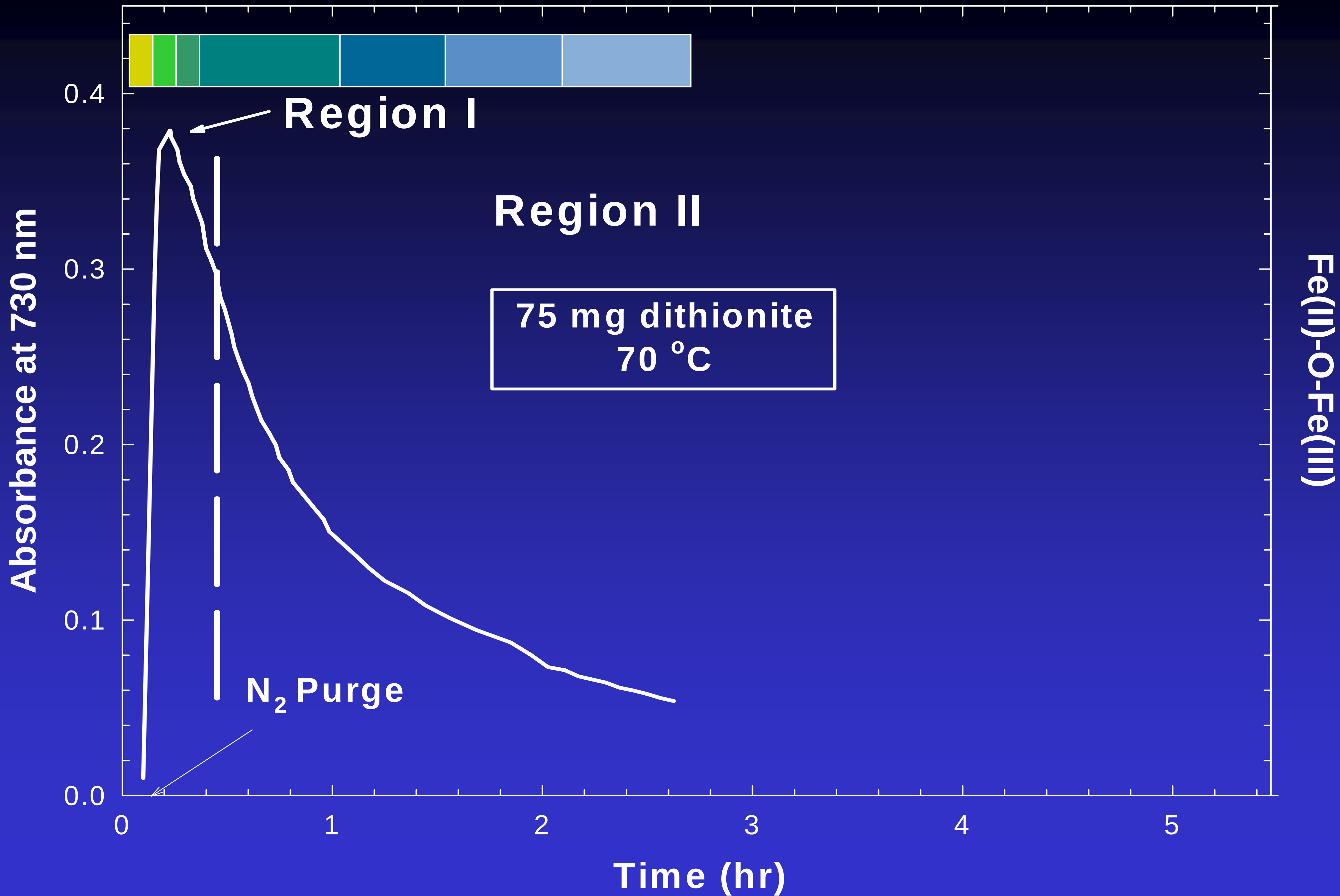

Region I
Region II
75 mg dithionite
70 °C
N2 Purge
Absorbance at 730 nm
Time (hr)
Fe(II)-O-Fe(III)
0.0
0.1
0.2
0.3
0.4
0
1
2
3
4
5

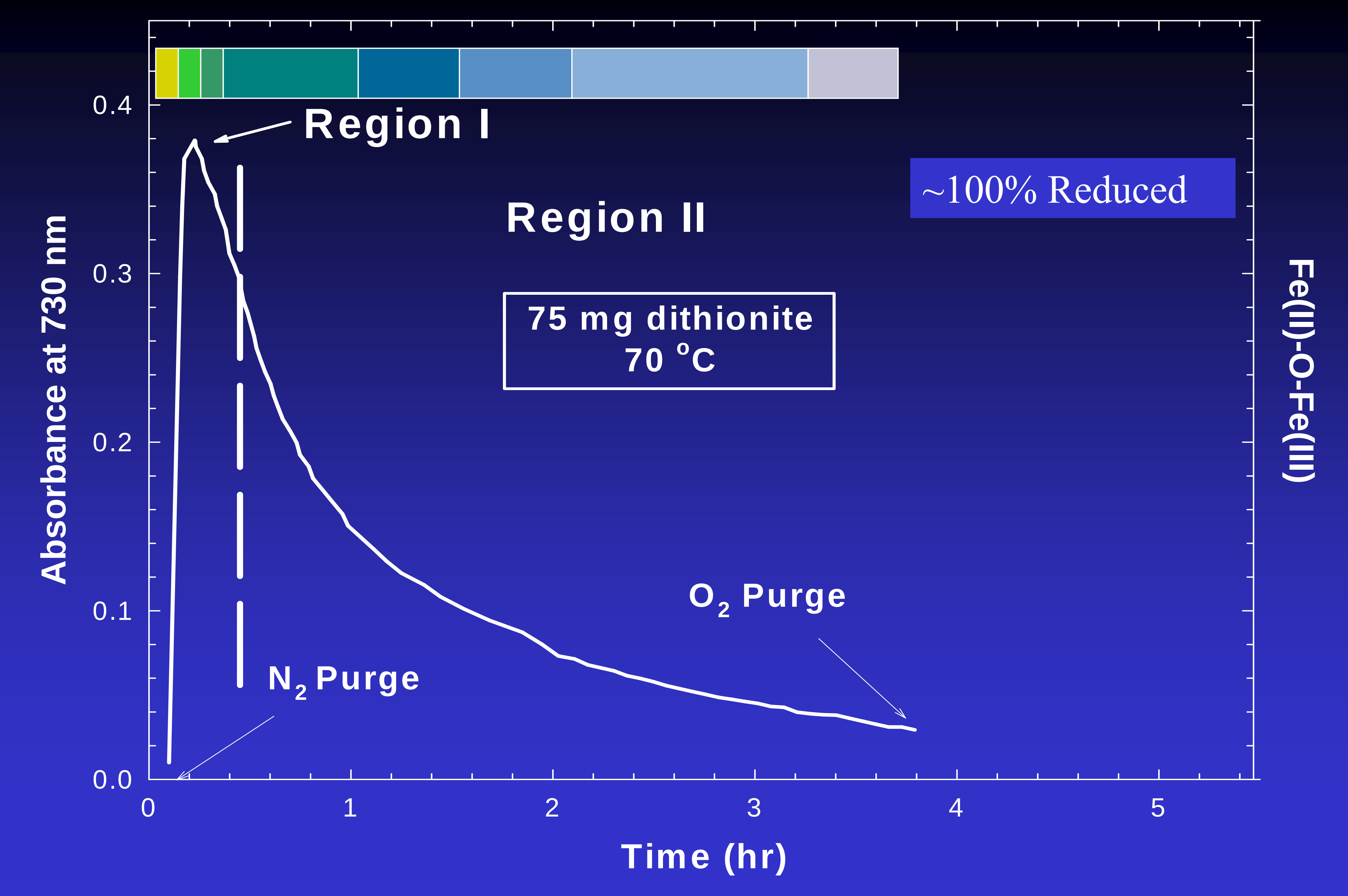
Region I
Region II
~100% Reduced
75 mg dithionite
70 °C
O_2 Purge
N_2 Purge
Absorbance at 730 nm
Time (hr)
Fe(II)-O-Fe(III)
0.0
0.1
0.2
0.3
0.4
0
1
2
3
4
5

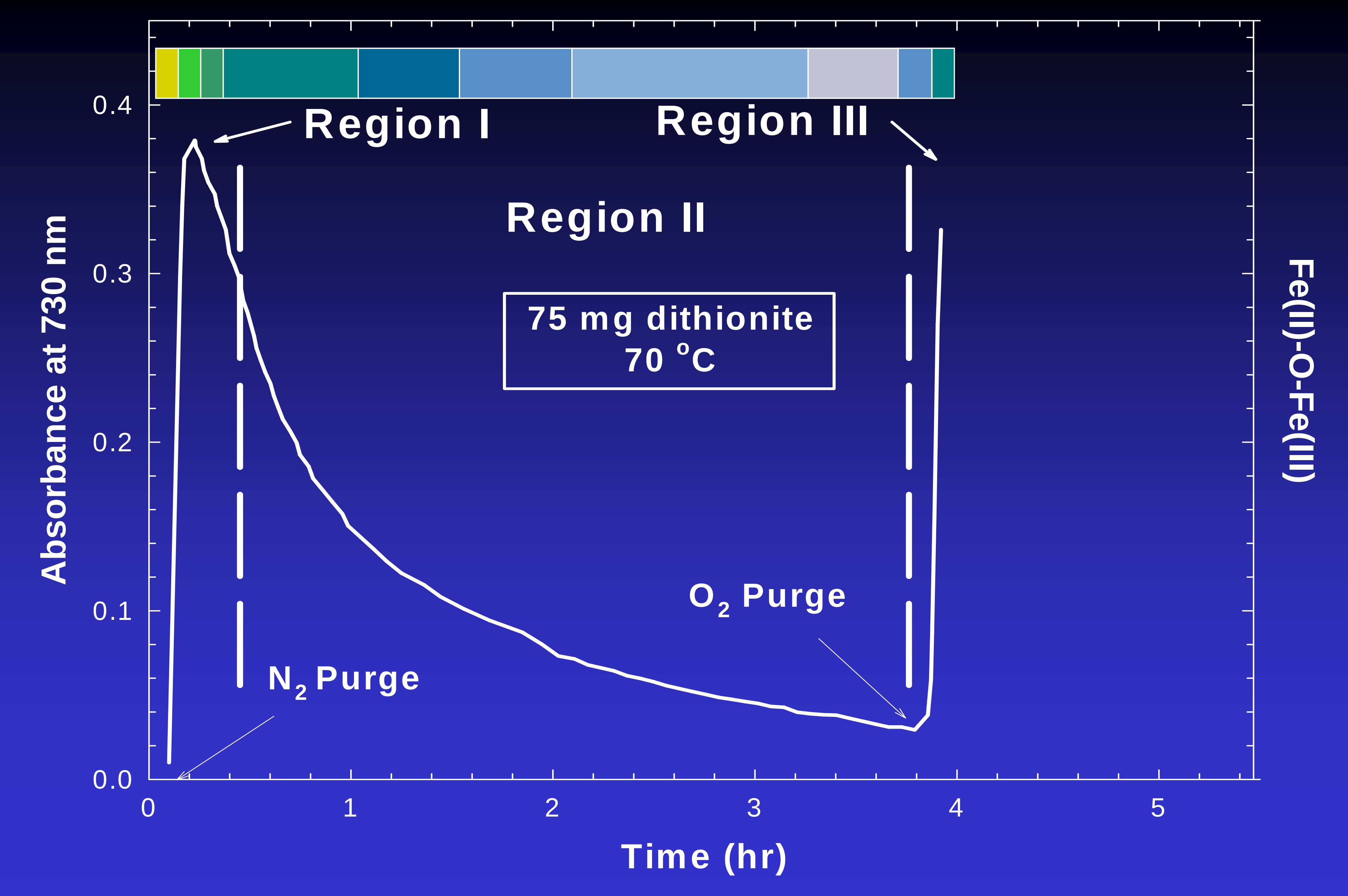
Region I
Region III
Region II
75 mg dithionite
70 °C
O2 Purge
N2 Purge
Absorbance at 730 nm
Fe(II)-O-Fe(III)
Time (hr)
0.0
0.1
0.2
0.3
0.4
0
1
2
3
4
5

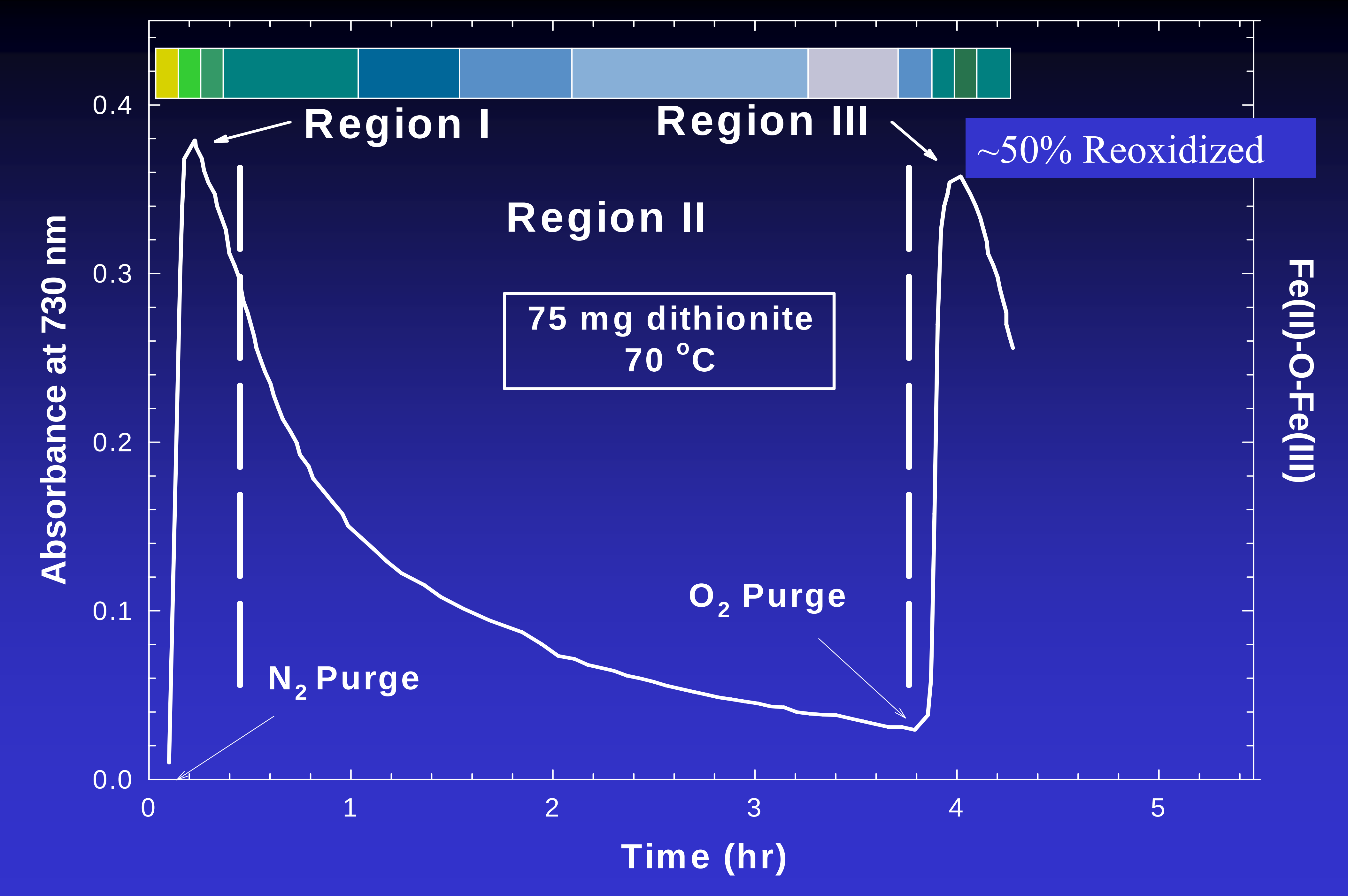
Region I
Region II
Region III
~50% Reoxidized
75 mg dithionite
70 °C
N2 Purge
O2 Purge
Absorbance at 730 nm
Fe(II)-O-Fe(III)
Time (hr)
0.0
0.1
0.2
0.3
0.4
0
1
2
3
4
5

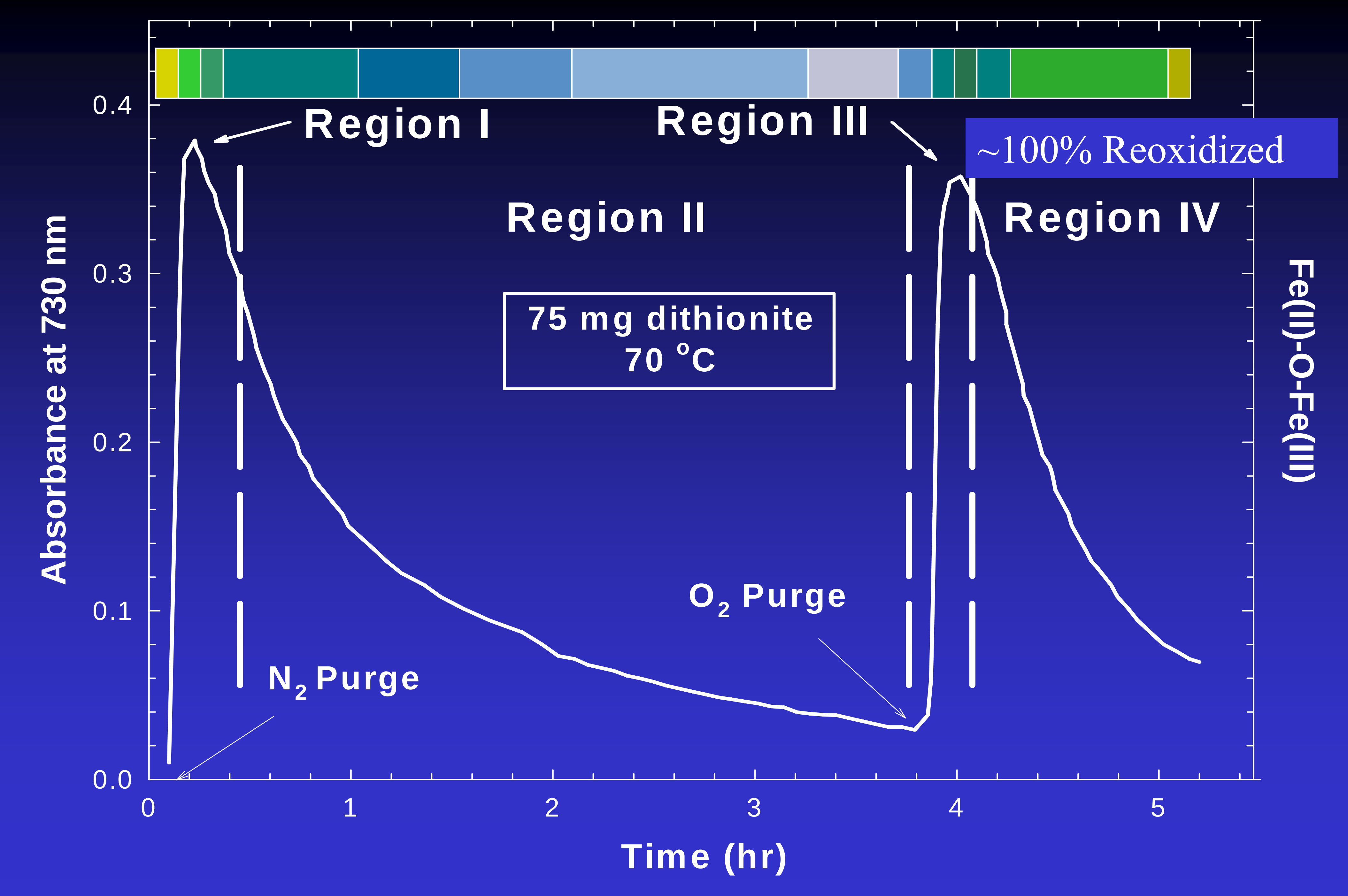

Region I
Region II
Region III
Region IV
~100% Reoxidized
75 mg dithionite
70 °C
N_2 Purge
O_2 Purge
Absorbance at 730 nm
Fe(II)-O-Fe(III)
Time (hr)
0.0
0.1
0.2
0.3
0.4
0
1
2
3
4
5

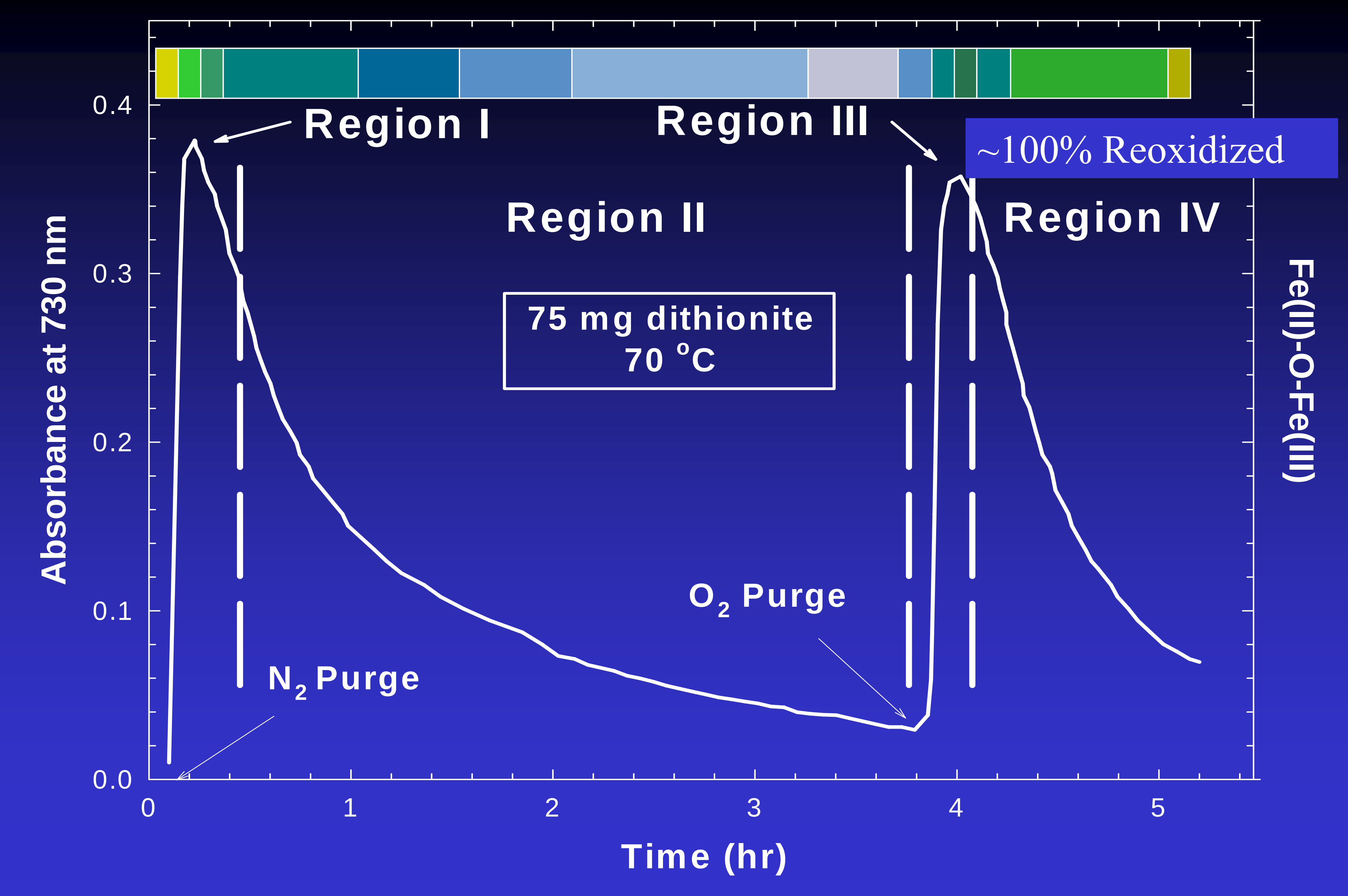
Region I
Region II
Region III
Region IV
~100% Reoxidized
75 mg dithionite
70 °C
N_2 Purge
O_2 Purge
Absorbance at 730 nm
Fe(II)-O-Fe(III)
Time (hr)
0.0
0.1
0.2
0.3
0.4
0
1
2
3
4
5

COLORS

REDUCING AGENTS

- Dithionite
- Hydrazine
- Sulfide
- Hydrogen Gas
- Hydroquinone
- Nitrobenzene
- Tetraphenylboron
- **Bacteria**

Microorganisms Used (FeRB)

Indigenous	Unclassified from SWa-1, paddy soil, upland soil, and subsurface sediments
Pseudomonas	*fluroescens, aureofaciens, putida*
Shewanella	*oneidensis (putrefaciens)* MR-1 & CN32, *alga* BrY
δ-Proteobacteria	*Geobacteraceae*
Low-G+C gram-positive bacteria	*Bacillus, Desulfitobacterium, Desulfotomaculum*
Others	List is open for expansion

*Smectite Reduction by Bacteria**

* *Schewanella putrefaciens* (strain MR-1) (from Wu and Kostka)


SWa-1
Nontronite
Reduced
By Bacteria
SWa-1
Nontronite
Non-Reduced
(Un-treated)

Summary of Observations

- The oxidation state of structural iron in clay minerals has a profound effect on their physical, chemical, and colloidal properties

Summary of Observations

- The oxidation state of structural iron in clay minerals has a profound effect on their physical, chemical, and colloidal properties
- Commonly occurring bacteria are capable of reducing structural iron in clay minerals

Summary of Observations

- The oxidation state of structural iron in clay minerals has a profound effect on their physical, chemical, and colloidal properties
- Commonly occurring bacteria are capable of reducing structural iron in clay minerals
- Increases in clay layer charge are less than predicted by levels of iron reduction

Summary of Observations

- The oxidation state of structural iron in clay minerals has a profound effect on their physical, chemical, and colloidal properties
- Commonly occurring bacteria are capable of reducing structural iron in clay minerals
- Increases in clay layer charge are less than predicted by levels of iron reduction
- Iron reduction affects soil fertility by fixing K^+ and other cations between clay layers

Summary of Observations

- **Reduced clay surfaces are more active with respect to degradation of chloro- and nitro-organics**

Summary of Observations

- Reduced clay surfaces are more active with respect to degradation of chloro- and nitro-organics
- Surface pH and redox potential are altered by structural iron reduction

Summary of Observations

- Reduced clay surfaces are more active with respect to degradation of chloro- and nitro-organics
- Surface pH and redox potential are altered by structural iron reduction
- The clay mineral layer exhibits frustrated anti-ferromagnetic behavior in the oxidized state and ferromagnetism in the reduced state

Summary of Observations

- Reduced clay surfaces are more active with respect to degradation of chloro- and nitro-organics
- Surface pH and redox potential are altered by structural iron reduction
- The clay mineral layer exhibits frustrated anti-ferromagnetic behavior in the oxidized state and ferromagnetism in the reduced state
- Iron reduction decreases specific surface area and clay swelling in water

Summary of Observations

- Mössbauer spectra reveal that the pathway for electron transfer into the clay structure upon chemical reduction may be different from bacterial reduction

Summary of Observations

- Mössbauer spectra reveal that the pathway for electron transfer into the clay structure upon chemical reduction may be different from bacterial reduction
- Pesticide degradation can be greatly affected by exposure to reduced-clay surfaces

Summary of Observations

- Mössbauer spectra reveal that the pathway for electron transfer into the clay structure upon chemical reduction may be different from bacterial reduction
- Pesticide degradation can be greatly affected by exposure to reduced-clay surfaces
- The structure and stability of reduced clays are governed by the extent of reduction, the reducing agent, and the presence of organic acids

Summary of Observations

- Redox-modified clay minerals have been characterized by:

Summary of Observations

- Redox-modified clay minerals have been characterized by:
  - Mössbauer spectroscopy

Summary of Observations

- Redox-modified clay minerals have been characterized by:
  - Mössbauer spectroscopy
  - FTIR

Summary of Observations

- Redox-modified clay minerals have been characterized by:
  - Mössbauer spectroscopy
  - FTIR
  - EXAFS and Polarized EXAFS

Summary of Observations

- Redox-modified clay minerals have been characterized by:
  - Mössbauer spectroscopy
  - FTIR
  - EXAFS and Polarized EXAFS
  - UV-Visible spectroscopy

Summary of Observations

- Redox-modified clay minerals have been characterized by:
  - Mössbauer spectroscopy
  - FTIR
  - EXAFS and Polarized EXAFS
  - UV-Visible spectroscopy
  - Magnetic susceptibility

Summary of Observations

- Redox-modified clay minerals have been characterized by:
  - Mössbauer spectroscopy
  - FTIR
  - EXAFS and Polarized EXAFS
  - UV-Visible spectroscopy
  - Magnetic susceptibility
  - L-edge x-ray absorption spectroscopy

Summary of Observations

- Redox-modified clay minerals have been characterized by:
  - Mössbauer spectroscopy
  - FTIR
  - EXAFS and Polarized EXAFS
  - UV-Visible spectroscopy
  - Magnetic susceptibility
  - L-edge x-ray absorption spectroscopy
  - X-ray photoelectron spectroscopy

Summary of Observations

- Redox-modified clay minerals have been characterized by:
  - Mössbauer spectroscopy
  - FTIR
  - EXAFS and Polarized EXAFS
  - UV-Visible spectroscopy
  - Magnetic susceptibility
  - L-edge x-ray absorption spectroscopy
  - X-ray photoelectron spectroscopy
  - High-resolution transmission electron microscopy

Iron Reduction Increases Layer Charge

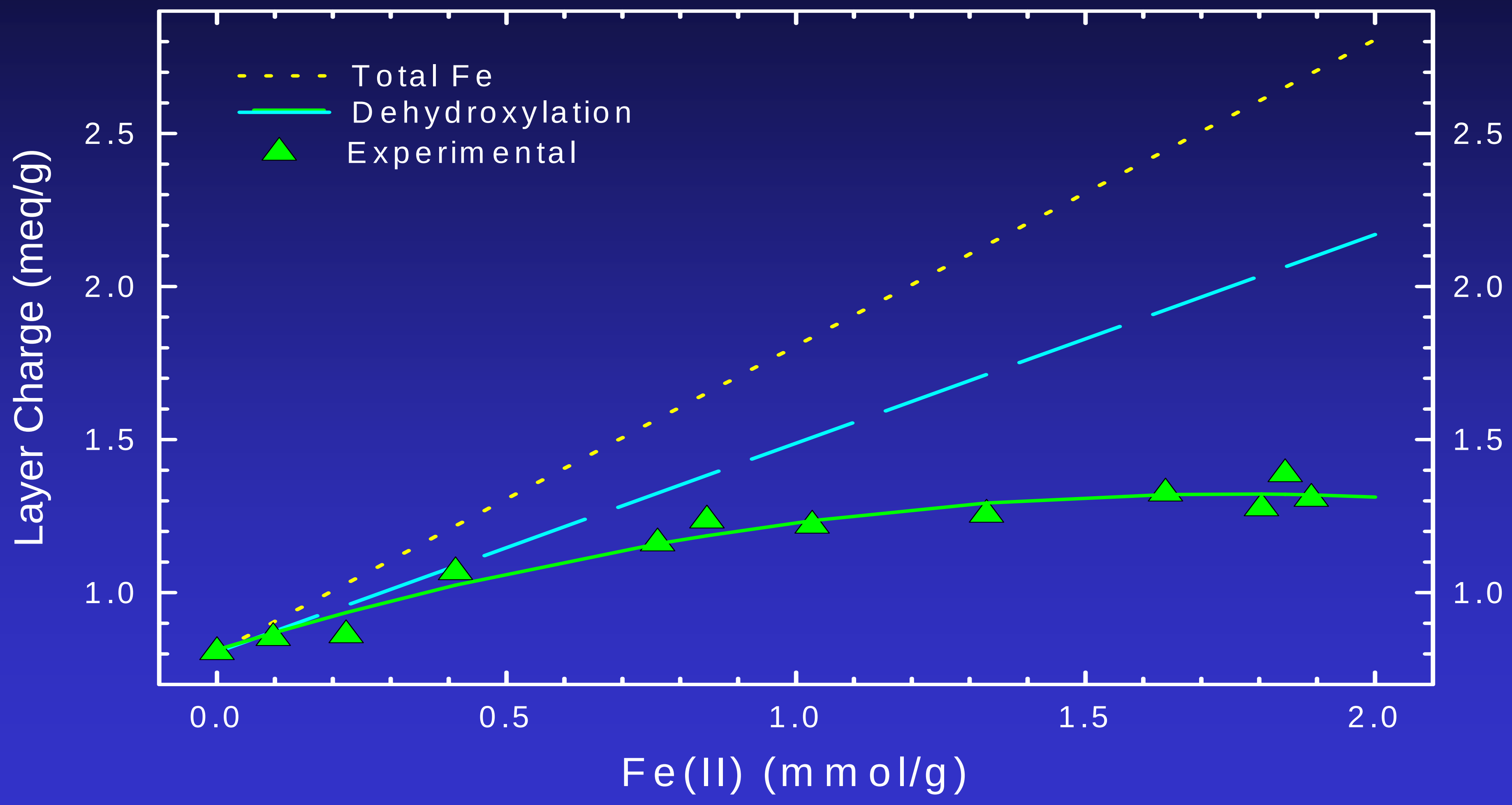

(from Lear and Stucki, 1985)

Cation Fixation by Reduced Clay

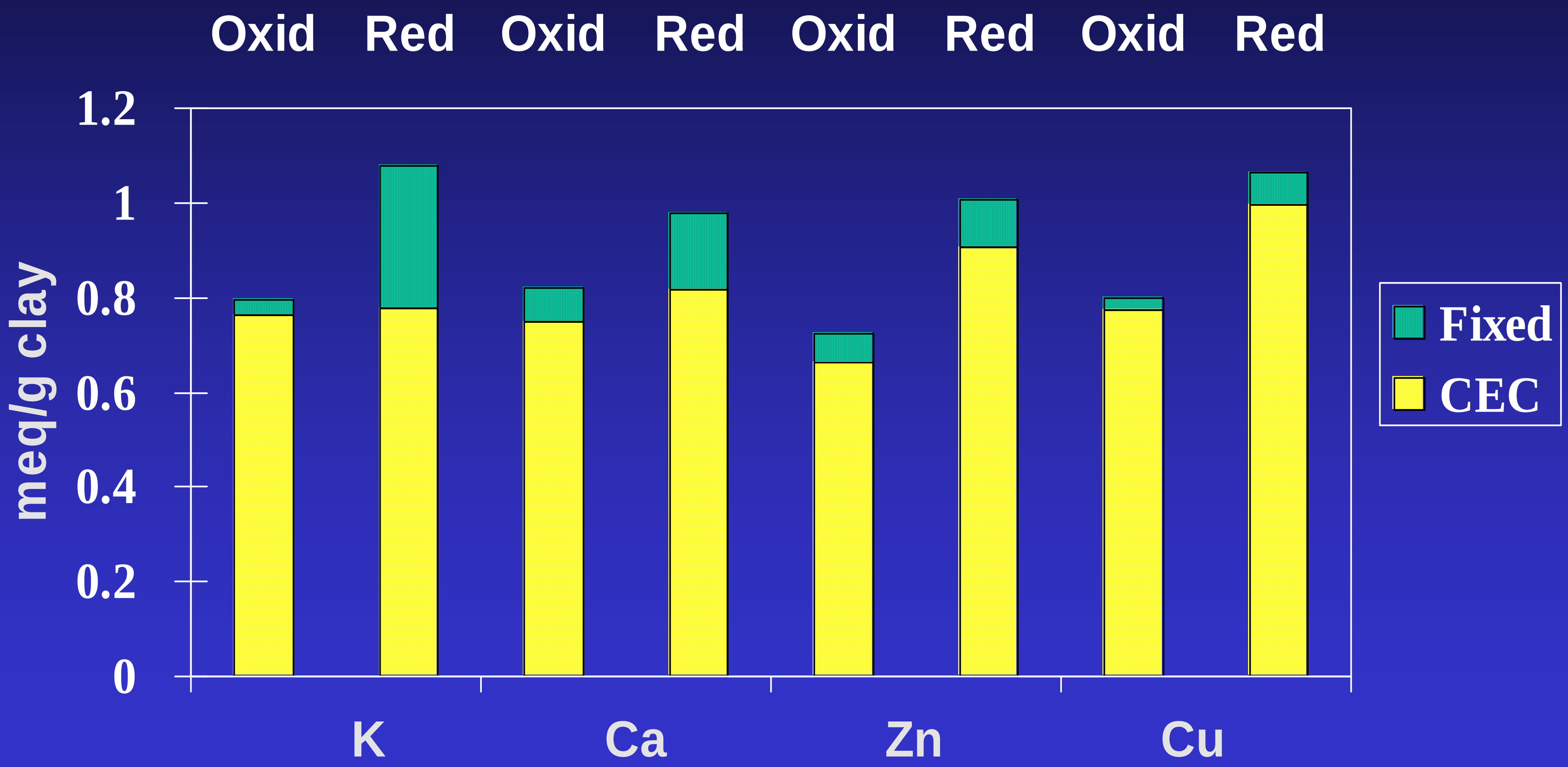

Potassium Fixation in Smectite

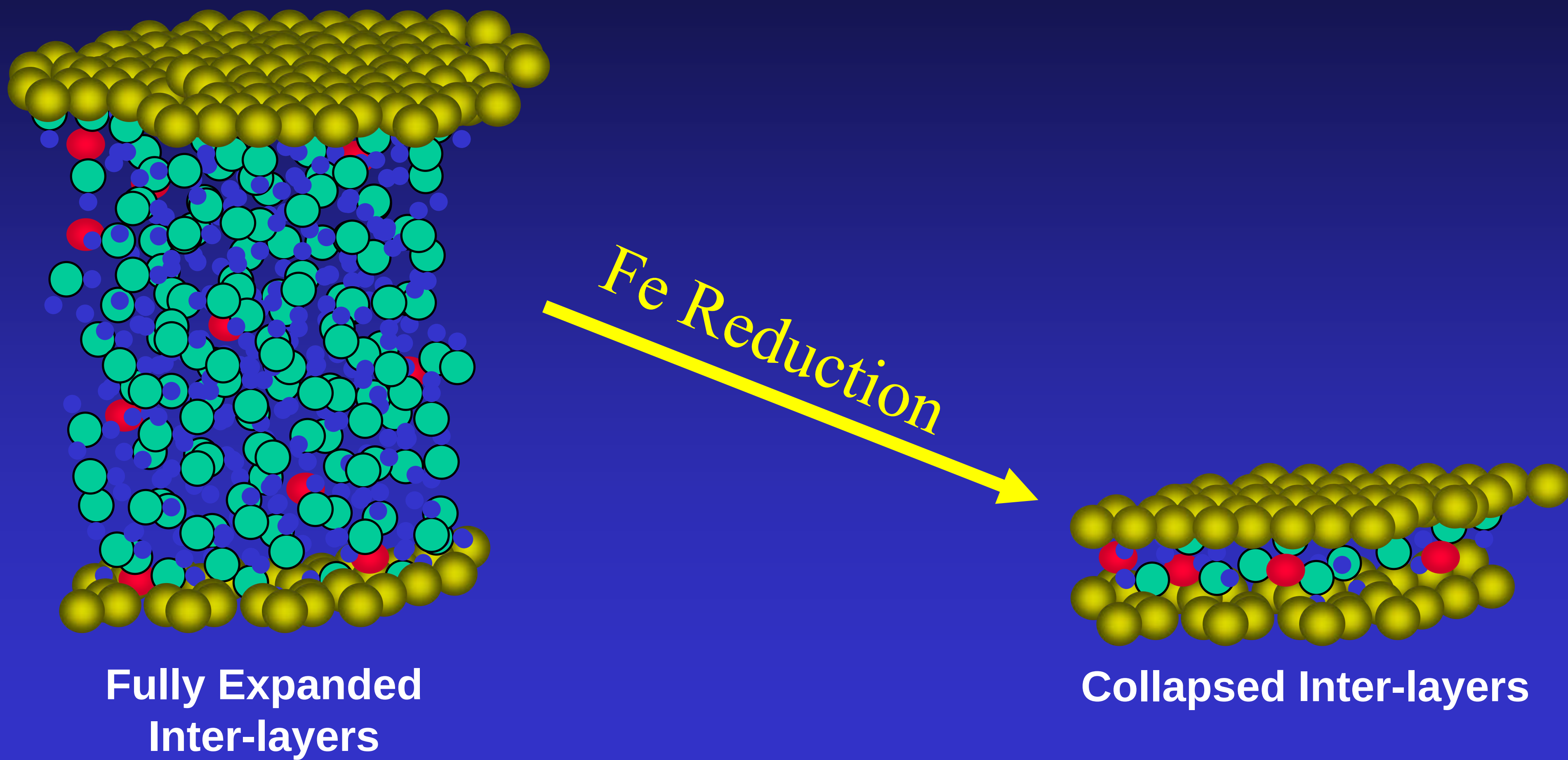

Cation Fixation by Reduced Clay

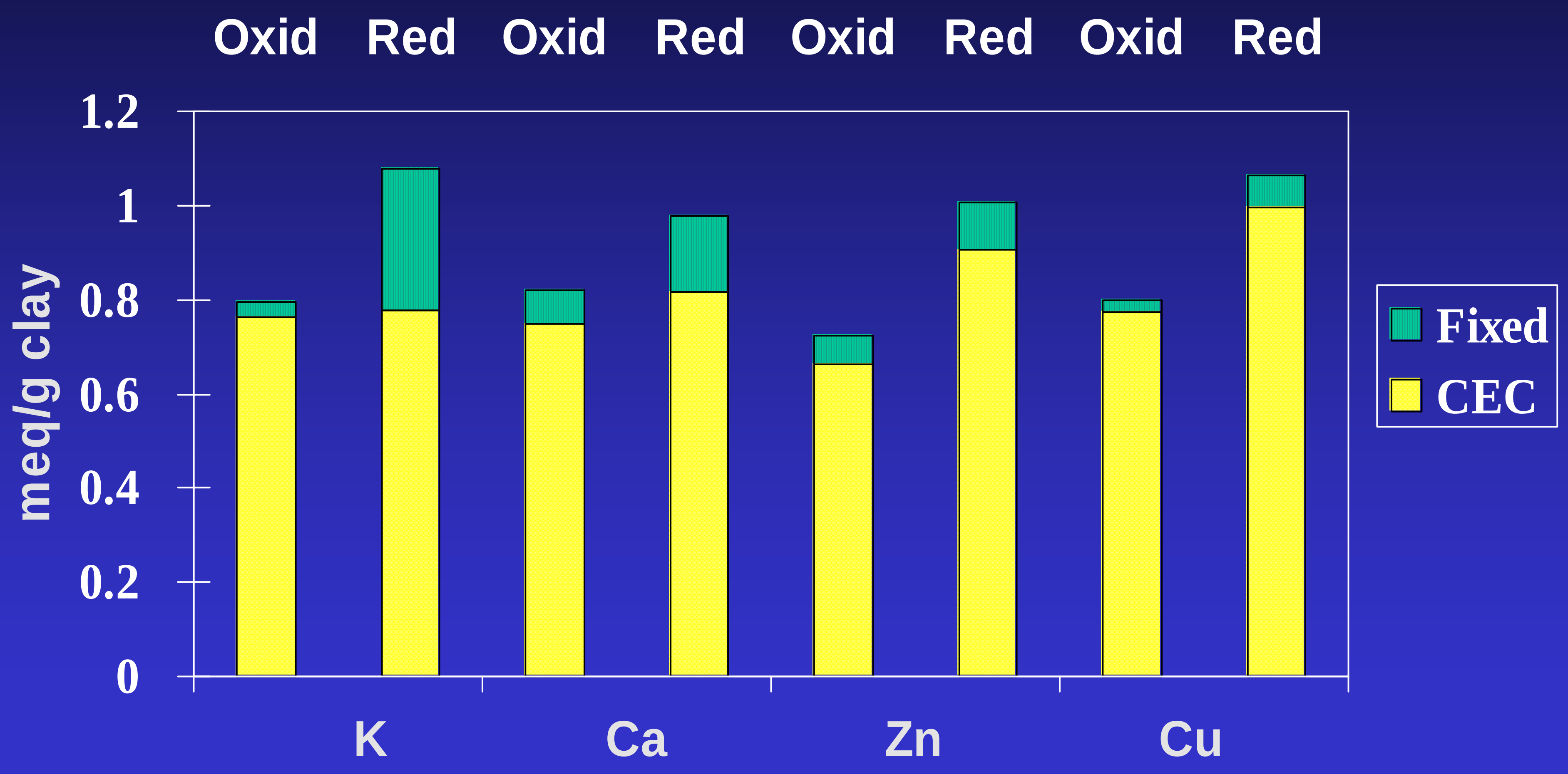

Potential for Potassium Fixation

Acre 6-in of Soil = 2 million lbs.

Medium Texture Soil = 15% Clay

K fixation @ 20% Fe(II) = 0.0047 lbs K_2O/lb. clay

$$\frac{0.0047 \text{ lbs } K_2O}{\text{lb. clay}} \times \frac{10 \text{ lbs. Clay}}{100 \text{ lbs soil}} \times \frac{2 \times 10^6 \text{ lbs. Soil}}{\text{Acre 6-in}}$$

Total Potential Fixation = 940 lbs K_2O/Acre 6-in

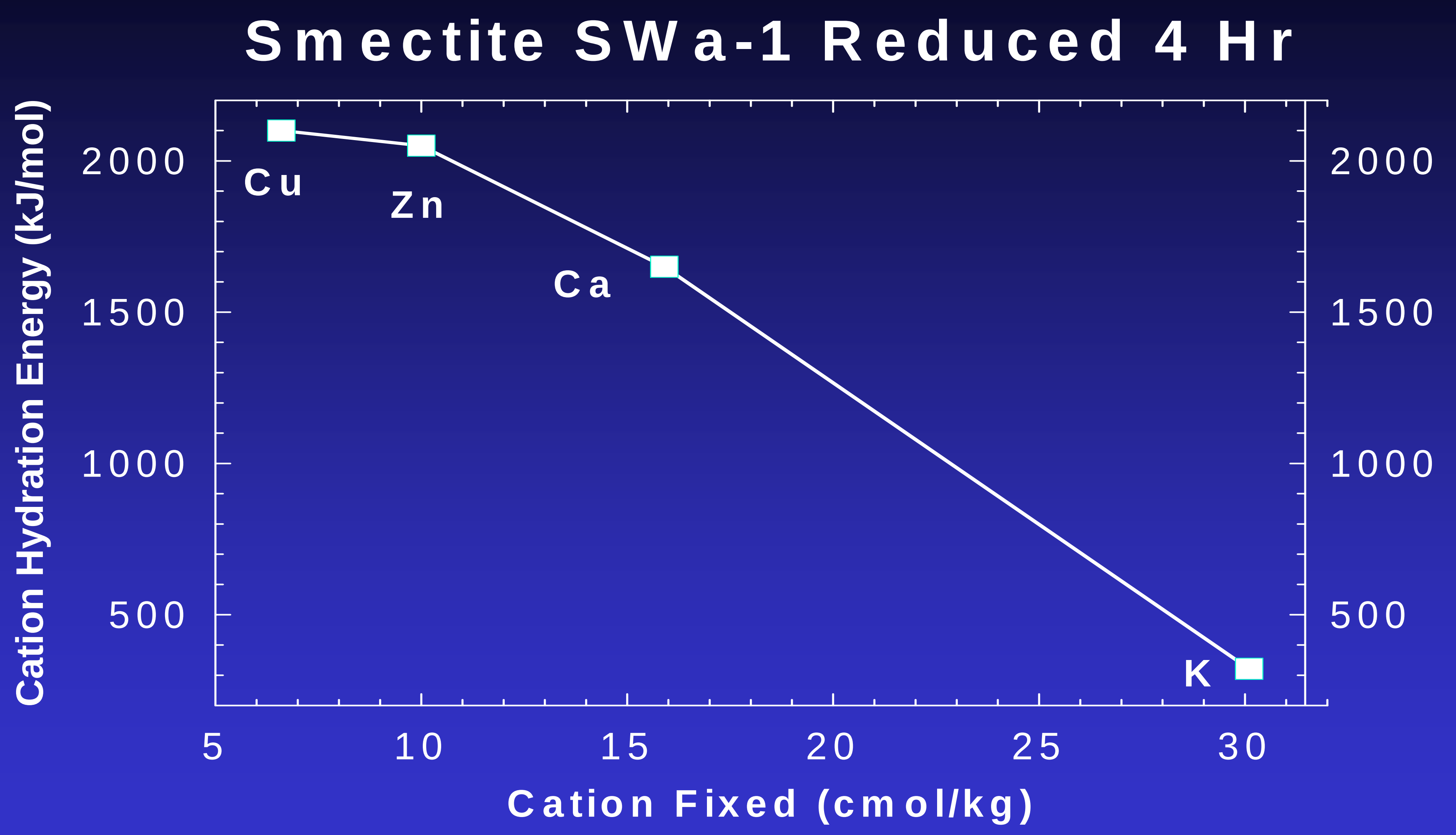
Smectite SWa-1 Reduced 4 Hr
Cation Hydration Energy (kJ/mol)
Cation Fixed (cmol/kg)
Cu
Zn
Ca
K
2000
1500
1000
500
5
10
15
20
25
30

Smectite SWa-1

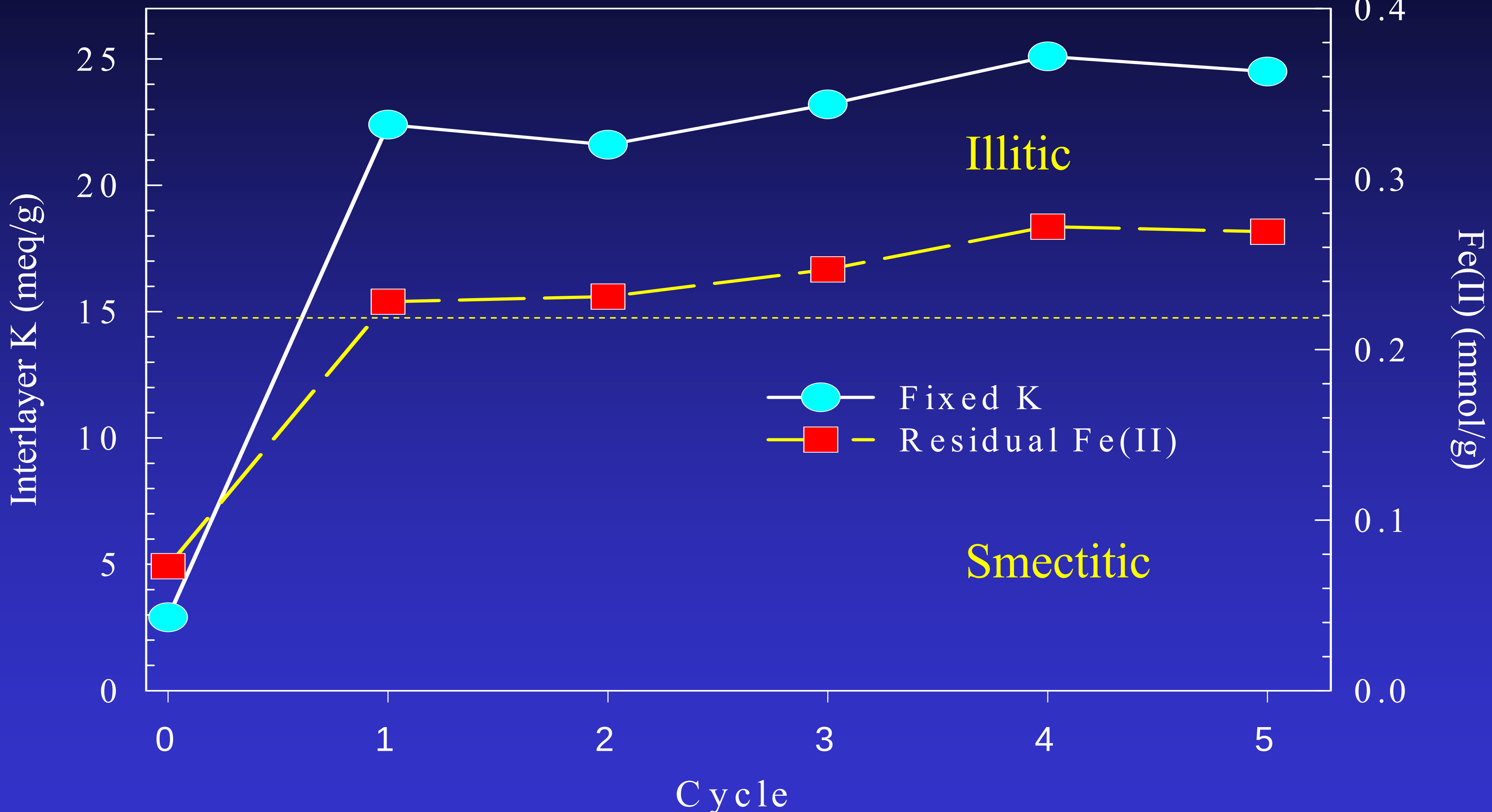

K Fixation in Na- and K-Exchanged Reduced SWa-1

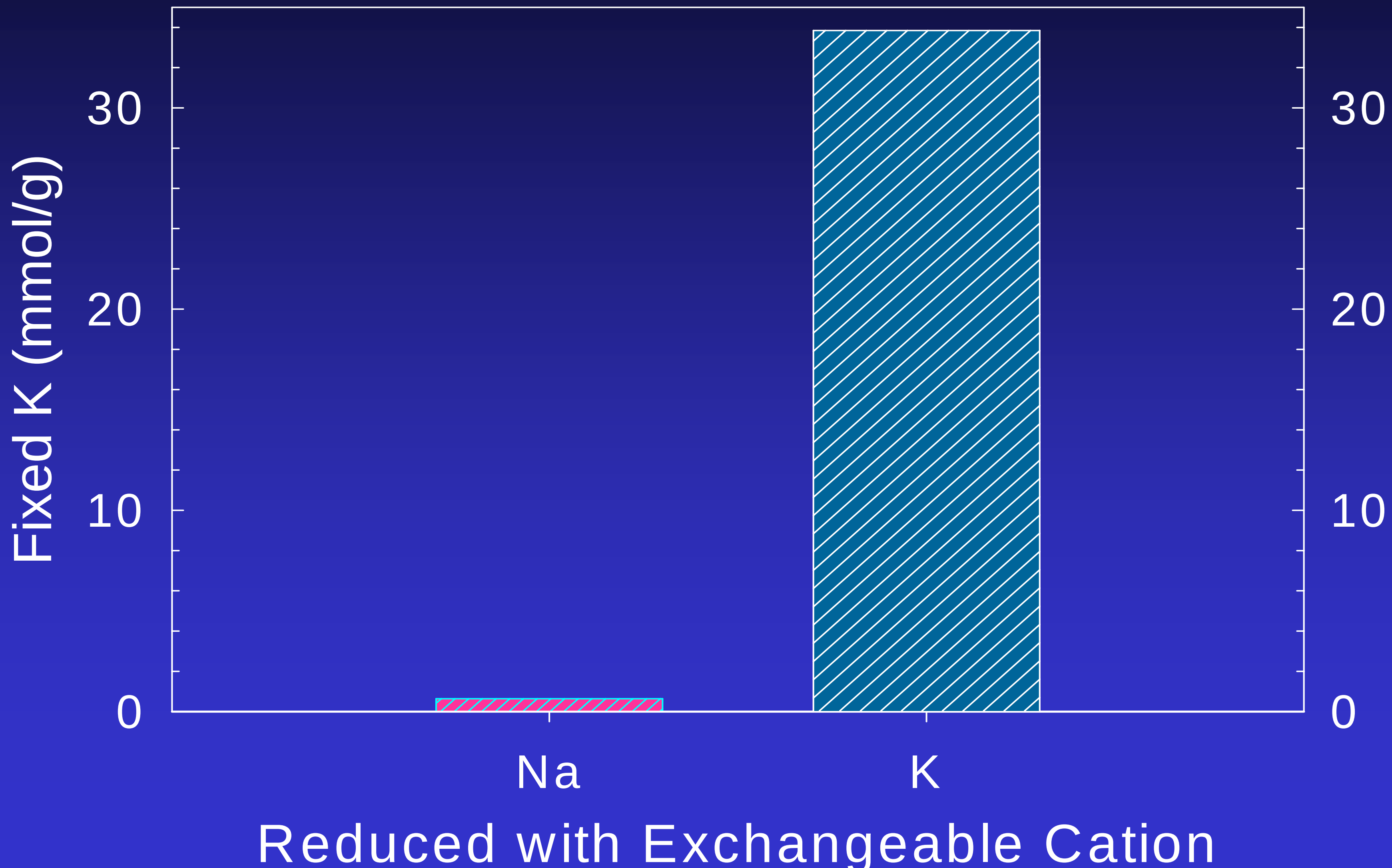

Oxidized SWa-1

Reduced SWa-1

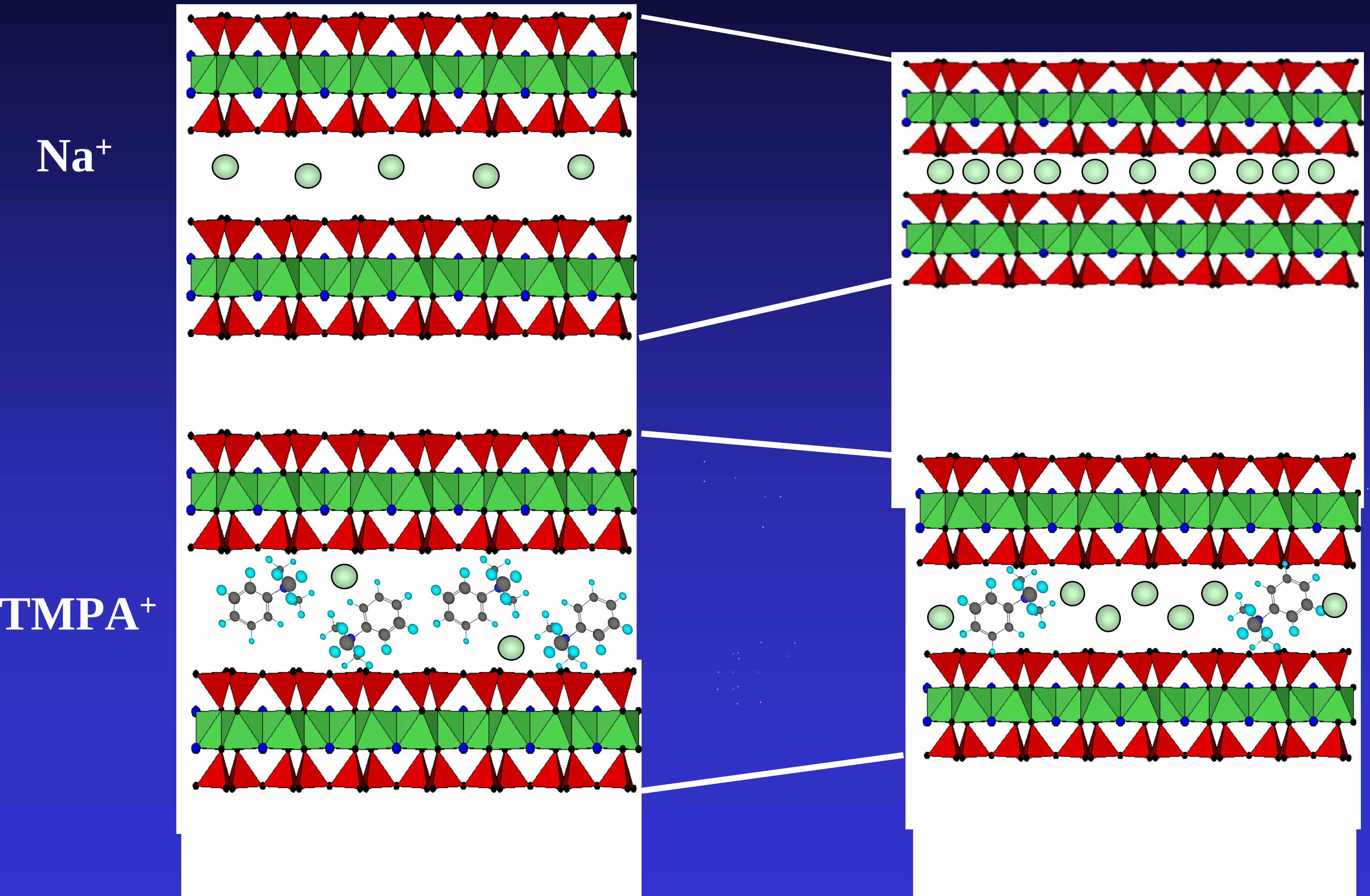

TMPA C Content in Unaltered SWa-1

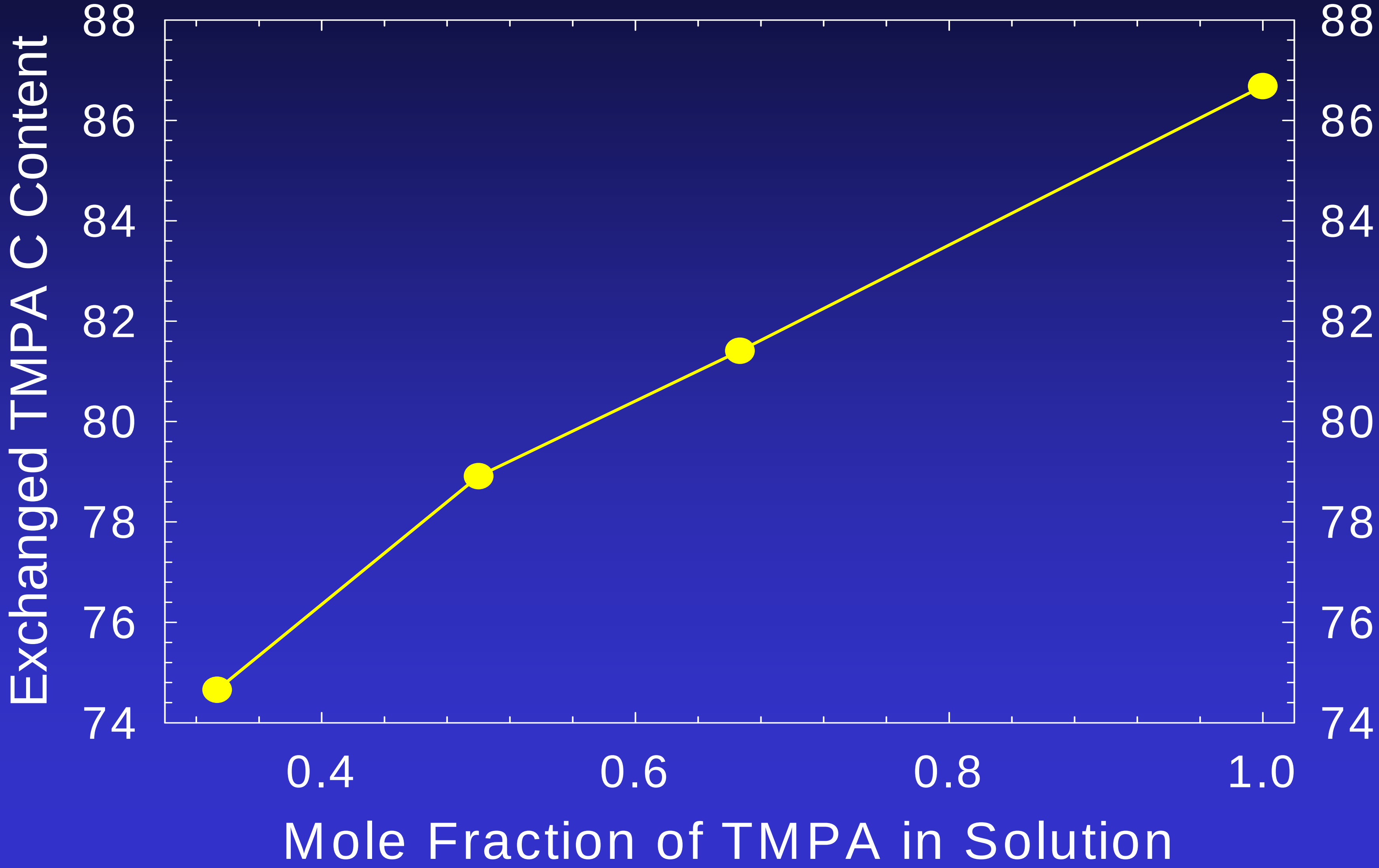

Effect of TMPA on Fixed K in Reduced SWa-1

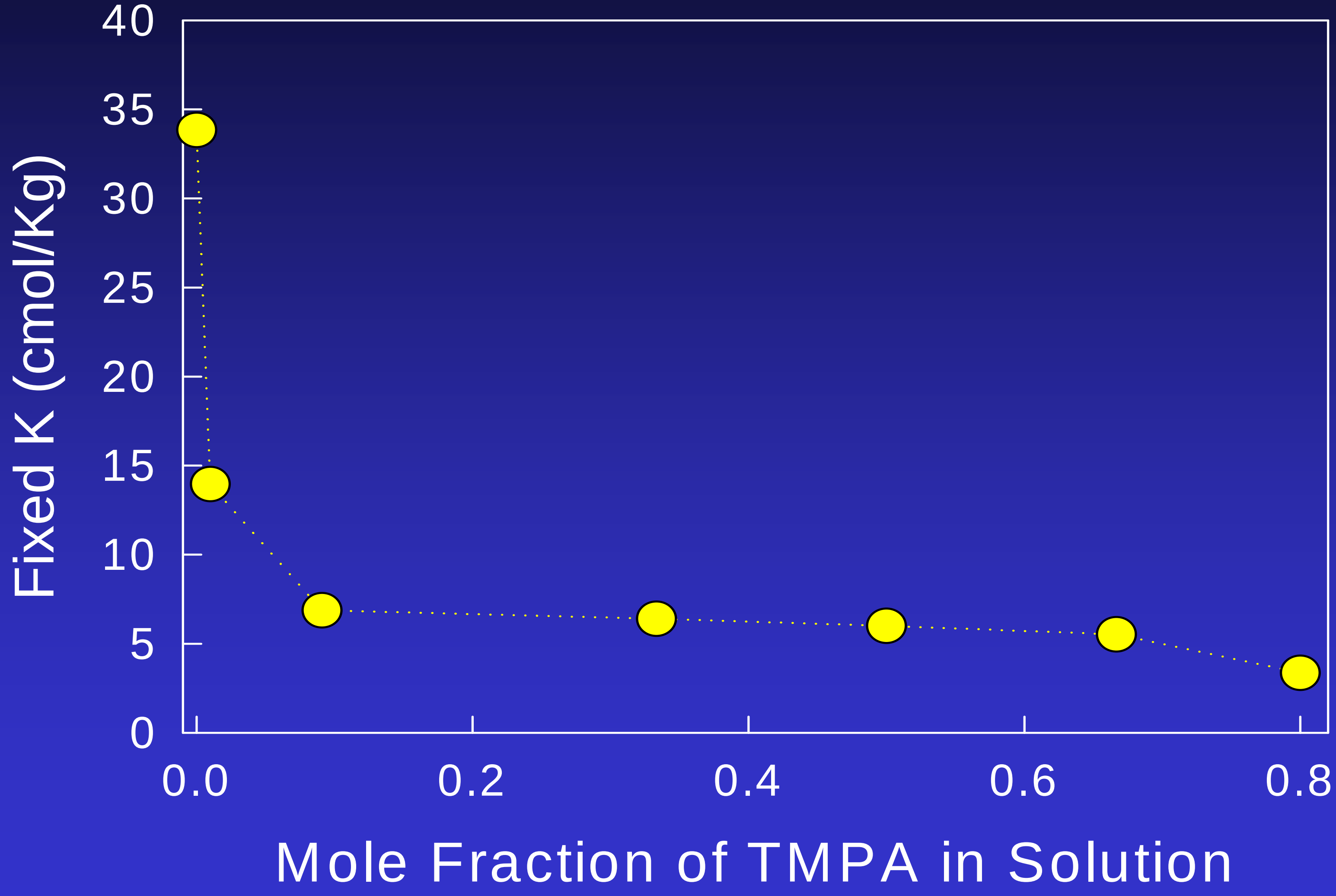

Effect of Glucosamine on K Fixation*

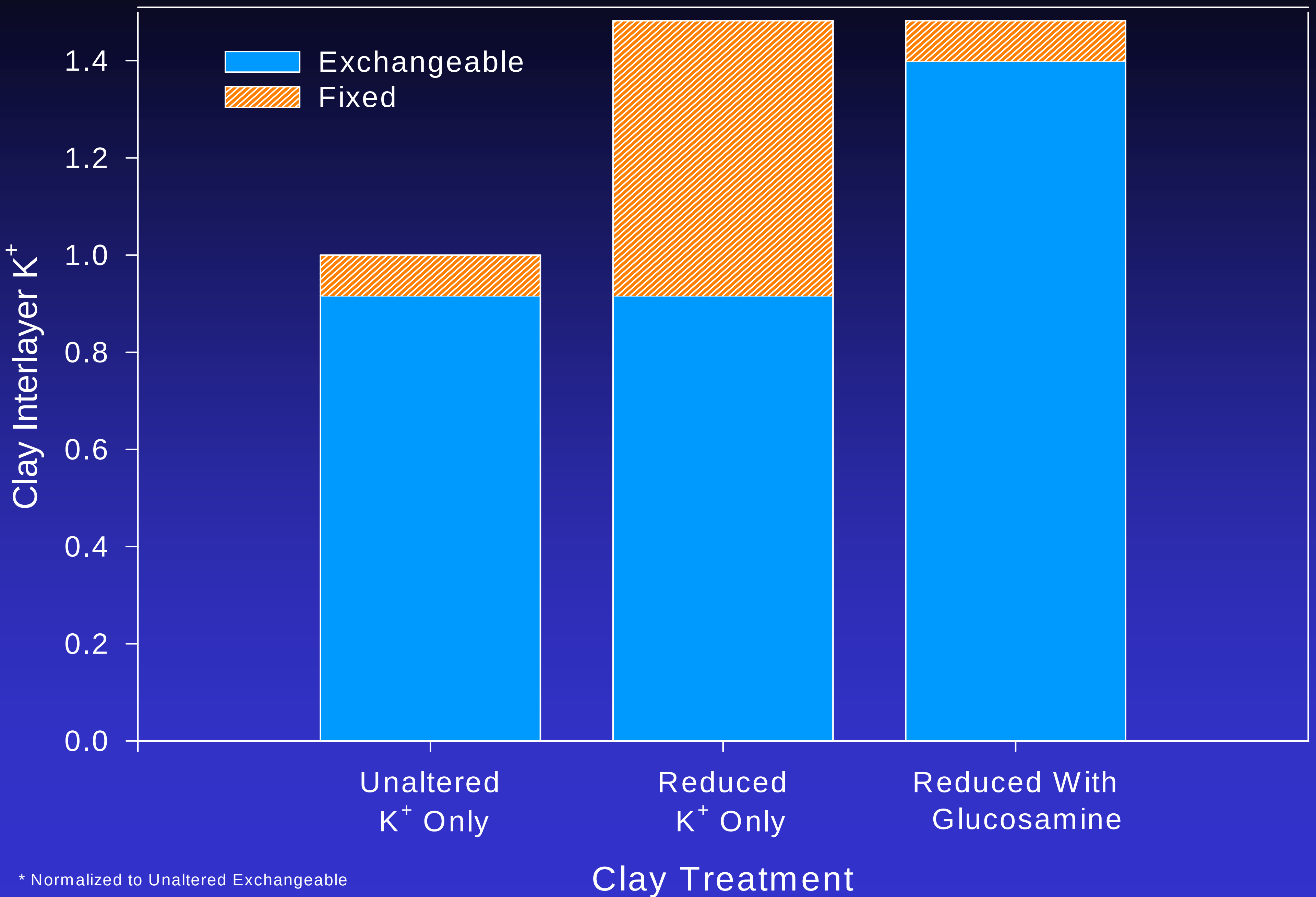

* Normalized to Unaltered Exchangeable

CLAY-ORGANIC INTERACTIONS

Joseph W. Stucki
University of Illinois

Pentachloroethane Transformation

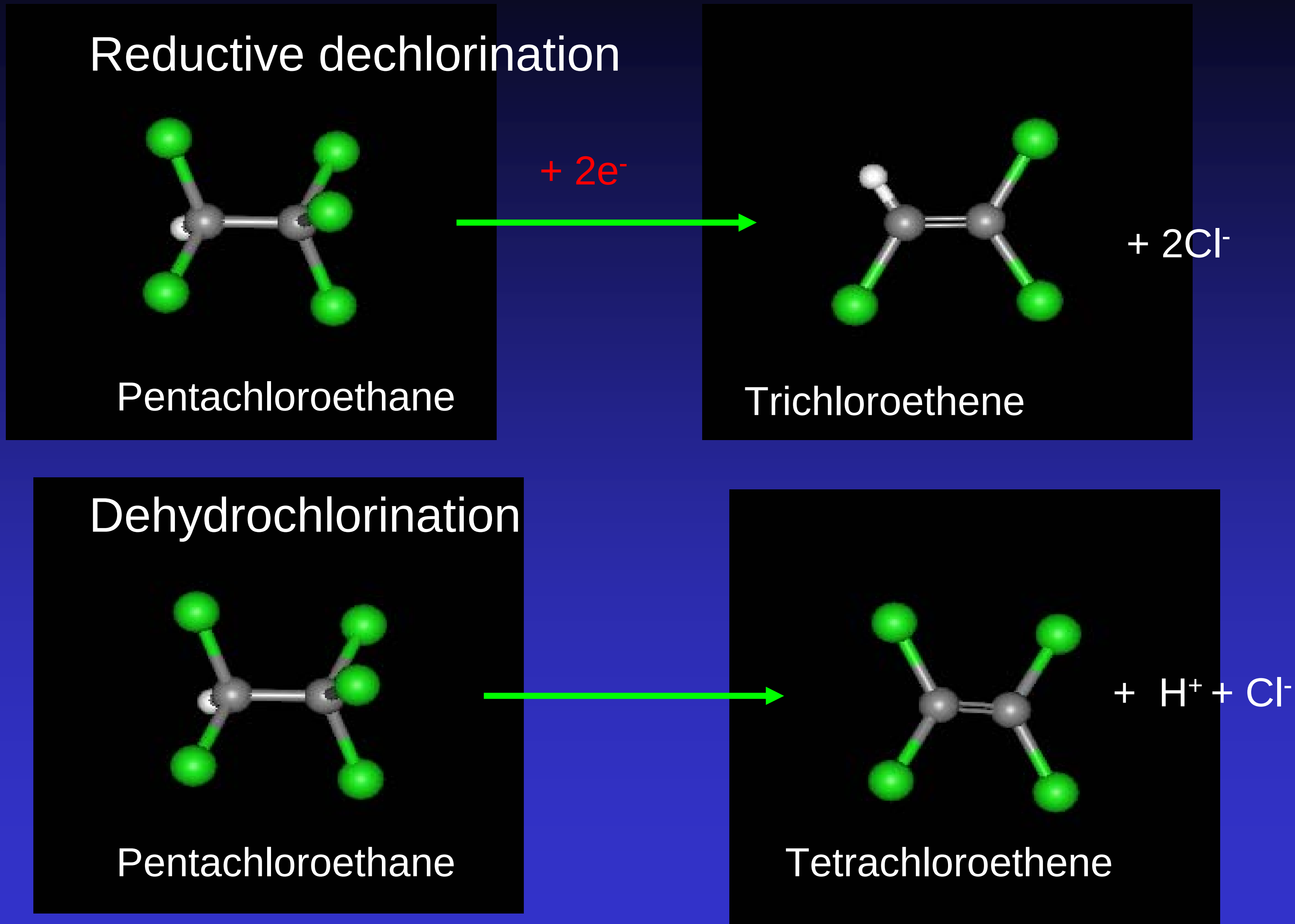

Figure drawn by Javiera Cervini-Silva

Rate of Pentachloroethane Transformation in NG-1

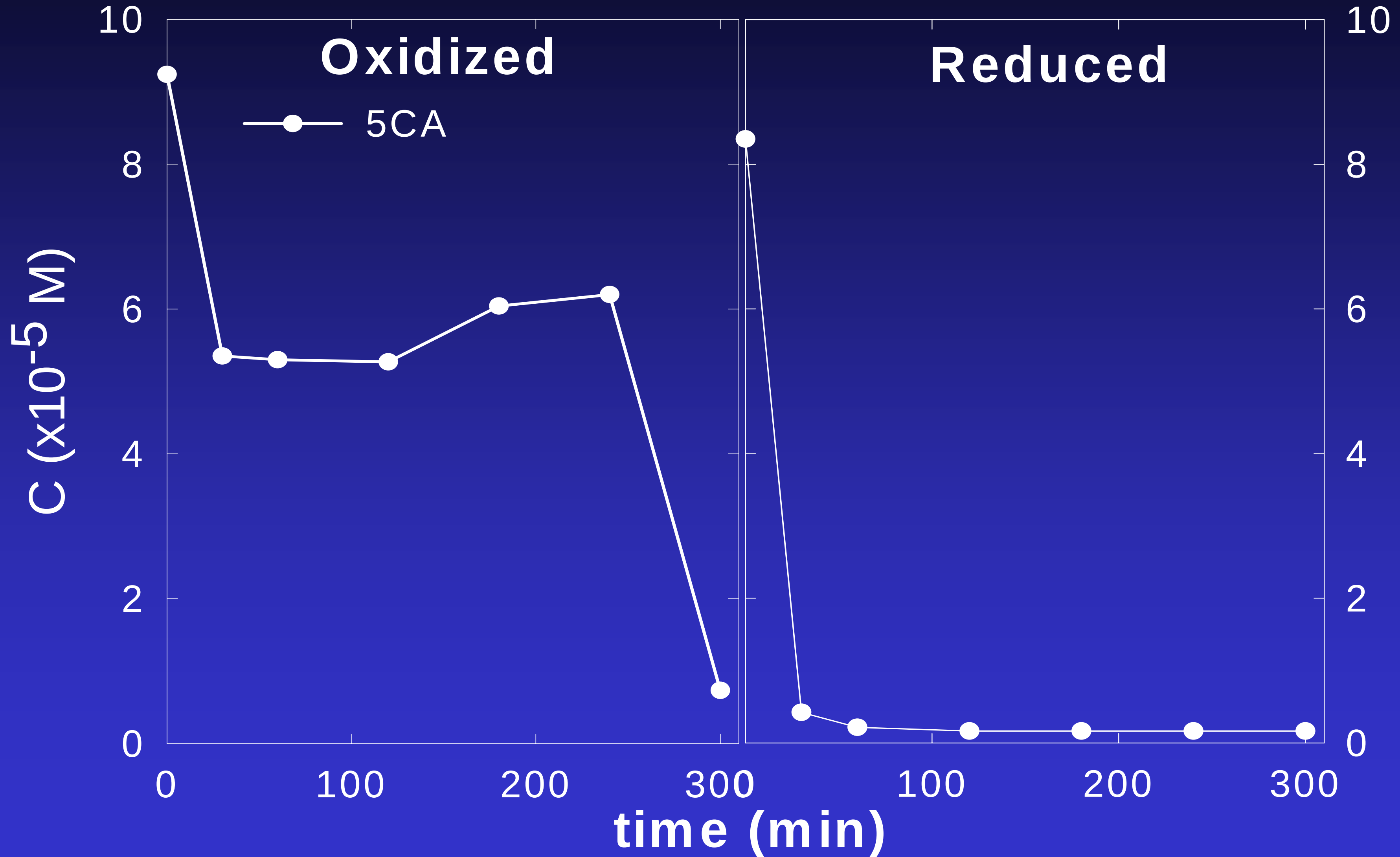

From Cervini-Silva et al., 2000, Clays Clay Miner. 48:132-138

Rate of Pentachloroethane Transformation in NG-1

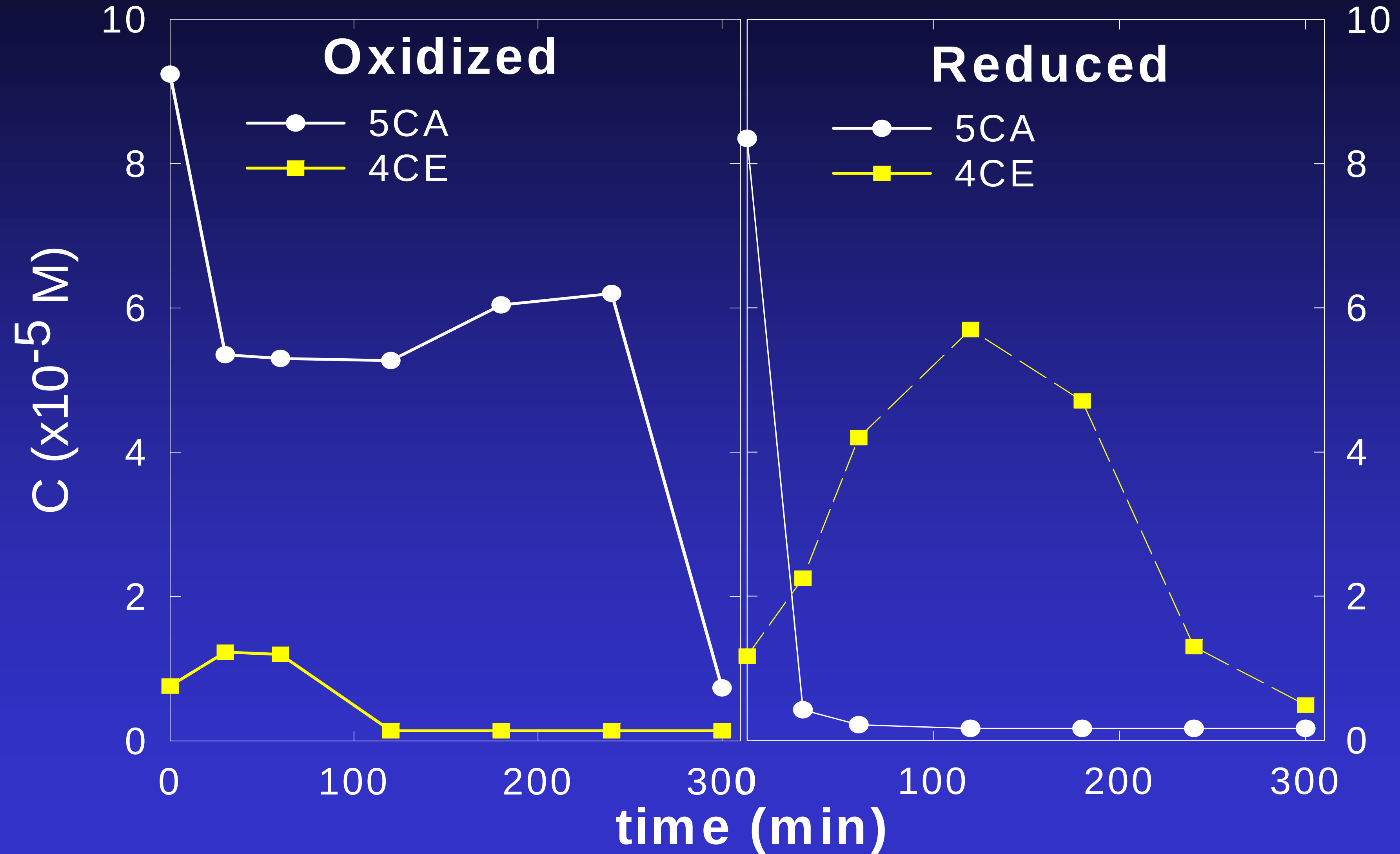

From Cervini-Silva et al., 2000, Clays Clay Miner. 48:132-138

Rate of Pentachloroethane Transformation

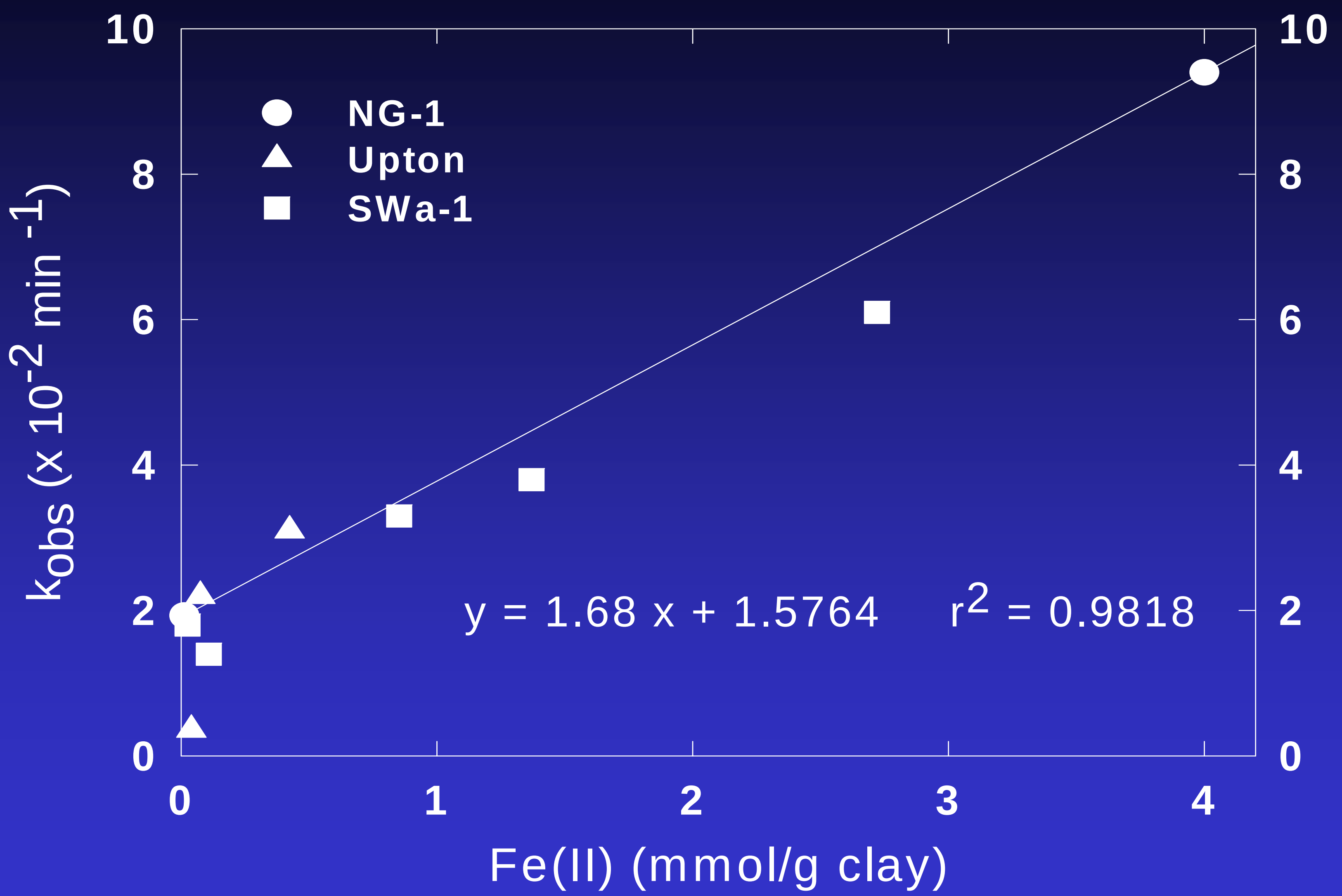

From Cervini-Silva et al., 2000, Clays Clay Miner. 48:132-138

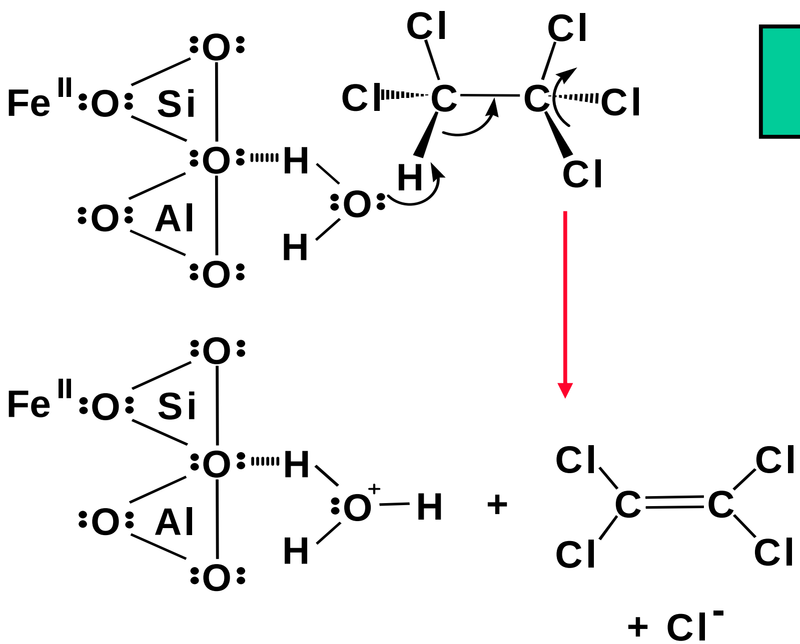

pentachloroethane

reduced smectite acts as a Bronsted base

tetrachloroethene

From Cervini-Silva et al., 2000, Clays Clay Miner. 48:132-138

Atrazine Transformation

Structure of Atrazine

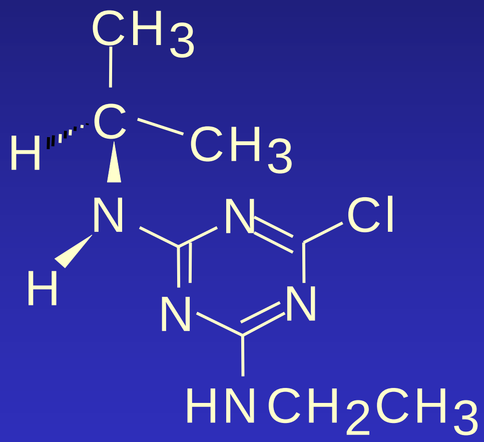

Atrazine Reacted with SWa-1

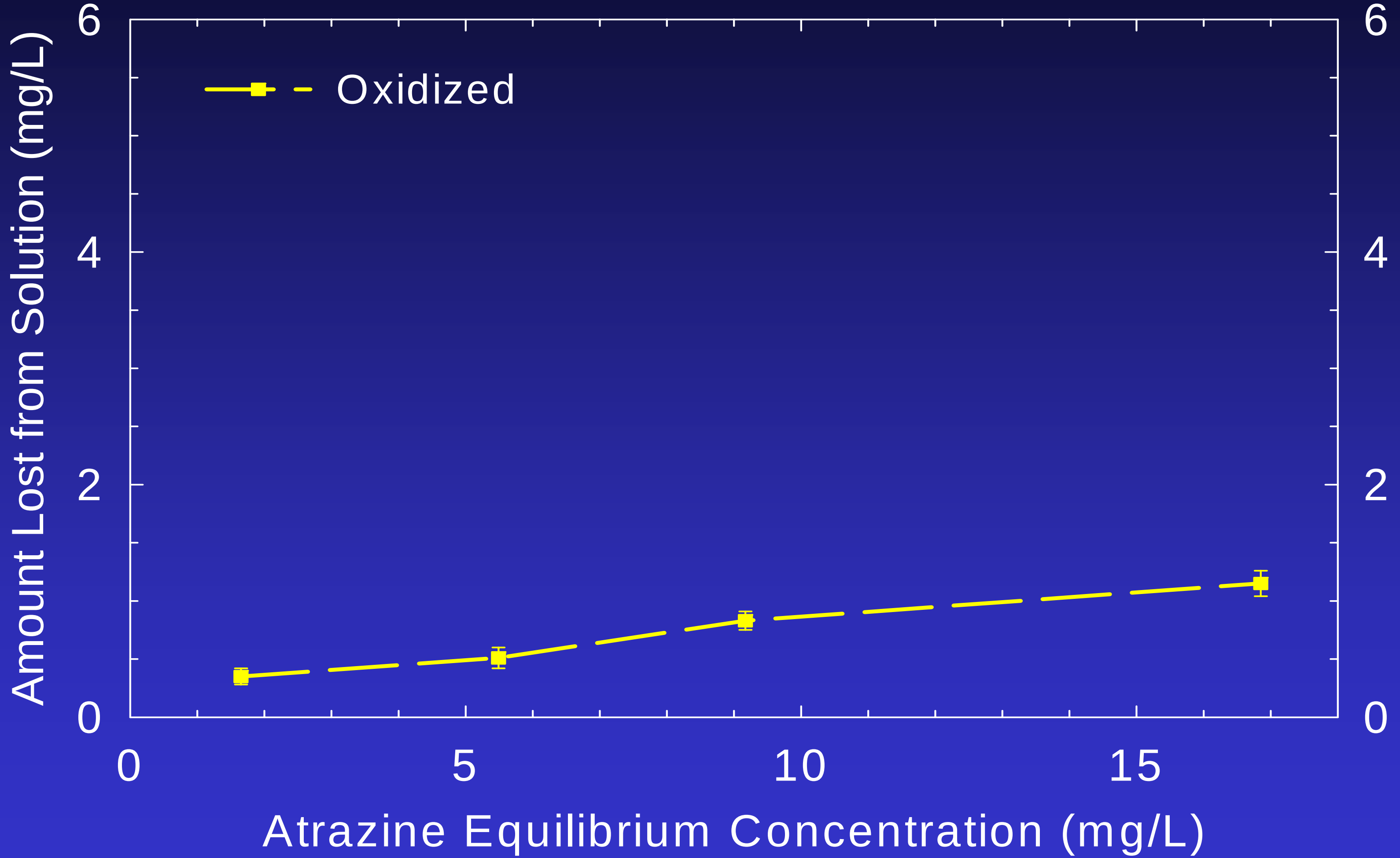

From Xu et al., 2001, Environ. Toxicol. Chem (in press)

Atrazine Reacted with SWa-1

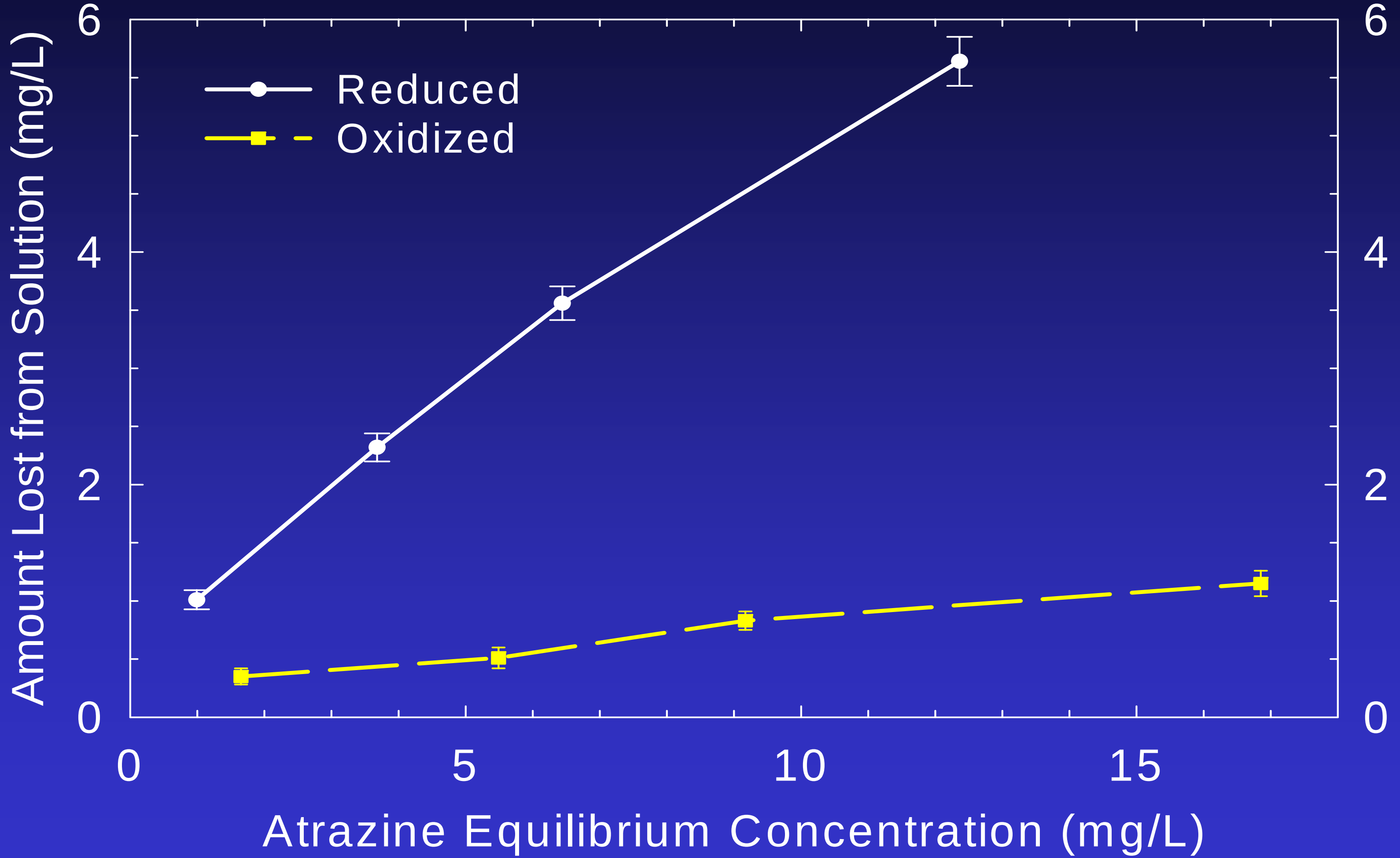

From Xu et al., 2001, Environ. Toxicol. Chem (in press)

Atrazine Reacted with SWa-1

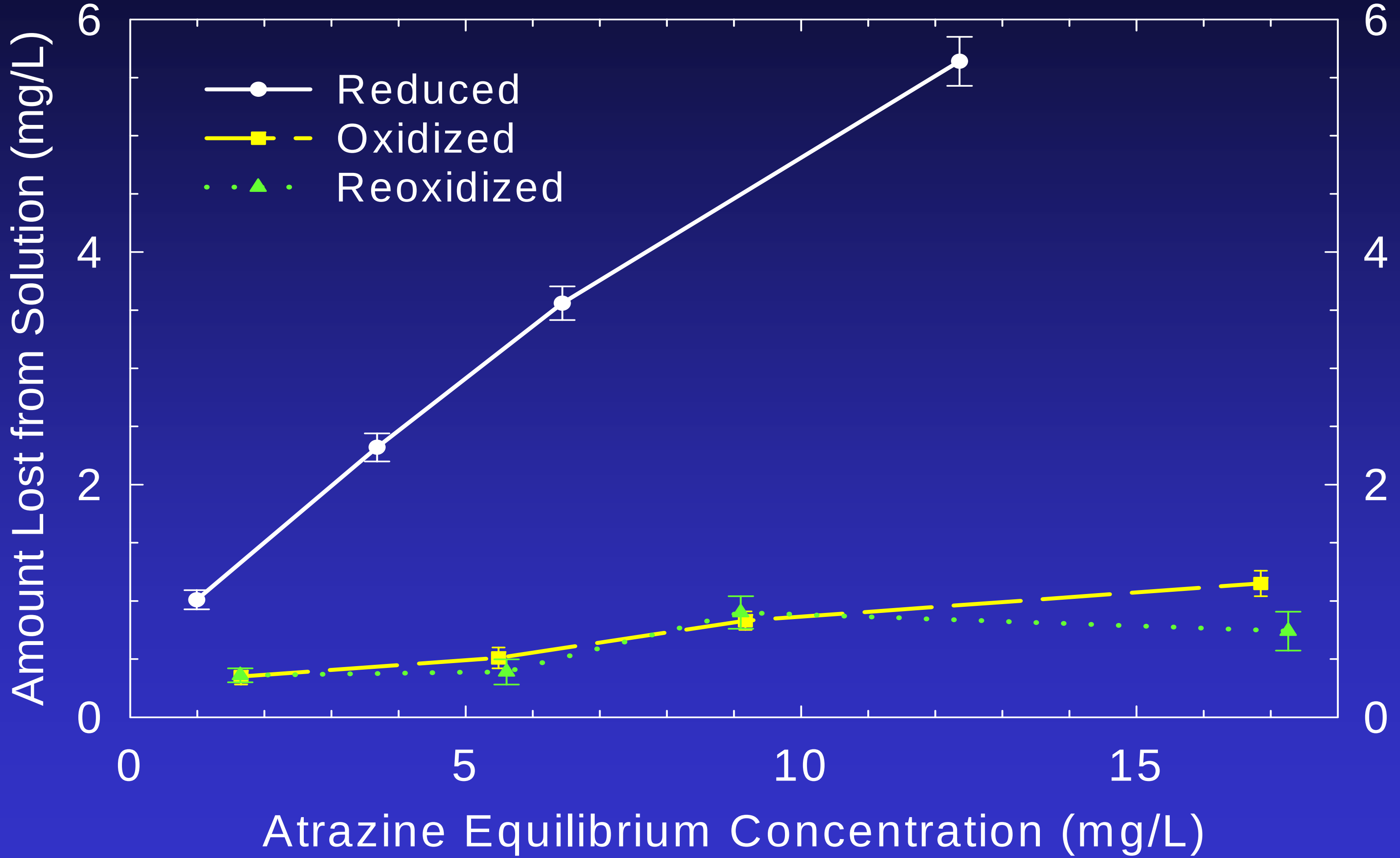

From Xu et al., 2001, Environ. Toxicol. Chem (in press)

Atrazine Reacted with SWa-1

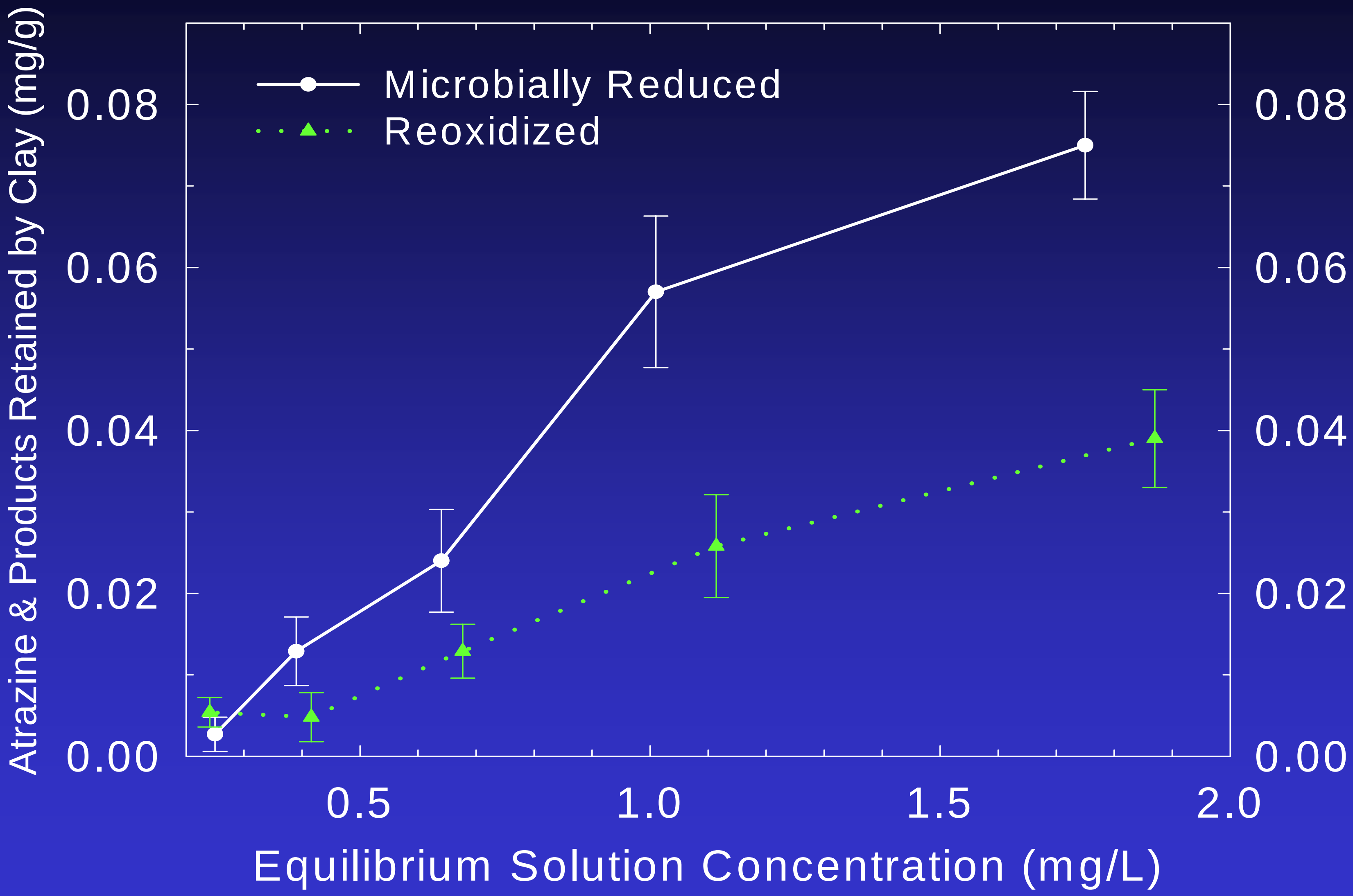

From Xu et al., 2001, Environ. Toxicol. Chem (in press)

HPLC of ^{14}C-Atrazine with Oxidized SWa-1

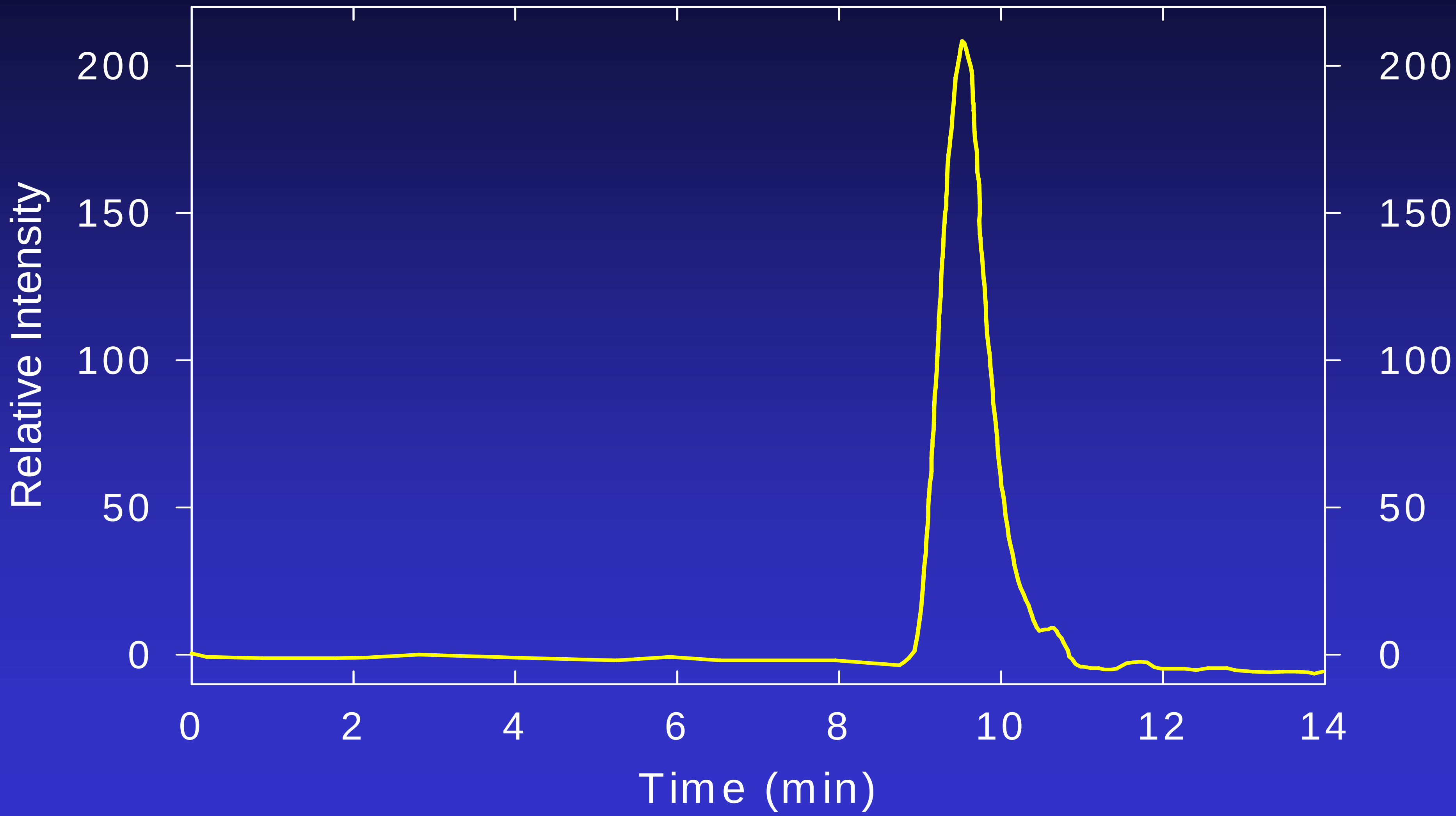

(from Xu, 1998)

HPLC of ^{14}C-Atrazine with Reduced SWa-1

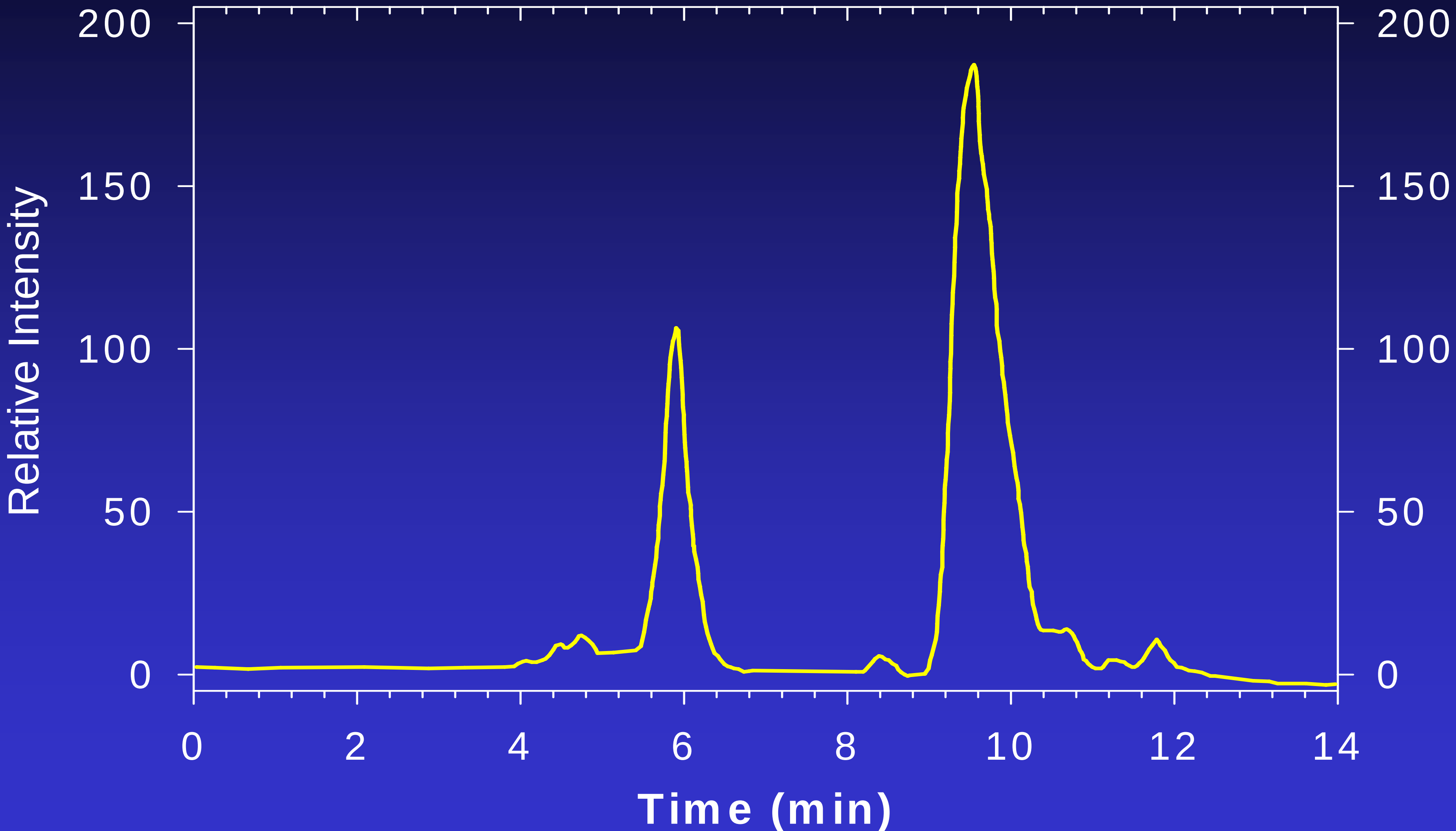

(from Xu, 1998)

Atrazine

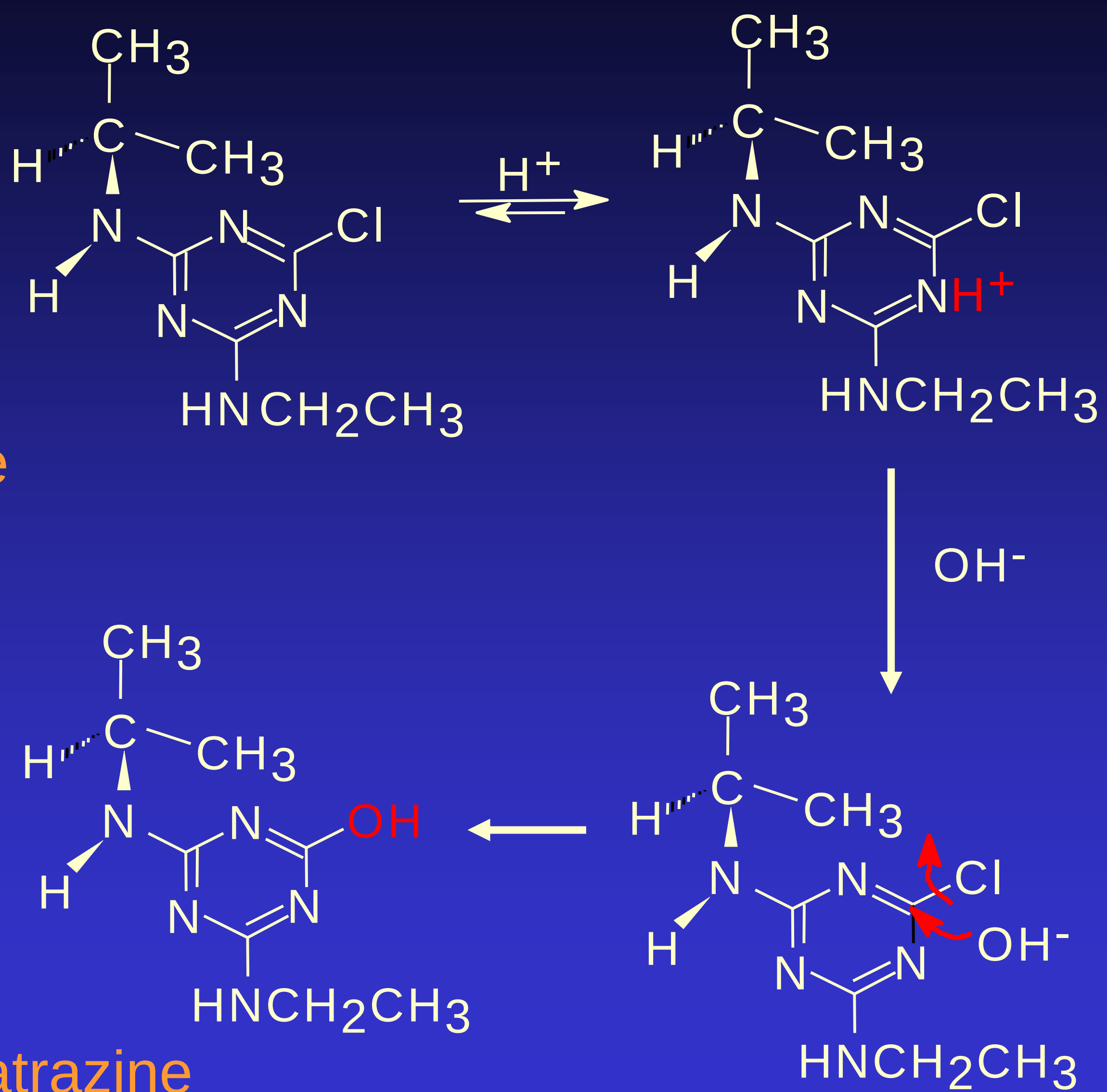

Bimolecular substitution (S_N2)

Hydroxyatrazine

Alachlor Transformation

Structure of Alachlor

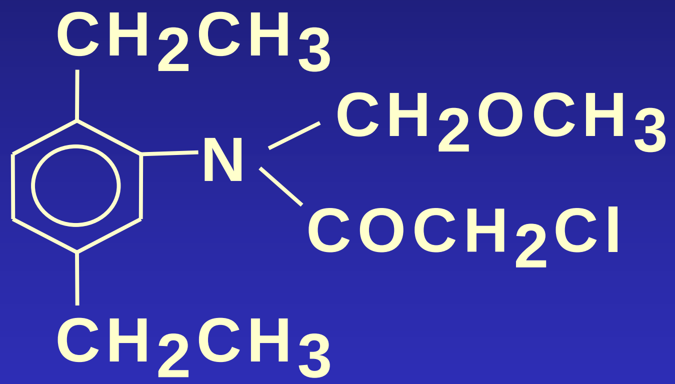

Alachlor Reacted with SWa-1

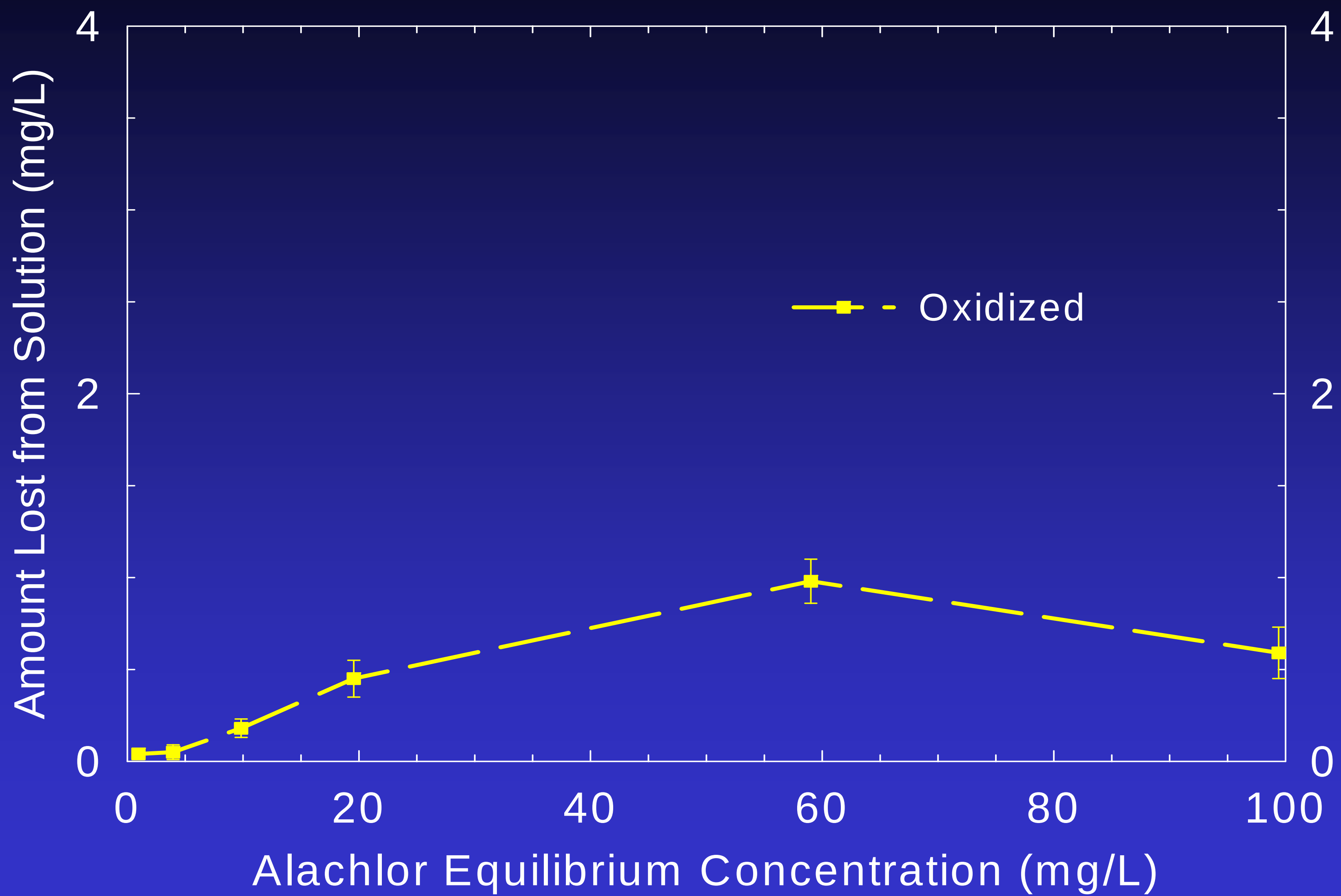

From Xu et al., 2001, Environ. Toxicol. Chem (in press)

Alachlor Reacted with SWa-1

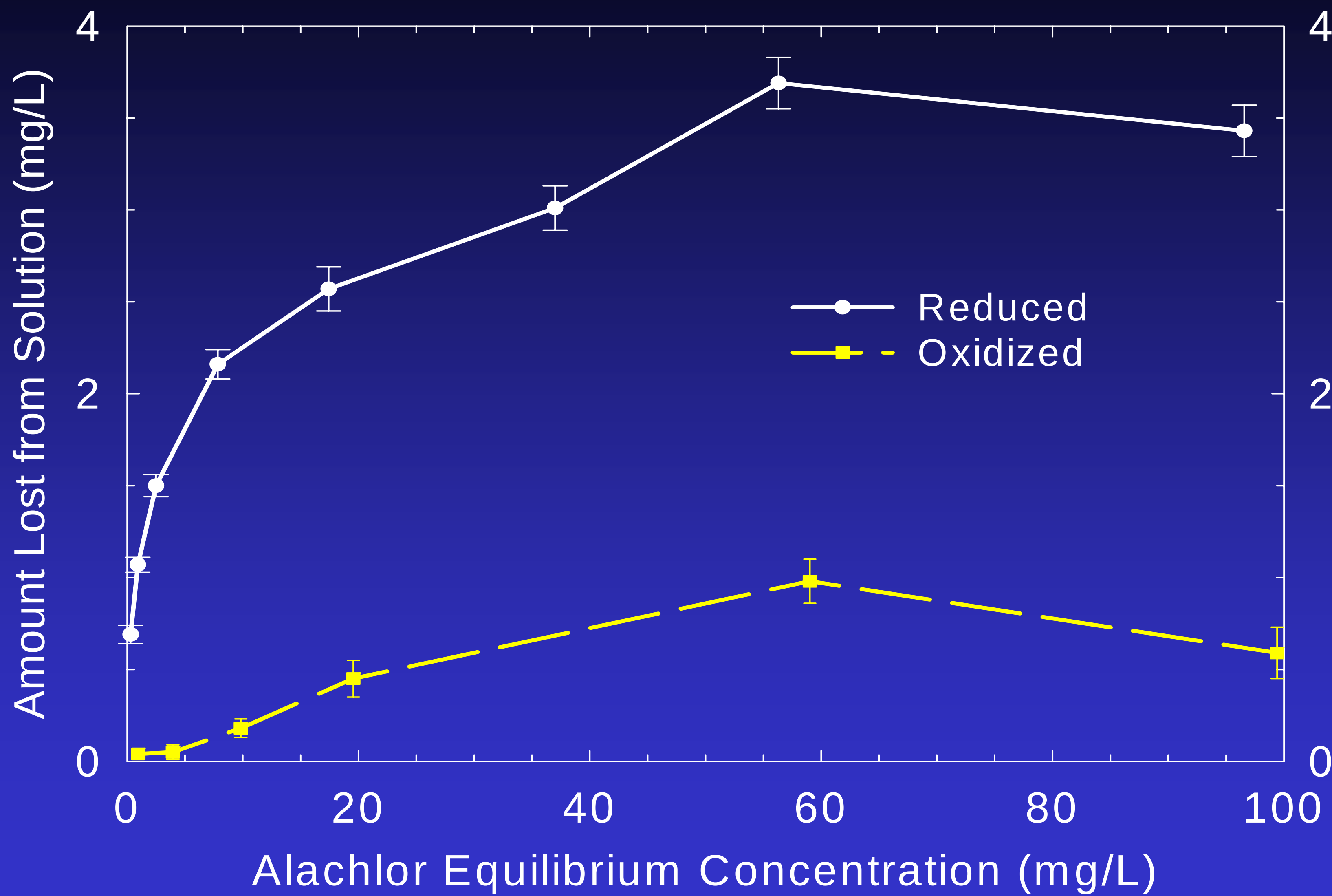

From Xu et al., 2001, Environ. Toxicol. Chem (in press)

Alachlor Reacted with SWa-1

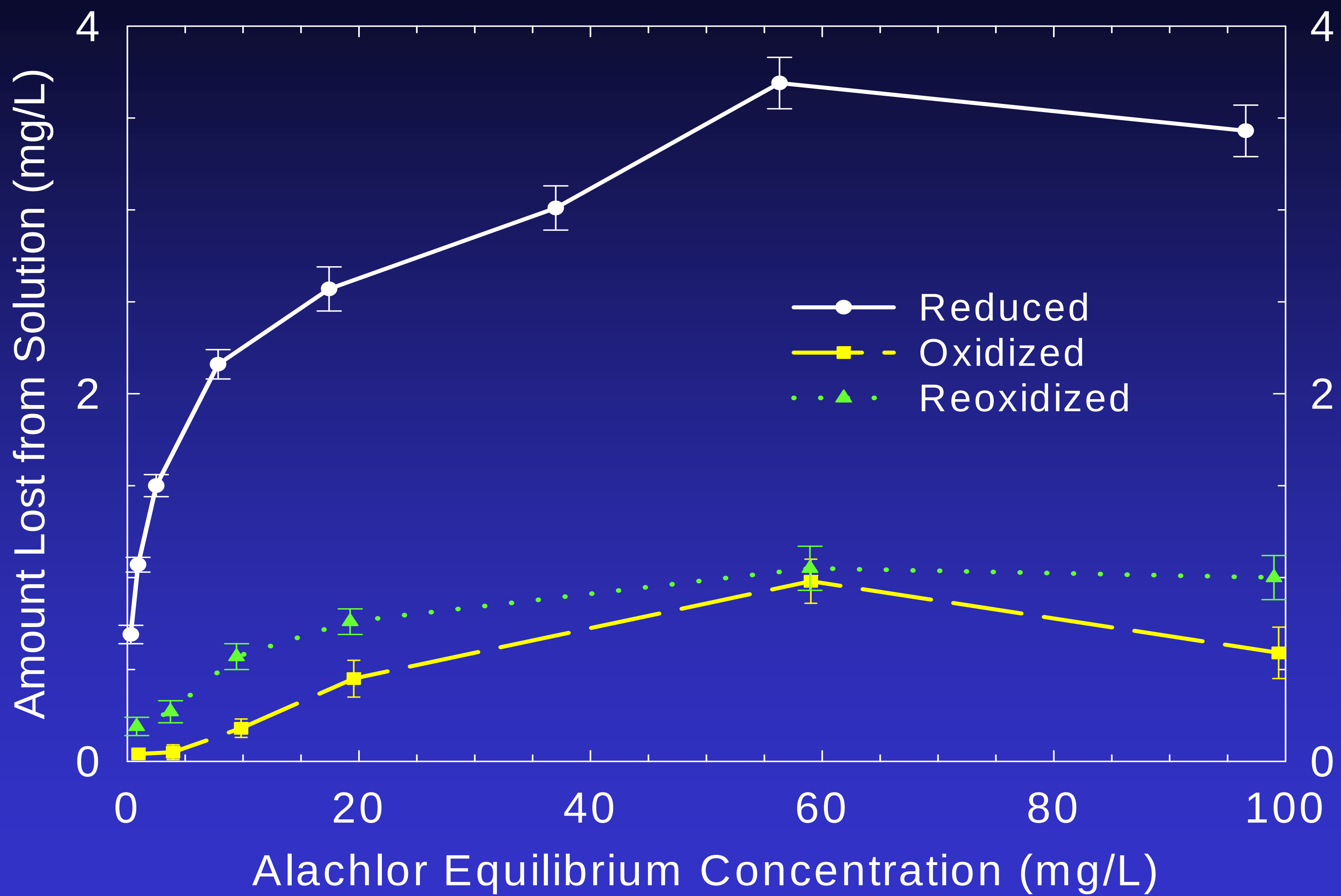

From Xu et al., 2001, Environ. Toxicol. Chem (in press)

Alachlor Reacted with SWa-1

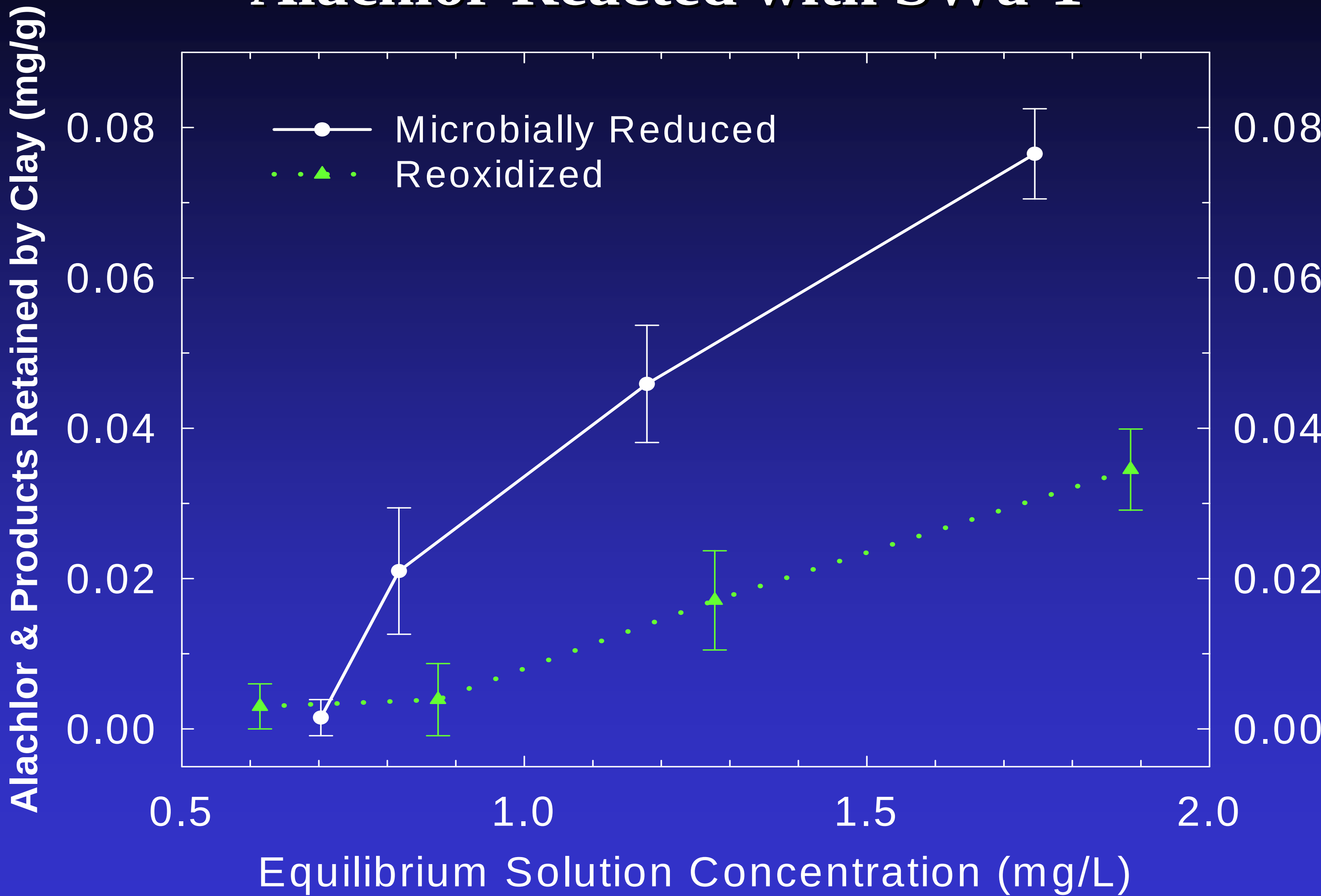

From Xu et al., 2001, Environ. Toxicol. Chem (in press)

HPLC of Alachlor with Oxidized SWa-1

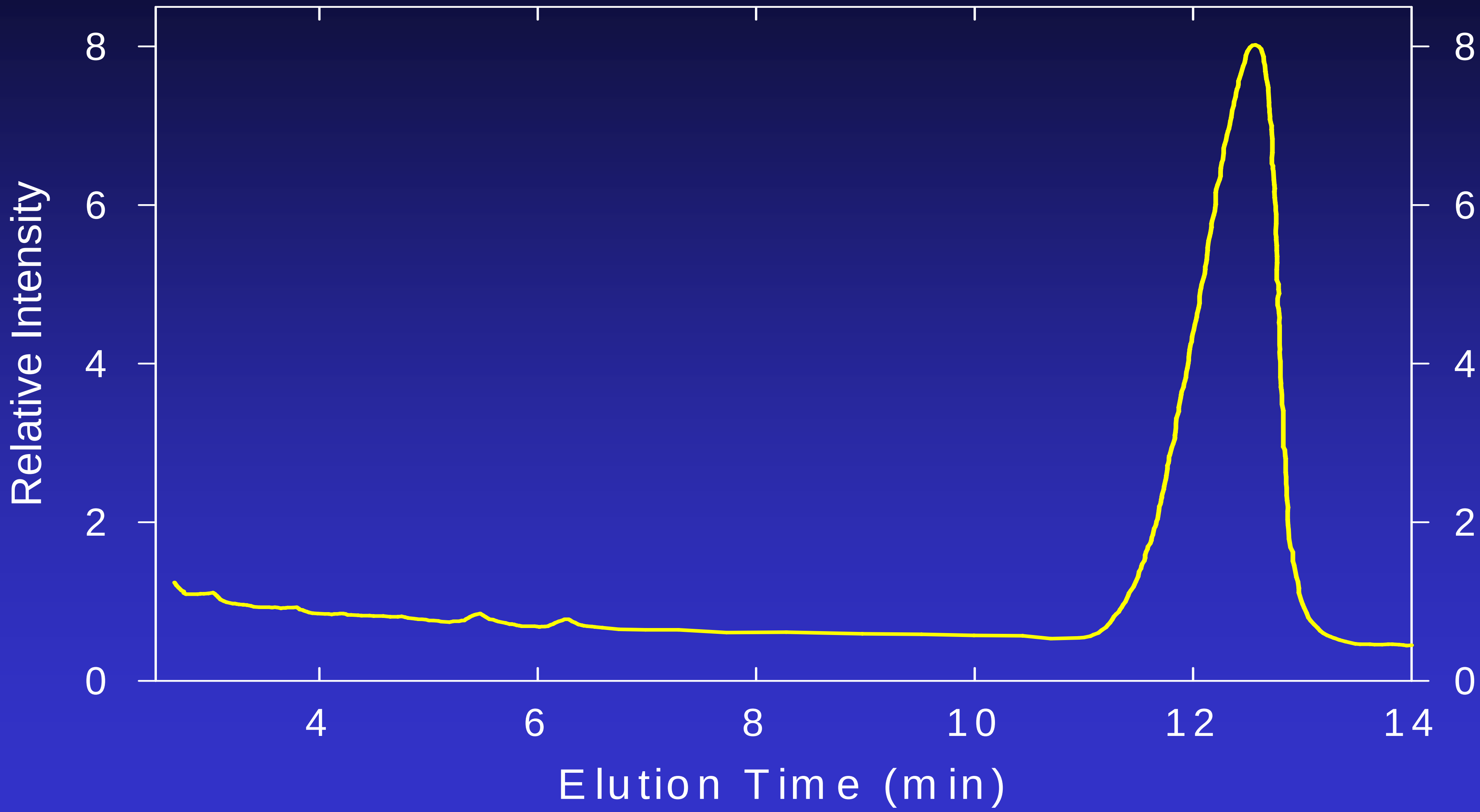

(from Xu, 1998)

HPLC of Alachlor in Reduced SWa-1

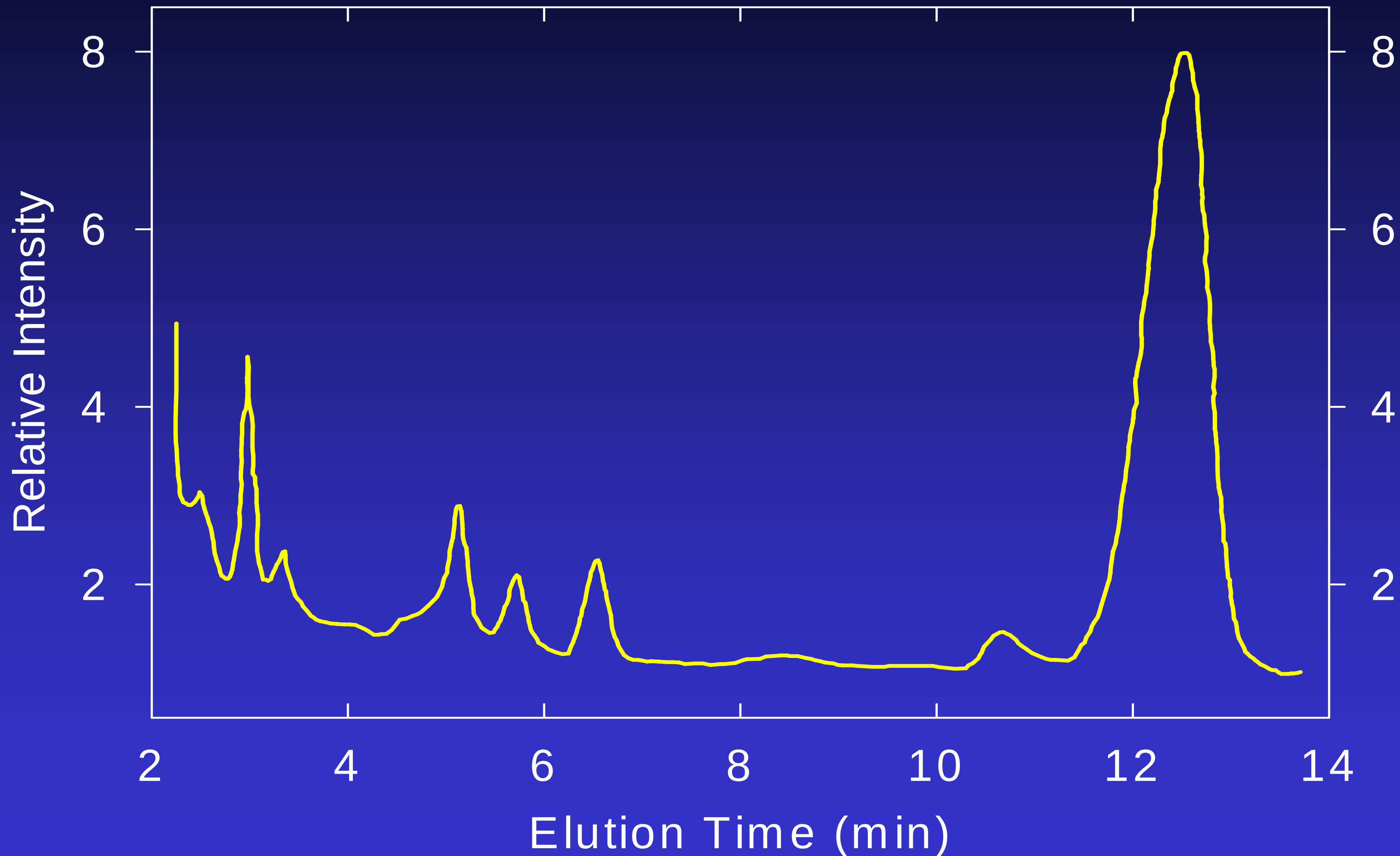

(from Xu, 1998)

Alachlor

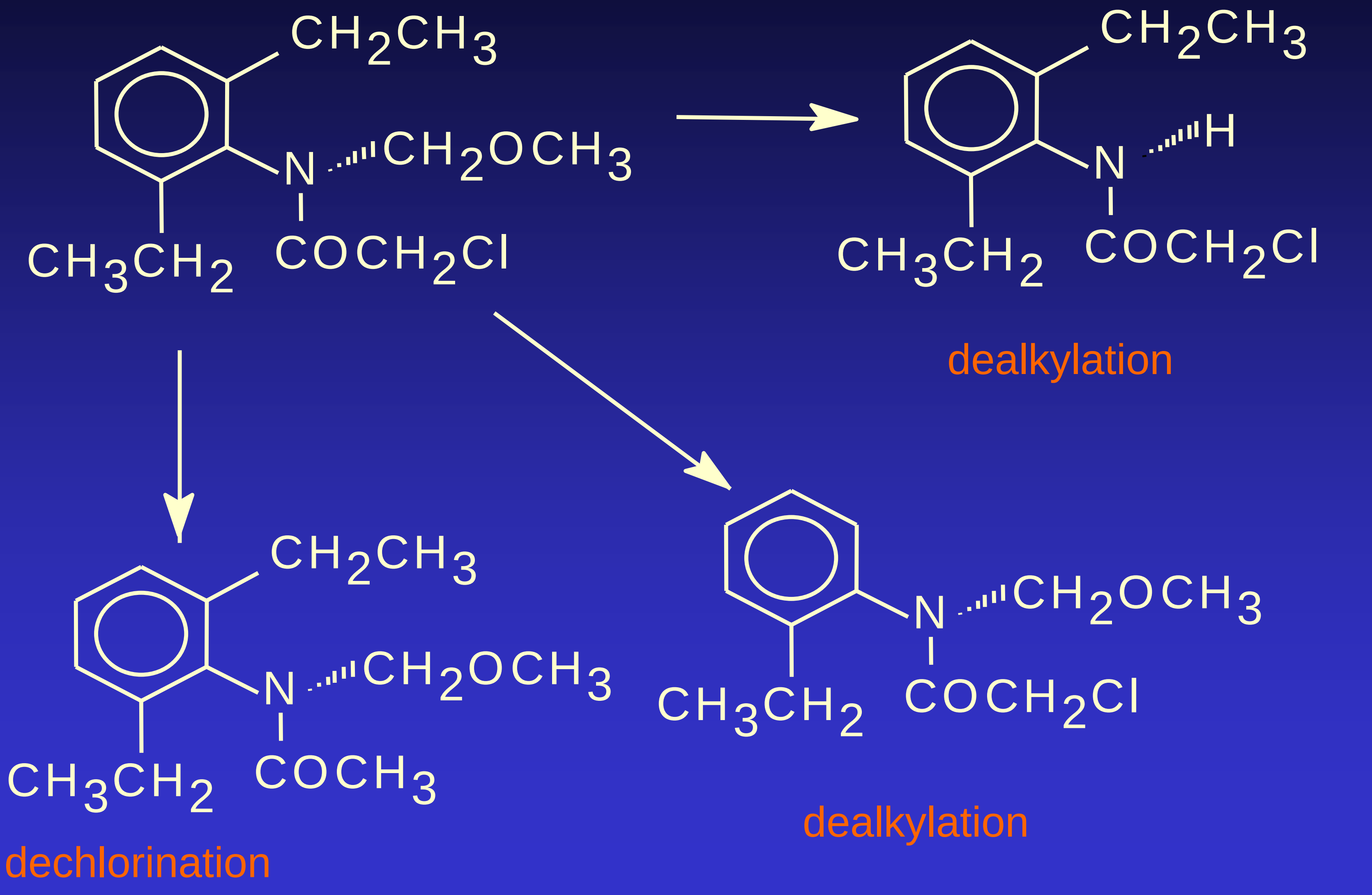

CH2CH3
N
CH2OCH3
CH3CH2
COCH2Cl
CH2CH3
N
H
CH3CH2
COCH2Cl
dealkylation
CH2CH3
N
CH2OCH3
CH3CH2
COCH3
dechlorination
N
CH2OCH3
CH3CH2
COCH2Cl
dealkylation

Trifluralin Transformation

Structure of Trifluralin

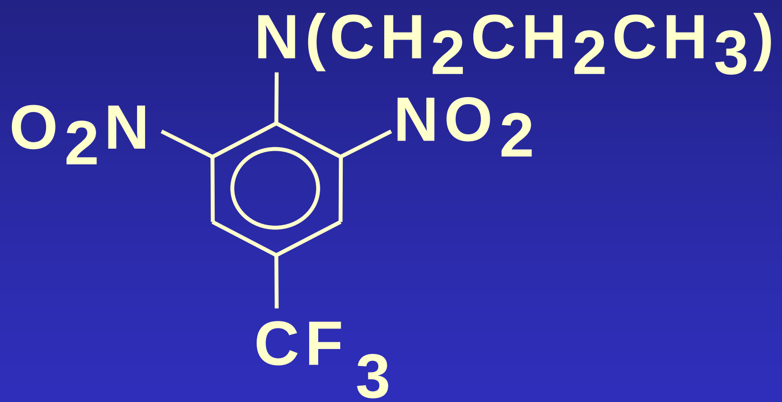

Trifluralin Reacted with SWa-1

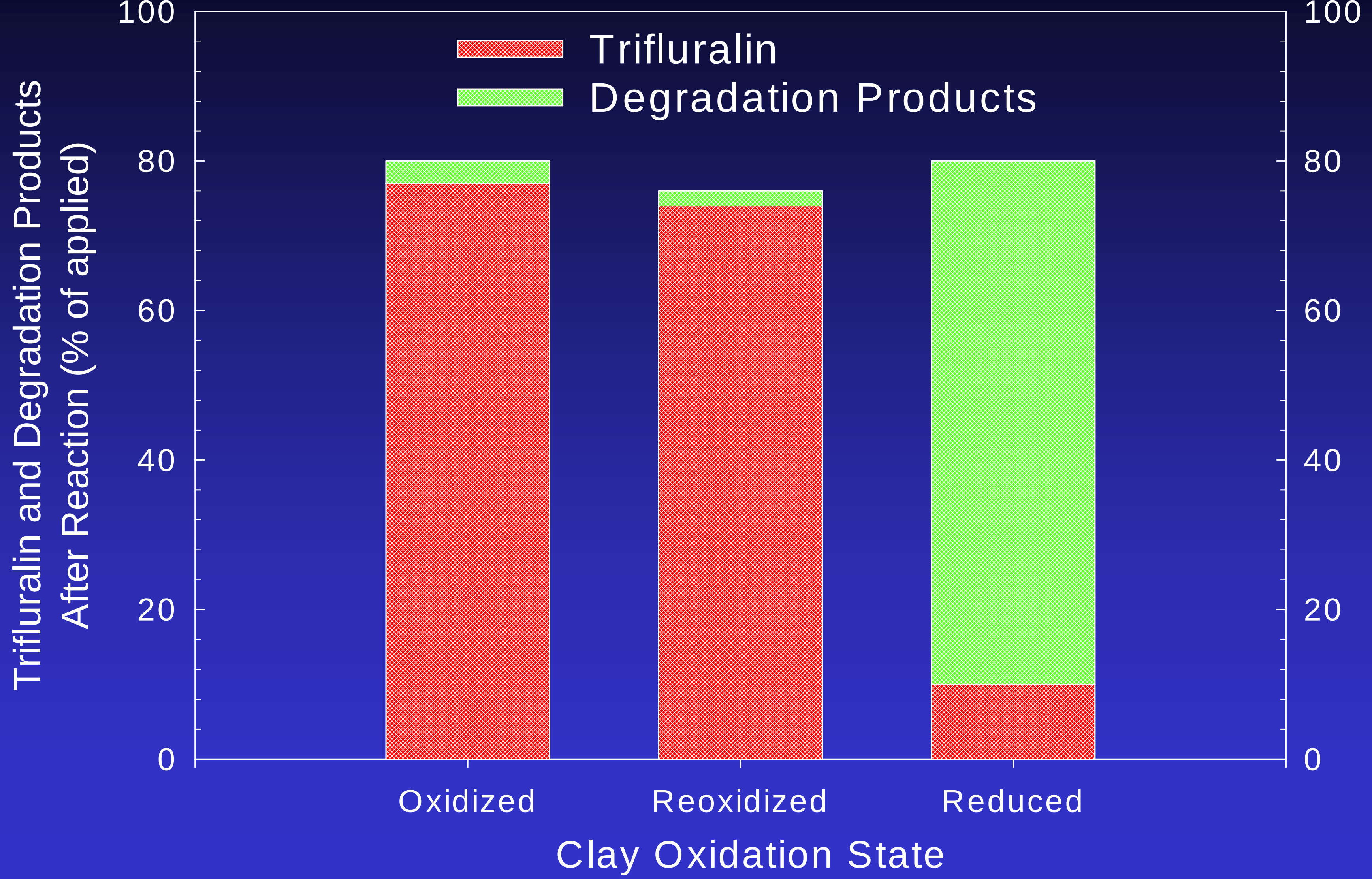

From Tor et al., 2000, Environ. Sci. Technol. 34:3148-3152

Chloropicrin Transformation

Structure of Chloropicrin

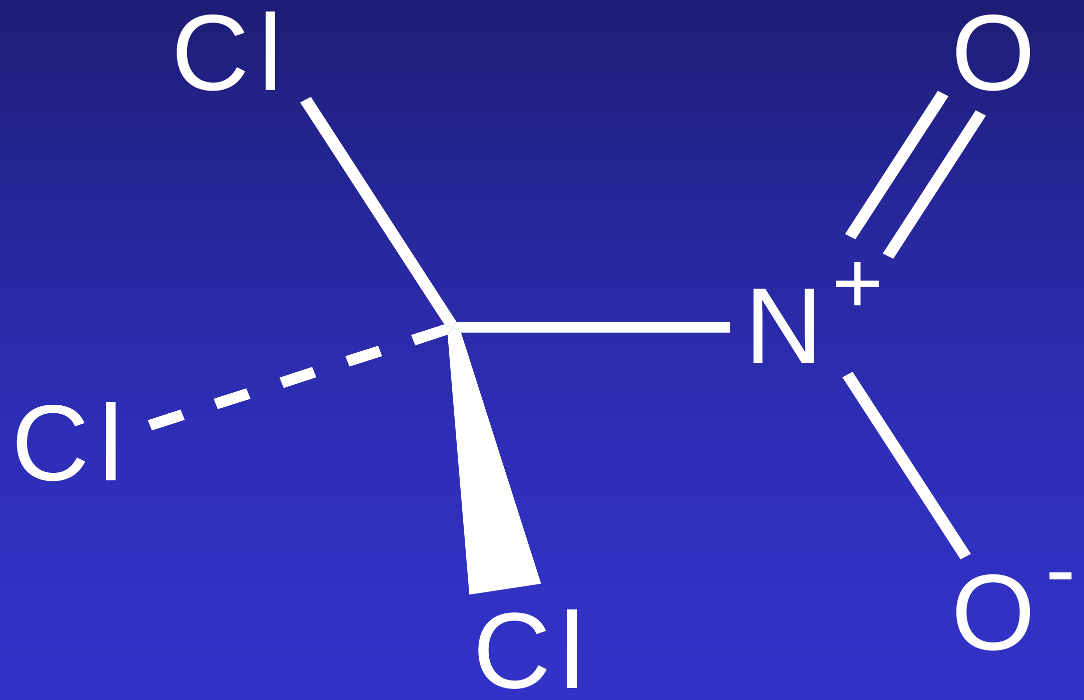

Trichloronitromethane

Chloropicrin Reaction Products

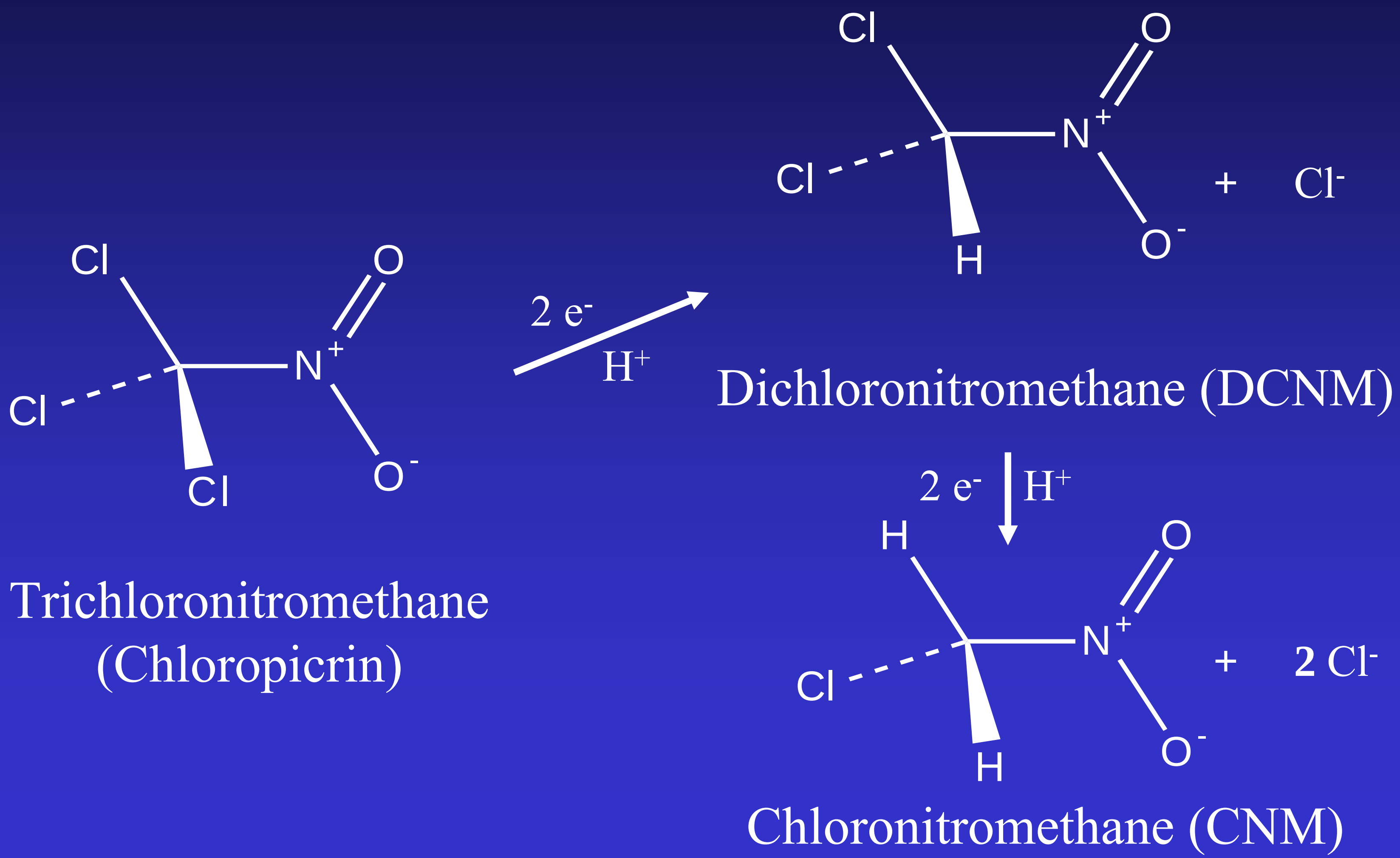

Chloropicrin Reacted with SWa-1

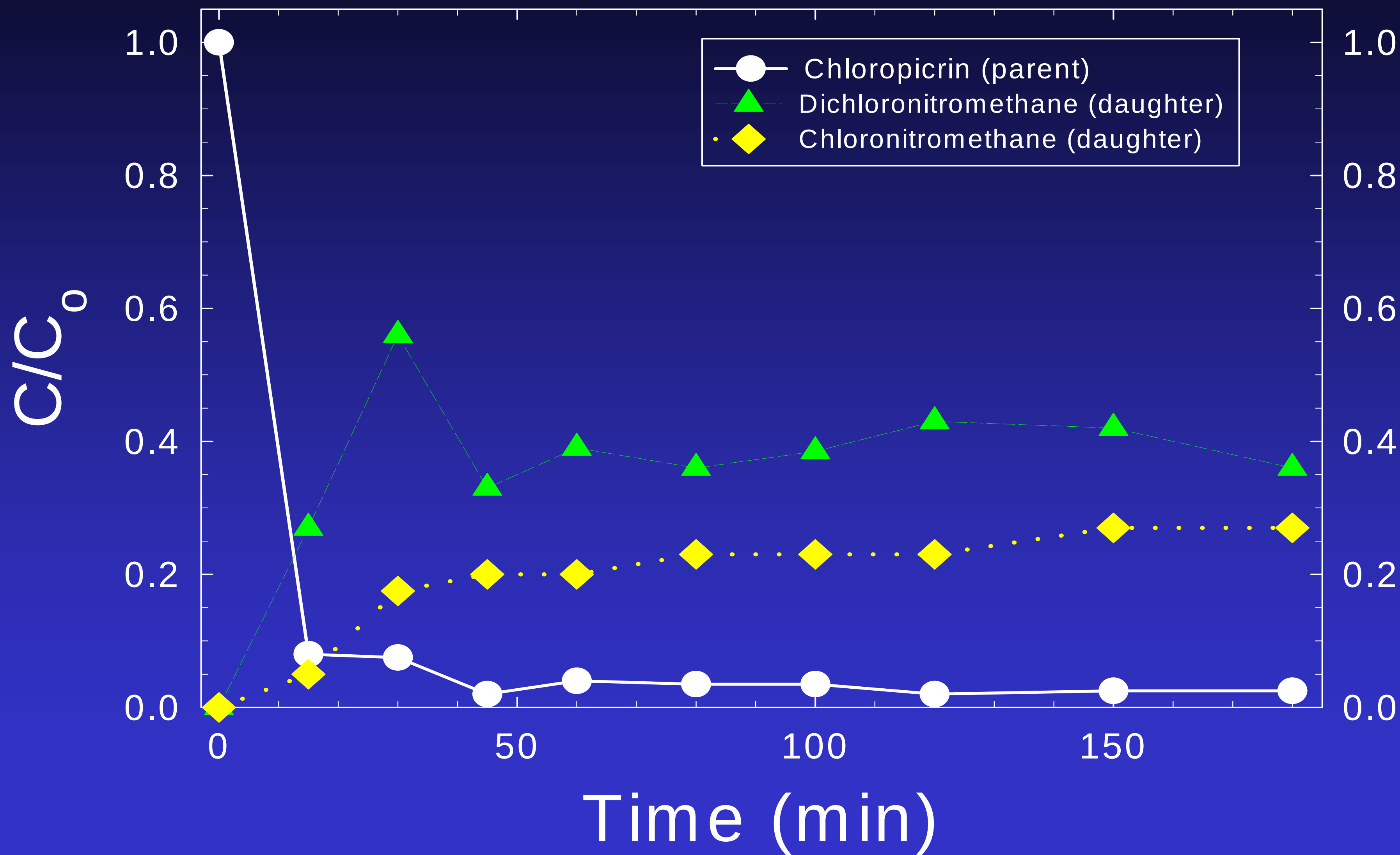

From Cervini-Silva et al., 2000, Environ. Sci. Technol. 34:915-917

Chloropicrin Reaction Products

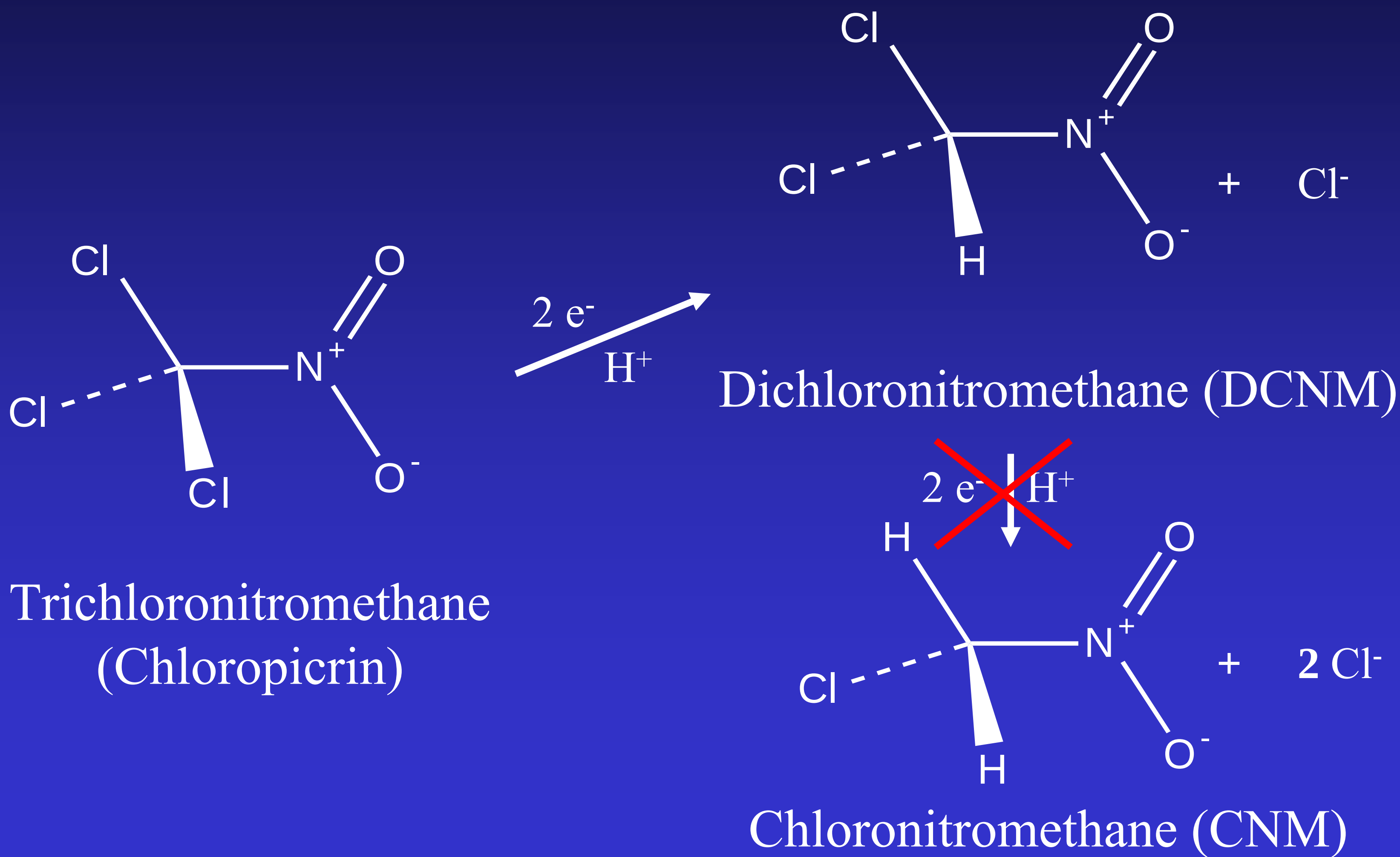

Chloropicrin Reaction Products

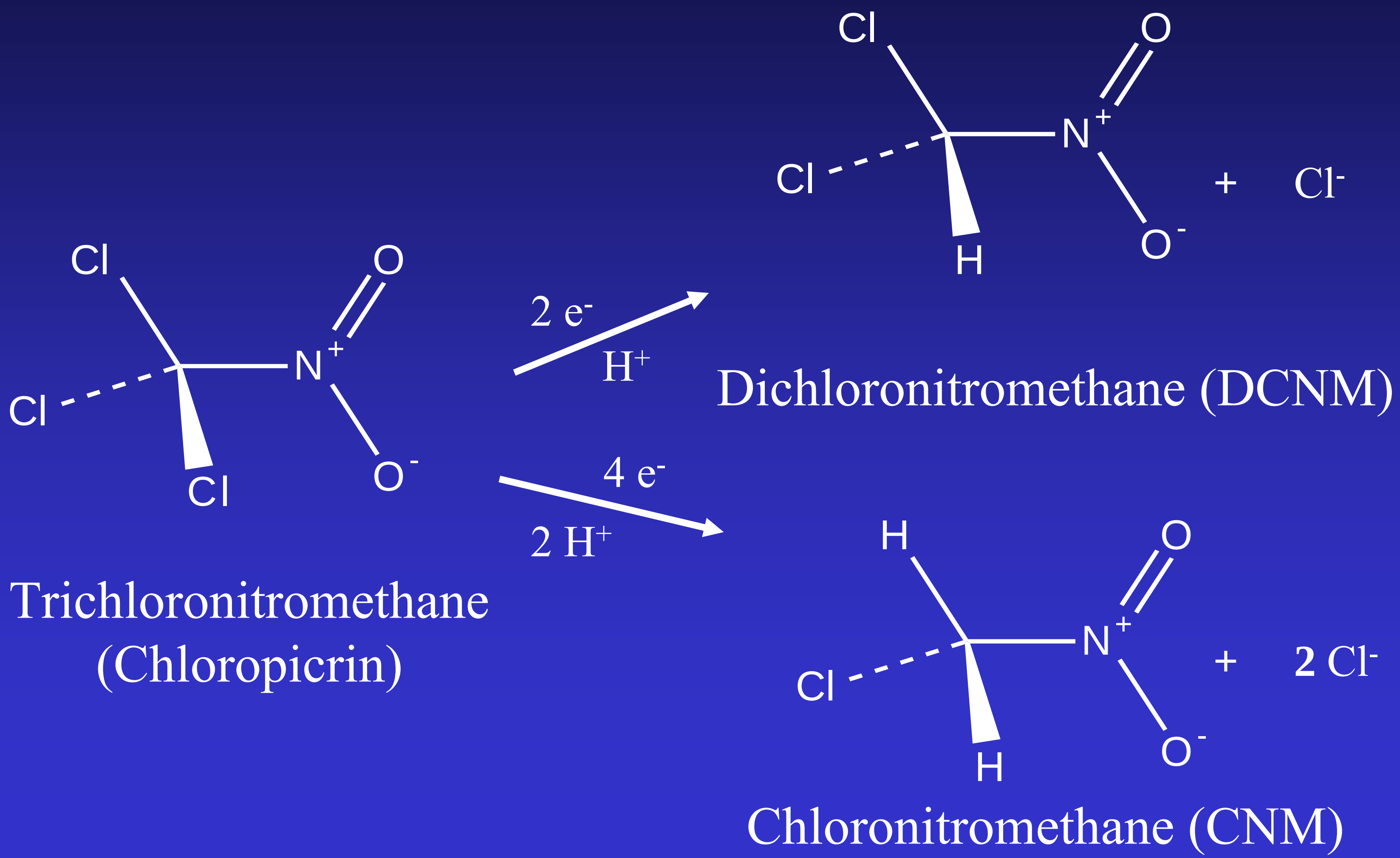

CONCLUSIONS

- Reduction of structural Fe activates smectite surfaces relative to organic compound transformation.
- Degradation pathways include base-catalyzed eliminations and reductive dehalogenation.
- Reduced smectite surfaces also contain significant acidic sites due to increased population of exchangeable cations.

Oxamyl Transformation

Structure of Oxamyl

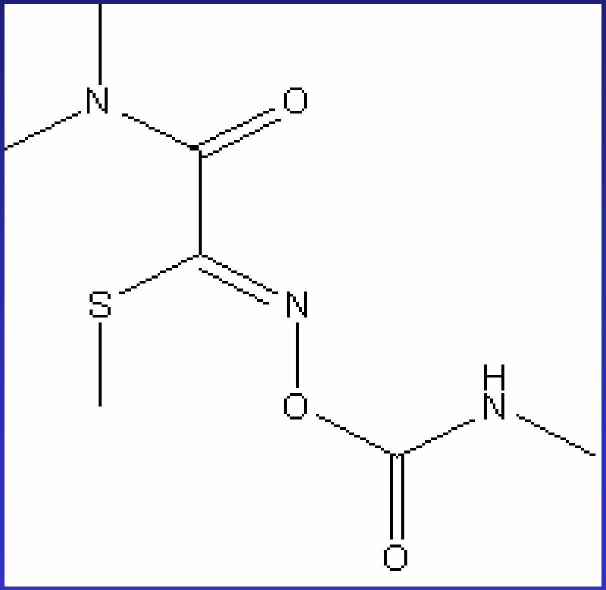

Oxamyl Reacted with Redox-Modified SWa-1

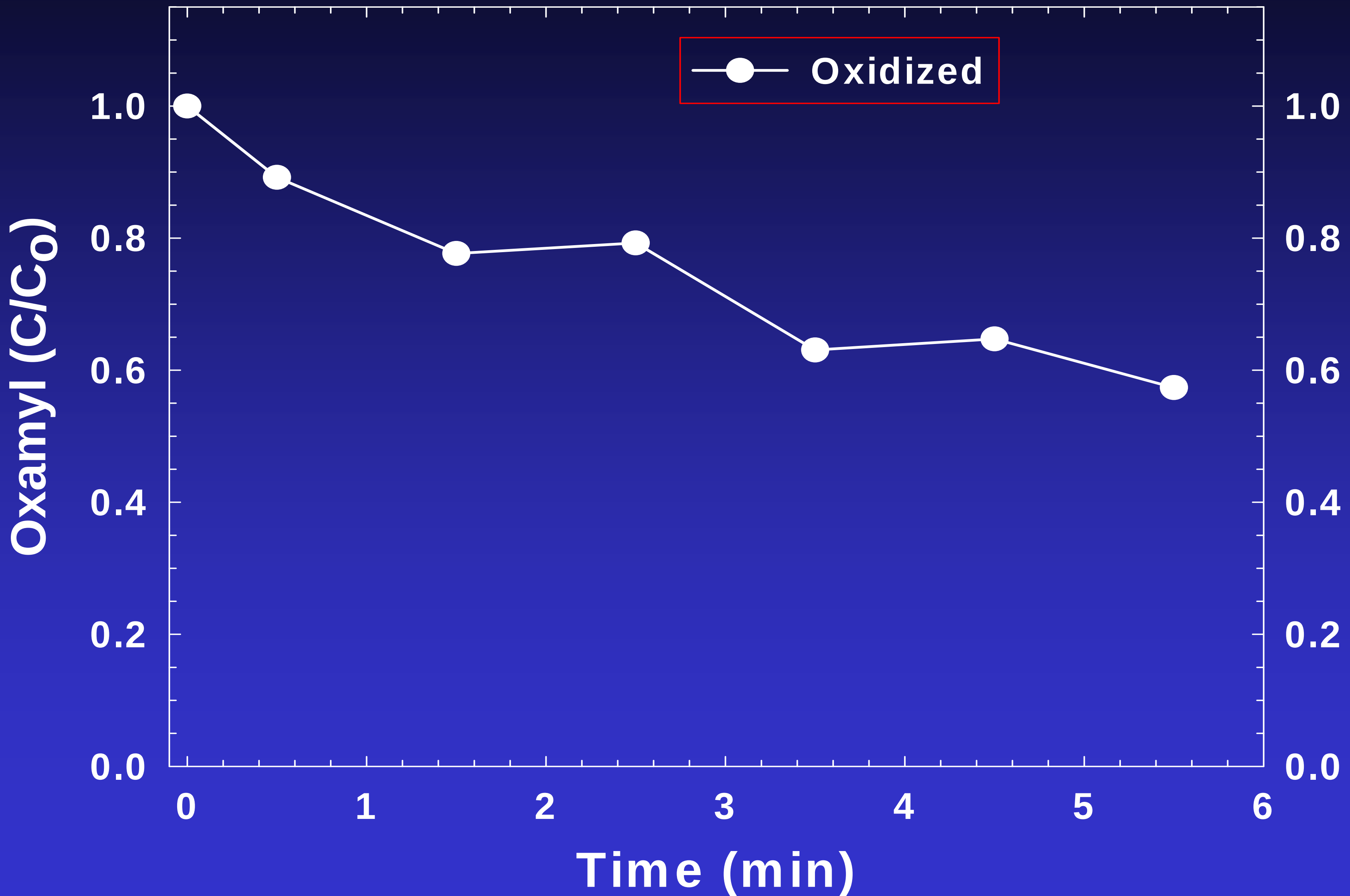

Oxamyl Reacted with Redox-Modified SWa-1

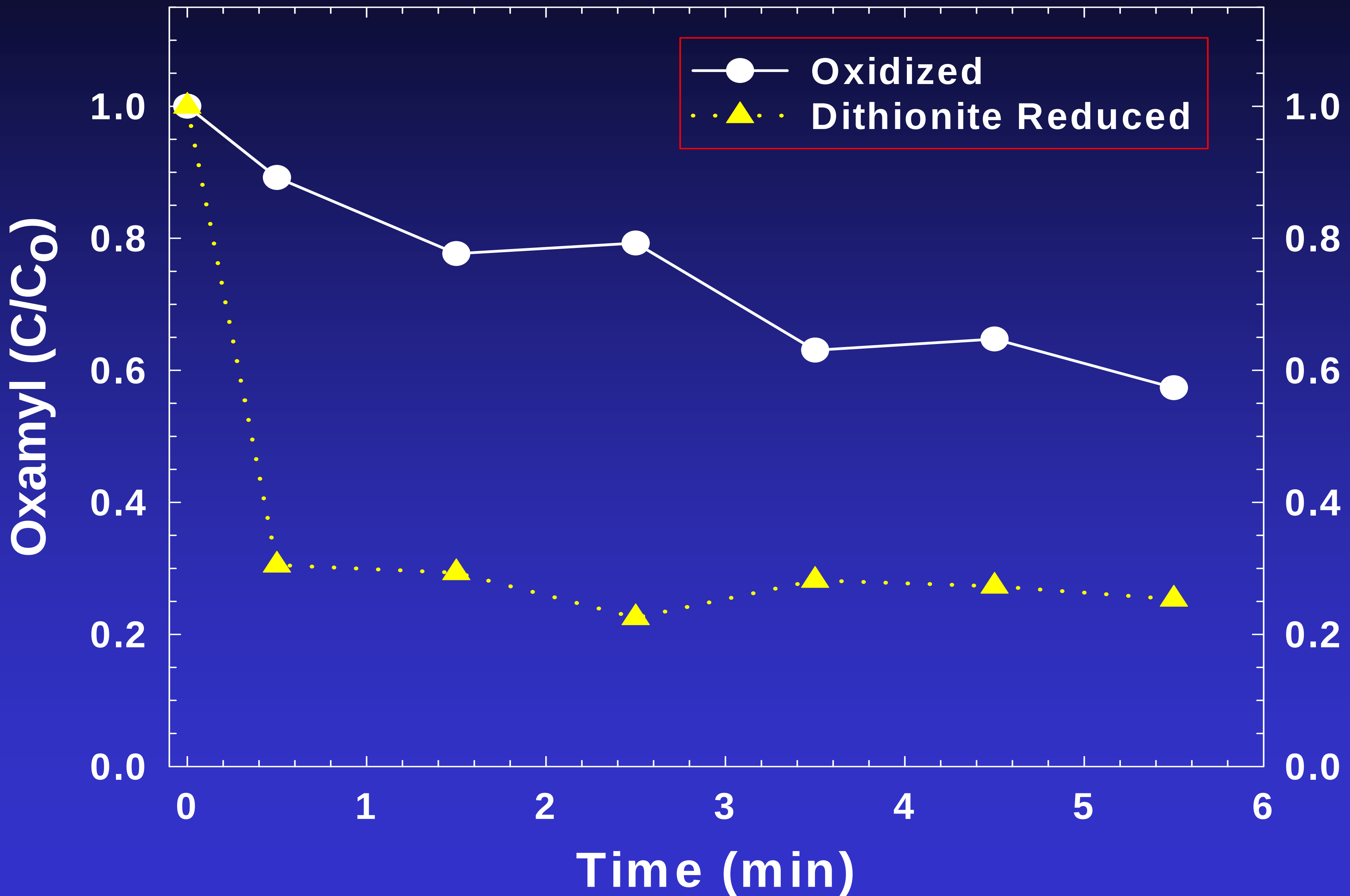

Oxamyl Reacted with Redox-Modified SWa-1

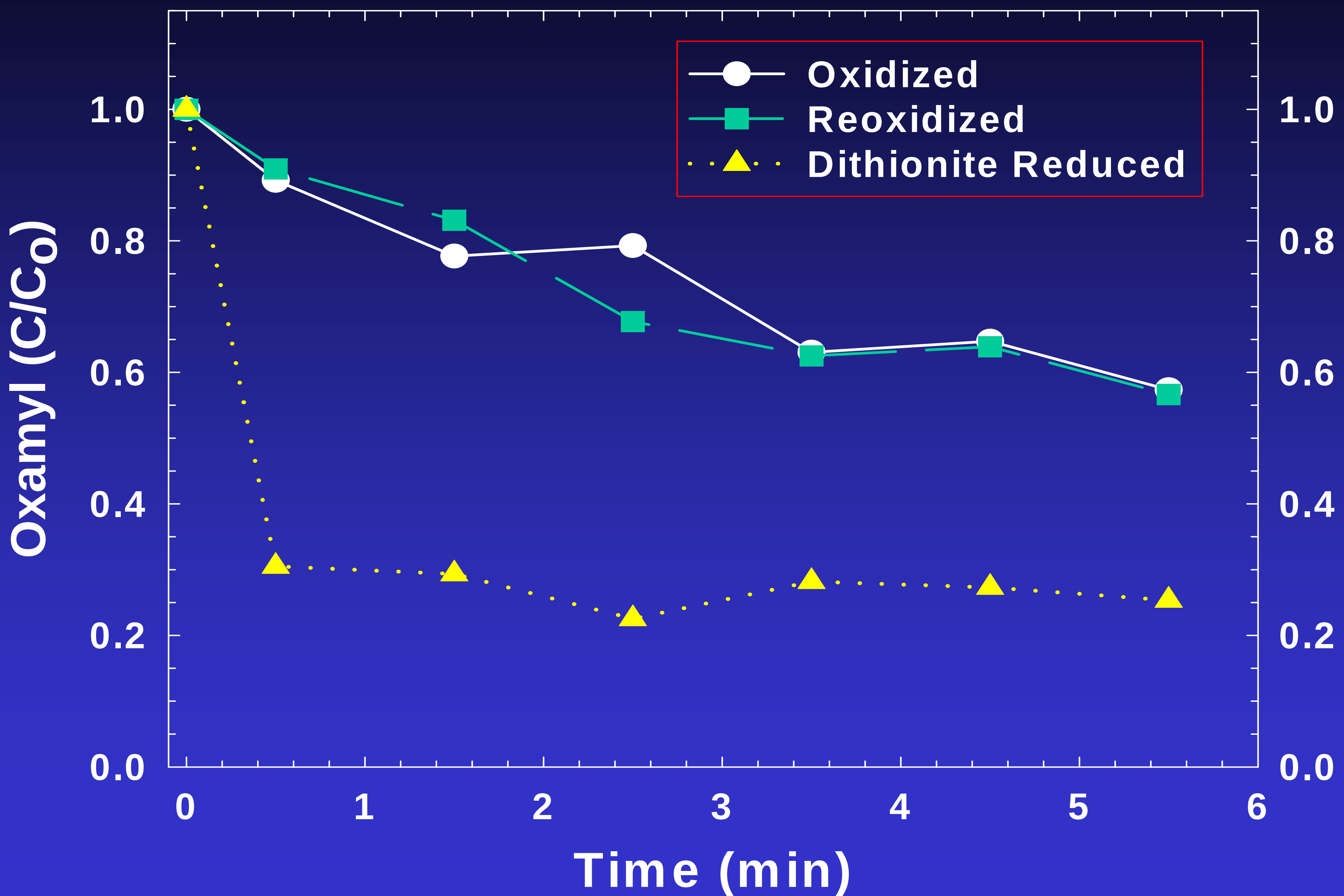

Oxamyl Reacted with Redox-Modified SWa-1

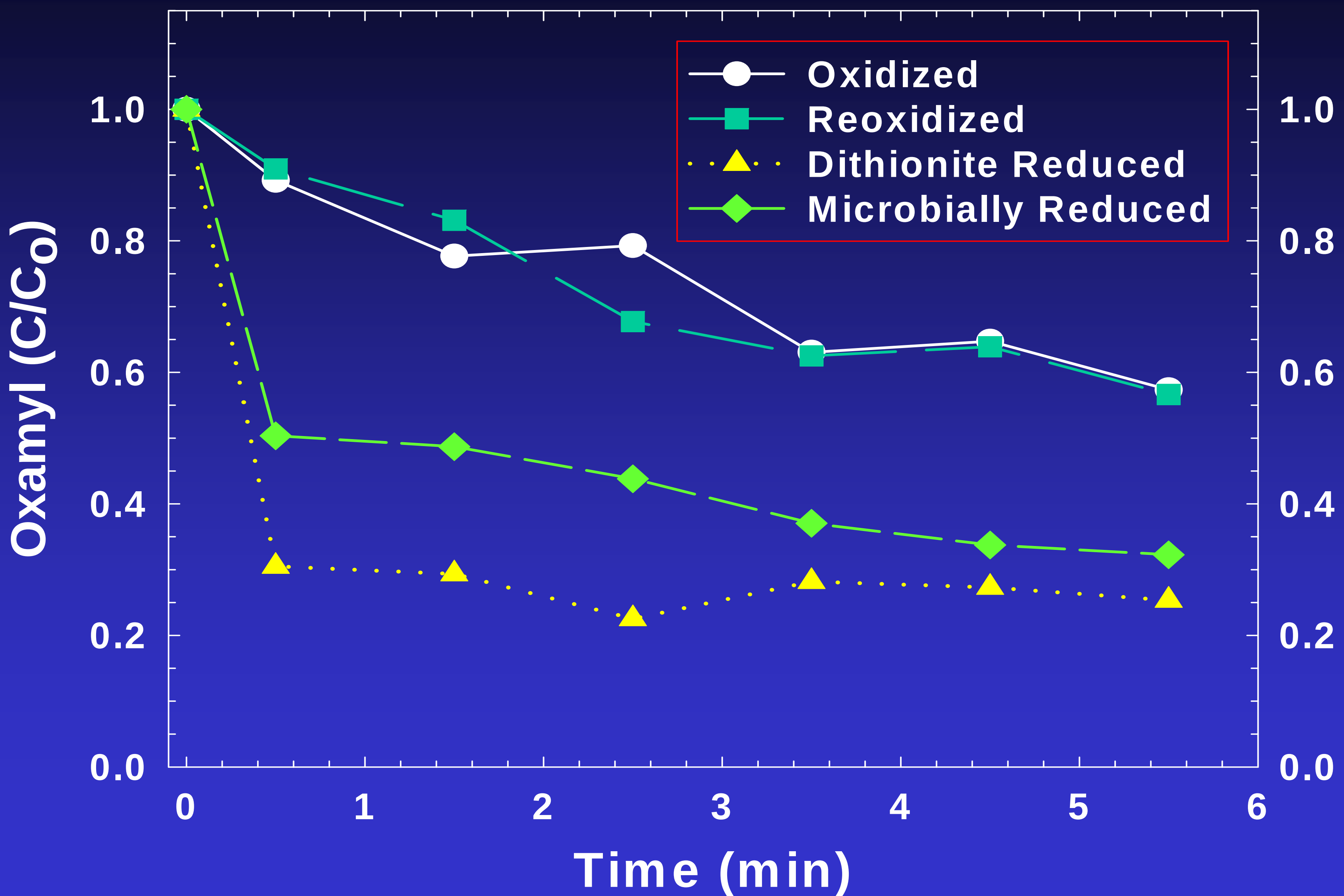

Oxamyl Structure

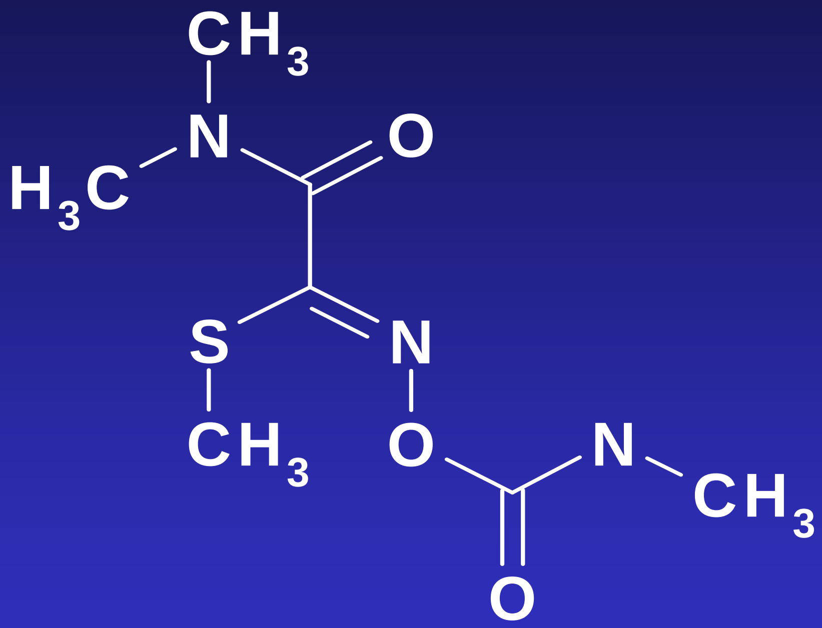

Oxamyl

Degrades by two mechanisms: hydrolysis and reduction

Hydrolysis of Oxamyl

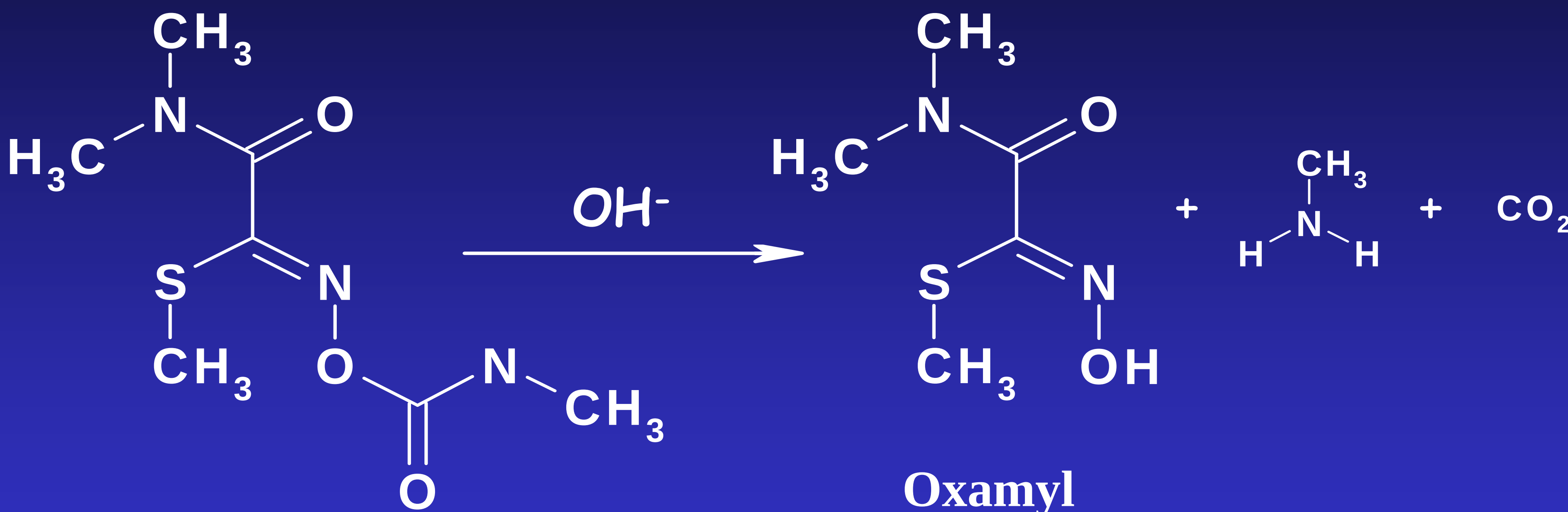

Oxamyl

Oxamyl Oxime

Reduction of Oxamyl

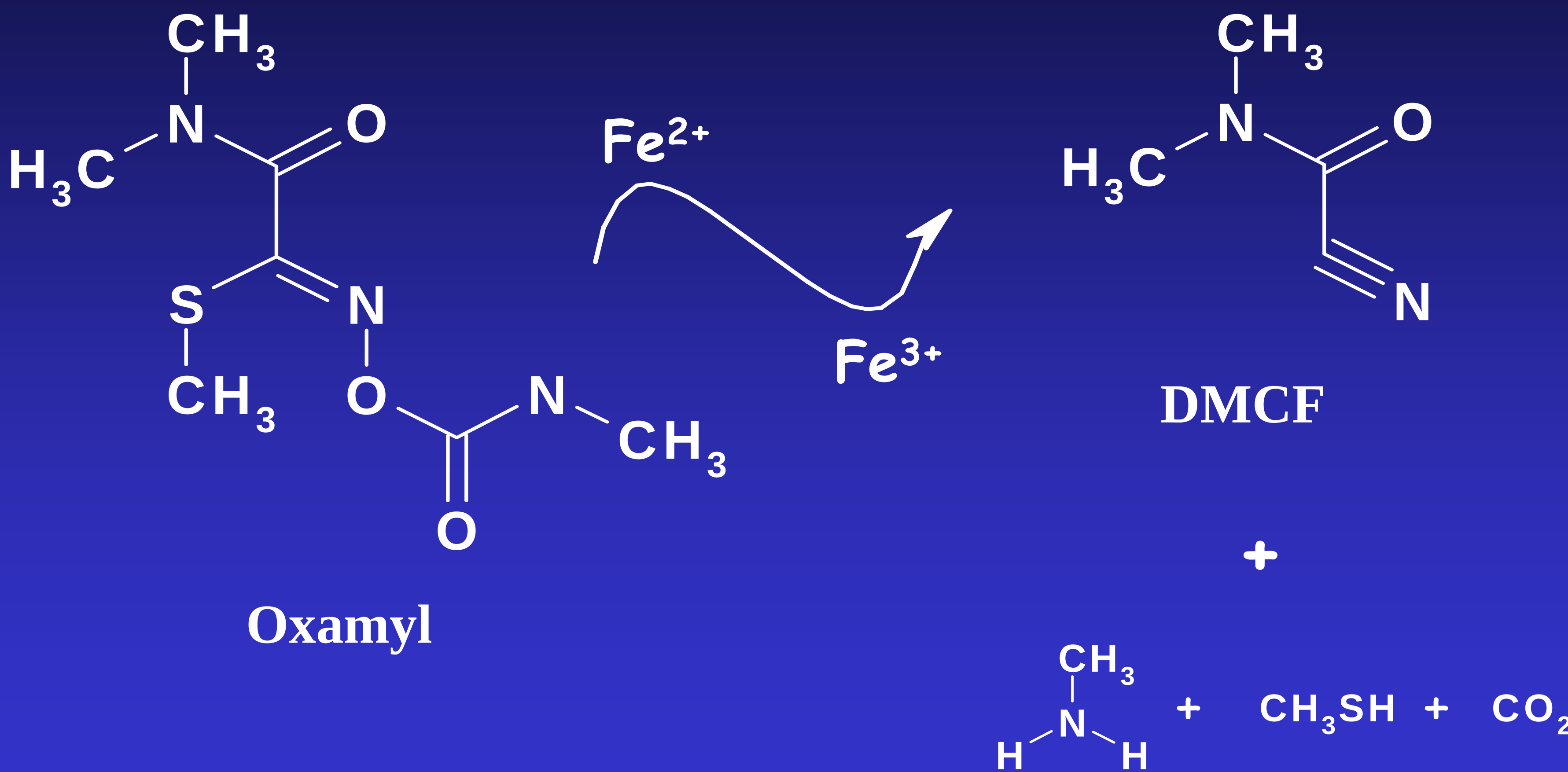

DMCF = N, N-dimethyl-1-cyanoformamide

pH vs. Oxidation State of SWa-1

Ox. state	Ox
Fe(II)/% of clay	0.09
	Solution pH
Without Oxamyl	6.9
Oxamyl pH = 3.5	3.4
Oxamyl pH = 7.0	6.6

pH vs. Oxidation State of SWa-1

Ox. state	Ox	D-Red
Fe(II)/% of clay	0.09	13.20
	Solution pH	
Without Oxamyl	6.9	8.4
Oxamyl pH = 3.5	3.4	7.1
Oxamyl pH = 7.0	6.6	9.0

pH vs. Oxidation State of SWa-1

Ox. state	Ox	D-Red
Fe(II)/% of clay	0.09	13.20
	Solution pH	
Without Oxamyl	6.9	8.4
Oxamyl pH = 3.5	3.4	7.1
Oxamyl pH = 7.0	6.6	9.0

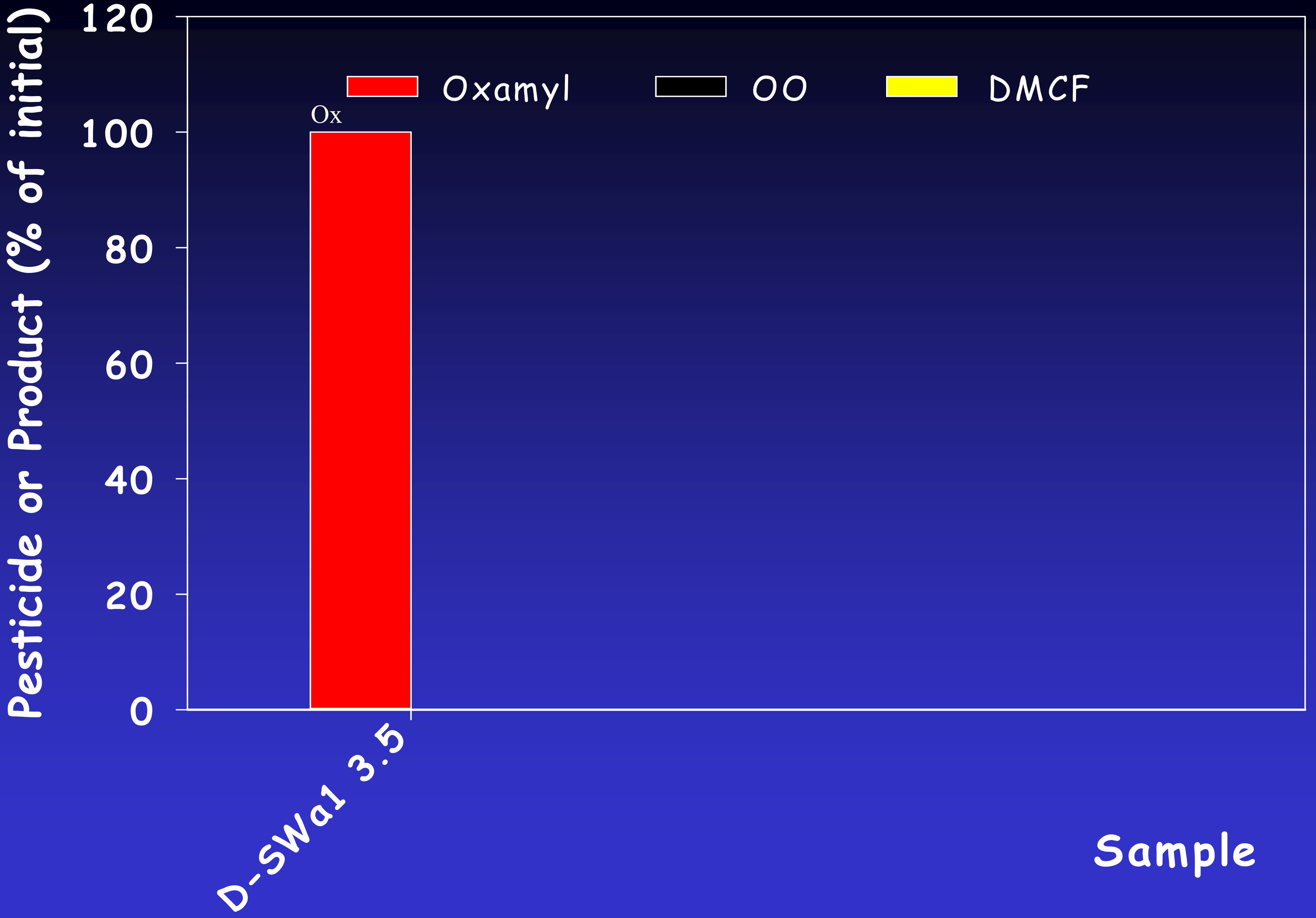
Pesticide or Product (% of initial)
120
100
80
60
40
20
0
Oxamyl
OO
DMCF
Ox
D-SWa1 3.5
Sample

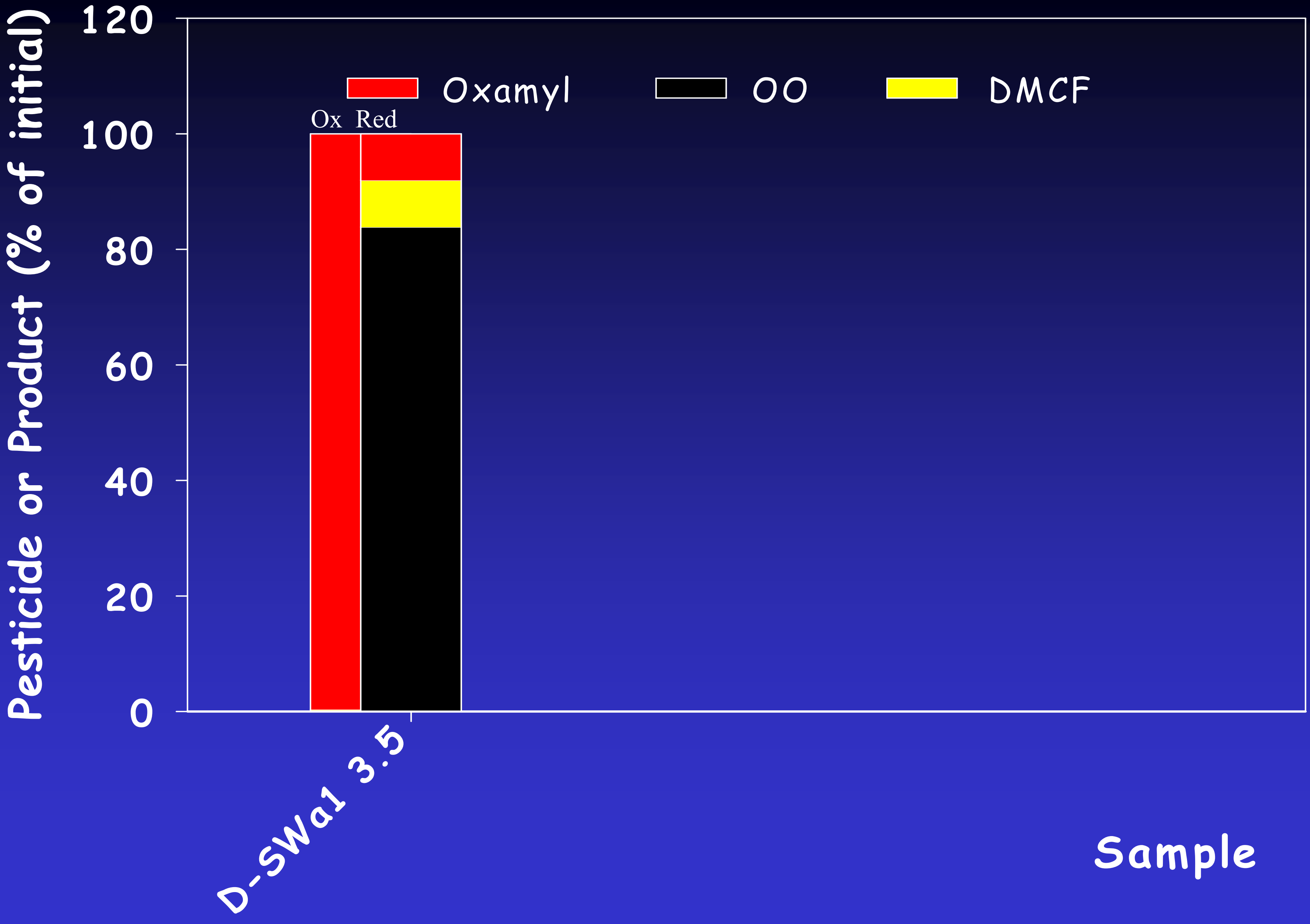

Pesticide or Product (% of initial)
0
20
40
60
80
100
120
Oxamyl
OO
DMCF
Ox
Red
D-SWa1 3.5
Sample

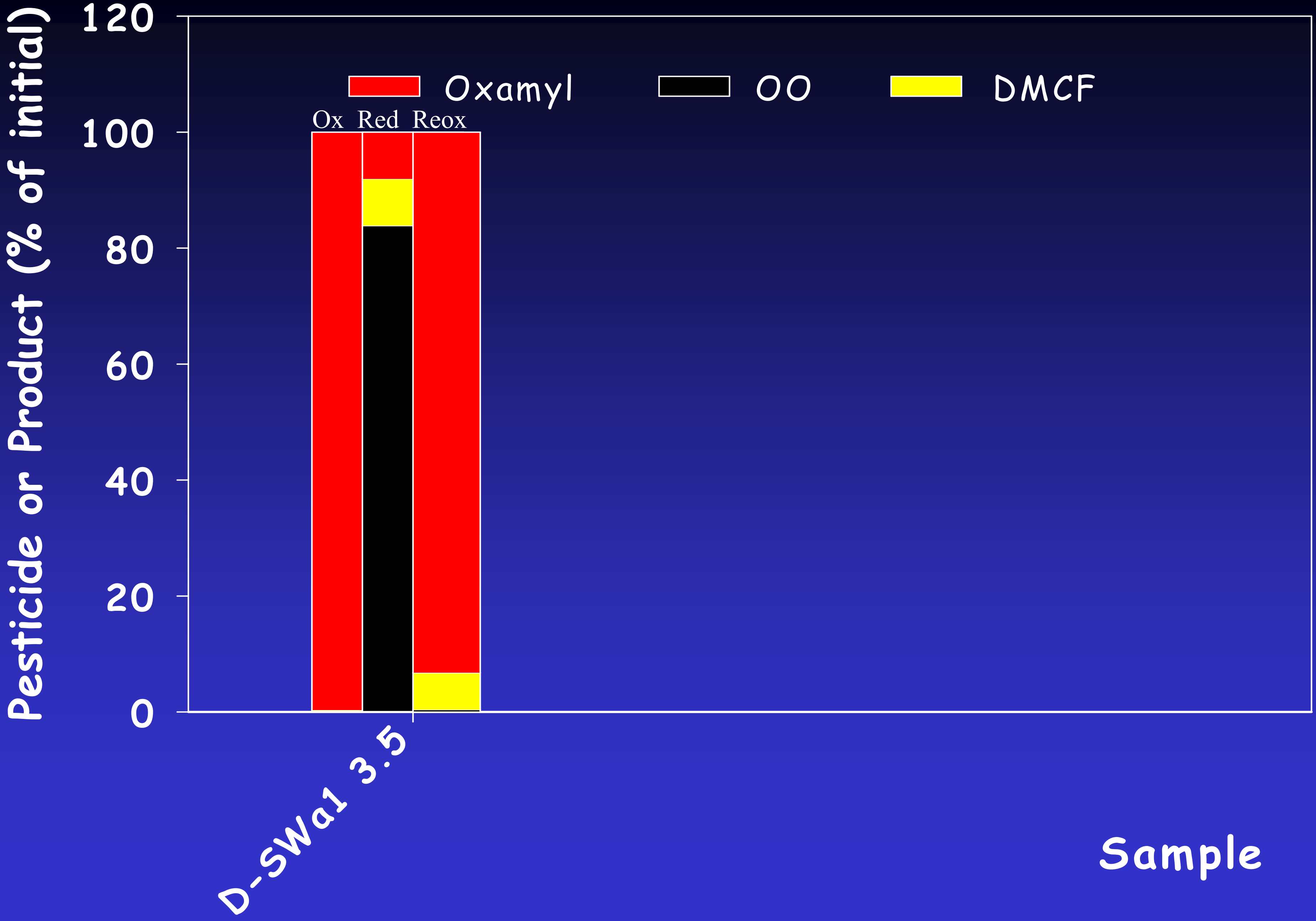
Pesticide or Product (% of initial)
120
100
80
60
40
20
0
Oxamyl
OO
DMCF
Ox
Red
Reox
D-SWa1 3.5
Sample

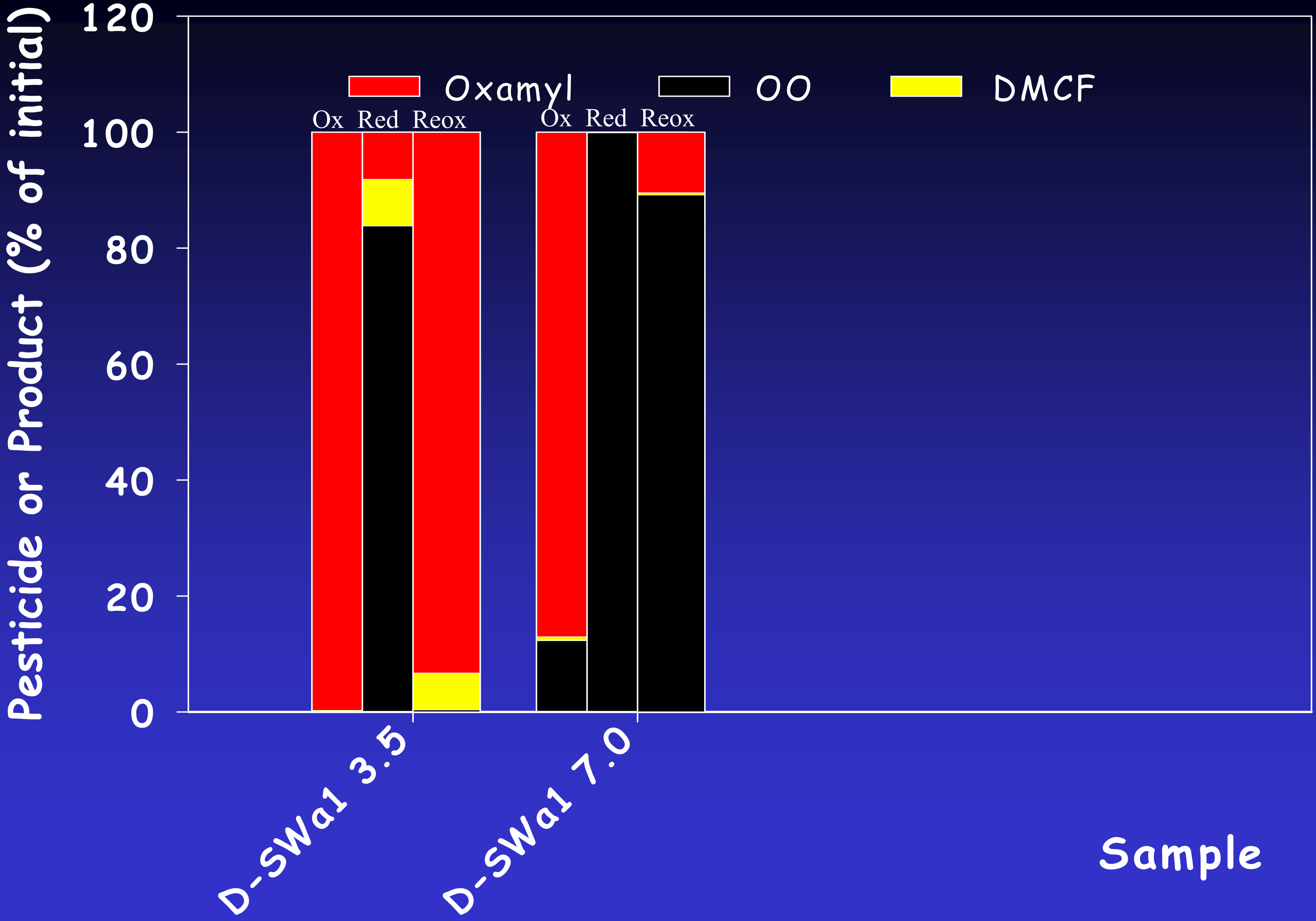

Pesticide or Product (% of initial)
120
100
80
60
40
20
0
Oxamyl
OO
DMCF
Ox Red Reox
Ox Red Reox
D-SWa1 3.5
D-SWa1 7.0
Sample

Summary

- Oxidized clay: no change in clay pH; no oxamyl degradation at low pH (3.5); some at neutral pH (7.0).
- Chemically reduced clay:
  - Clay pH increases as structural Fe(II) increases;
  - Oxamyl is partially degraded into OO (mostly) and DMCF at low pH;
  - Oxamyl degrades completely into OO at neutral pH;

Conclusions

- **Oxamyl degrades rapidly in the presence of reduced smectite.**
- **Oxamyl oxime (hydrolyis) product dominates in reduced SWa-1 at higher pHs.**
- **DMCF (reduction) product occurs only at low pH.**

Mitigating Pesticide Toxicity

Objective:

Determine ways to mitigate the human toxicity of pesticides in the environment

2_4_D

ESTIMATED ANNUAL AGRICULTURAL USE

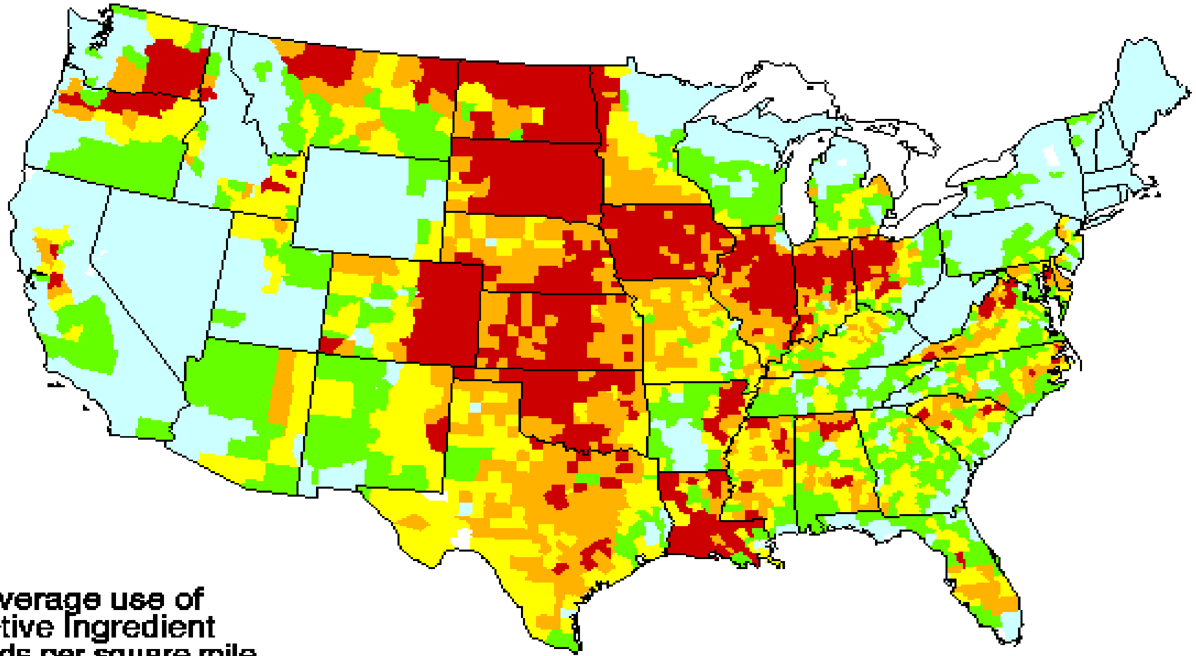

Average use of
Active Ingredient
Pounds per square mile
of county per year

- No Estimated Use
- < 3.253
- 3.253 – 8.881
- 8.882 – 15.668
- 15.669 – 23.562
- >= 23.563

Crops	Total Pounds Applied	Percent National Use
pasture	16, 106, 460	43. 25
wheat and grains	7, 928, 326	21. 29
corn	4, 550, 447	12. 22
other hay	3, 718, 124	9. 98
soybeans	2, 044, 003	5. 49
barley	908, 808	2. 44
rice	556, 462	1. 49
sorghum	453, 258	1. 22
oats	275, 812	0. 74
sugar cane: sugar & seed	164, 703	0. 44

ALACHLOR

ESTIMATED ANNUAL AGRICULTURAL USE

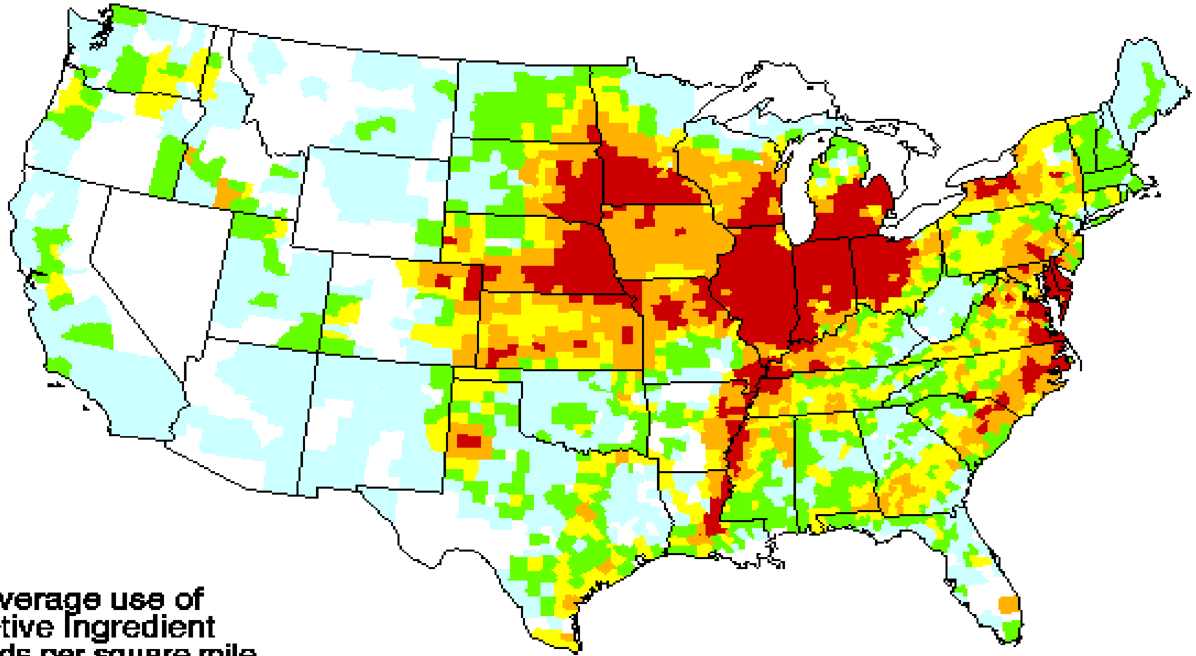

Average use of
Active Ingredient
Pounds per square mile
of county per year

- No Estimated Use
- < 0.415
- 0.415 – 2.456
- 2.457 – 9.988
- 9.989 – 29.195
- >= 29.196

Crops	Total Pounds Applied	Percent National Use
corn	13, 902, 747	54. 21
soybeans	8, 862, 899	34. 56
sorghum	1, 829, 617	7. 13
sweet corn	507, 232	1. 98
dry beans	336, 853	1. 31
peanuts	122, 871	0. 48
cotton	61, 870	0. 24
sunflower	23, 794	0. 09

ATRAZINE

ESTIMATED ANNUAL AGRICULTURAL USE

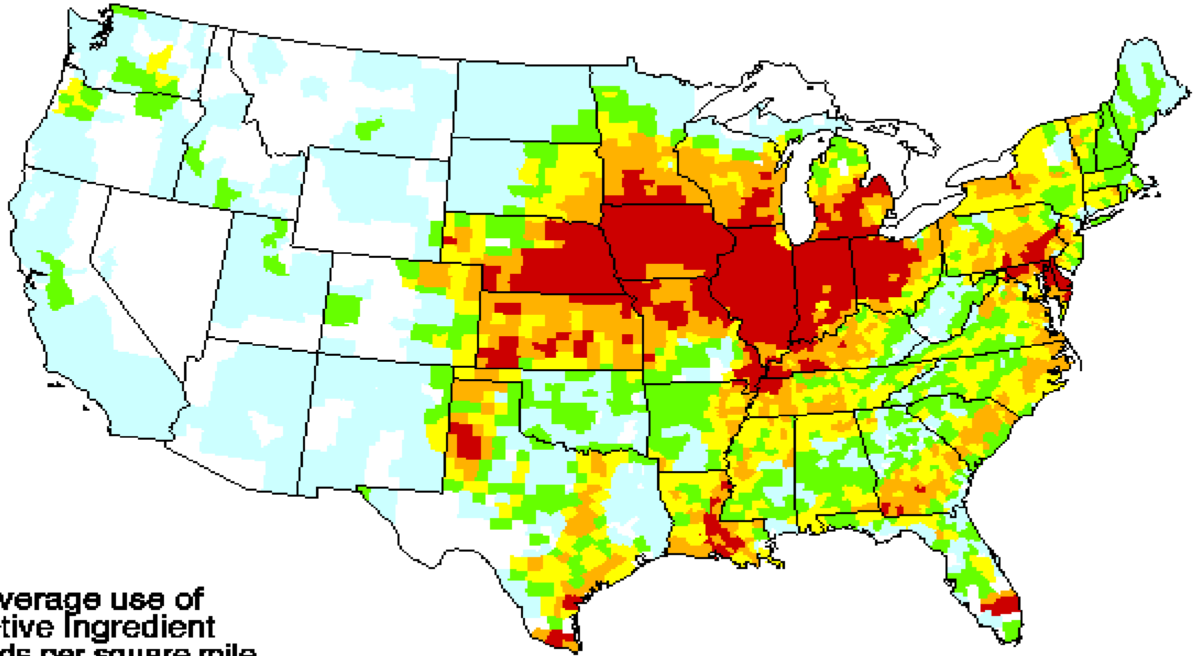

Average use of Active Ingredient Pounds per square mile of county per year

- No Estimated Use
- < 1.080
- 1.080 – 5.587
- 5.588 – 21.211
- 21.212 – 66.515
- >= 66.516

Crops	Total Pounds Applied	Percent National Use
corn	53, 796, 206	84. 13
sorghum	7, 339, 963	11. 48
sugar cane: sugar & seed	1, 711, 322	2. 68
pasture	518, 074	0. 81
sweet corn	444, 523	0. 70
sod	119, 182	0. 19
proso millet	11, 937	0. 02
field and grass seed	6, 305	0. 01

DICAMBA

ESTIMATED ANNUAL AGRICULTURAL USE

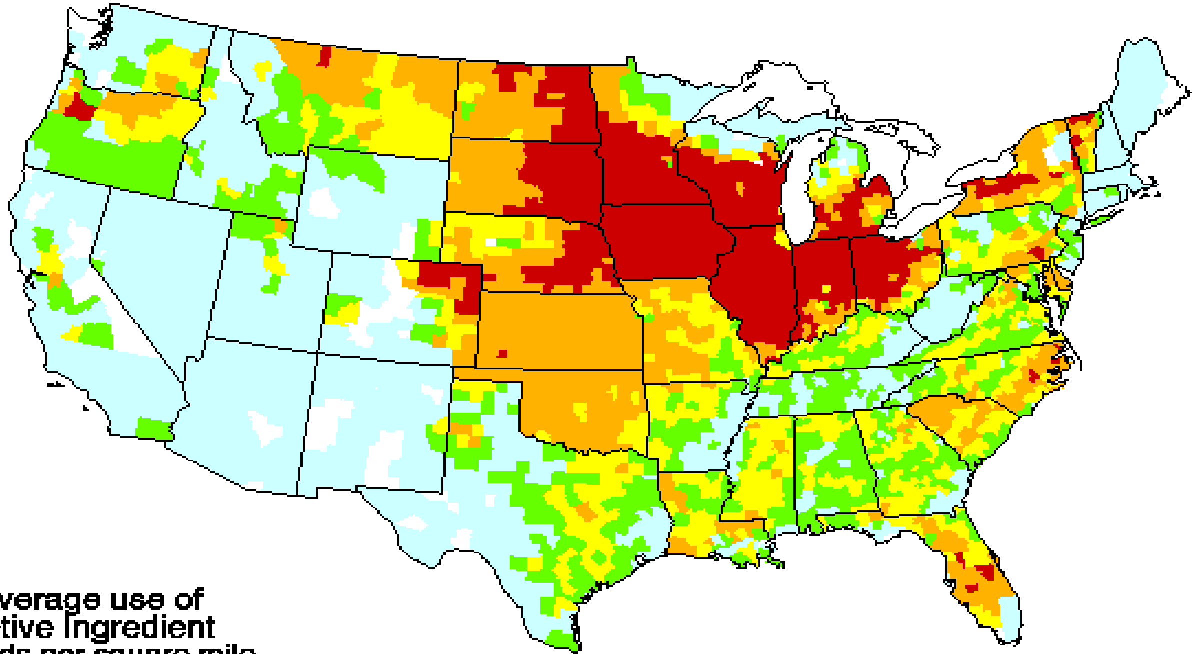

Average use of Active Ingredient Pounds per square mile of county per year

- No Estimated Use
- < 0.302
- 0.302 – 0.931
- 0.932 – 2.138
- 2.139 – 6.432
- >= 6.433

Crops	Total Pounds Applied	Percent National Use
corn	6, 907, 941	72. 03
pasture	1, 175, 374	12. 26
wheat and grains	861, 932	8. 99
other hay	398, 438	4. 15
barley	89, 182	0. 93
sorghum	59, 065	0. 62
field and grass seed	50, 572	0. 53
oats	32, 167	0. 34
sod	11, 518	0. 12
prosomillet	1, 726	0. 02

OXAMYL

ESTIMATED ANNUAL AGRICULTURAL USE

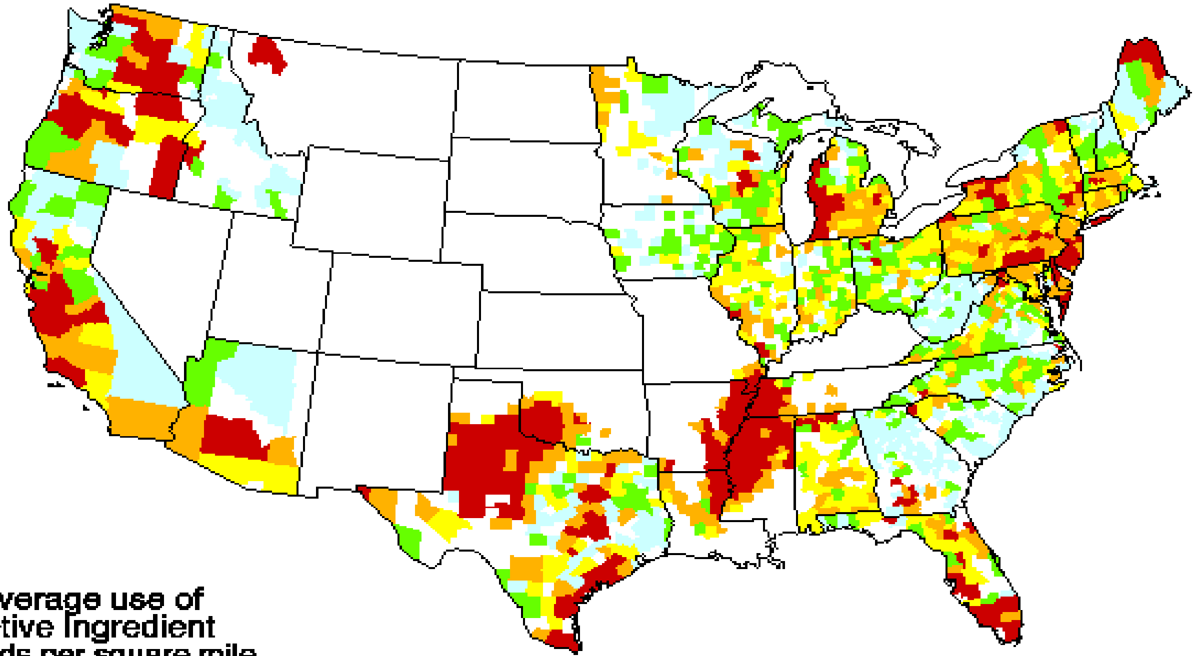

Average use of
Active Ingredient
Pounds per square mile
of county per year

- No Estimated Use
- < 0.004
- 0.004 – 0.016
- 0.017 – 0.079
- 0.080 – 0.467
- >= 0.468

Crops	Total Pounds Applied	Percent National Use
cotton	477, 086	58. 62
potatoes	75, 625	9. 29
apples	72, 819	8. 95
mint	61, 554	7. 56
sweet peppers	27, 967	3. 44
celery	23, 599	2. 90
tomatoes	21, 537	2. 65
cucumbers	12, 269	1. 51
onions	11, 075	1. 36
melons	9, 379	1. 15

TRIFLURALIN

ESTIMATED ANNUAL AGRICULTURAL USE

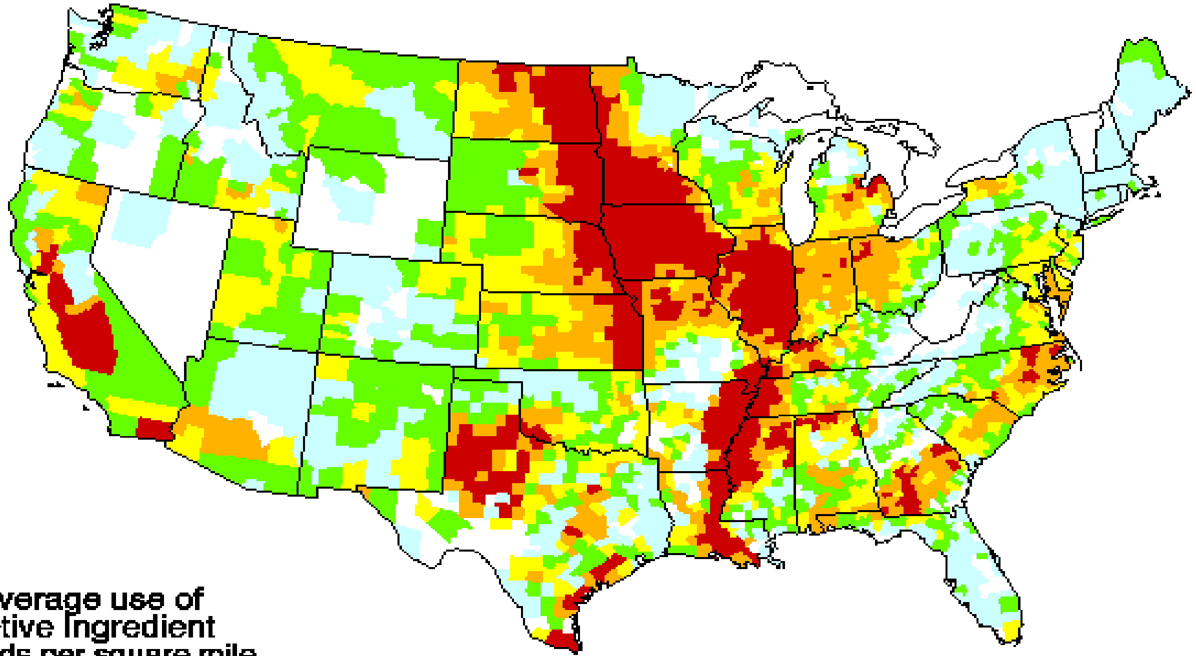

Average use of
Active Ingredient
Pounds per square mile
of county per year

- No Estimated Use
- < 0.181
- 0.181 – 1.226
- 1.227 – 5.155
- 5.156 – 16.325
- >= 16.326

Crops	Total Pounds Applied	Percent National Use
soybeans	11,099,394	56.10
cotton	4,736,822	23.94
alfalfa hay	991,611	5.01
sunflower	645,436	3.26
wheat and grains	558,665	2.82
dry beans	324,002	1.64
barley	290,602	1.47
sugar cane: sugar & seed	245,381	1.24
tomatoes	126,594	0.64
green peas	96,034	0.49

The Team:

Kara C. Sorensen: Ph.D. Student

Richard E. Warner -- wildlife ecologist

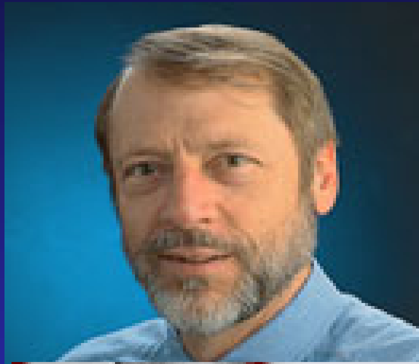

Michael J. Plewa -- geneticist and toxicologist

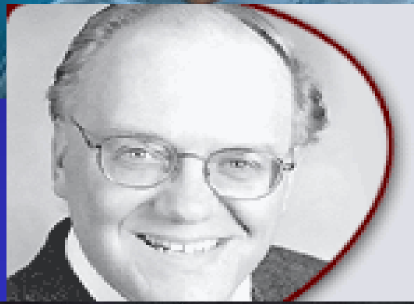

Joseph W. Stucki -- clay chemist

Mitigating Pesticide Toxicity

Studied Four Pesticides:

Alachlor, 2,4-D, Dicamba, Oxamyl

Measured:

Cytotoxicity & Genotoxicity

Mitigating Pesticide Toxicity

Cells Representing Human Cells:

Chinese Hamster Ovary Cells (CHO)

Clay Used Was Iron Smectite

Common in Soils; Bacteria Change Iron From +3 to +2; Changes Chemistry

Mitigating Pesticide Toxicity

Objective:

Determine ways to mitigate the human toxicity of pesticides in the environment

Treatment of Pesticide

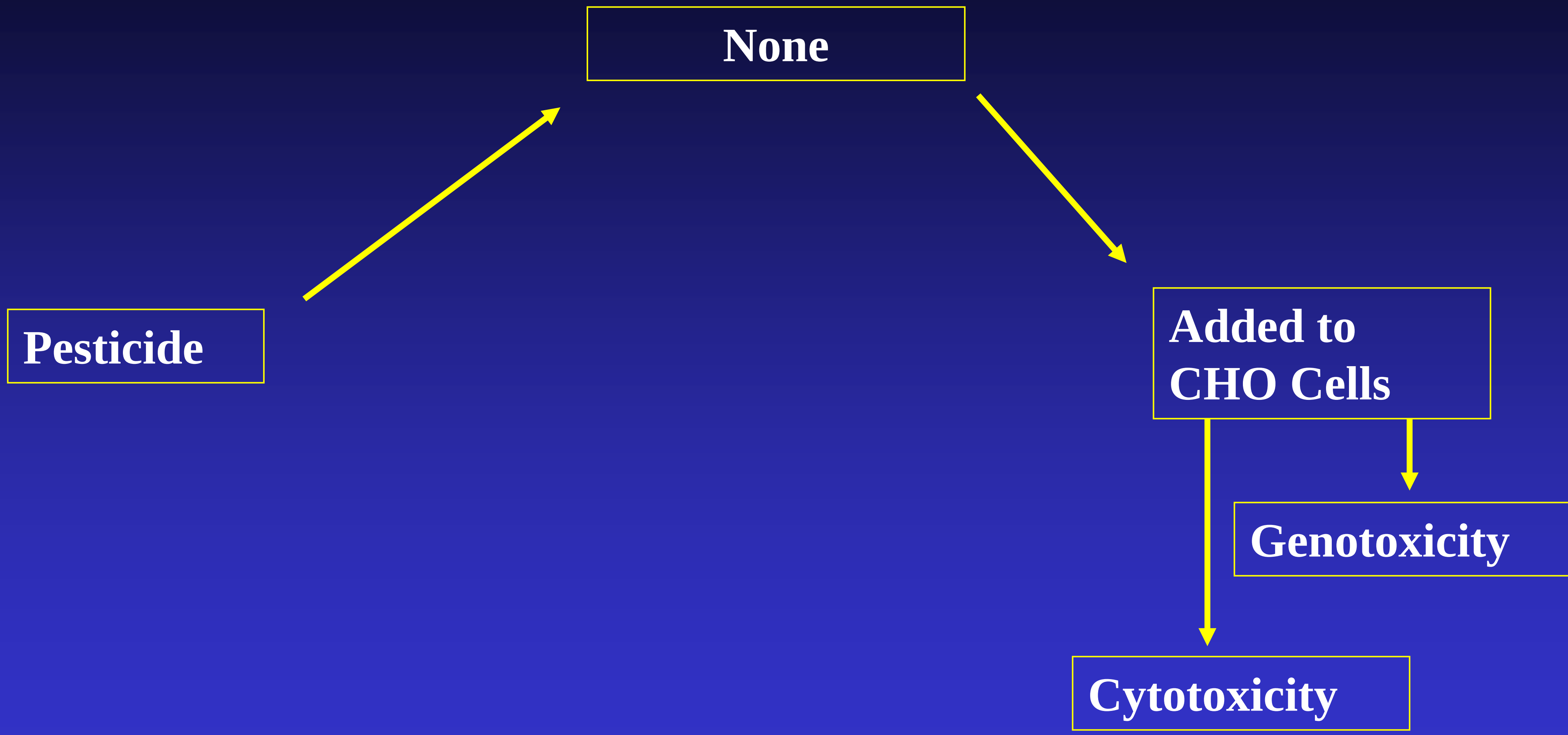

Treatment of Pesticide

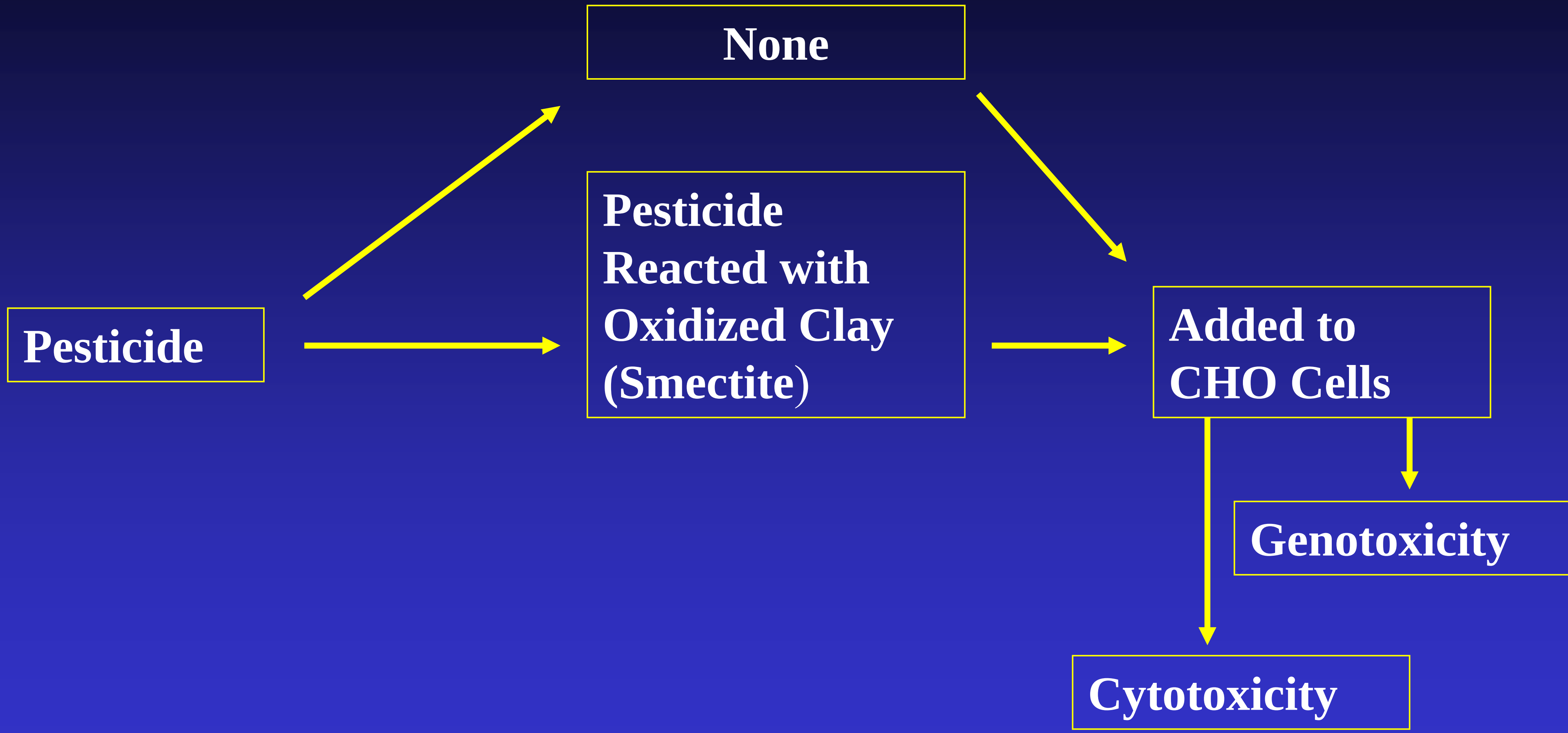

Treatment of Pesticide

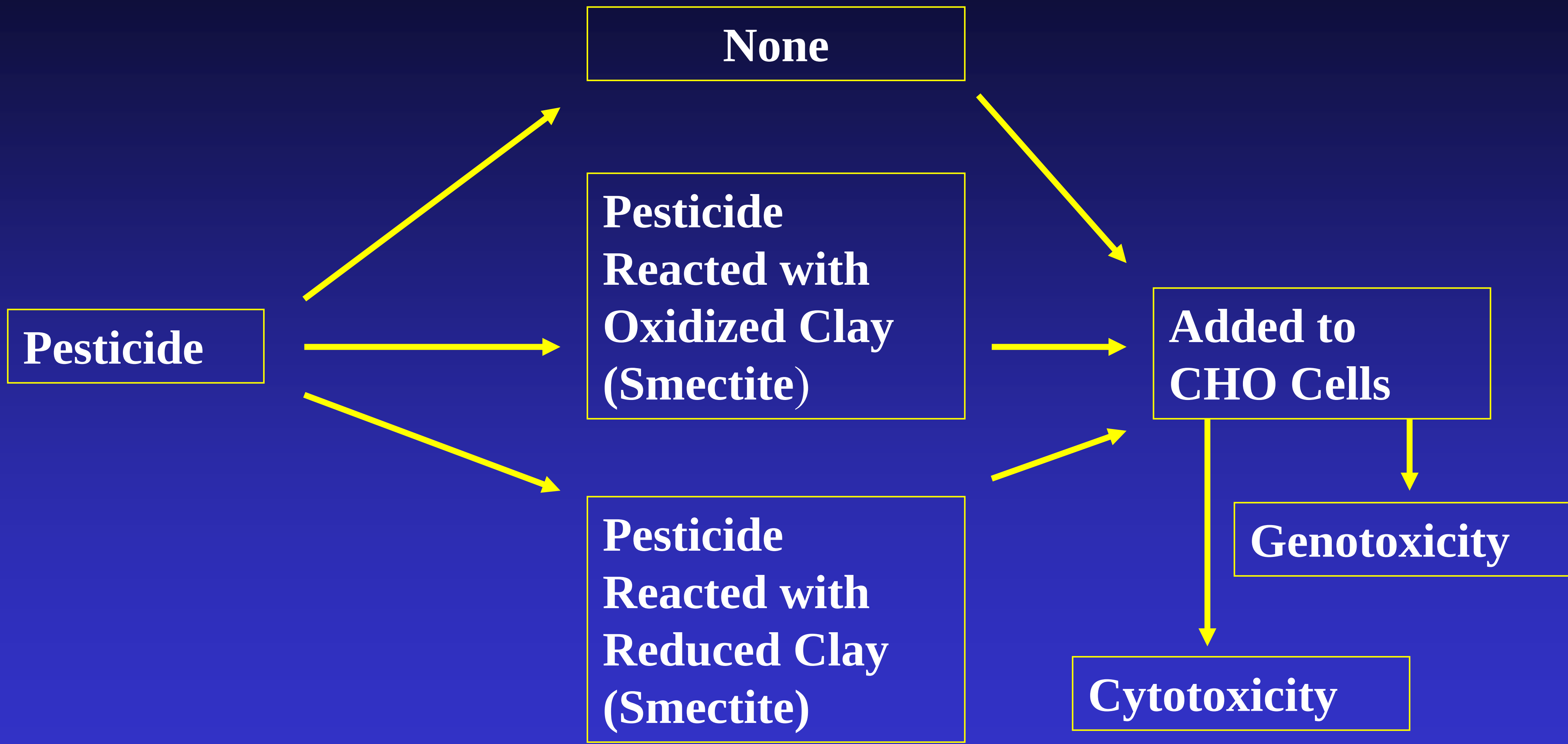

Treatment of Pesticide

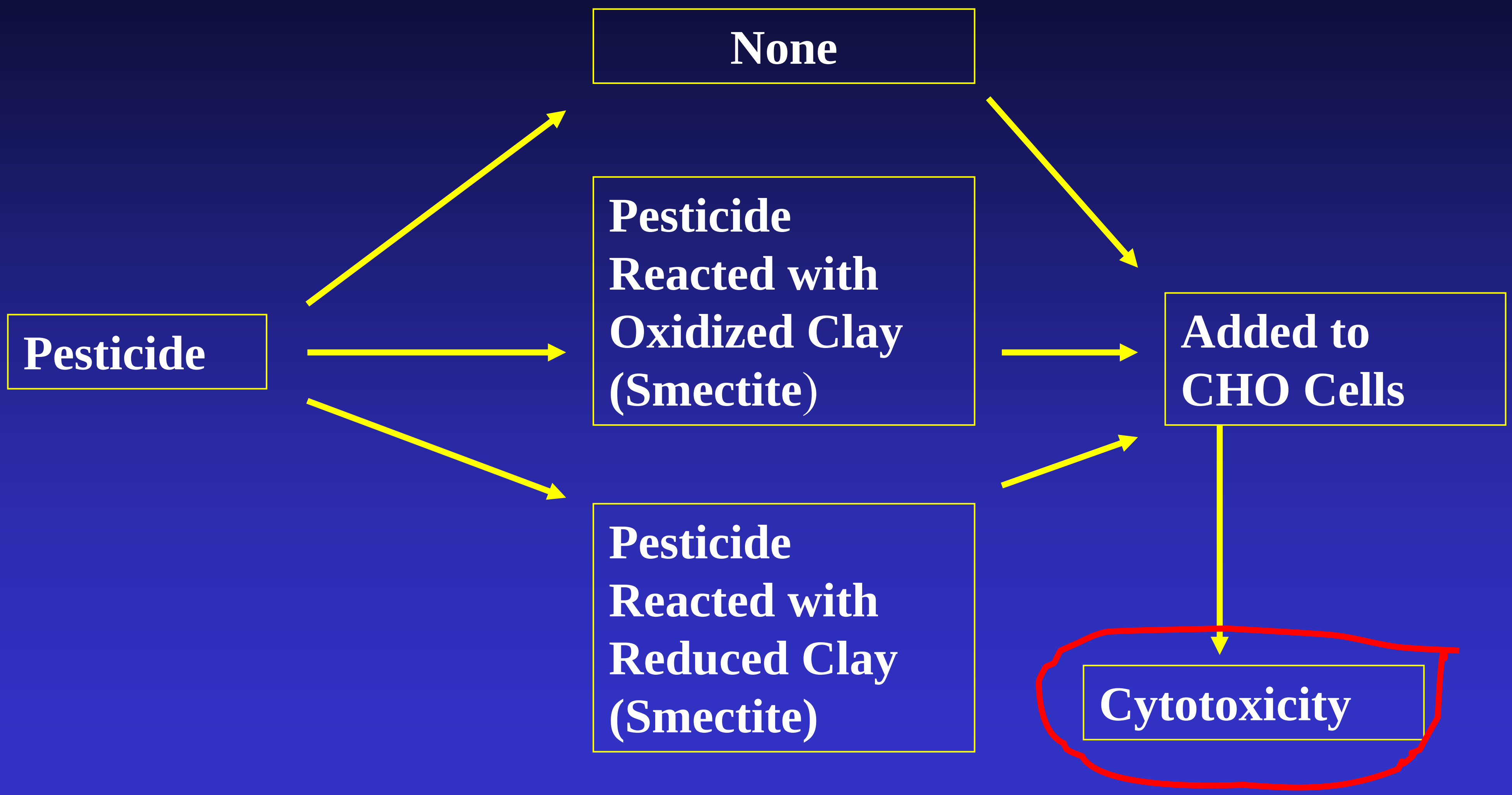

Cytotoxicity Method

- Solutions containing pesticide were separated from the solid clay fraction by centrifugation.

Cytotoxicity Method

- Solutions containing pesticide were separated from the solid clay fraction by centrifugation.
- In order to avoid collateral damage to CHO cells due to ancillary reactions, solutions were filter sterilized and the pH and ionic strength were carefully controlled under an inert atmosphere.

Cytotoxicity Method

- Solutions containing pesticide were separated from the solid clay fraction by centrifugation.
- In order to avoid collatoral damage to CHO cells due to ancillary reactions, solutions were filter sterilized and the pH and ionic strength were carefully controlled under an inert atmosphere.
- The fraction of surviving cells after treatment with pesticide solutions was measured by live-cell density, using visible absorption spectroscopy at 450 nm after live-cell fixation with crystal violet.

Alachlor Transformation

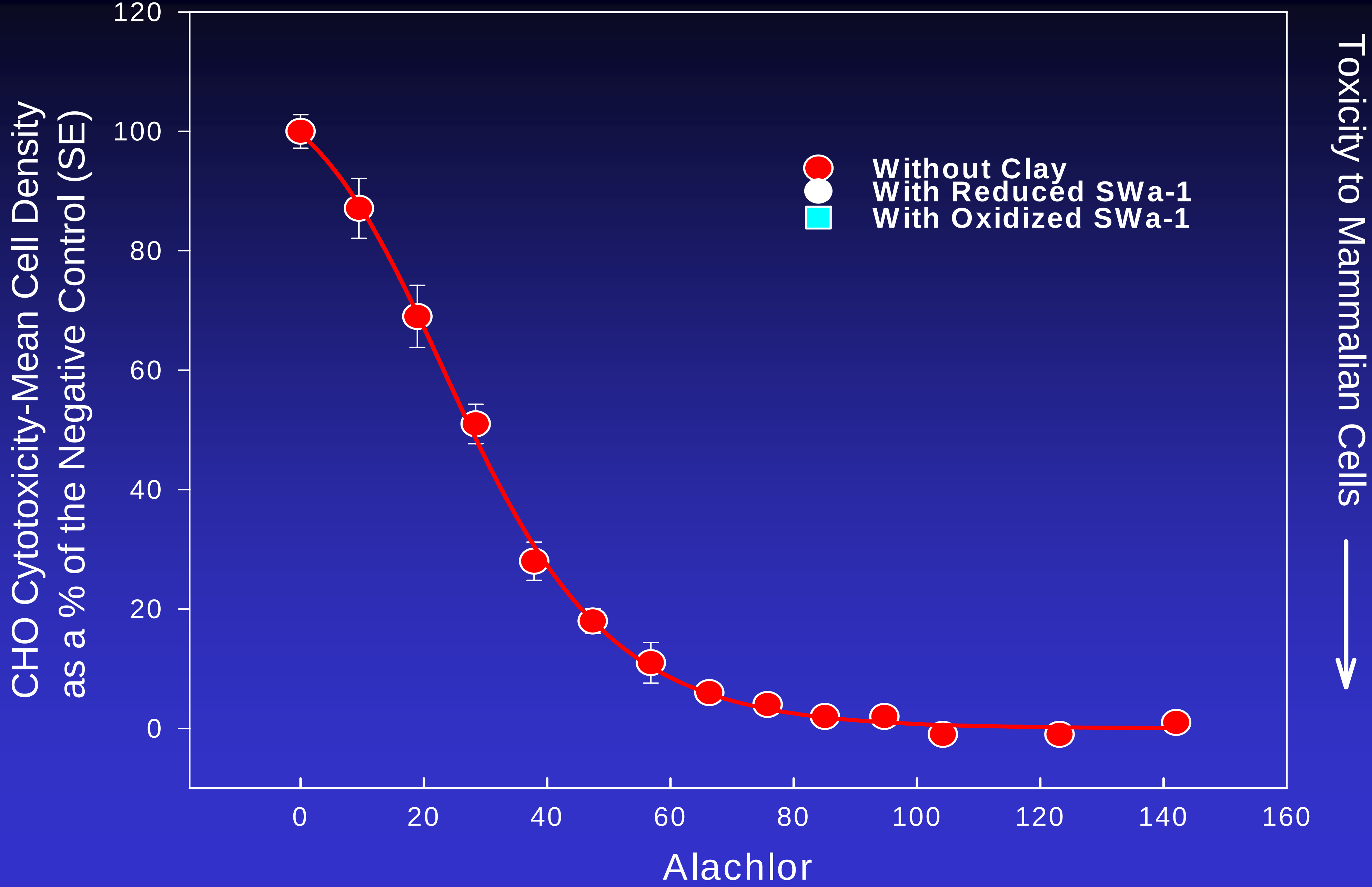
CHO Cytotoxicity-Mean Cell Density
as a % of the Negative Control (SE)
120
100
80
60
40
20
0
0
20
40
60
80
100
120
140
160
Alachlor
Without Clay
With Reduced SWa-1
With Oxidized SWa-1
Toxicity to Mammalian Cells

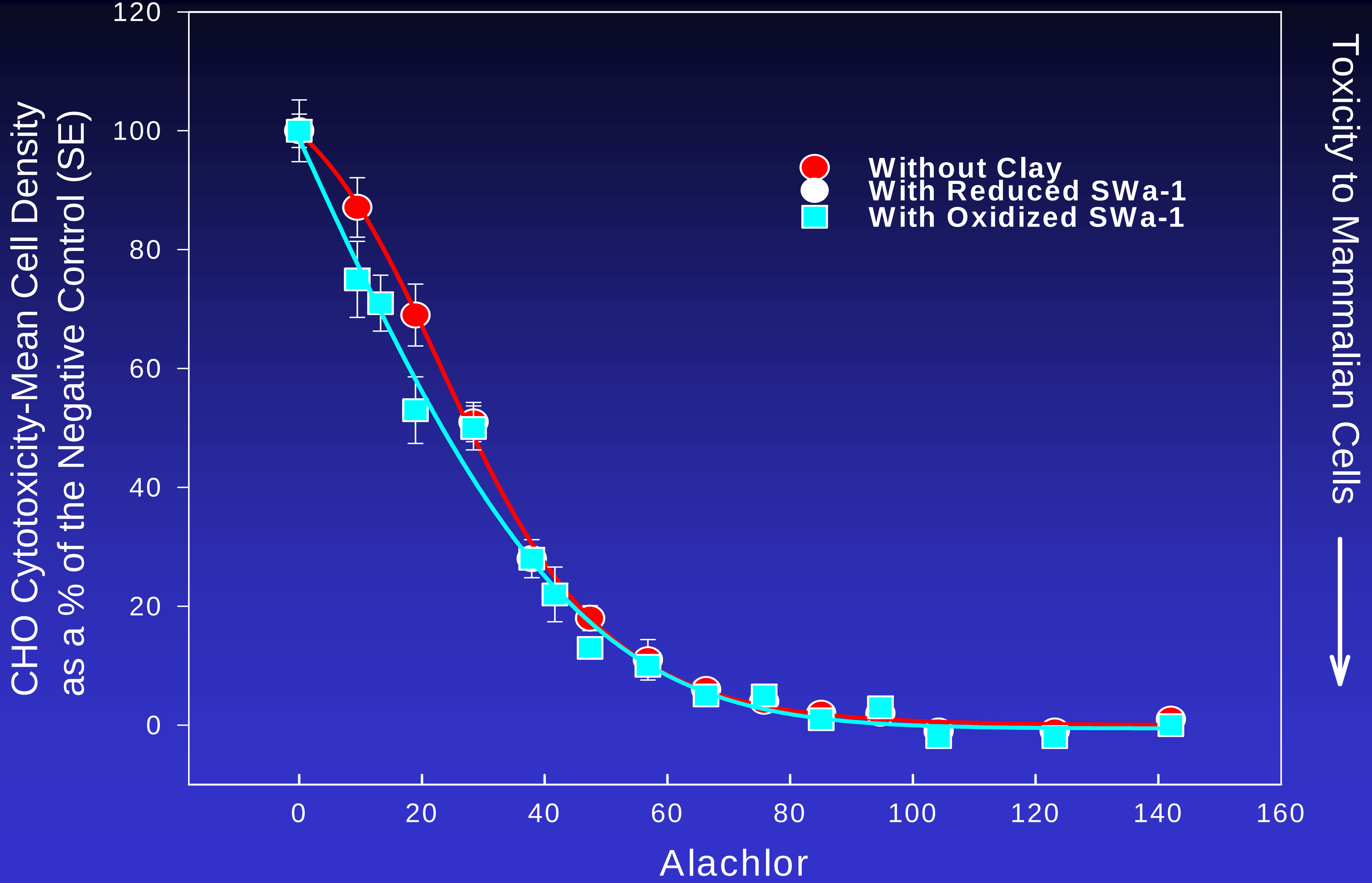

CHO Cytotoxicity-Mean Cell Density as a % of the Negative Control (SE)
Without Clay
With Reduced SWa-1
With Oxidized SWa-1
Toxicity to Mammalian Cells
Alachlor
0
20
40
60
80
100
120
140
160

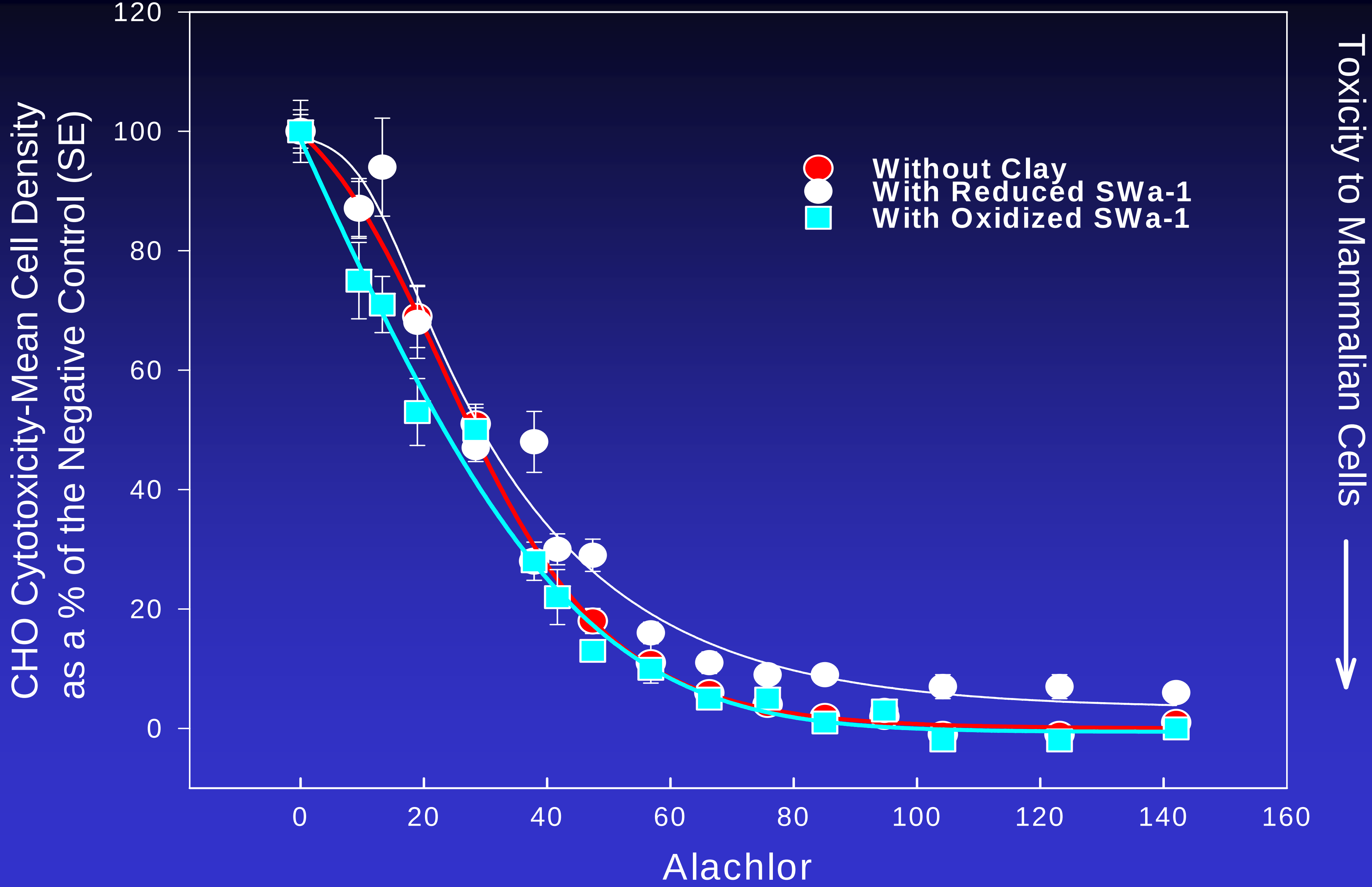

CHO Cytotoxicity-Mean Cell Density
as a % of the Negative Control (SE)
Toxicity to Mammalian Cells
Without Clay
With Reduced SWa-1
With Oxidized SWa-1
Alachlor
0
20
40
60
80
100
120
140
160

Conclusions -- Alachlor

- Alachlor evokes a cytotoxic response in the CHO cells.
- Prior reaction of alachlor with oxidized (unaltered) smectite clay has no effect on cytotoxicity of the pesticide.
- Reaction of alachlor with reduced smectite clay has a small, but statistically significant effect on decreasing its cytotoxicity.

Oxamyl Transformation

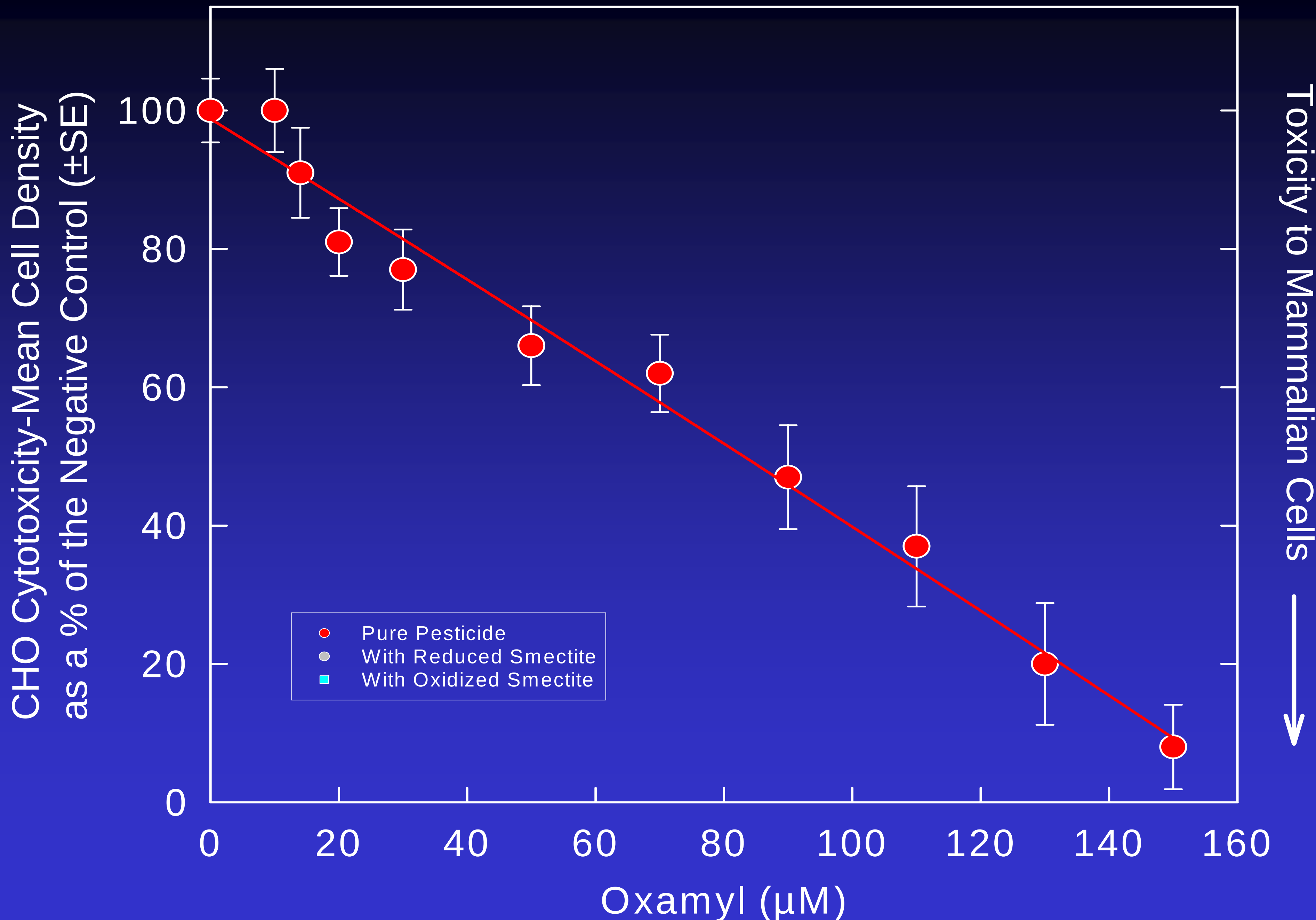
CHO Cytotoxicity-Mean Cell Density
as a % of the Negative Control (±SE)
Toxicity to Mammalian Cells
Pure Pesticide
With Reduced Smectite
With Oxidized Smectite
0
20
40
60
80
100
0
20
40
60
80
100
120
140
160
Oxamyl (μM)

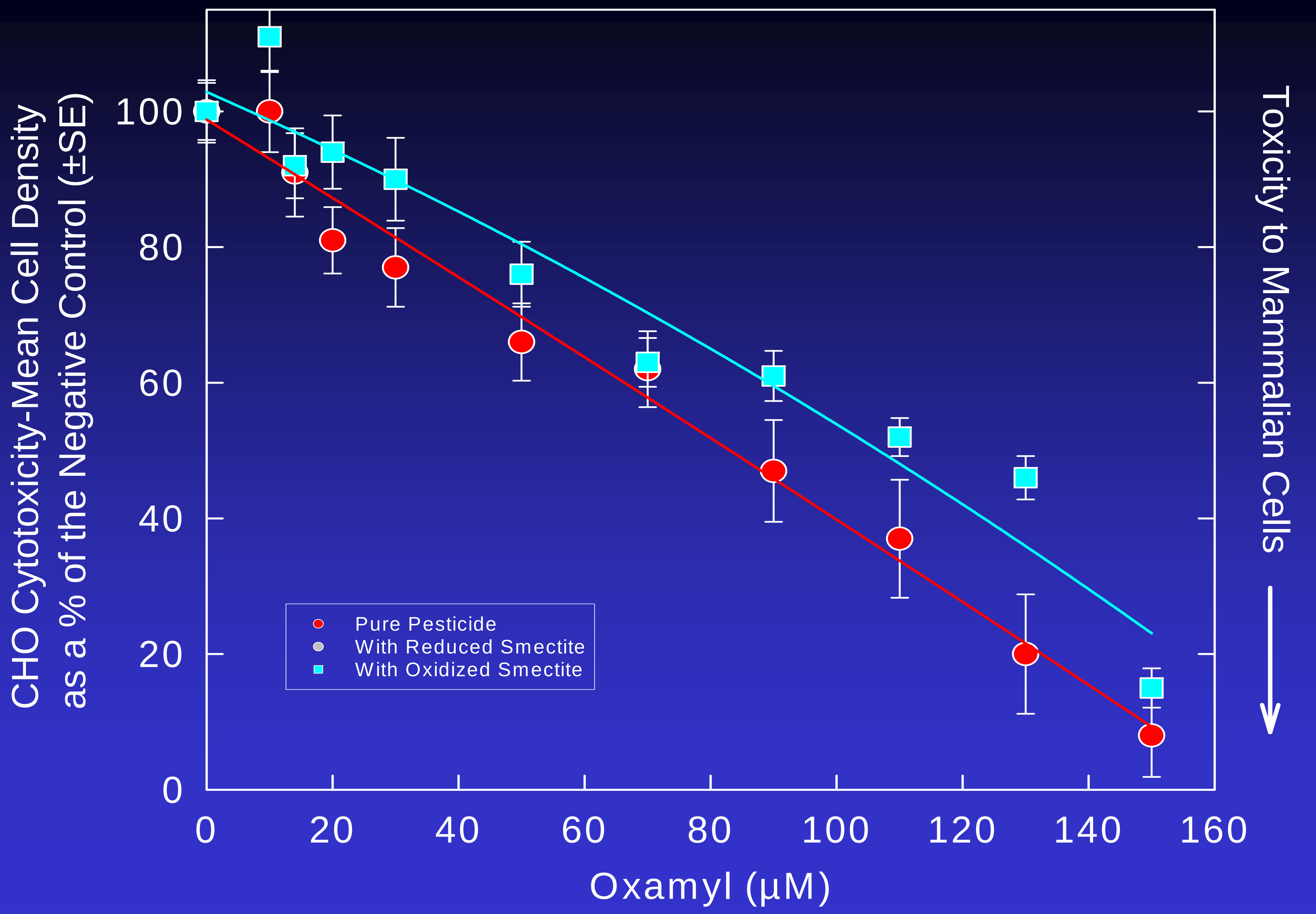
CHO Cytotoxicity-Mean Cell Density
as a % of the Negative Control (±SE)
Toxicity to Mammalian Cells
Pure Pesticide
With Reduced Smectite
With Oxidized Smectite
Oxamyl (µM)
0
20
40
60
80
100
120
140
160

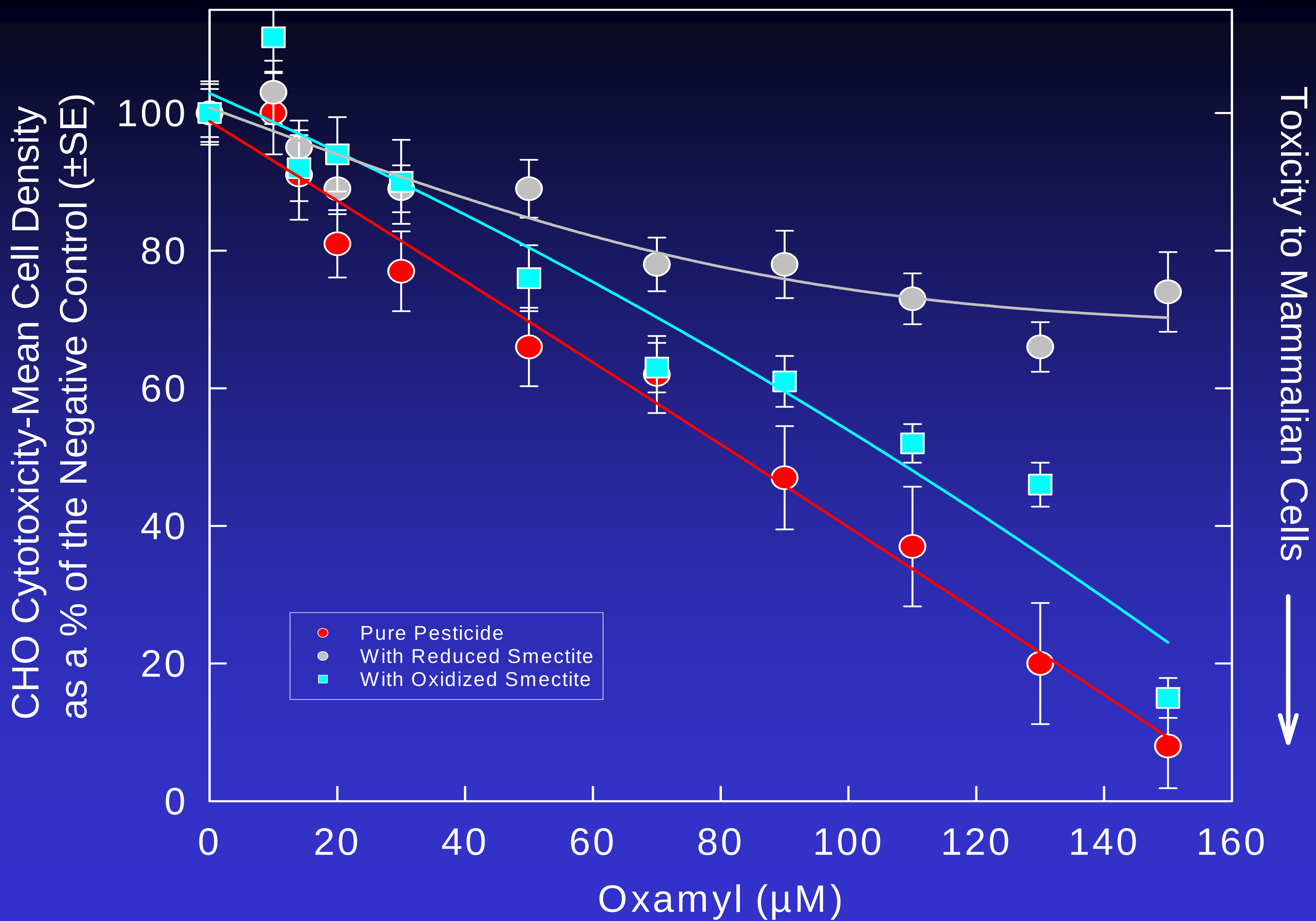

CHO Cytotoxicity-Mean Cell Density
as a % of the Negative Control (±SE)
Toxicity to Mammalian Cells
Pure Pesticide
With Reduced Smectite
With Oxidized Smectite
0
20
40
60
80
100
0
20
40
60
80
100
120
140
160
Oxamyl (µM)

Conclusions -- Oxamyl

- Oxamyl evokes a cytotoxic response in the CHO cells.
- Prior reaction of oxamyl with oxidized (unaltered) smectite clay has no effect on cytotoxicity of the pesticide.
- Reaction of oxamyl with reduced smectite clay mitigates a large fraction of its cytotoxicity.

2,4-D Transformation

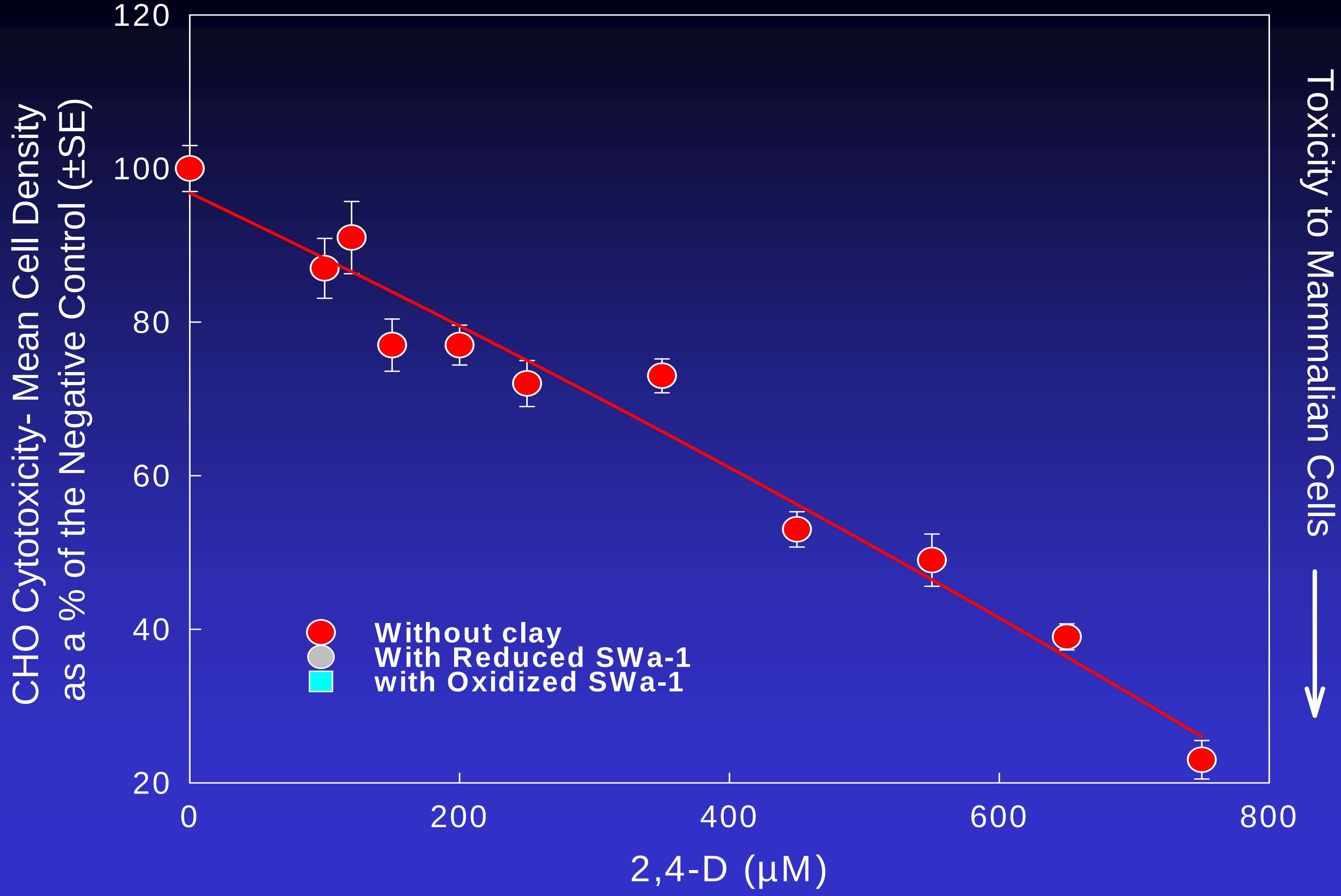

CHO Cytotoxicity- Mean Cell Density
as a % of the Negative Control (±SE)
120
100
80
60
40
20
0
200
400
600
800
2,4-D (μM)
Without clay
With Reduced SWa-1
with Oxidized SWa-1
Toxicity to Mammalian Cells

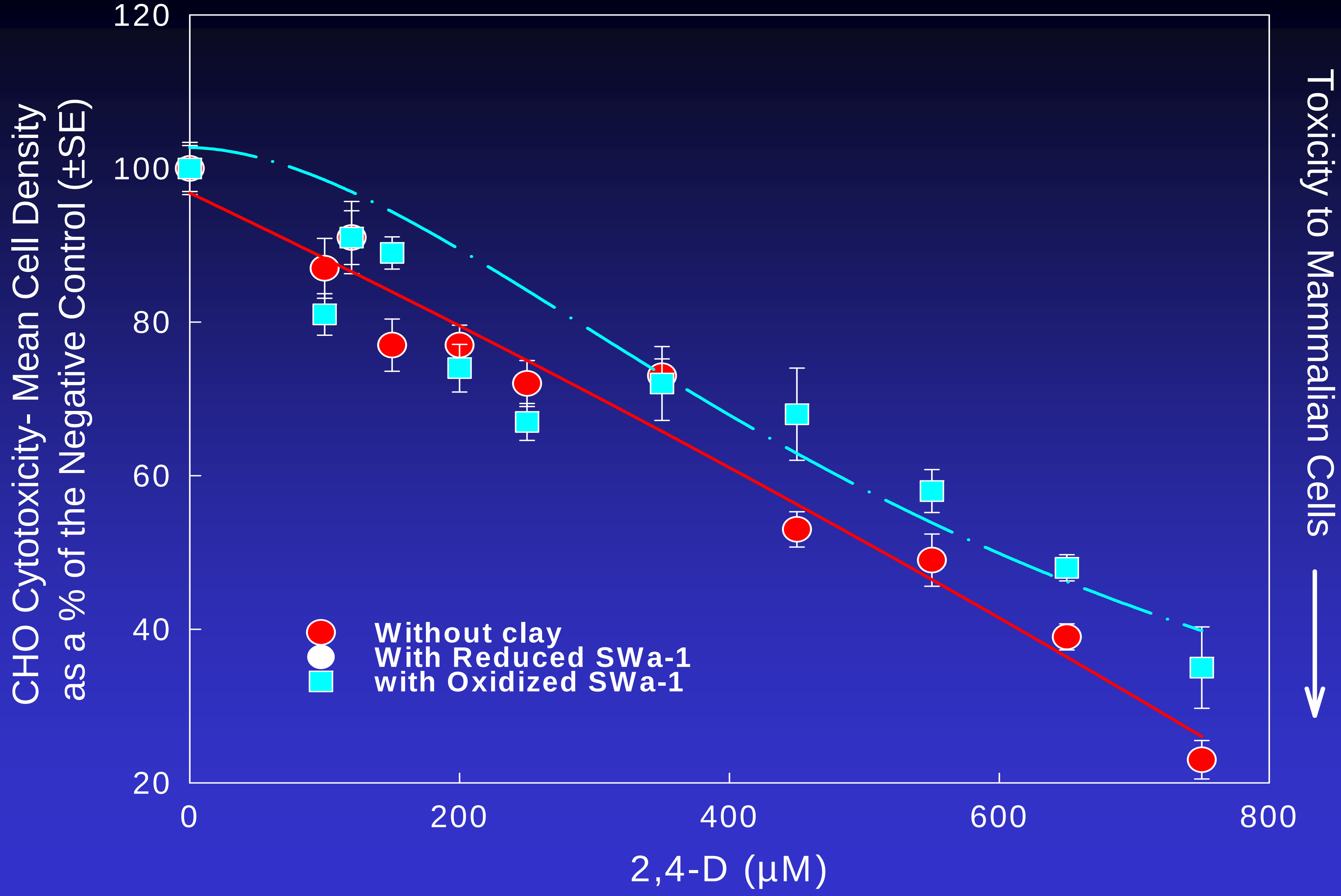
CHO Cytotoxicity- Mean Cell Density
as a % of the Negative Control (±SE)
120
100
80
60
40
20
0
200
400
600
800
2,4-D (µM)
Without clay
With Reduced SWa-1
with Oxidized SWa-1
Toxicity to Mammalian Cells

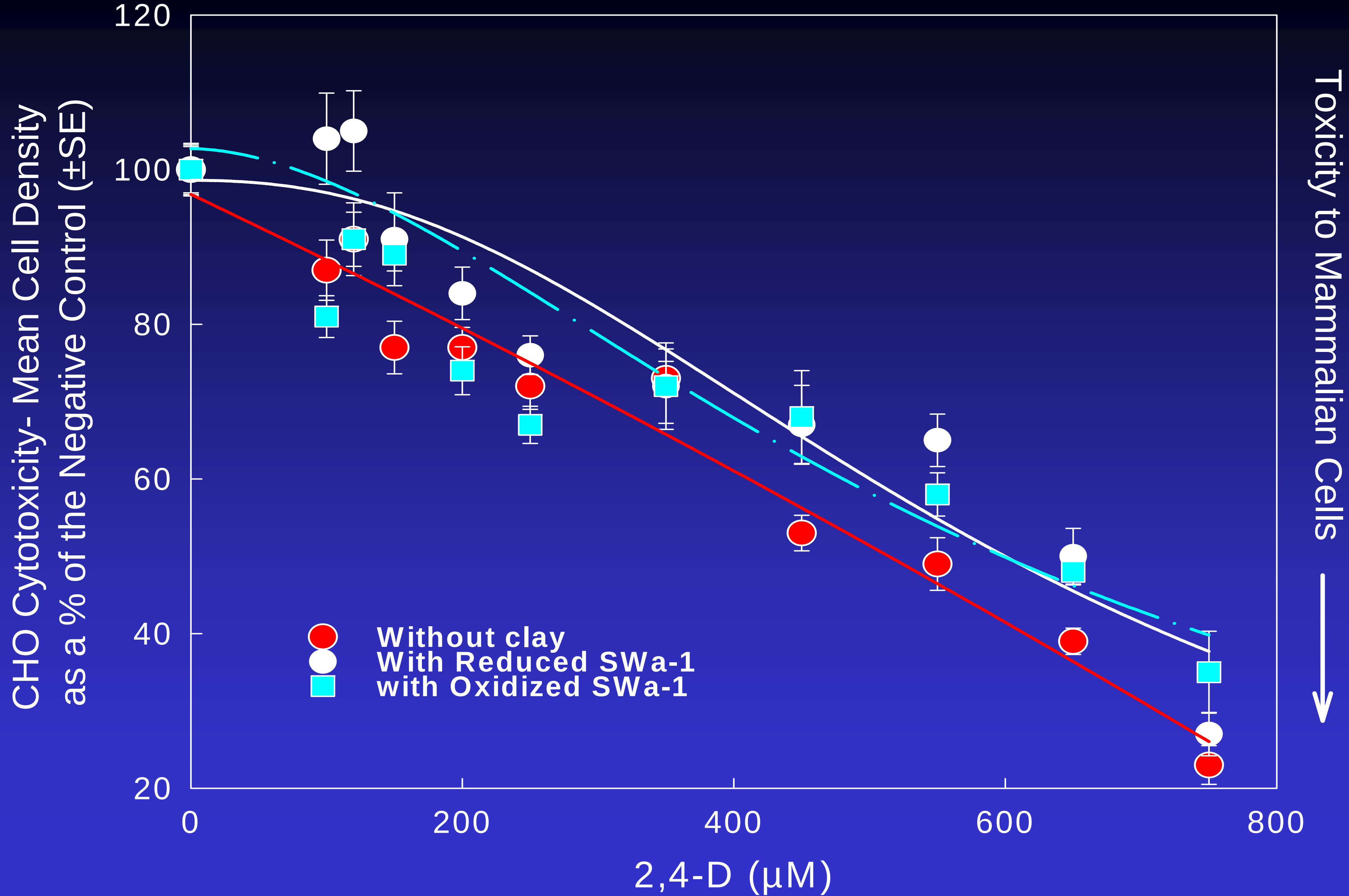

CHO Cytotoxicity- Mean Cell Density
as a % of the Negative Control (±SE)
Toxicity to Mammalian Cells
120
100
80
60
40
20
0
200
400
600
800
2,4-D (µM)
Without clay
With Reduced SWa-1
with Oxidized SWa-1

Conclusions – 2,4-D

- 2,4-D evokes a cytotoxic response in the CHO cells.
- Prior reaction of 2,4-D with either oxidized (unaltered) or reduced smectite clay has no effect on cytotoxicity of this pesticide.

Dicamba Transformation

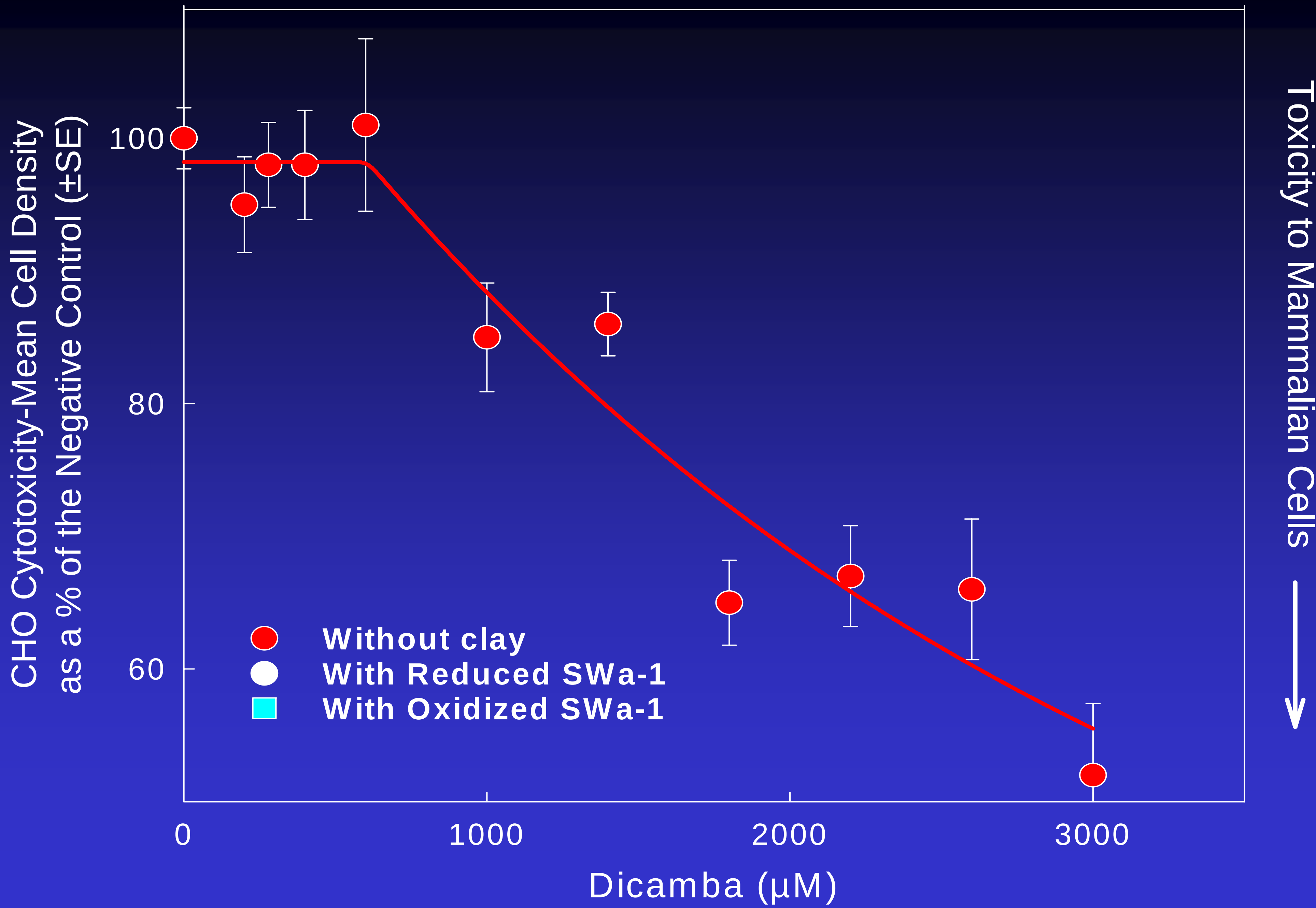
CHO Cytotoxicity-Mean Cell Density
as a % of the Negative Control (±SE)
100
80
60
0
1000
2000
3000
Dicamba (µM)
Toxicity to Mammalian Cells
Without clay
With Reduced SWa-1
With Oxidized SWa-1

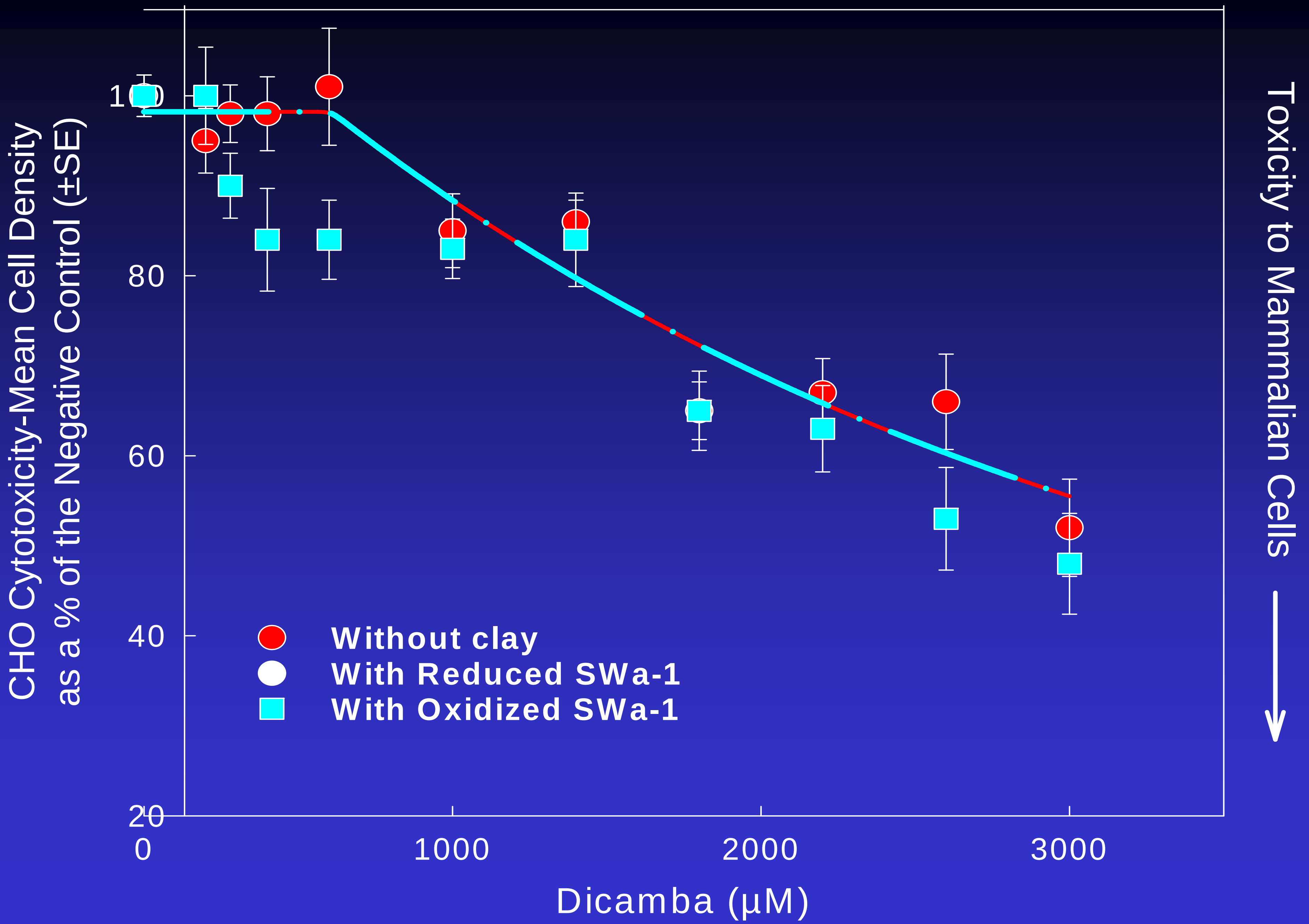

CHO Cytotoxicity-Mean Cell Density
as a % of the Negative Control (±SE)
100
80
60
40
20
0
1000
2000
3000
Dicamba (µM)
Without clay
With Reduced SWa-1
With Oxidized SWa-1
Toxicity to Mammalian Cells

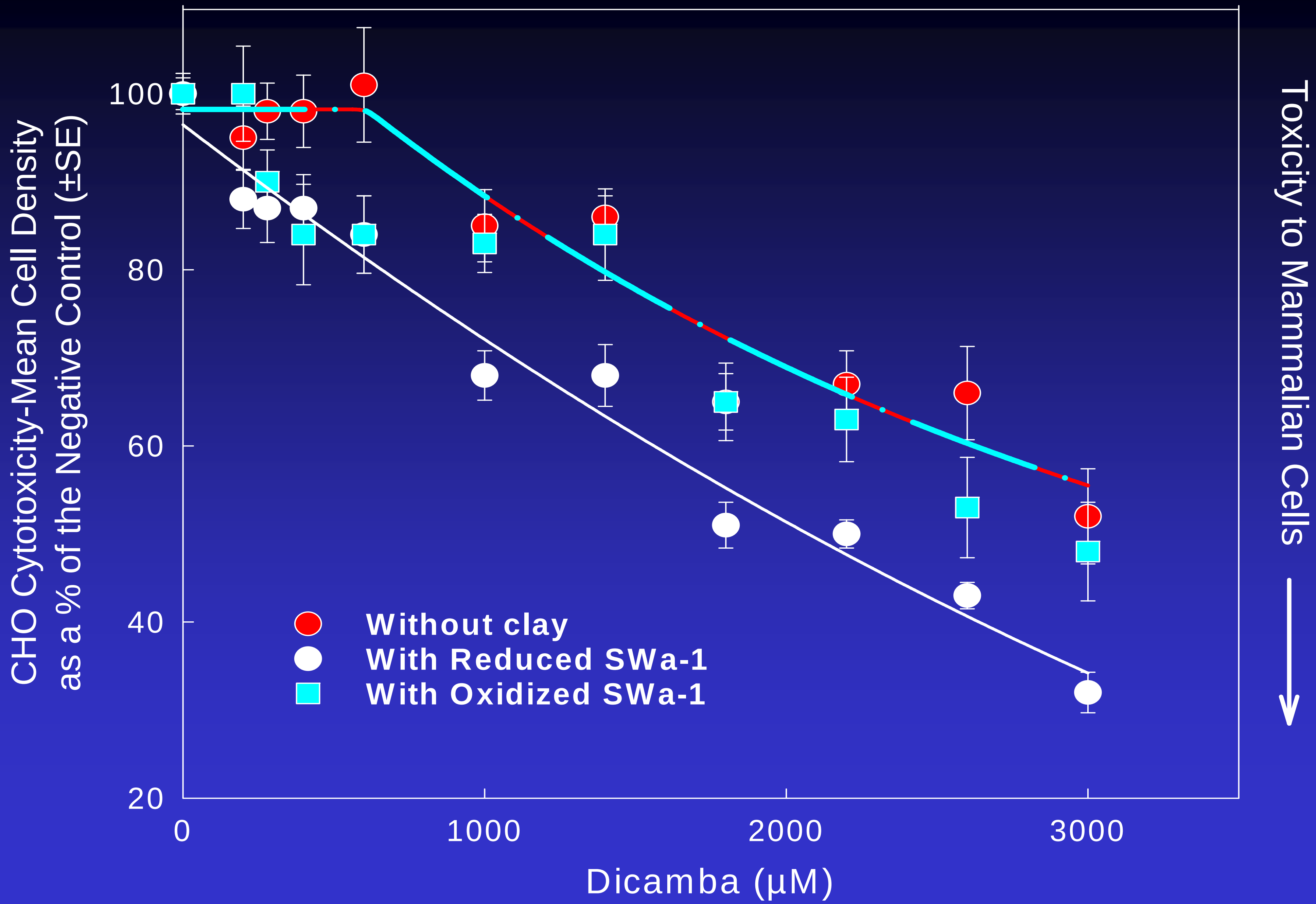

CHO Cytotoxicity-Mean Cell Density
as a % of the Negative Control (±SE)
100
80
60
40
20
0
1000
2000
3000
Dicamba (µM)
Without clay
With Reduced SWa-1
With Oxidized SWa-1
Toxicity to Mammalian Cells

Conclusions -- Dicamba

- Dicamba evokes a cytotoxic response in the CHO cells.
- Prior reaction of dicamba with oxidized (unaltered) smectite clay has little effect on cytotoxicity of the pesticide.
- Reaction of dicamba with reduced smectite clay actually enhances its cytotoxicity to CHO cells.

Treatment of Pesticide

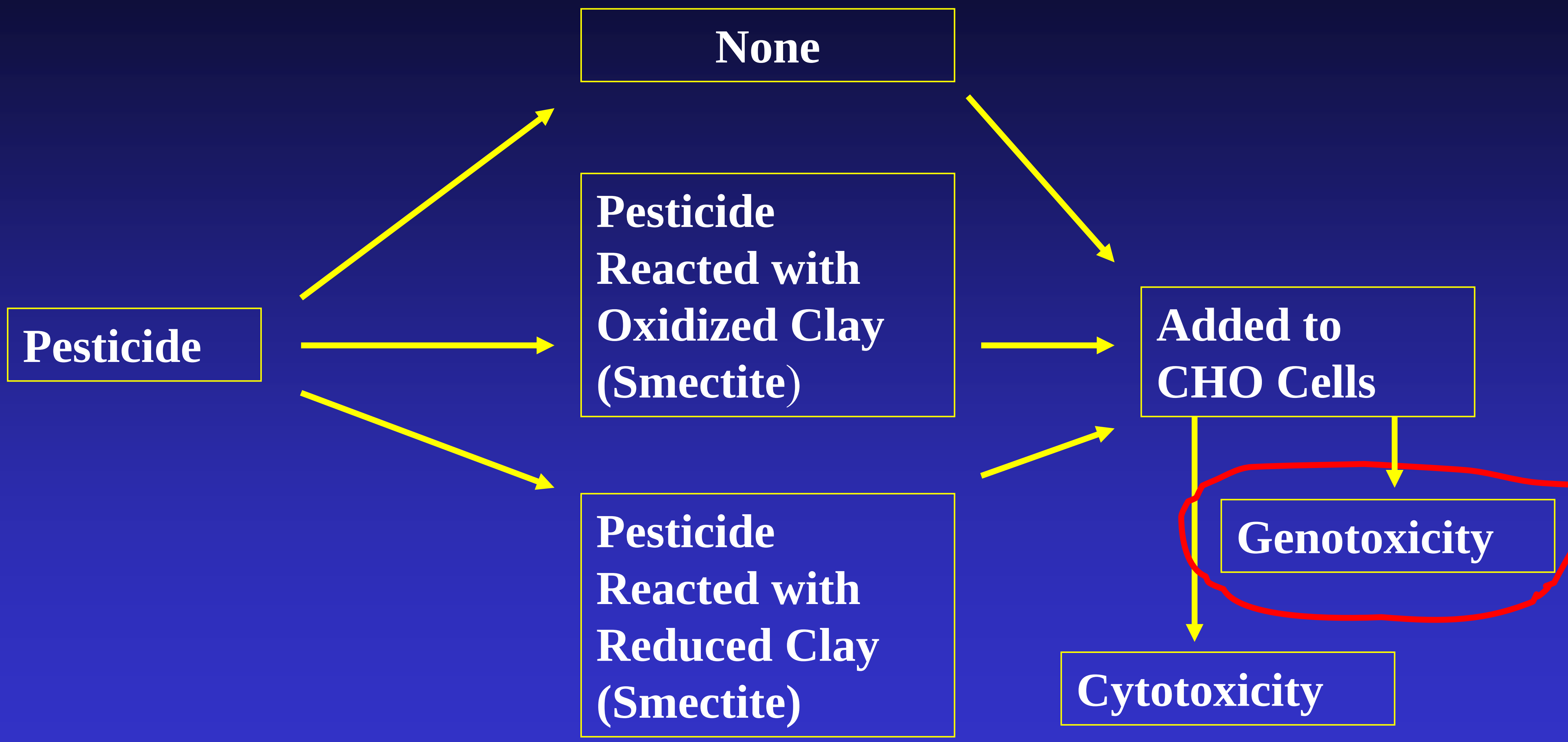

Genotoxicity Method

- DNA was stained with ethidium bromide then submitted to Single-cell Gel Electrophoresis.

Genotoxicity Method

- DNA was stained with ethidium bromide then submitted to Single-cell Gel Electrophoresis.
- A fluorescence microscope was used to digitize and record images of DNA in a CCD camera.

Genotoxicity Method

- DNA was stained with ethidium bromide then submitted to Single-cell Gel Electrophoresis.
- A fluorescence microscope was used to digitize and record images of DNA in a CCD camera.
- Damaged DNA migrated away from the nucleus, creating a tail in the medium – like a comet.

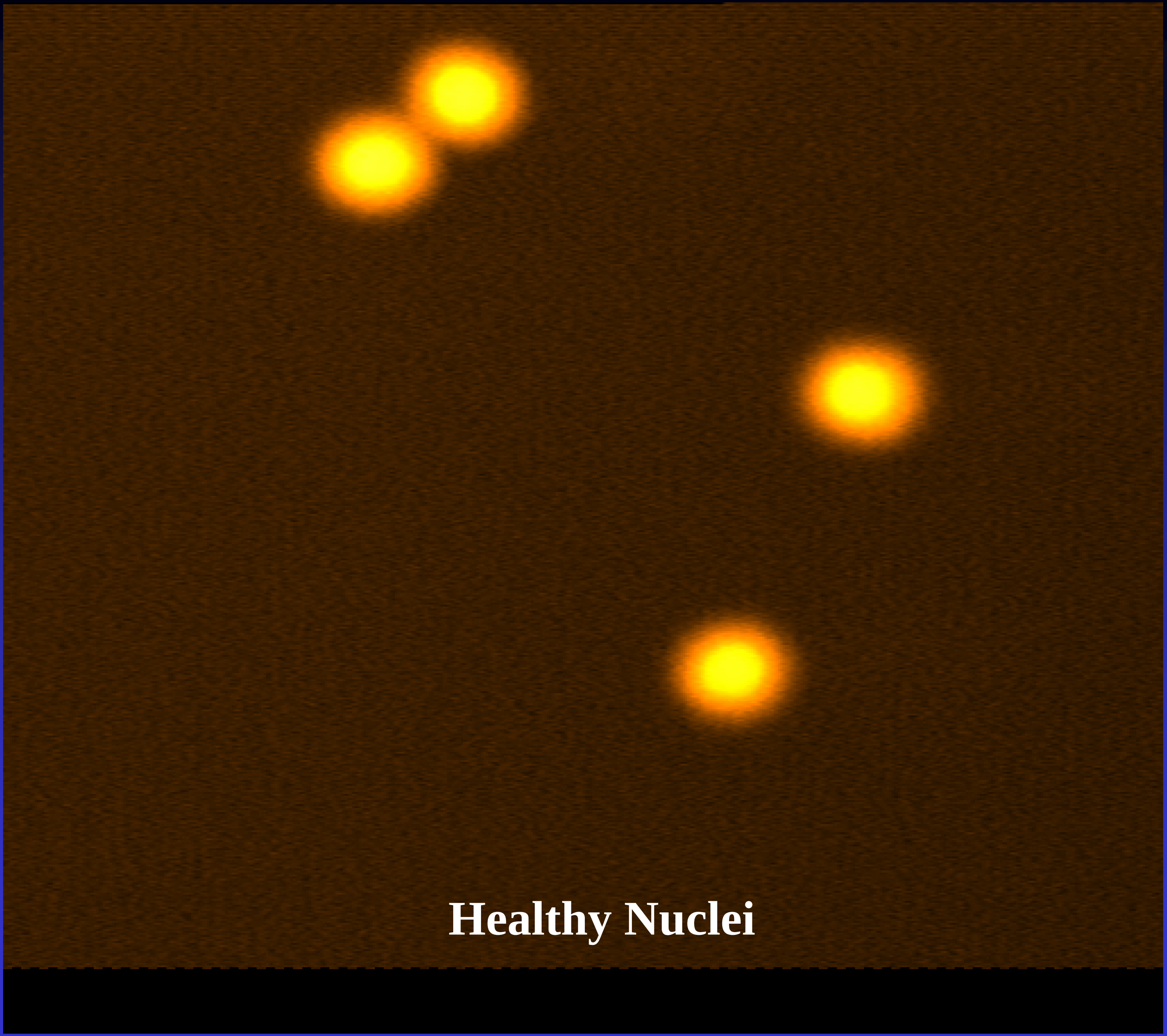
Healthy Nuclei

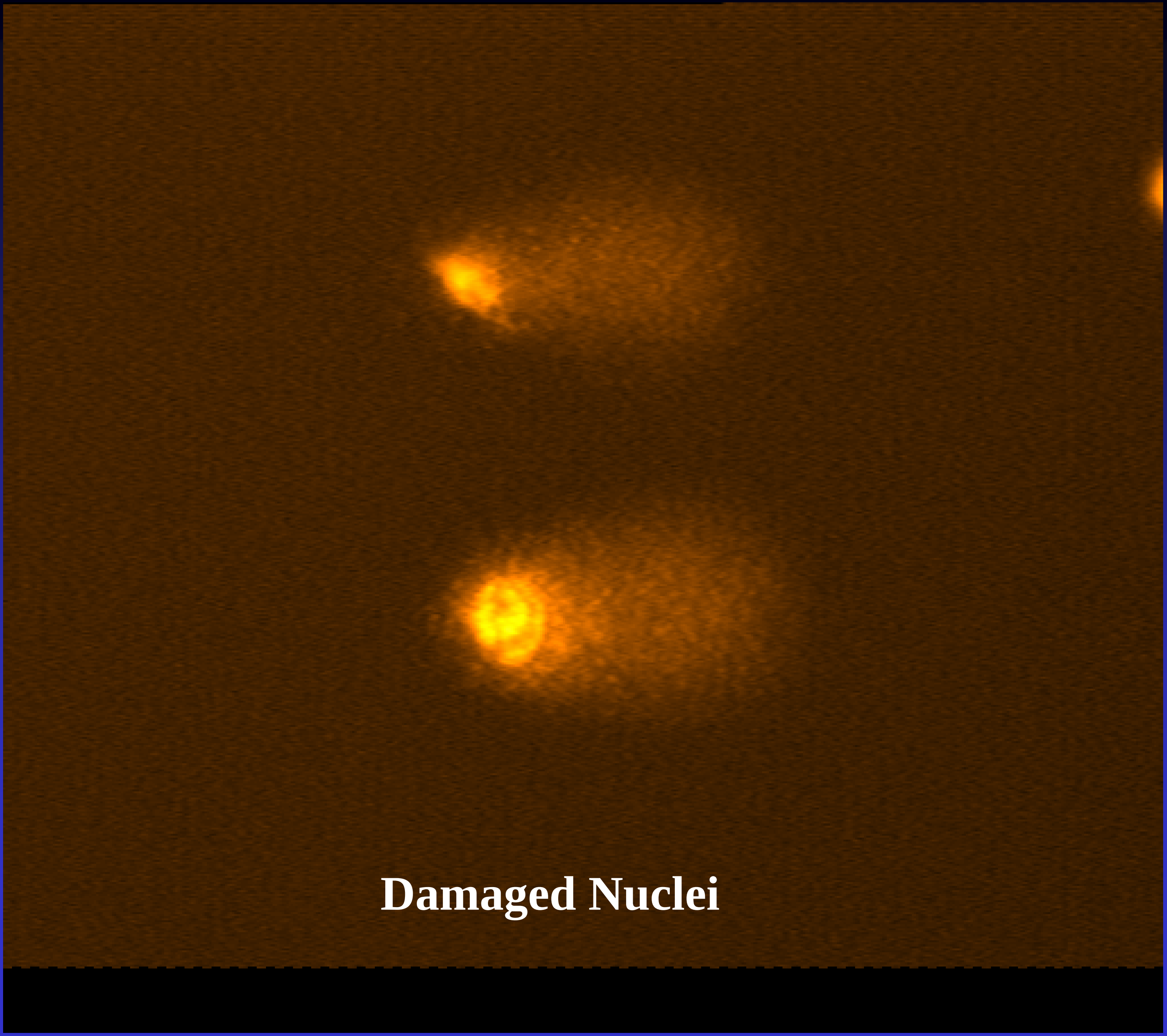
Damaged Nuclei

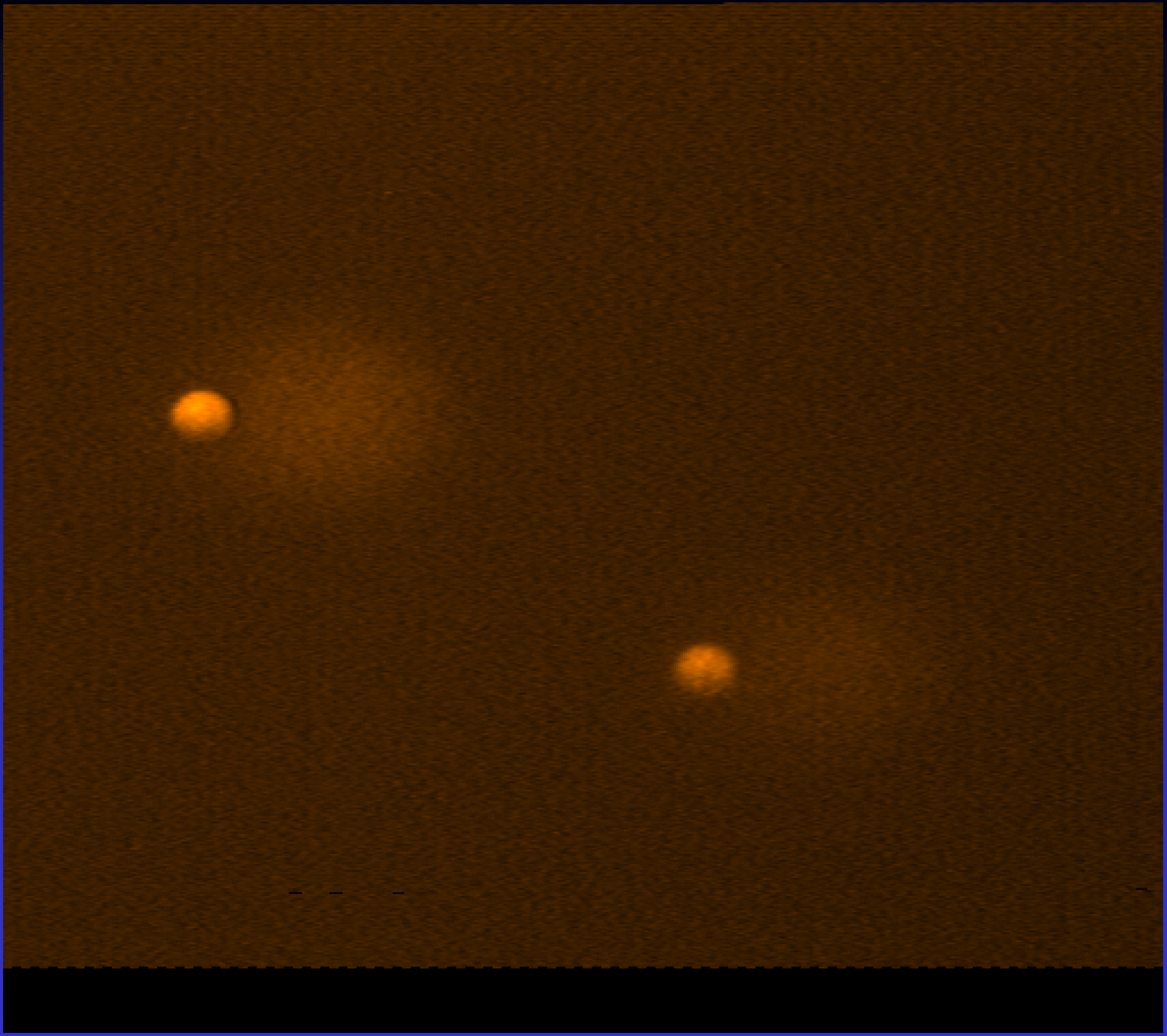

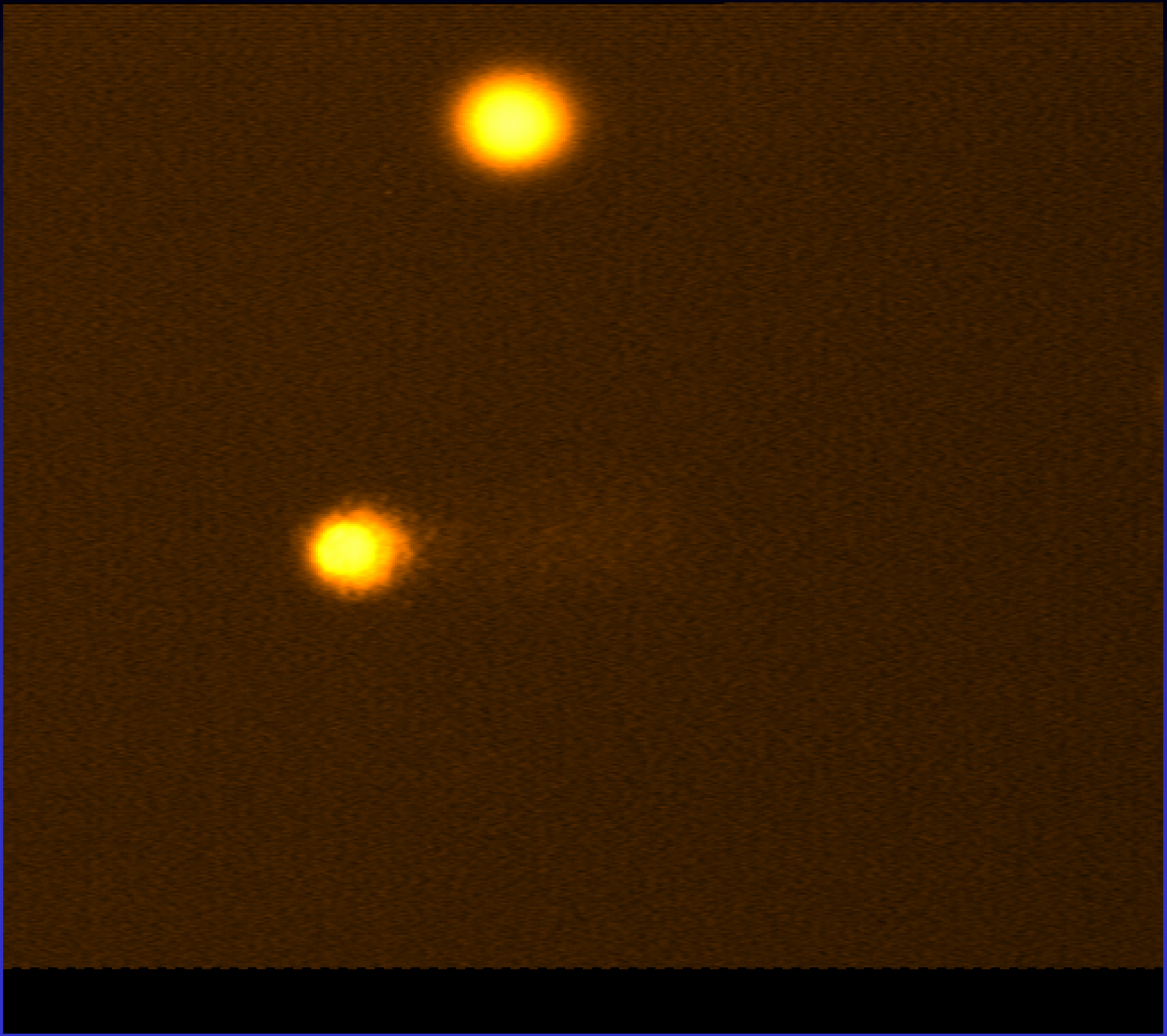

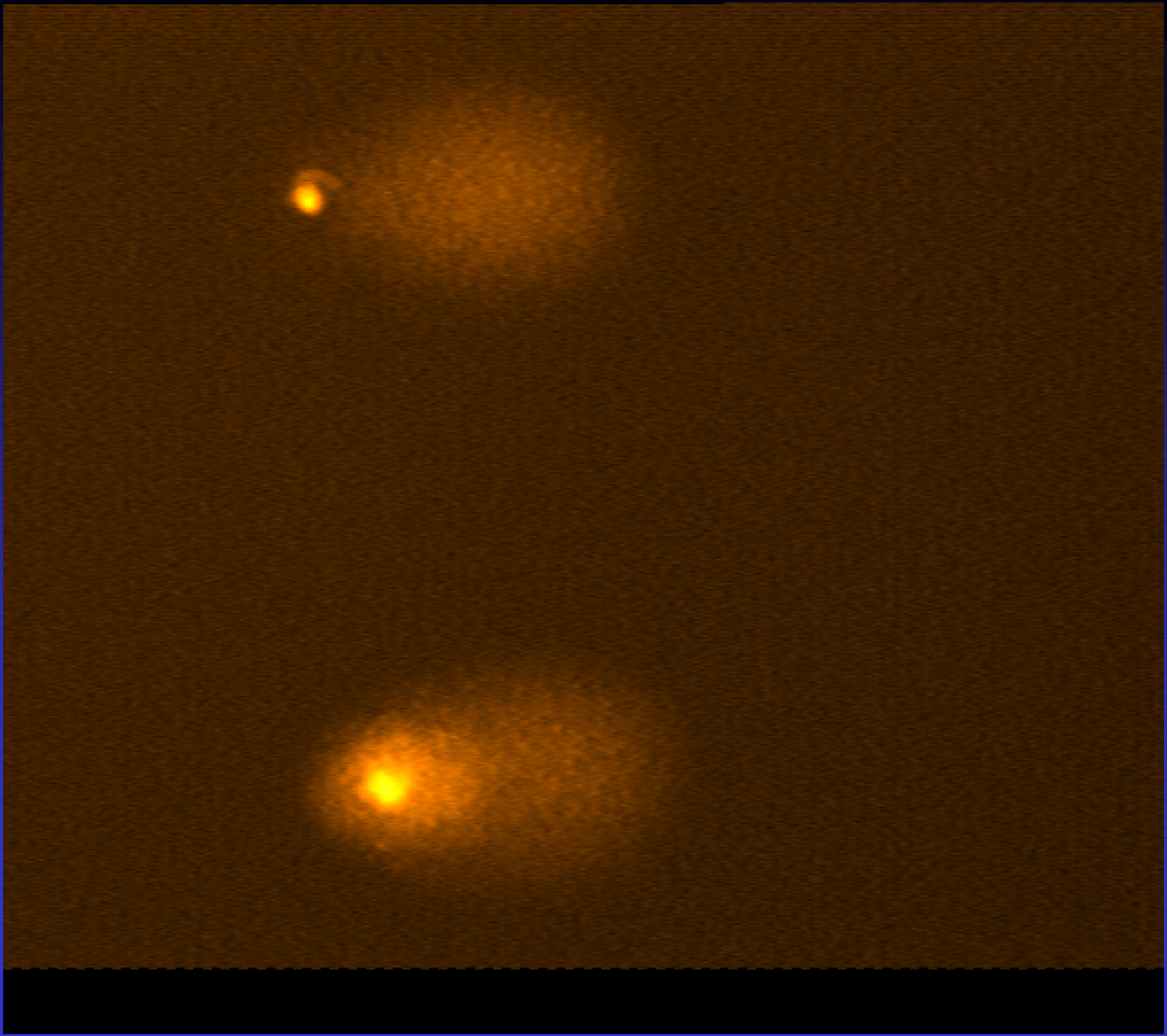

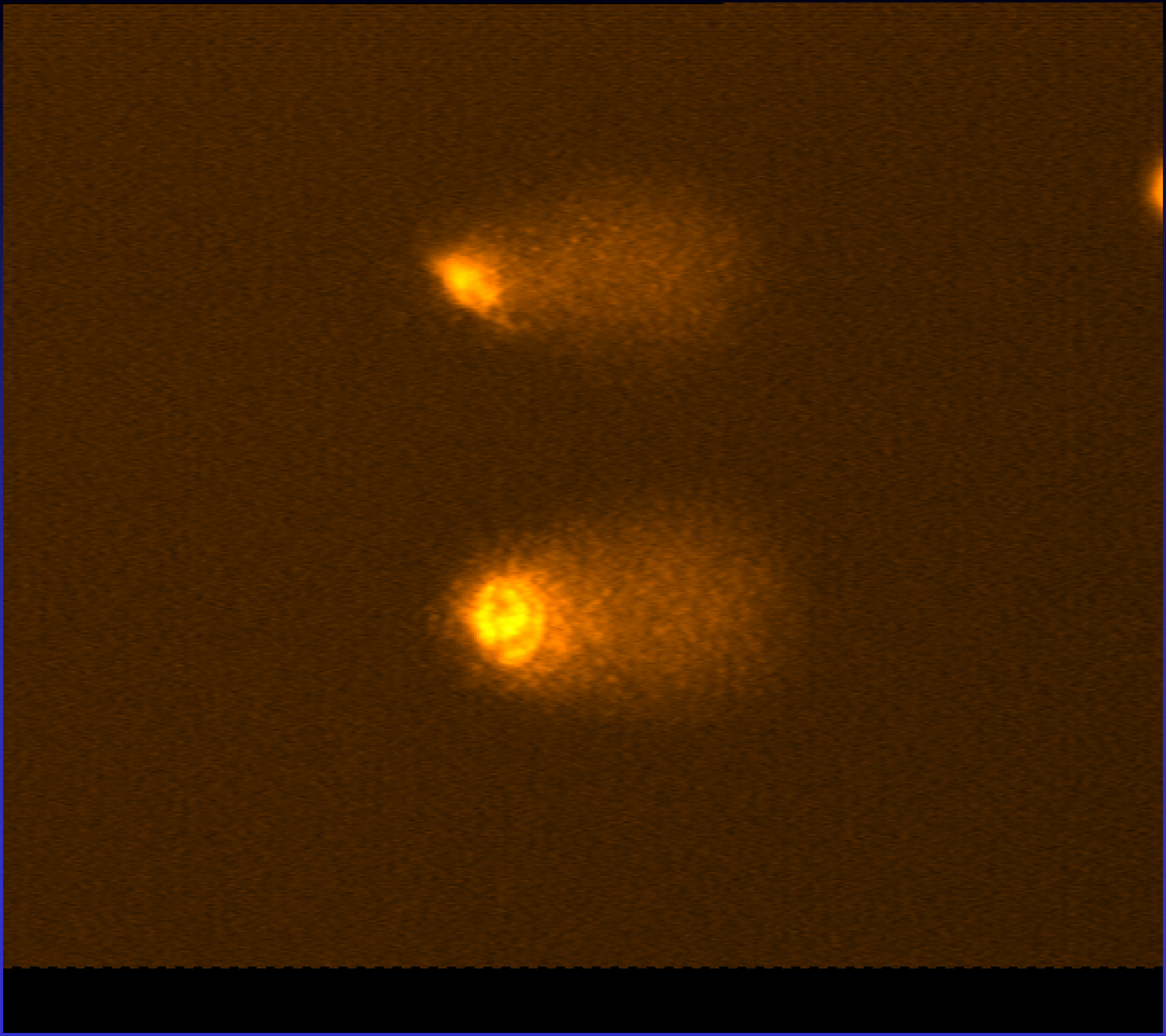

Genotoxicity Method

- DNA was stained with ethidium bromide then submitted to Single-cell Gel Electrophoresis.
- A fluorescence microscope was used to digitize and record images of DNA in a CCD camera.
- Damaged DNA migrated away from the nucleus, creating a tail in the medium – like a comet.
- Extent of damage was recorded as % tail of a concurrent positive control using (EMS).

Genotoxicity Method

- DNA was stained with ethidium bromide then submitted to Single-cell Gel Electrophoresis.
- A fluorescence microscope was used to digitize and record images of DNA in a CCD camera.
- Damaged DNA migrated away from the nucleus, creating a tail in the medium – like a comet.
- Extent of damage was recorded as % tail of a concurrent positive control using (EMS).
- Level of exposure to pesticide was in the range where cytotoxicity was low.

All Pesticides with No Clay

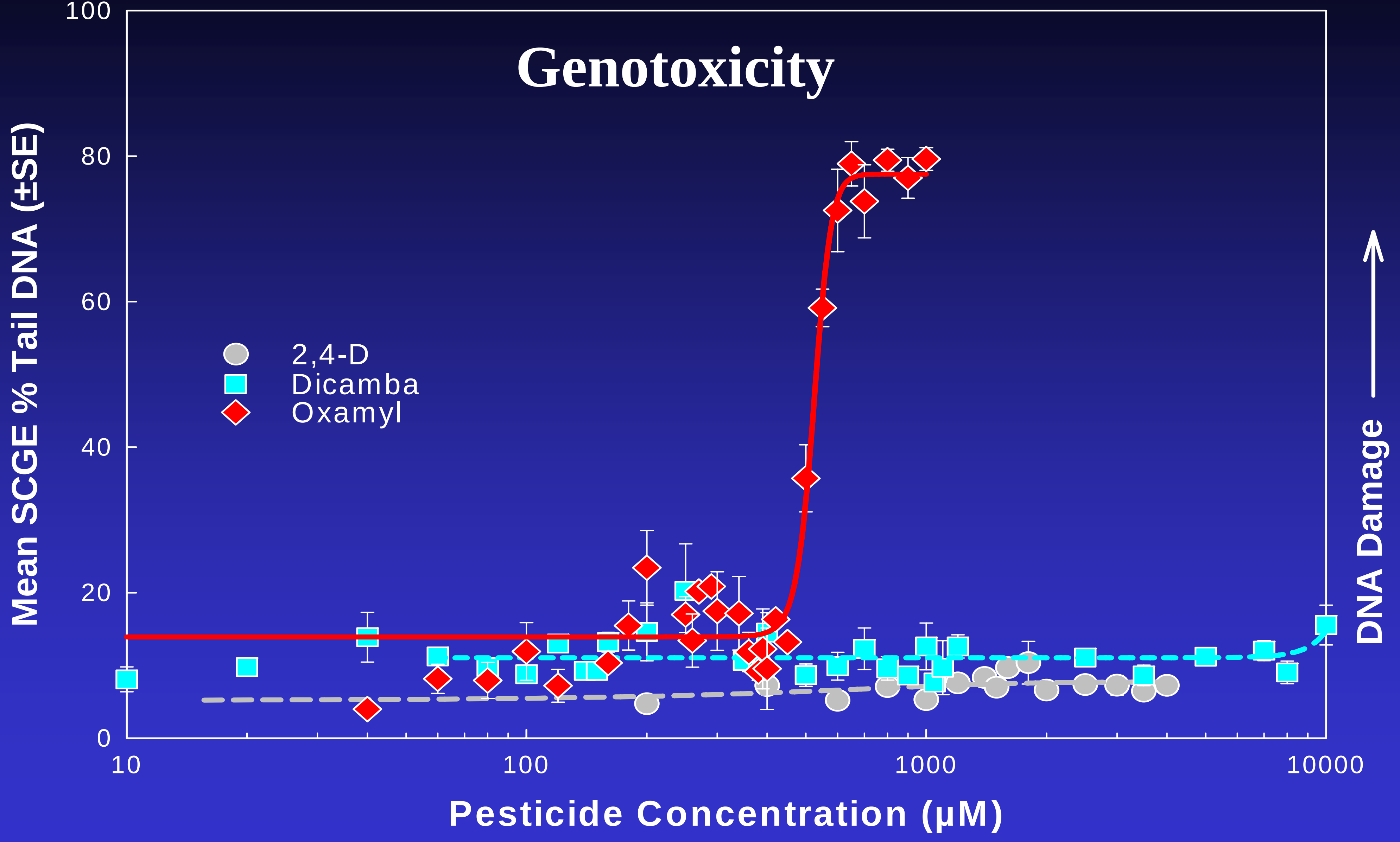
Genotoxicity
Mean SCGE % Tail DNA (±SE)
100
80
60
40
20
0
2,4-D
Dicamba
Oxamyl
10
100
1000
10000
Pesticide Concentration (μM)
DNA Damage

Oxamyl

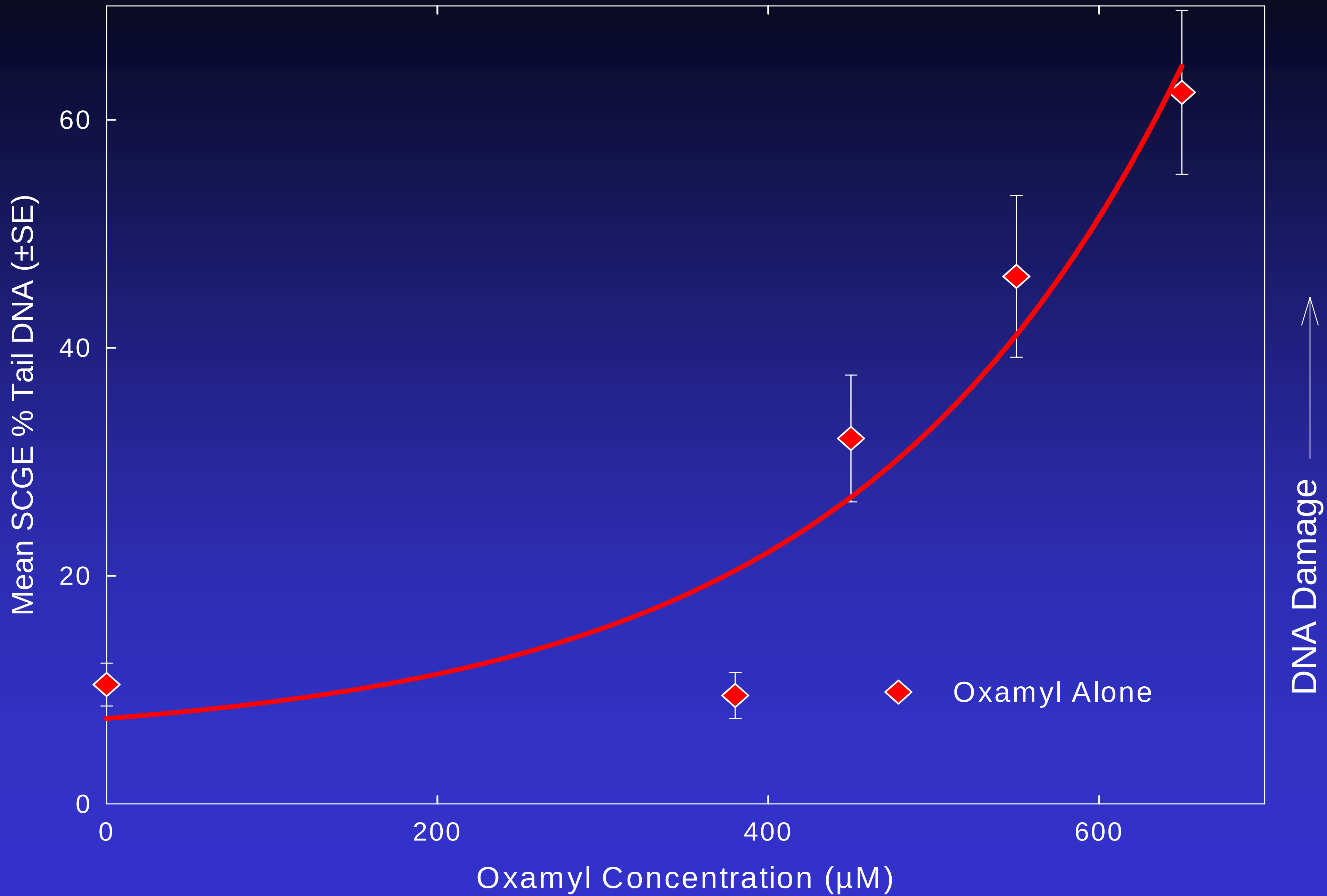

Mean SCGE % Tail DNA (±SE)
60
40
20
0
0
200
400
600
Oxamyl Concentration (µM)
Oxamyl Alone
DNA Damage

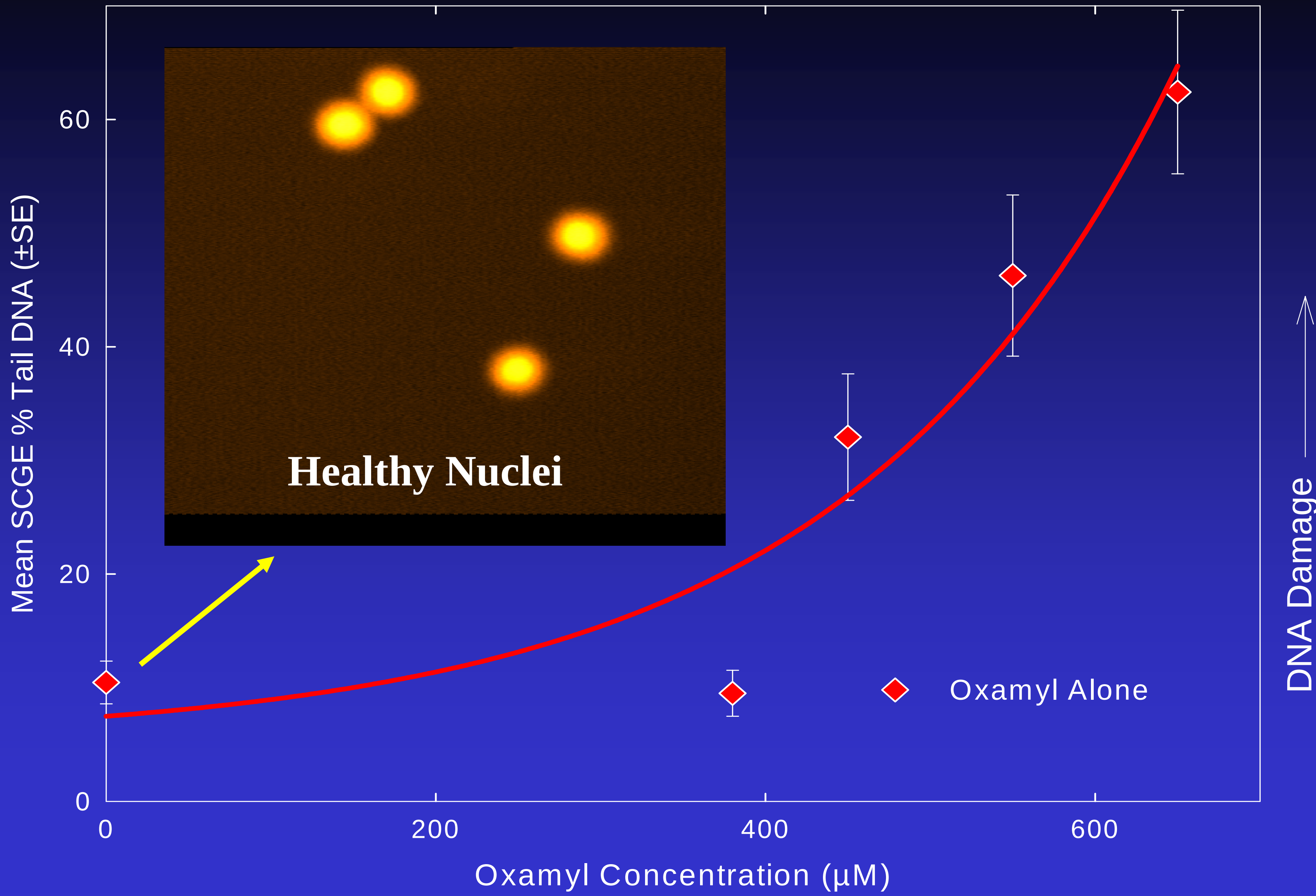

Healthy Nuclei
Mean SCGE % Tail DNA (±SE)
0
20
40
60
0
200
400
600
Oxamyl Concentration (µM)
Oxamyl Alone
DNA Damage

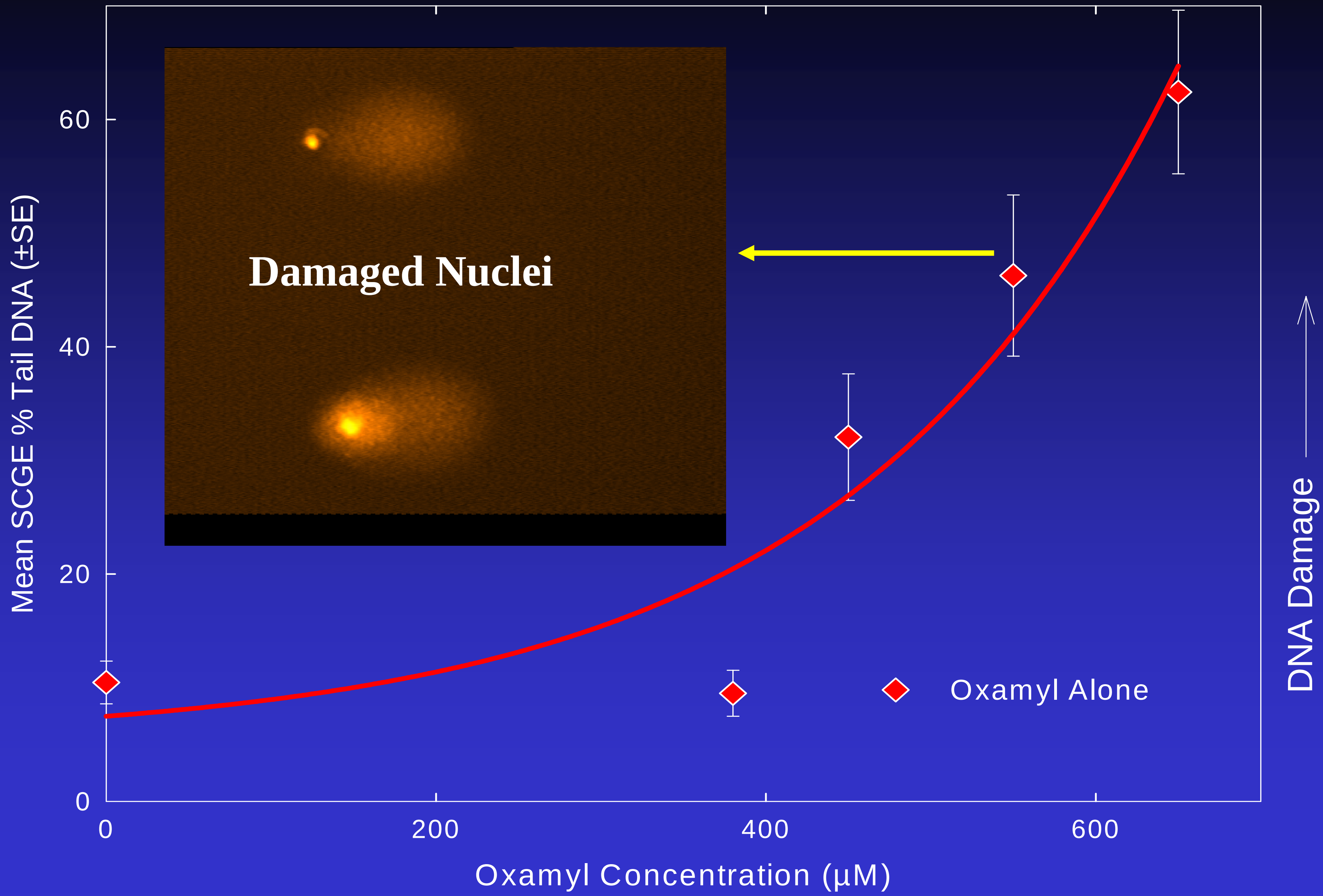
Damaged Nuclei
Mean SCGE % Tail DNA (±SE)
0
20
40
60
0
200
400
600
Oxamyl Concentration (μM)
Oxamyl Alone
DNA Damage

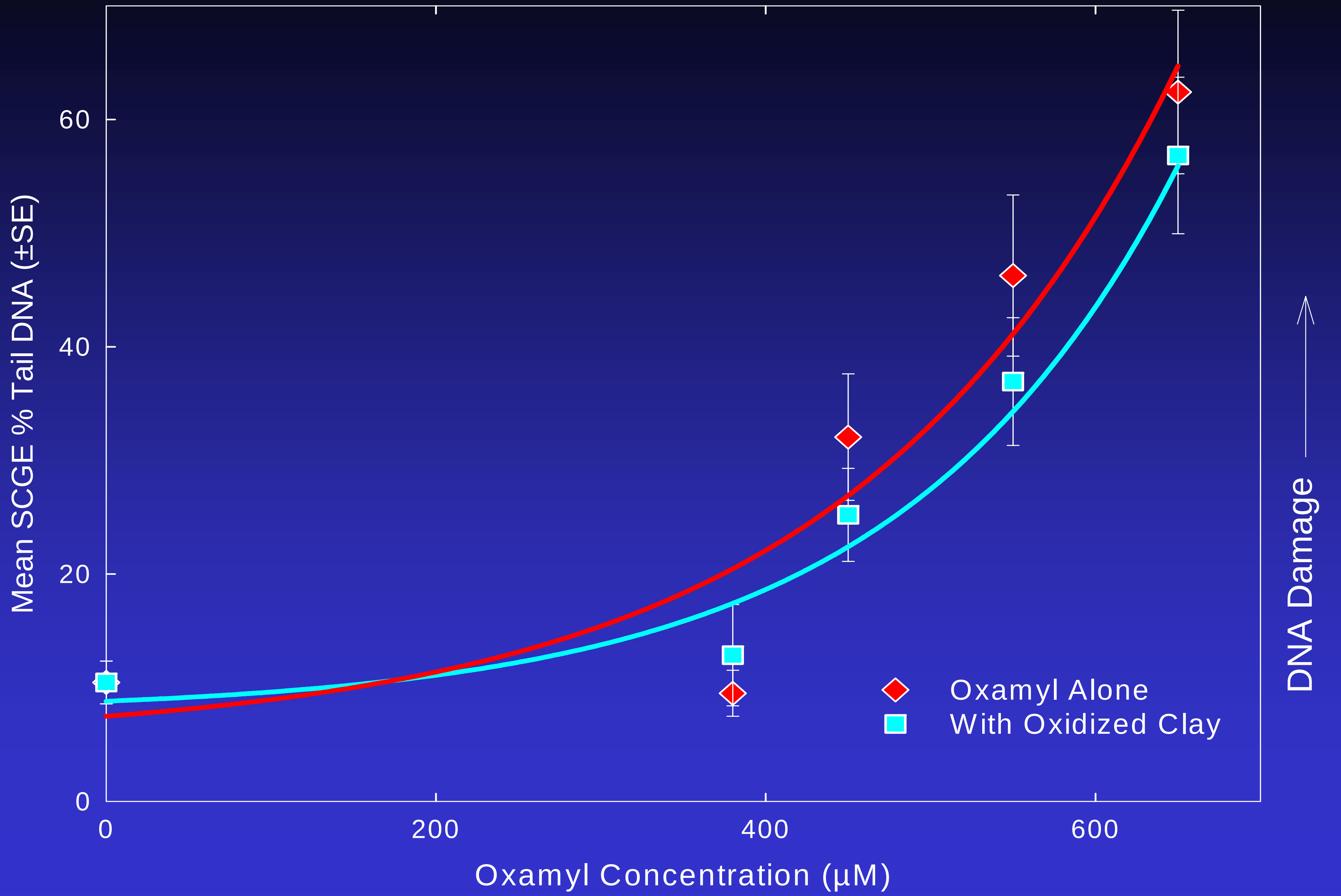

Mean SCGE % Tail DNA (±SE)
60
40
20
0
0
200
400
600
Oxamyl Concentration (μM)
Oxamyl Alone
With Oxidized Clay
DNA Damage

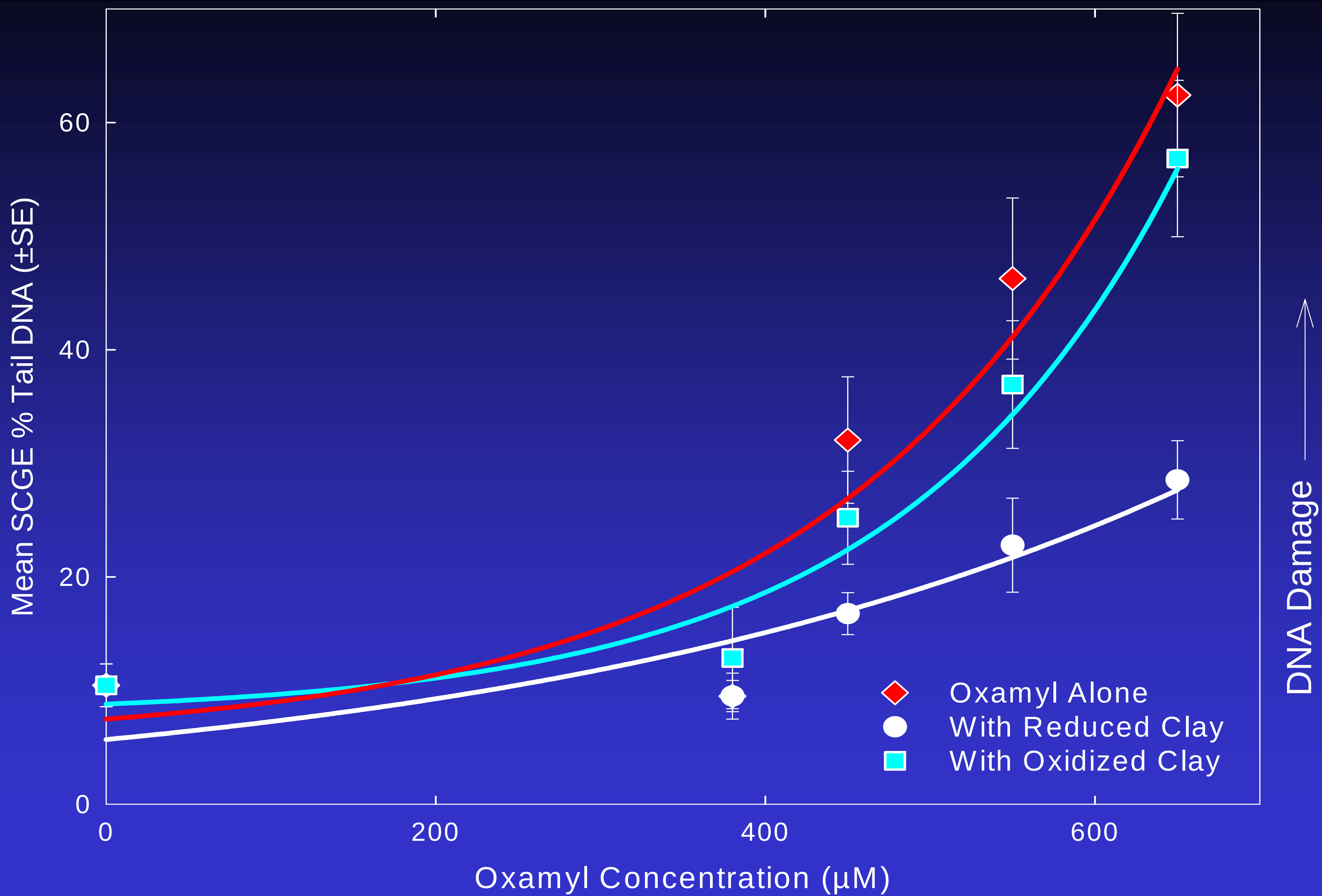

Mean SCGE % Tail DNA (±SE)
0
20
40
60
0
200
400
600
Oxamyl Concentration (μM)
Oxamyl Alone
With Reduced Clay
With Oxidized Clay
DNA Damage

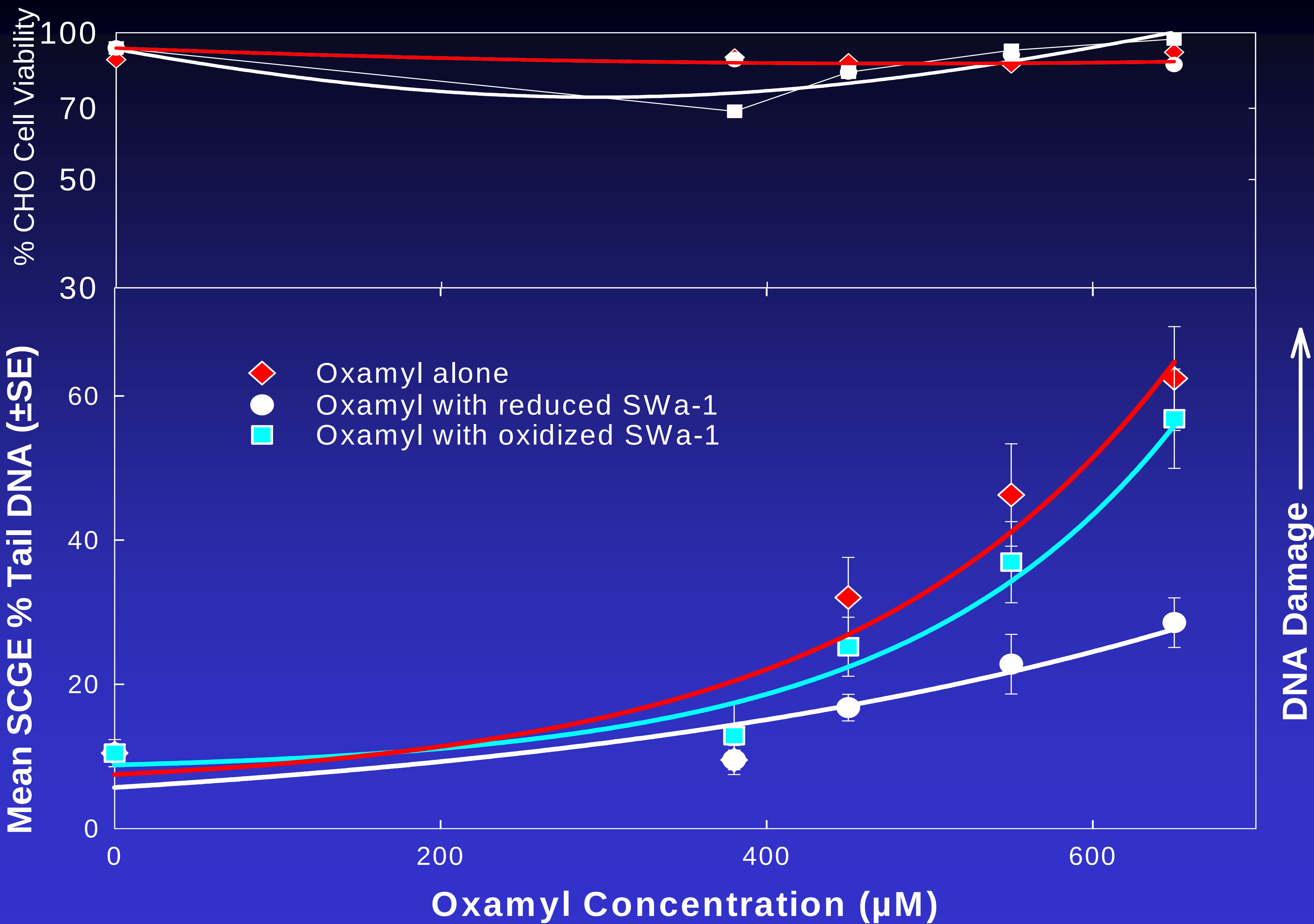

% CHO Cell Viability
100
70
50
30
Mean SCGE % Tail DNA (±SE)
60
40
20
0
Oxamyl alone
Oxamyl with reduced SWa-1
Oxamyl with oxidized SWa-1
DNA Damage
0
200
400
600
Oxamyl Concentration (μM)

Conclusions -- Oxamyl

- To our knowledge this is the first report that the pesticide oxamyl manifests genotoxic properties.

Conclusions -- Oxamyl

- To our knowledge this is the first report that the pesticide oxamyl manifests genotoxic properties.
- Reaction of oxamyl with oxidized (unaltered) smectite clay has no effect on genotoxicity of the pesticide.

Conclusions -- Oxamyl

- To our knowledge this is the first report that the pesticide oxamyl manifests genotoxic properties.
- Reaction of oxamyl with oxidized (unaltered) smectite clay has no effect on genotoxicity of the pesticide.
- Reaction of oxamyl with reduced smectite clay mitigates a large fraction of its genotoxicity.

2,4-D

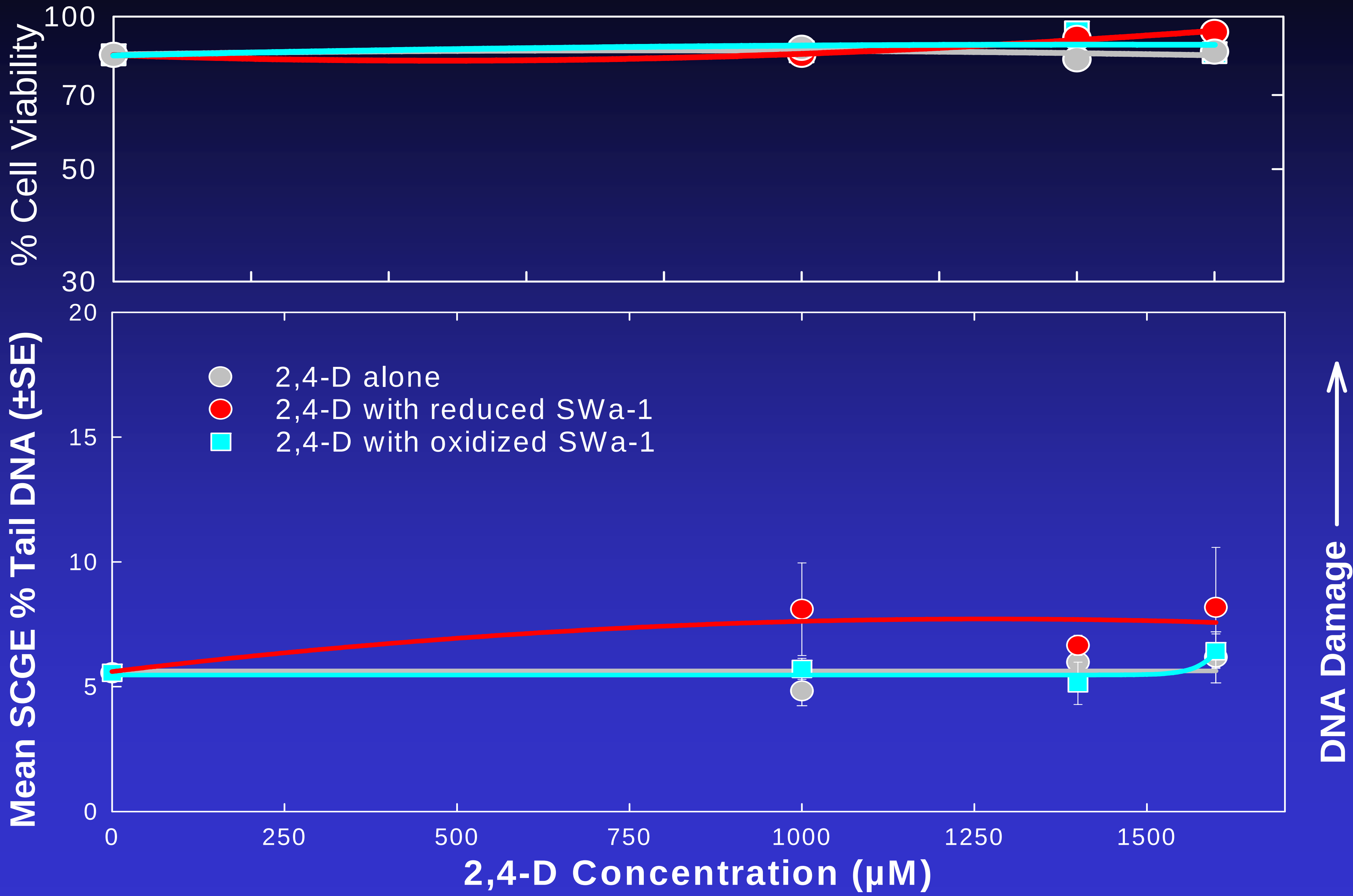
100
70
50
30
% Cell Viability
20
15
10
5
0
Mean SCGE % Tail DNA (±SE)
2,4-D alone
2,4-D with reduced SWa-1
2,4-D with oxidized SWa-1
DNA Damage
0
250
500
750
1000
1250
1500
2,4-D Concentration (μM)

Conclusions -- 2,4-D

- **2,4-D genotoxicity is less than oxamyl and about the same as dicamba.**

Conclusions -- 2,4-D

- 2,4-D genotoxicity is less than oxamyl and about the same as dicamba.
- Its genotoxicity is unaffected by either oxidized (unaltered) or reduced smectite clay.

Dicamba

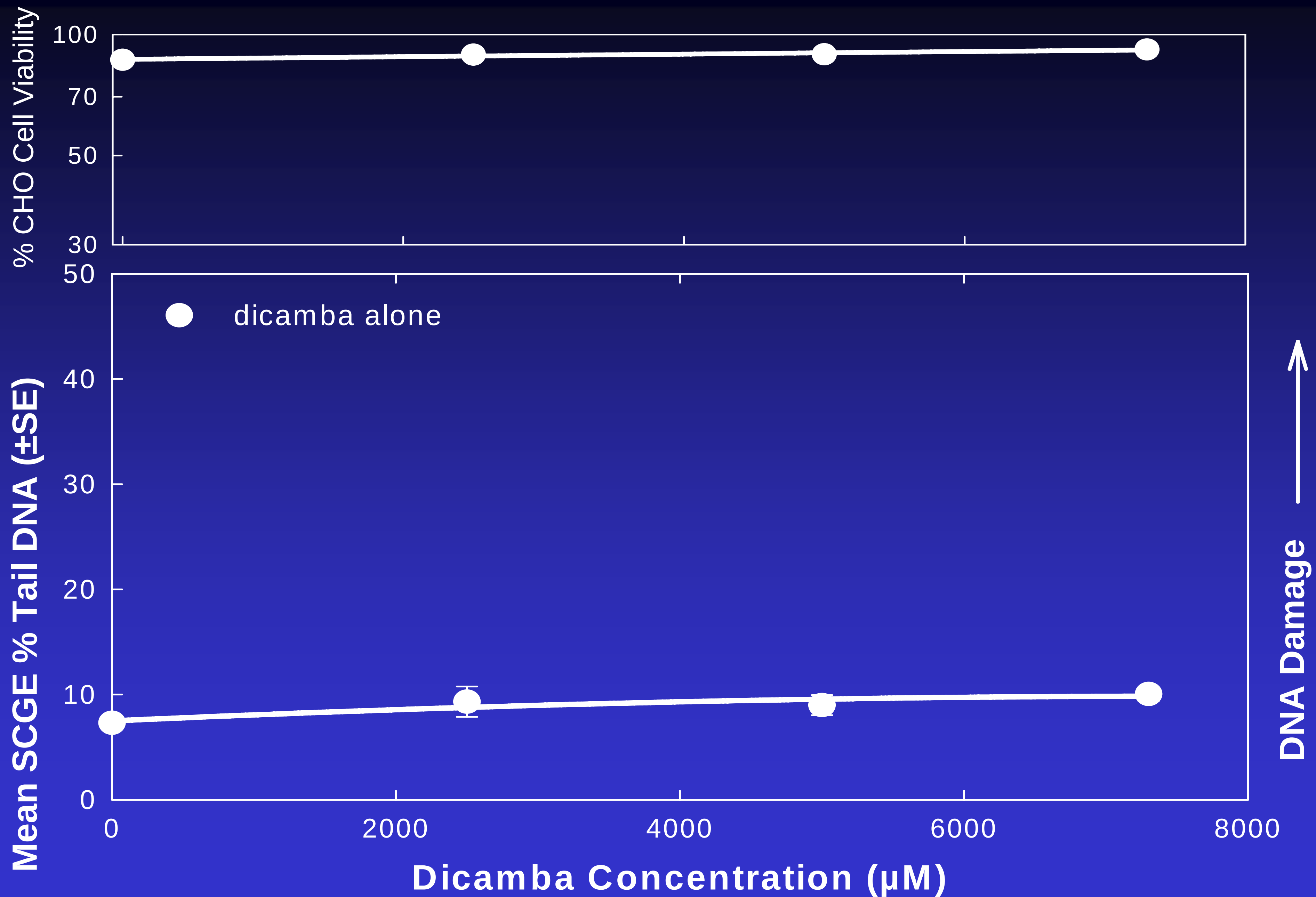

% CHO Cell Viability
100
70
50
30
50
40
30
20
10
0
dicamba alone
Mean SCGE % Tail DNA (±SE)
DNA Damage
0
2000
4000
6000
8000
Dicamba Concentration (μM)

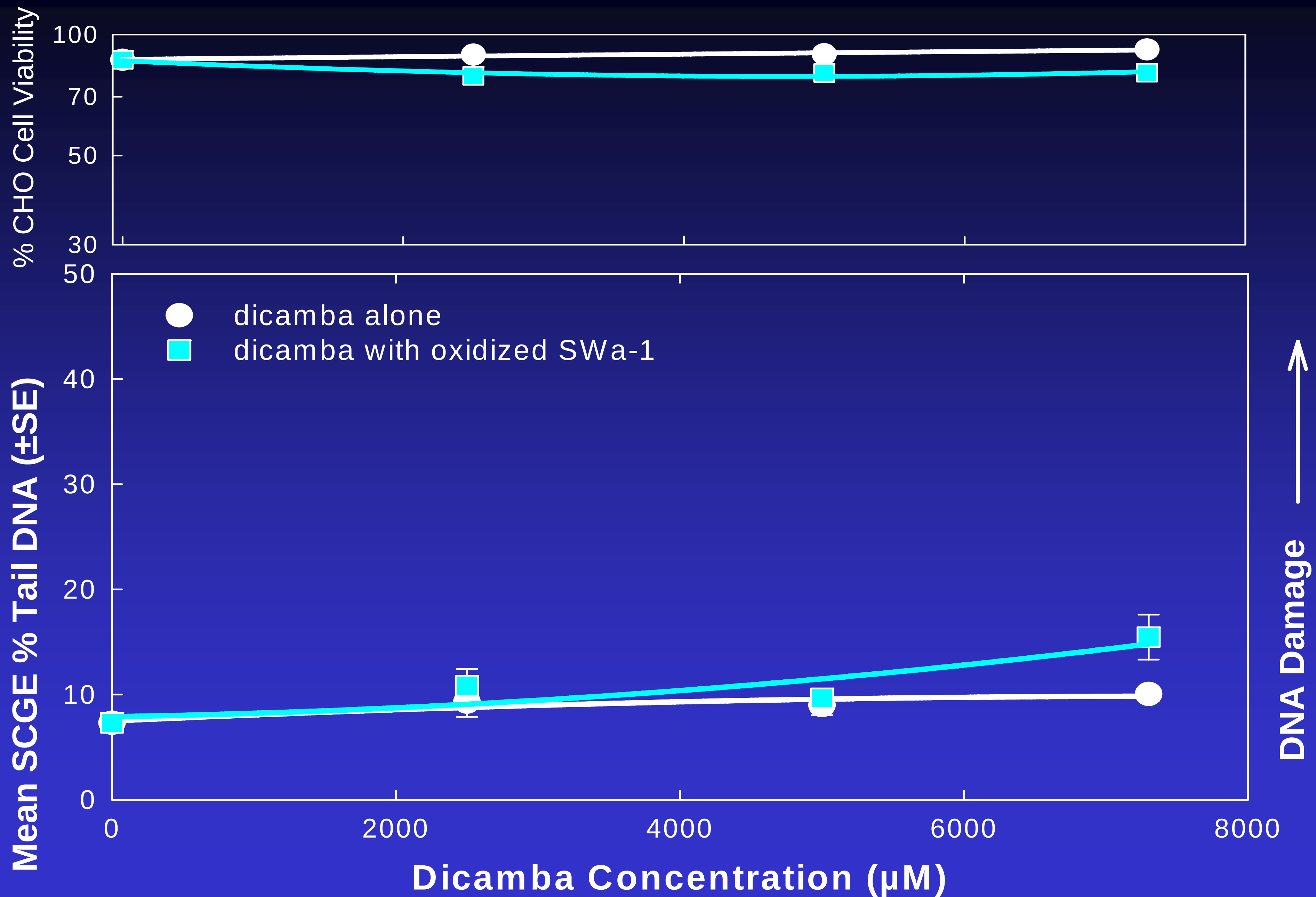

% CHO Cell Viability
100
70
50
30
50
40
30
20
10
0
dicamba alone
dicamba with oxidized SWa-1
Mean SCGE % Tail DNA (±SE)
DNA Damage
0
2000
4000
6000
8000
Dicamba Concentration (µM)

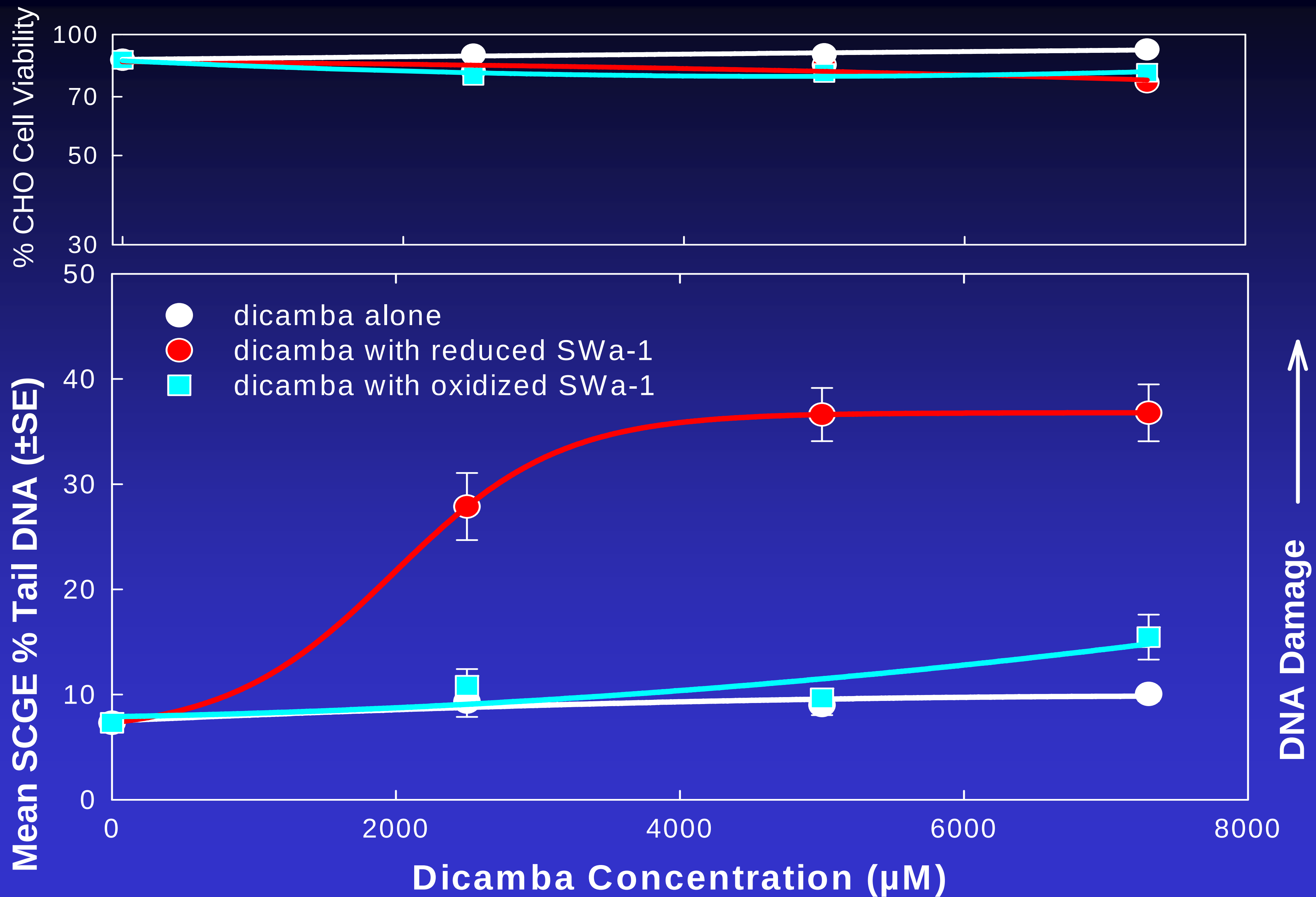

% CHO Cell Viability
100
70
50
30
50
40
30
20
10
0
dicamba alone
dicamba with reduced SWa-1
dicamba with oxidized SWa-1
Mean SCGE % Tail DNA (±SE)
DNA Damage
0
2000
4000
6000
8000
Dicamba Concentration (µM)

Conclusions -- Dicamba

- Dicamba genotoxicity is less than oxamyl and about the same as 2,4-D.
- Reaction of dicamba with oxidized (unaltered) smectite clay has a slight enhancement effect on its genotoxicity.
- Reaction of dicamba with reduced smectite clay causes a significant increase in the genotoxicity of this pesticide.

Mitigating Pesticide Toxicity

- The redox state of iron in smectite clay minerals has a large effect on the cyto- and genotoxicity of some pesticides.

Mitigating Pesticide Toxicity

- The redox state of iron in smectite clay minerals has a large effect on the cyto- and genotoxicity of some pesticides.
- On the pesticides where an effect is observed, it may be positive or negative, depending on the pesticide.

Mitigating Pesticide Toxicity

- The redox state of iron in smectite clay minerals has a large effect on the cyto- and genotoxicity of some pesticides.
- On the pesticides where an effect is observed, it may be positive or negative, depending on the pesticide.
- The toxicity of some pesticides is unaffected by the smectite.

Mitigating Pesticide Toxicity

- The redox state of iron in smectite clay minerals has a large effect on the cyto- and genotoxicity of some pesticides.
- On the pesticides where an effect is observed, it may be positive or negative, depending on the pesticide.
- The toxicity of some pesticides is unaffected by the smectite.
- Evaluations of pesticide fate must include effects of redox-modified clays.

Current & Future Work

Current work in Professor Plewa's laboratory is focussed on linking biological toxicological endpoints with alterations in gene expression in normal (non-transformed) human cells (student Mark Rundell). This will be one of the next steps in our work with the clays.

Current & Future Work

Current work in Professor Plewa's laboratory is focussed on linking biological toxicological endpoints with alterations in gene expression in normal (non-transformed) human cells (student Mark Rundell). This will be one of the next steps in our work with the clays. Studies with bacteria altered clays are also needed.